

**PIXEL-BASED AND OBJECT-BASED IMAGE  
ANALYSIS COMPARISON FOR LAND USE  
AND LAND COVER CLASSIFICATION**



**A Thesis Submitted in Partial Fulfillment of the Requirements for the  
Degree of Master of Science in Geoinformatics  
Suranaree University of Technology  
Academic Year 2017**

การเปรียบเทียบการวิเคราะห์ข้อมูลภาพเชิงจุดภาพและเชิงวัตถุ  
สำหรับการจำแนกการใช้ประโยชน์ที่ดินและสิ่งปกคลุมดิน



นางสาวศลิษา สาทรัมย์สำโรง

วิทยานิพนธ์นี้เป็นส่วนหนึ่งของการศึกษาตามหลักสูตรปริญญาวิทยาศาสตรมหาบัณฑิต

สาขาวิชาภูมิสารสนเทศ

มหาวิทยาลัยเทคโนโลยีสุรนารี

ปีการศึกษา 2560

**PIXEL-BASED AND OBJECT-BASED IMAGE ANALYSIS**  
**COMPARISON FOR LAND USE AND LAND COVER**  
**CLASSIFICATION**

Suranaree University of Technology has approved this thesis submitted in partial fulfillment of the requirements for a Master's Degree.

Thesis Examining Committee

S. Dasananda  
(Assoc. Prof. Dr. Songkot Dasananda)

Chairperson

Suwit Ong.  
(Assoc. Prof. Dr. Suwit Ongsomwang)

Member (Thesis Advisor)

S. Sarapirome  
(Asst. Prof. Dr. Sunya Sarapirome)

Member

Pantip  
(Dr. Pantip Piyatadsananon)

Member

S.M.  
(Prof. Dr. Santi Maensiri)  
Vice Rector for Academic Affairs  
and Internationalisation

W. Meevasana  
(Asst. Prof. Dr. Worawat Meevasana)  
Dean of Institute of Science

ศลิษา สาขาวิชา : การเปรียบเทียบการวิเคราะห์ข้อมูลภาพเชิงจุดภาพและเชิงวัตถุ  
สำหรับการจำแนกการใช้ประโยชน์ที่ดินและสิ่งปกคลุมดิน (PIXEL-BASED AND  
OBJECT-BASED IMAGE ANALYSIS COMPARISON FOR LAND USE AND LAND  
COVER CLASSIFICATION) อาจารย์ที่ปรึกษา : รองศาสตราจารย์ ดร.สุวิทย์ อ่องสมหวัง,  
192 หน้า.

ข้อมูลการใช้ประโยชน์ที่ดินและสิ่งปกคลุมดิน เป็นข้อมูลพื้นฐานของระบบสารสนเทศ  
ภูมิศาสตร์ ที่มีผู้ต้องการใช้งานหลากหลาย เช่น ผู้จัดการที่ดินและทรัพยากร นักผังเมือง หรือผู้  
ตัดสินใจ เพราะการใช้ประโยชน์ที่ดินและสิ่งปกคลุมดินเปลี่ยนแปลงอย่างรวดเร็ว แผนที่การใช้  
ประโยชน์ที่ดินและสิ่งปกคลุมดินจึงจำเป็นต้องมีการปรับปรุงจากข้อมูลการรับรู้จากระยะไกล  
ภายในระยะเวลาสั้น ฉะนั้น วิธีการของการจำแนกที่เหมาะสมเป็นสิ่งสำคัญสำหรับนำไปใช้ในการ  
ปรับปรุงแผนที่การใช้ประโยชน์ที่ดินและสิ่งปกคลุมดิน วัตถุประสงค์หลักของการศึกษา คือ (1)  
เพื่อจำแนกข้อมูลการใช้ประโยชน์ที่ดินและสิ่งปกคลุมดินโดยเลือกใช้วิธีการต่าง ๆ ของการ  
วิเคราะห์ข้อมูลภาพเชิงจุดภาพและการวิเคราะห์ข้อมูลภาพเชิงวัตถุ (2) เพื่อระบุวิธีการที่เหมาะสม  
ของการวิเคราะห์ข้อมูลภาพเชิงจุดภาพหรือ/และการวิเคราะห์ข้อมูลภาพเชิงวัตถุสำหรับการจำแนก  
การใช้ประโยชน์ที่ดินและสิ่งปกคลุมดิน ในการศึกษาครั้งนี้ใช้ข้อมูลแพนชาร์ปเพนนิ่งของ  
ดาวเทียมแลนด์แซท 8 เพื่อจำแนกการใช้ประโยชน์ที่ดินและสิ่งปกคลุมดินบริเวณอำเภอวังน้ำเขียว  
จังหวัดนครราชสีมา กรอบงานของวิธีการวิจัยประกอบด้วย 3 องค์ประกอบหลัก คือ (1) การ  
รวบรวมและจัดเตรียมข้อมูล (2) การจำแนกการใช้ประโยชน์ที่ดินและสิ่งปกคลุมดินภายใต้การ  
วิเคราะห์ข้อมูลภาพเชิงจุดภาพและการวิเคราะห์ข้อมูลภาพเชิงวัตถุ และ (3) การประเมินความ  
ถูกต้องของการใช้ประโยชน์ที่ดินและสิ่งปกคลุมดิน และวิธีการที่เหมาะสมสูงสุดสำหรับการ  
จำแนกการใช้ประโยชน์ที่ดินและสิ่งปกคลุมดินภายใต้การวิเคราะห์ข้อมูลภาพเชิงจุดภาพและการ  
วิเคราะห์ข้อมูลภาพเชิงวัตถุ

จากผลการประเมินประสิทธิภาพของตัวแทนวิธีการจำแนก 3 วิธี ที่ดีที่สุดของการวิเคราะห์  
ข้อมูลภาพเชิงจุดภาพ ประกอบด้วย (1) การจำแนกแบบความควรจะเป็นสูงสุดกับข้อมูลภาพ 9  
แบนด์ (2) โครงข่ายประสาทเทียมที่ใช้อัตราการเรียนรู้เท่ากับ 0.1 กับข้อมูลภาพ 6 แบนด์ (3) การ  
จำแนกแบบต้นไม้การตัดสินใจที่ไม่แบ่งแยกตัวอย่างกับข้อมูลภาพ 6 แบนด์ พบว่า วิธีการจำแนก  
ของการวิเคราะห์ข้อมูลภาพเชิงจุดภาพที่เหมาะสมสูงสุดสำหรับการจำแนกการใช้ประโยชน์ที่ดิน  
และสิ่งปกคลุมดินในการศึกษาครั้งนี้ได้แก่ การจำแนกแบบความควรจะเป็นสูงสุดกับข้อมูลภาพ 9  
แบนด์ (แบนด์ 2 3 4 5 6 และ 7 NDVI MNDWI และ NDBI) ซึ่งให้ค่าความถูกต้องโดยรวมเท่ากับ

ร้อยละ 86.01 และค่าสัมประสิทธิ์แคปปาเท่ากับร้อยละ 81.93 นอกจากนี้ จากผลการทดสอบค่า Z ระหว่างวิธีการจำแนกที่มีประสิทธิภาพสูงสุด 3 วิธีของการวิเคราะห์ข้อมูลภาพเชิงจุดภาพ พบว่า ความถูกต้องของการจำแนกแบบความควรจะเป็นสูงสุดกับข้อมูลภาพ 9 แบนด์ มีความแตกต่างกันอย่างมีนัยสำคัญ ณ ระดับความเชื่อมั่นร้อยละ 80 จากโครงข่ายประสาทเทียมที่ใช้อัตราการเรียนรู้เท่ากับ 0.1 กับข้อมูลภาพ 6 แบนด์ ในขณะเดียวกัน จากผลการประเมินประสิทธิภาพของตัวแทนวิธีการจำแนก 2 วิธีที่ดีที่สุดของการวิเคราะห์ข้อมูลภาพเชิงวัตถุ ซึ่งประกอบด้วย (1) การจำแนกแบบจุดภาพข้างเคียงที่ใกล้ที่สุดกับข้อมูลภาพ 11 แบนด์ และ (2) การจำแนกแบบจุดภาพข้างเคียงที่ใกล้ที่สุดกับรูปลักษณะที่เหมาะสมกับการจัดกลุ่มรูปลักษณะแบบที่ 3 พบว่า วิธีการจำแนกของการวิเคราะห์ข้อมูลภาพเชิงวัตถุที่เหมาะสมสูงสุดสำหรับการจำแนกการใช้ประโยชน์ที่ดินและสิ่งปกคลุมดินคือ การจำแนกแบบจุดภาพข้างเคียงที่ใกล้ที่สุดกับข้อมูลภาพ 11 แบนด์ (แบนด์ 2 3 4 5 6 และ 7 NDVI MNDWI NDBI ระดับความสูง และความชัน) ให้ค่าความถูกต้องโดยรวมเท่ากับร้อยละ 81.35 และสัมประสิทธิ์แคปปาเท่ากับร้อยละ 75.68 นอกจากนี้ จากผลการทดสอบค่า Z ระหว่างวิธีการจำแนกที่มีประสิทธิภาพสูงสุด 2 วิธีของการวิเคราะห์ข้อมูลภาพเชิงวัตถุ พบว่า ความถูกต้องของการจำแนกแบบจุดภาพข้างเคียงที่ใกล้ที่สุดกับข้อมูลภาพ 11 แบนด์ มีความแตกต่างกันอย่างมีนัยสำคัญ ณ ระดับความเชื่อมั่นร้อยละ 80 จากการจำแนกแบบจุดภาพข้างเคียงที่ใกล้ที่สุดกับรูปลักษณะที่เหมาะสมกับการจัดกลุ่มรูปลักษณะแบบที่ 3

จากผลการศึกษาสามารถสรุปได้ว่า วิธีการจำแนกที่เหมาะสมมากที่สุดสำหรับการจำแนกการใช้ประโยชน์ที่ดินและสิ่งปกคลุมดินระหว่างการวิเคราะห์ข้อมูลภาพเชิงจุดภาพและการวิเคราะห์ข้อมูลภาพเชิงวัตถุ คือ การจำแนกแบบความควรจะเป็นสูงสุดกับข้อมูลภาพ 9 แบนด์ จากผลการทดสอบค่า Z ระหว่างวิธีการจำแนกที่เหมาะสมสูงสุดของการวิเคราะห์ข้อมูลภาพเชิงจุดภาพและการวิเคราะห์ข้อมูลเชิงวัตถุแสดงให้เห็นว่า ความถูกต้องของการจำแนกแบบความควรจะเป็นสูงสุดกับข้อมูลภาพ 9 แบนด์ ภายใต้การวิเคราะห์ข้อมูลภาพเชิงจุดภาพ มีความแตกต่างกันอย่างมีนัยสำคัญ ณ ระดับความเชื่อมั่นร้อยละ 80 จากการจำแนกแบบจุดภาพข้างเคียงที่ใกล้ที่สุดกับข้อมูลภาพ 11 แบนด์ภายใต้การวิเคราะห์ข้อมูลภาพเชิงวัตถุ

สาขาวิชาการรับรู้จากระยะไกล

ปีการศึกษา 2560

ลายมือชื่อนักศึกษา

ศศิธา ลานงาช้าง

ลายมือชื่ออาจารย์ที่ปรึกษา

ศศิธา

SALISA SARAIAMRONG : PIXEL-BASED AND OBJECT-BASED  
IMAGE ANALYSIS COMPARISON FOR LAND USE AND LAND  
COVER CLASSIFICATION. THESIS ADVISOR : ASSOC. PROF. SUWIT  
ONGSOMWANG, Dr. rer. Nat. 192 PP.

PBIA/ OBIA/ LAND USE AND LAND COVER CLASSIFICATION / WANG NAM  
KIEO/ NAKHON RATCHASIMA/ THAILAND

Land use and land cover (LULC) data is a basic GIS dataset require by various users, e.g. land and resources manager, city planner, or decision-maker. Due to rapid LULC change, LULC map is frequently required to update from the remotely sensed data within a short period of times. Thus, optimum classification method is necessary to identify for updating LULC map. The main objectives of the study area were (1) to classify LULC data by selection methods of pixel-based image analysis (PBIA) and object-based image analysis (OBIA), and (2) to identify an optimum method of PBIA or / and OBIA for LULC classification. In this study, pan-sharpened image of Landsat-8 image was applied to LULC classification in Wang Nam Khiao District of Nakhon Ratchasima Province. The research methodology framework consisted of three major components include (1) data collection and preparation (2) LULC classification under PBIA and OBIA and (3) thematic LULC accuracy assessment and the best practical method for LULC classification under PBIA and OBIA.

According to the best performances of three representative methods of PBIA including (1) maximum likelihood classifier (MLC) with nine bands, (2) artificial neural network (ANN) at learning rate of 0.1 with six bands and (3) decision tree

classifier (DT) without splitting samples with six bands, the optimum method of PBIA for LULC classification was MLC with nine bands (Band 2, 3, 4, 5, 6, and 7, NDVI, MNDWI, and NDBI) that provided overall accuracy of 86.01% and Kappa hat coefficient of 81.93%. Herewith, the pairwise Z test among the best performances of three representative methods of PBIA showed that accuracy of MLC with nine bands is significantly different at the 80% confidence level from ANN at learning rate of 0.1 with six bands. Meanwhile, the best performances of two representative methods of OBIA including (1) standard nearest neighbor classifier (SNN) with eleven bands and (2) nearest neighbor classifier with feature space optimization (FSO) with feature combination # 3, the optimum method of OBIA for LULC classification is SNN with eleven bands (Band 2, 3, 4, 5, 6, and 7, NDVI, MNDWI, NDBI, elevation and slope) that provided overall accuracy of 81.35% and Kappa hat coefficient of 75.68%. Herewith, the pairwise Z test between the best performance of two representative methods of OBIA showed that accuracy of SNN with eleven bands is significantly different at the 80% confidence level from FSO with features combination # 3.

In conclusion, the optimum method for LULC classification between PBIA and OBIA is MLC with nine bands. The pairwise Z test between the optimum method of PBIA and OBIA showed that accuracy of MLC with nine bands under PBIA is significantly different at the 80% confidence level from SNN with eleven bands under OBIA.

School of Remote Sensing

Academic Year 2017

Student's Signature salisa Saraisamrong

Advisor's Signature Surit Ong

## **ACKNOWLEDGEMENTS**

This thesis would not have been possible without the guidance and support of many people. I would like to express my sincere appreciation to my thesis advisor, Assoc. Prof. Dr. Suwit Ongsomwang for his extensive knowledge, guidance, encouragement and continuous support through the study periods at Suranaree University of Technology.

I am grateful my committee members, Assoc. Prof. Dr. Songkot Dasananda, Asst. Prof. Dr. Sunya Sarapirome and Dr. Pantip Piyatadsananon for providing suggestions to helpfully improve in this research, Additionally, I am also thank to Suranaree University of Technology for teaching assistants and research assistant scholarship.

Special thanks also to Dr. Yaowaret Jantakat of Rajamangala University of Technology Isan for encouragement and continuous support through in the past time. I extend my thanks to all of the staffs and my friends at School of Remote Sensing for their help and support during my study here, especially Mrs. Pimprapai Piphatnawakul, Miss. Warunee Aunphoklang, Miss. Wilawan Prasomsup, Mr. Athiwat Phinyoyang and Mr. Kompheak Mom.

Finally, I wish to express my love and gratitude to my beloved family for their financial supports, great love, care, and patience during my study.

Salisa Saraisamrong



# CONTENTS

	<b>Page</b>
ABSTRACT IN THAI.....	I
ABSTRACT IN ENGLISH .....	III
ACKNOWLEDGEMENTS .....	V
CONTENTS.....	VI
LIST OF TABLES .....	XI
LIST OF FIGURES .....	XIX
LIST OF ABBREVIATIONS.....	XV
<b>CHAPTER</b>	
<b>I INTRODUCTION.....</b>	<b>1</b>
1.1 Background and significance of the study .....	1
1.2 Research objectives .....	3
1.3 Scope of the study .....	4
1.4 Limitation of the study .....	5
1.5 Study area .....	5
1.6 Benefits of the study.....	7
1.7 Outline of the thesis.....	7
<b>II BASIC CONCEPTS AND LITERATURE REVIEWS .....</b>	<b>9</b>
2.1 Pixel-based image analysis (PBIA).....	9
2.1.1 Parametric classification method .....	9

## CONTENTS (Continued)

	<b>Page</b>
2.1.2 Nonparametric classification method.....	12
2.1.3 Nonmetric classification method.....	15
2.2 Object-Based Image Analysis (OBIA).....	19
2.2.1 Standard nearest neighbor classifier.....	20
2.2.2 Nearest neighbor classifier with feature space optimization.....	21
2.3 Literature reviews.....	21
<b>III RESEARCH METHODOLOGY.....</b>	<b>30</b>
3.1 Data collection and preparation .....	30
3.2 LULC classification under PBIA and OBIA .....	34
3.3 Thematic LULC accuracy assessment and the best practical method for LULC classification under PBIA and OBIA.....	35
<b>IV PREPROCESSING OF REMOTE SENSING AND GIS DATA .....</b>	<b>38</b>
4.1 Pan-sharpening processing.....	38
4.2 Optimum pan-sharpening method identification using UIQI .....	42
4.3 Additional spectral band generation.....	45
4.4 Elevation and slope extraction .....	47
4.5 Preparation of image dataset for PBIA and OBIA.....	50
4.5.1 Dataset of PBIA .....	51
4.5.2 Dataset of OBIA.....	52

## CONTENTS (Continued)

	<b>Page</b>
<b>V PIXEL-BASED IMAGE ANALYSIS</b> .....	53
5.1 LULC classification of MLC .....	53
5.1.1 LULC classification of MLC with six bands .....	55
5.1.2 LULC classification of MLC with nine bands .....	58
5.2 LULC classification of ANN .....	64
5.2.1 LULC classification of ANN at learning rate of 0.1 with six bands.....	66
5.2.2 LULC classification of ANN at learning rate of 0.2 with six bands.....	68
5.2.3 LULC classification of ANN at learning rate of 0.1 with nine bands.....	74
5.2.4 LULC classification of ANN at learning rate of 0.2 with nine bands.....	76
5.3 LULC classification of DT.....	83
5.3.1 LULC classification of DT without splitting samples with six bands.....	84
5.3.2 LULC classification of DT without splitting samples with nine bands.....	89
5.3.3 LULC classification of DT without splitting samples with eleven bands .....	95

## CONTENTS (Continued)

	<b>Page</b>
5.3.4 LULC classification of DT with splitting samples with six bands.....	104
5.3.5 LULC classification of DT with splitting samples with nine bands.....	110
5.3.6 LULC classification of DT with splitting samples with eleven bands .....	116
<b>VI OBJECT-BASED IMAGE ANALYSIS</b> .....	<b>129</b>
6.1 LULC classification of SNN.....	129
6.1.1 LULC classification of SNN with six bands.....	134
6.1.2 LULC classification of SNN with nine bands.....	136
6.1.3 LULC classification of SNN with eleven bands .....	139
6.2 LULC classification of FSO .....	145
6.2.1 LULC classification of FSO with feature combination # 1 .....	146
6.2.2 LULC classification of FSO with feature combination # 2 .....	149
6.2.3 LULC classification of FSO with feature combination # 3 .....	152
6.2.4 LULC classification of FSO with feature combination # 4 .....	155
6.2.5 LULC classification of FSO with feature combination # 5 .....	158
<b>VII OPTIMUM METHOD FOR LULC CLASSIFICATION</b> .....	<b>164</b>
7.1 Optimum method of PBIA for LULC classification.....	164
7.2 Optimum method of OBIA for LULC classification .....	168

## CONTENTS (Continued)

	<b>Page</b>
7.3 Optimum method for LULC classification .....	171
<b>VIII CONCLUSION AND RECOMMENDATION .....</b>	<b>175</b>
8.1 Conclusion .....	175
8.1.1 Optimum method of PBIA for LULC classification .....	175
8.1.2 Optimum method of OBIA for LULC classification .....	177
8.1.3 Optimum method for LULC classification .....	178
8.2 Recommendation.....	179
REFERENCES .....	180
CURRICULUM VITAE.....	192

## LIST OF TABLES

Table	Page
1.1 Major land use types of Wang Nam Khiao District.....	6
2.1 Advantage and disadvantage of maximum likelihood decision rule .....	11
2.2 Advantage and disadvantage of ANN.....	15
2.3 Advantages and disadvantage of expert system.....	18
2.4 Synthesis of literature reviews .....	27
3.1 Specification of Landsat 8 products.....	33
3.2 Sensors and number band of Landsat 8 .....	33
3.3 The error matrix .....	35
4.1 Basic statistical data of pan-sharpened image with MIHS .....	41
4.2 Basic statistical data of pan-sharpened image with WT .....	41
4.3 Basic statistical data of pan-sharpened image with HPF .....	42
4.4 Basic statistical data of pan-sharpened image with EF.....	42
4.5 Basic statistical data of pan-sharpened image with GS .....	42
4.6 Comparison of the image quality from different pan-sharpening methods for Landsat 8 data of 2015 based on average UIQI value.....	44
4.7 Area and percentage of elevation classification in the study area .....	50
4.8 Area and percentage of slope classification in the study area .....	50
5.1 Area and percentage of final LULC classification of MLC with 6 bands .....	55

## LIST OF TABLES (Continued)

<b>Table</b>		<b>Page</b>
5.2	Error matrix and accuracy assessment of LULC classification of MLC with 6 bands .....	58
5.3	Area and percentage of final LULC classification of MLC with 9 bands .....	59
5.4	Error matrix and accuracy assessment of LULC classification of MLC with 9 bands .....	61
5.5	Pairwise Z test of Kappa hat coefficient value for LULC classification of MLC with six and nine bands.....	64
5.6	Area and percentage of final LULC classification of ANN at learning rate of 0.1 with six bands .....	66
5.7	Error matrix and accuracy assessment of LULC classification of ANN at learning rate of 0.1 with six bands.....	68
5.8	Area and percentage of final LULC classification of ANN at learning rate of 0.2 with six bands .....	69
5.9	Error matrix and accuracy assessment of LULC classification of ANN at learning rate of 0.2 with six bands.....	71
5.10	Pairwise Z test of Kappa hat coefficient value for LULC classification of ANN from six bands dataset with different learning rate.....	74
5.11	Area and percentage of final LULC classification of ANN at learning rate of 0.1 with nine bands.....	74

## LIST OF TABLES (Continued)

<b>Table</b>	<b>Page</b>
5.12 Error matrix and accuracy assessment of LULC classification of ANN at learning rate of 0.1 with nine bands.....	76
5.13 Area and percentage of final LULC classification of ANN at learning rate of 0.2 with 9 bands.....	77
5.14 Error matrix and accuracy assessment of LULC classification of ANN at learning rate of 0.2 with nine bands.....	79
5.15 Pairwise Z test of Kappa hat coefficient value for LULC classification of ANN from nine bands dataset with different learning rate .....	81
5.16 Pairwise Z test of Kappa hat coefficient value for LULC classification of ANN at learning rate at 0.1 and 0.2 with two different datasets (six and nine bands) .....	83
5.17 Model summary of DT without splitting samples with six bands: specifications and results .....	84
5.18 Accuracy assessment of the model based on training data as model-based inference statistics.....	86
5.19 Area and percentage of final LULC classification of DT without splitting samples with six bands.....	87
5.20 Error matrix and accuracy assessment of LULC classification of DT without splitting samples with six bands .....	89



## LIST OF TABLES (Continued)

<b>Table</b>	<b>Page</b>
5.21 Model summary of DT without splitting samples with nine bands: specifications and results .....	90
5.22 Accuracy assessment of the model based on training data as model-based inference statistics .....	92
5.23 Area and percentage of final LULC classification of DT without splitting samples with nine bands .....	93
5.24 Error matrix and accuracy assessment of LULC classification of DT without splitting samples with nine bands .....	95
5.25 Model summary of DT without splitting samples with eleven bands: specifications and results .....	96
5.26 Accuracy assessment of the model based on training data as model-based inference statistics .....	98
5.27 Area and percentage of final LULC classification of DT without splitting samples with eleven bands .....	99
5.28 Error matrix and accuracy assessment of LULC classification of DT without splitting samples with eleven bands .....	101
5.29 Pairwise Z test of Kappa hat coefficient value for LULC extraction in DT without splitting samples .....	104
5.30 Model summary of DT with splitting samples with six bands: specifications and results .....	105

## LIST OF TABLES (Continued)

<b>Table</b>	<b>Page</b>
5.31 Accuracy assessment of the model based on training data as model-based inference statistics .....	107
5.32 Area and percentage of final LULC classification of DT with splitting samples with six bands .....	108
5.33 Error matrix and accuracy assessment of LULC classification of DT with splitting samples with six bands .....	110
5.34 Model summary of DT with splitting samples with nine bands: specifications and results .....	111
5.35 Accuracy assessment of the model based on training data as model-based inference statistics .....	113
5.36 Area and percentage of final LULC classification of DT with splitting samples with nine bands .....	114
5.37 Error matrix and accuracy assessment of LULC classification of DT with splitting samples with nine bands .....	116
5.38 Model summary of DT without splitting samples with eleven bands: specifications and results .....	117
5.39 Accuracy assessment of the model based on training data as model-based inference statistics .....	119
5.40 Area and percentage of final LULC classification of DT with splitting samples with eleven bands.....	120

## LIST OF TABLES (Continued)

<b>Table</b>		<b>Page</b>
5.41	Error matrix and accuracy assessment of LULC classification of DT with splitting samples with eleven bands.....	122
5.42	Pairwise Z test of Kappa hat coefficient value for LULC extraction in DT with splitting samples from three datasets .....	125
5.43	Pairwise Z test of Kappa hat coefficient value for LULC extraction in DT with splitting samples .....	128
6.1	Parameter setting of multiresolution segmentation and number of the derived image objects of three datasets for LULC classification with SNN .....	130
6.2	List of features of SNN with three different dataset .....	133
6.3	Area and percentage of final LULC classification of SNN with six bands..	134
6.4	Error matrix and accuracy assessment of LULC classification of SNN with six bands .....	136
6.5	Area and percentage of final LULC classification of SNN with nine bands	137
6.6	Error matrix and accuracy assessment of LULC classification of SNN with nine bands .....	139
6.7	Area and percentage of final LULC classification of SNN with eleven bands.....	140
6.8	Error matrix and accuracy assessment of LULC classification of SNN with eleven bands.....	142

## LIST OF TABLES (Continued)

<b>Table</b>		<b>Page</b>
6.9	Pairwise Z test of Kappa hat coefficient value for LULC extraction in SNN .....	145
6.10	Area and percentage of final LULC classification of FSO with feature combination # 1.....	146
6.11	Error matrix and accuracy assessment of LULC classification of FSO with feature combination # 1 .....	148
6.12	Area and percentage of final LULC classification of FSO with feature combination # 2.....	149
6.13	Error matrix and accuracy assessment of LULC classification of FSO with feature combination # 2 .....	151
6.14	Area and percentage of final LULC classification of FSO with feature combination # 3.....	152
6.15	Error matrix and accuracy assessment of LULC classification of FSO with feature combination # 3 .....	154
6.16	Area and percentage of final LULC classification of FSO with feature combination # 4.....	155
6.17	Error matrix and accuracy assessment of LULC classification of FSO with feature combination # 4 .....	157
6.18	Area and percentage of final LULC classification of FSO with feature combination # 5.....	158

## LIST OF TABLES (Continued)

<b>Table</b>		<b>Page</b>
6.19	Error matrix and accuracy assessment of LULC classification of FSO with feature combination # 5 .....	160
6.20	Pairwise Z test of Kappa hat coefficient value for LULC classification with FSO .....	163
7.1	Accuracy assessment of the best three representative methods of PBIA .....	164
7.2	Pairwise Z test of among the best performance of three representative methods of PBIA.....	167
7.3	Accuracy assessment of the best two methods of OBIA .....	168
7.4	Pairwise Z test of among the best two methods of OBIA.....	170
7.5	Accuracy assessment of the optimum method of PBIA and OBIA.....	171
7.6	Pairwise Z test of between optimum method of PBIA and OBIA.....	173

## LIST OF FIGURES

Figure	Page
1.1 Comparison of agricultural land utilization in Nakhon Ratchasima Province during 2002 to 2013 .....	3
1.2 Study area.....	6
1.3 Structure of the thesis.....	8
2.1 Basic structure of a three layer ANN.....	13
2.2 Mathematic model of neuron.....	14
2.3 Example of a decision tree branch.....	17
2.4 Split rule decision tree branch.....	17
2.5 General scheme and components of an expert system for image analysis .....	18
2.6 Workflow of object-based image analysis in eCognition.....	20
3.1 A Workflow of research methodology framework.....	31
3.2 Landsat 8 data acquired date 15 December 2015.....	34
4.1 False color composite image of pan-sharpened image of modified IHS transformation .....	39
4.2 False color composite image of pan-sharpened image of wavelet fusion .....	39
4.3 False color composite image of pan-sharpened image of high pass filtering .	40
4.4 False color composite image of pan-sharpened image of Ehlers fusion.....	40
4.5 False color composite image of pan-sharpened image of Gram-Schmidt pan-sharpening .....	41

## LIST OF FIGURES (Continued)

<b>Figure</b>	<b>Page</b>
4.6 Universal Image Quality Index Model .....	43
4.7 Comparison of color composite of pan-sharpened image for visual test: (a) WT and (b) HPF methods.....	45
4.8 Normalized Difference Vegetation Index (NDVI) image .....	46
4.9 Modified Normalized Difference Water Index (MNDWI) image.....	46
4.10 Normalized Difference Built-up Index (NDBI) image.....	47
4.11 Elevation data.....	48
4.12 Slope data.....	48
4.13 Distribution of elevation classification .....	49
4.14 Distribution of slope classification .....	49
5.1 Examples of training areas of 9 LULC classes for MLC.....	54
5.2 LULC classification of 2015 of maximum likelihood classifier with 6 bands .....	56
5.3 Distribution of 193 sampling points for accuracy assessment.....	57
5.4 LULC classification of 2015 of MLC with 9 bands .....	60
5.5 Comparison area of LULC classification of MLC .....	62
5.6 Comparison of producer's accuracy and user's accuracy of MLC with six and nine bands.....	63
5.7 Example training areas of 9 LULC classes for ANN .....	65
5.8 LULC classification of 2015 of ANN at learning rate of 0.1 with six bands .	67

## LIST OF FIGURES (Continued)

<b>Figure</b>	<b>Page</b>
5.9	LULC classification of 2015 of ANN at learning rate of 0.2 with 6 bands .... 70
5.10	Comparison area of LULC classification of ANN from six bands with different learning rates (0.1 and 0.2)..... 72
5.11	Comparison of producer's accuracy and user's accuracy of LULC classes of ANN from six bands with different learning rates ..... 73
5.12	LULC classification of 2015 of ANN at learning rate of 0.1 with 9 bands .... 75
5.13	LULC classification of 2015 of ANN at learning rate of 0.2 with 9 bands .... 78
5.14	Comparison area of LULC classification of ANN from nine bands with different learning rates (0.1 and 0.2)..... 80
5.15	Comparison of producer's accuracy and user's accuracy of LULC classes of ANN from nine bands with different learning rates ..... 81
5.16	Binary decision tree structure for LULC classification without splitting samples with six bands..... 85
5.17	LULC classification of 2015 of DT without splitting samples with six bands ..... 88
5.18	Binary decision tree structure for LULC classification without splitting samples with nine bands ..... 91
5.19	LULC classification of 2015 of DT without splitting samples with nine bands ..... 94



## LIST OF FIGURES (Continued)

<b>Figure</b>	<b>Page</b>
5.20 Binary decision tree structure for LULC classification without splitting samples with eleven bands.....	97
5.21 LULC classification of 2015 of DT without splitting samples with eleven bands.....	100
5.22 Comparison area of LULC classification of DT without splitting samples..	102
5.23 Comparison of producer's accuracy and user's accuracy of LULC classes of DT without splitting samples from six, nine, and eleven bands.....	103
5.24 Binary decision tree structure for LULC classification with splitting samples with six bands .....	106
5.25 LULC classification of 2015 of DT with splitting samples with six bands..	109
5.26 Binary decision tree structure for LULC classification with splitting samples with nine bands .....	112
5.27 LULC classification of 2015 of DT with splitting samples with nine bands	115
5.28 Binary decision tree structure for LULC classification with splitting samples with eleven bands.....	118
5.29 LULC classification of 2015 of DT with splitting samples with eleven bands.....	121
5.30 Comparison area of LULC classification of DT with splitting samples from six, nine, and eleven bands .....	123

## LIST OF FIGURES (Continued)

<b>Figure</b>	<b>Page</b>
5.31 Comparison of producer's accuracy and user's accuracy of LULC classes of DT with splitting samples from six, nine, and eleven bands.....	124
5.32 Accuracy assessment of DT classification with and without splitting sample for decision tree construction in each dataset (six, nine, eleven bands) .....	126
5.33 Comparison of producer's accuracy and user's accuracy of LULC classes of DT classification with and without splitting sample for decision tree construction in each dataset (six, nine, eleven bands) .....	127
6.1 Image segmentation as image objects using multiresolution segmentation with the scale factor of 15, color parameter of 0.9 and compactness of 0.5.	130
6.2 Training areas of 9 LULC classes for SNN and FSO methods .....	132
6.3 LULC classification of 2015 of SNN with six bands .....	135
6.4 LULC classification of 2015 of SNN with nine bands.....	138
6.5 LULC classification of 2015 of SNN with eleven bands .....	141
6.6 Comparison area of LULC classification of SNN with three different dataset.....	143
6.7 Accuracy assessment of SNN with three different datasets.....	143
6.8 Comparison producer's and user's accuracy of LULC classification of SNN .....	144
6.9 LULC classification of 2015 of FSO with feature combination # 1.....	147
6.10 LULC classification of 2015 of FSO with feature combination # 2.....	150

## LIST OF FIGURES (Continued)

<b>Figure</b>	<b>Page</b>
6.11 LULC classification of 2015 of FSO with feature combination # 3.....	153
6.12 LULC classification of 2015 of FSO with feature combination # 4.....	156
6.13 LULC classification of 2015 of FSO with feature combination # 5.....	159
6.14 Comparison area of LULC classification of FSO with five features combinations .....	161
6.15 Accuracy assessment of FSO with five different features combination .....	161
6.16 Comparison producer's and user's accuracy of LULC classification of FSO with five different features combination.....	162
7.1 Accuracy assessment of the best three representative methods of PBIA .....	165
7.2 Producer's accuracy and user's accuracy of the best three representative methods of PBIA.....	166
7.3 Accuracy assessment of the best two methods of OBIA.....	169
7.4 Producer's accuracy and user's accuracy of the best two methods of OBIA .....	170
7.5 Accuracy assessment of optimum method of PBIA and OBIA.....	171
7.6 Producer's accuracy and user's accuracy of optimum method of PBIA and OBIA.....	172

## LIST OF ABBREVIATIONS

ANN	=	Artificial Neural Network
CV	=	Cassava
DT	=	Decision Tree Classifier
EF	=	Ehlers Fusion
FA	=	Forest Area
FSO	=	Nearest Neighbor Classifier with Feature Space Optimization
GIS	=	Geographic Information System
GLCM	=	Gray Level Co-Occurrence Matrices
GS	=	Gram-Schmidt Pan-Sharpener
HPF	=	High Pass Filtering
km <sup>2</sup>	=	Square Kilometer
LDD	=	Land Development Department
LULC	=	Land Use and Land Cover
m	=	Meter
MA	=	Maize
MIHS	=	Modified IHS Transformation
ML	=	Miscellaneous Land
MLC	=	Maximum Likelihood Classifier
MNDWI	=	Modified Normalized Difference Water Index
NDBI	=	Normalized Difference Built-up Index

**LIST OF ABBREVIATIONS (Continued)**

NDVI	=	Normalized Difference Vegetation Index
NIR	=	Near Infrared
OBIA	=	Object-Based Image Analysis
OP	=	Orchard and Perennial Trees
PBIA	=	Pixel-Based Image Analysis
PD	=	Paddy Field
SNN	=	Standard Nearest Neighbor Classifier
sq. km	=	Square Kilometer
Std.	=	Standard Deviation
SU	=	Sugarcane
SWIR	=	Short-Wavelength Infrared
UB	=	Urban and Built-Up Area
UIQI	=	Universal Image Quality Index
USGS	=	United States Geological Survey
WB	=	Water Bodies
WT	=	Wavelet Fusion

# CHAPTER I

## INTRODUCTION

### 1.1 Background and significance of the study

Digital image analysis is the science by using the pixel value for image interpretation or processing, which relies on multispectral data of remote sensing sensors to record reflection of objects on the earth (Ongsomwang, 2011). In practice, there is two main digital image analysis methods include pixel-based image analysis (PBIA) and object-based image analysis (OBIA).

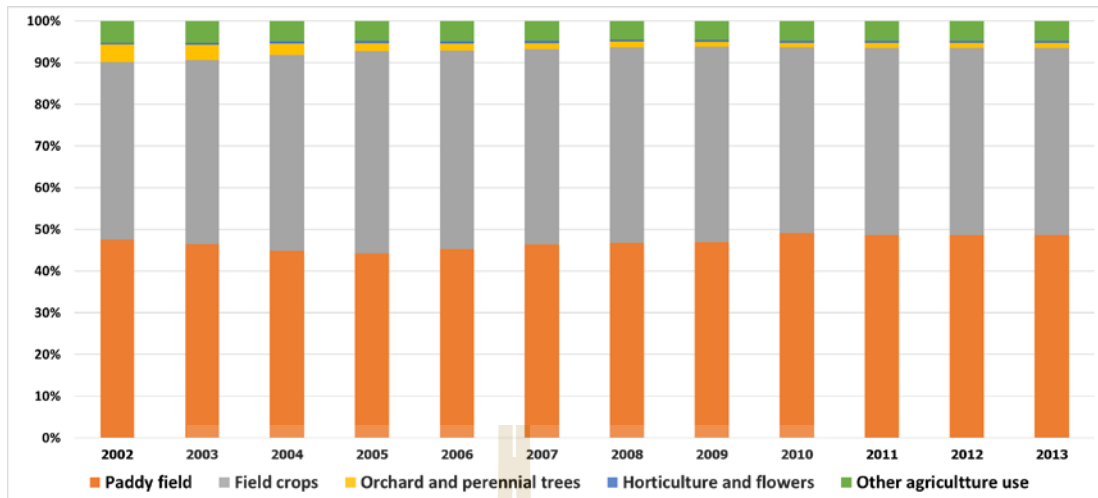
In general, PBIA is hitherto the most commonly used types of classification in remote sensing and it is described in detail and mathematically derived in the specialist textbooks (Nussbaum and Menz, 2008) such as Canty (1999), Richards and Jia (1999), Albertz (2001), Lillesand, Kiefer, and Chipman (2004). In contrast, OBIA is applied in several fields (Nussbaum and Menz, 2008) such as the wide-area monitoring of landscape areas (Blaschke, 2005; Chandra, Moreira, and Keydel, 2005; Crase and Hempel, 2005; Laliberte, Rango and Fredrickson, 2005; Witheside, 2005); the monitoring of densely settled urban areas (Chunyang, Li, Zhang, Pan, and Chen, 2005; Grenzdoerfer, 2005; Moeller, 2005); disasters assessment (Bitelli, Camassi, Gusella, and Mongol, 2004; Heremans, Willekens, Borghys, Verbeeck, Valckenborgh, and Perneel, 2005; Kouchi and Yamazaki, 2005); and data fusion and the establishment of GIS systems (Benz, Hofmann, Willhauck, Lingenfelder, and Heynen, 2004; Langanke,

Blaschke, and Lang, 2004; Sim, 2005; Cabral, Gilg, and Painho, 2005; Kosugi and Kosaka, 2005).

However, the purely PBIA has increasingly reached its limit despite further development in recent years. One reason is the fact that with increasing spatial resolution of the satellite data, the (small) feature basis of spectral values often only provides insufficient results for classification. Furthermore, there is an increasing amount of additional data such as information from GIS system or digital elevation model (DEM). It appears meaningful for future investigation to integrate these additional data into satellite image analysis. OBIA offers great potential, since it has a very large feature basis for classification and additional data from other data sources can be readily integrated and used for analysis (Nussbaum and Menz, 2008).

Meanwhile, land use and land cover (LULC) data is a basic GIS dataset require by various users, e.g. land and resources manager, city planner, or decision-maker. Due to rapid LULC change, LULC map is frequently required to update from the remotely sensed data within a short period of times. Weih and Riggan (2010) stated that LULC data have proven to be valuable assets for resource managers interested in landscape characteristics and the changes that occur over time.

According to annual report of the Office of Agricultural Economics on agricultural land utilization in Nakhon Ratchasima Province during 2002-2013, areas of major agricultural land use types, namely paddy field, field crop, orchards and perennial trees, horticulture and flowers and other agricultural use are fluctuate (Figure 1.1). This information confirms status and its change over the study area, Wang Nam Khieo District, Nakhon Ratchasima Province. Thus, optimum classification method is necessary to identify for updating recent LULC status.



**Source:** Office of Agricultural Economics, 2016.

**Figure 1.1** Comparison of agricultural land utilization in Nakhon Ratchasima Province during 2002 to 2013.

Therefore, PBIA and OBIA are here examined to classify LULC data from moderate spatial resolution of the free-downloaded Landsat-data instead of very high spatial resolution data of IKONOS or QuickBird satellite. The derived results are then compared to identify an optimum method of PBIA and/or OBIA for LULC classification. The expected results can provide the basic guideline to image analyst for LULC classification in the future. In addition, the derived LULC can be used to update recent LULC information.

## 1.2 Research objectives

The aim of this research is to identify an optimum method of PBIA and/or OBIA for LULC classification from moderate free-downloaded Landsat data. The specific research objectives on PBIA and OBIA comparison for LULC classification are as follows:



- (1) To classify LULC data by selection methods of PBIA and OBIA,
- (2) To identify an optimum method of PBIA or / and OBIA for LULC classification.

### **1.3 Scope of the study**

Scope of this study can be summarized as follows:

(1) Landsat 8 data (multispectral and panchromatic bands) acquiring in December 2015 is processed pan-sharpening image with predefined methods: (1) Modified IHS transformation (MIHS), (2) Wavelet fusion (WT), (3) High Pass Filtering (HPF), (4) Ehlers fusion (EF), and (5) Gram-Schmidt pan-sharpening (GS) to create optimum pan-sharpened image based on Universal Image Quality Index (UIQI) for LULC classification under PBIA and OBIA. In addition, the derived pan-sharpened image is further used to create additional bands for LULC classification methods include spectral indices (Normalized Difference Vegetation Index (NDVI), Modified Normalized Difference Water Index (MNDWI) and Normalized Difference Built-up Index (NDBI)) and physical data (elevation and slope).

(2) Selected classification method for LULC classification under PBIA consists of maximum likelihood classifier (MLC), artificial neural network (ANN) and decision tree classifier (DT) while standard nearest neighbor classifier (SNN) and nearest neighbor classifier with feature space optimization (FSO) are applied under OBIA.

(3) LULC classification system that is modified from standard land use classification system of LDD includes (1) urban and built-up area, (2) paddy field, (3) cassava, (4) maize, (5) sugarcane, (6) orchard and perennial trees, (7) forest area, (8)

water bodies, and (9) miscellaneous land.

(4) Thematic LULC accuracy (overall accuracy and Kappa hat coefficient) is assessed using random stratified sampling points based on multinomial distribution theory by field survey in January 2017. In addition, pairwise Z test is also applied to examine significantly different of Kappa hat coefficient among selected classification methods.

(5) An optimum classification method is identified under PBIA, OBIA and between PBIA and OBIA based on overall accuracy and Kappa hat coefficient.

#### **1.4 Limitations of the study**

Accuracy assessment of thematic map from various methods of PBIA and OBIA was conducted based on field survey January in 2017. It can be here observed that date of remotely sensed data and field survey data are different due to time constraint. However, the effect of phenological change on LULC in December and January are not significantly different.

#### **1.5 Study area**

Wang Nam Khiao District of Nakhon Ratchasima Province, Thailand is chosen as study area. It situates in the southern parts of Nakhon Ratchasima Province and has neighboring districts, namely Pak Thong Chai, Khon Buri, Pak Chong of Nakhon Ratchasima Province and Na Di, Prachantakham of Prachinburi Province. The district is subdivided into 5 sub-districts include Wang Nam Khiao, Wang Mhee, Ra Roeng, Udom Sap and Thai Samakkhi (Figure 1.2).

Wang Nam Khiao District has area of 1,054.30 km<sup>2</sup> which consists of various LULC types with rapid LULC change. According to land use data of LDD in 2011, two main land use types in the study area are forest land (54.04%) and agricultural land (35.52%) as summarized in Table 1.1.

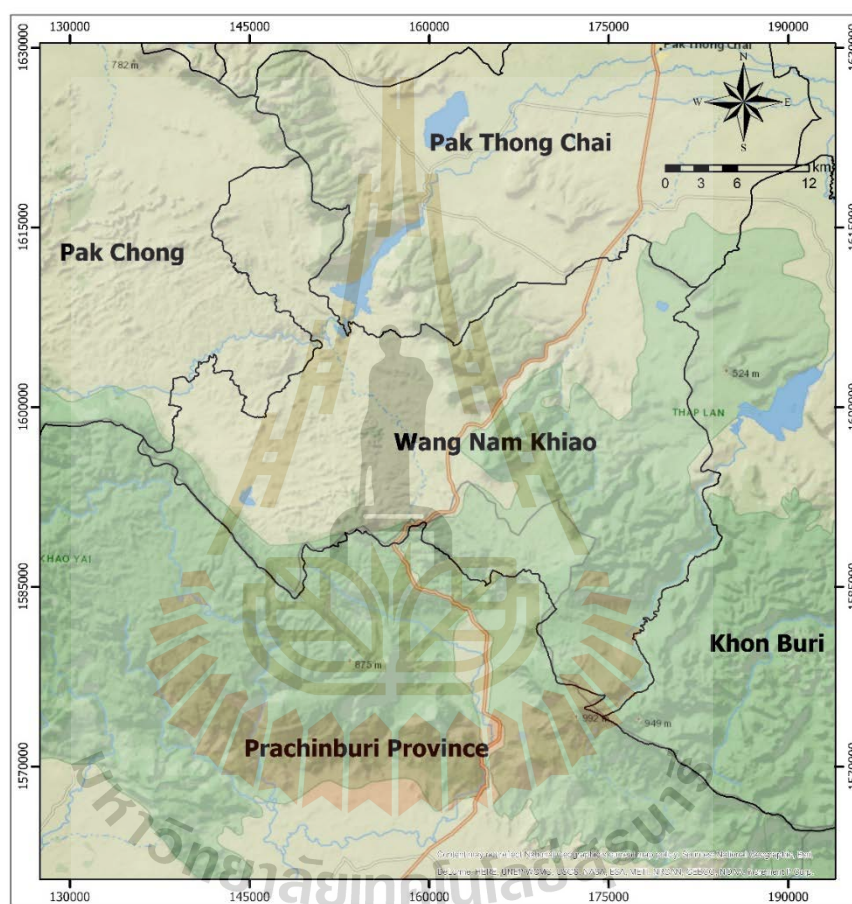


**Figure 1.2** Study area.

**Table 1.1** Major land use types of Wang Nam Khiao District (LDD, 2011).

No.	Land use type	Area in sq. km	Percent
1	Urban and built-up area	49.99	4.74
2	Agricultural land	374.50	35.52
3	Forest land	569.70	54.04
4	Water body	10.20	0.97
5	Miscellaneous land	49.91	4.73
<b>Total</b>		<b>1,054.30</b>	<b>100.00</b>

## 1.6 Benefits of the study

The benefits of the study are as follows:

1. LULC data of pixel-based and object-based image analysis.
2. An optimum method of PBIA for LULC classification.
3. An optimum method of OBIA for LULC classification.
4. An optimum method for LULC classification.

## 1.7 Outline of the thesis

The thesis is structured in two parts and follows a hierarchical organization as shown in Figure 1.3. Key information of each chapter in each part is summarized in the following section.

The first part includes Chapters I “Introduction”, Chapter II “Basic Concepts and Literature Reviews” and Chapter III “Research Methodology”. Chapter I contains background problem and significance of the study, research objectives, scope of the study, limitation of the study, study area, benefits of the study and outline of the thesis. Chapter II consists of PBIA, OBIA and literature reviews. Meanwhile, Chapter III explains details of research methodology including (1) data collection and preparation (2) LULC classification under PBIA and OBIA and (3) thematic LULC accuracy assessment and the best practical method for LULC classification under PBIA and OBIA.

The second part consists of four chapters of the results with discussion, which separately describe according to objectives and one chapter presents conclusion and recommendation. Chapter IV “Preprocessing of Remote Sensing and GIS Data” contains (1) pan-sharpening processing, (2) optimum pan-sharpening method

identification using UIQI, (3) additional spectral band generation, (4) elevation and slope extraction, and (5) preparation of image dataset for PBIA and OBIA. Chapter V “Pixel-Based Image Analysis” explains results of LULC classification of PBIA including MLC, ANN, and DT. Likewise, Chapter VI “Object-Based Image Analysis” describes results of LULC classification using SNN and FSO under OBIA. Chapter VII “Optimum Method for LULC Classification” explains an optimum method of PBIA and/or OBIA for LULC classification. Chapter VIII “Conclusion and Recommendation” comprises conclusion of the study and recommendation.

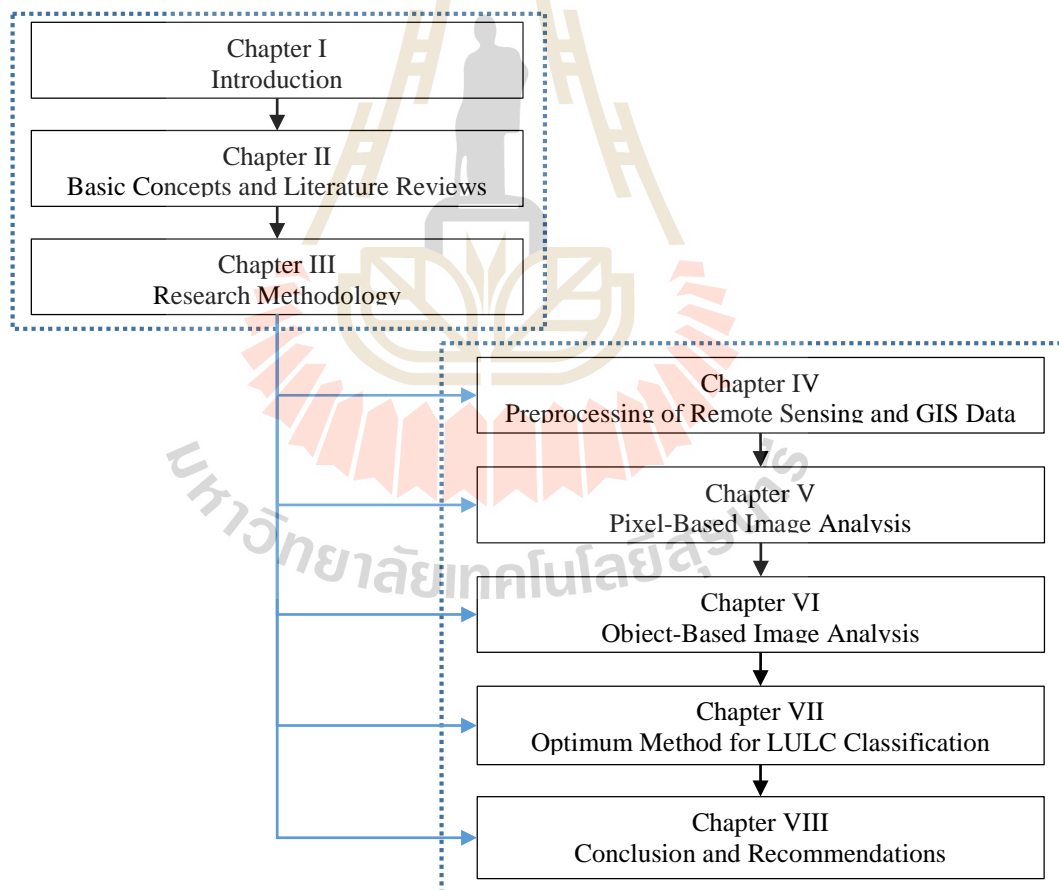


**Figure 1.3** Structure of the thesis.

## **CHAPTER II**

### **BASIC CONCEPTS AND LITERATURE REVIEWS**

Basic concepts include (1) pixel-based image analysis (PBIA), and (2) object-based image analysis (OBIA) and (3) literature reviews are briefly described in this chapter.

#### **2.1 Pixel-based image analysis (PBIA)**

The common image classification methods of PBIA that are frequently applied with multispectral remotely sensed data for LULC classification are here separately summarized into three groups: parametric, nonparametric and nonmetric classification methods.

##### **2.1.1 Parametric classification method**

Parametric classification method relies on assumption about the form of the probability distribution for each class. The most notable popular is maximum likelihood classifier (MLC), which explicitly uses a probability model to determine the decision boundaries. The necessary parameters for the model are estimates from training data. A useful property of parametric classifiers is theoretical estimation of classifiers error from the assumed distribution that is not possible with nonparametric classifiers (Schowengerdt, 1997).

In general, classifier of parametric classification method includes maximum likelihood classifier (MLC) and clustering classifier. In this study, MLC is chosen as representative of parametric classification method and it can be summarized its characteristics and advantage/disadvantage as below.

The maximum likelihood decision rule is based on probability. The probability of a pixel belonging to each of a predefined set of  $m$  classes is calculated, and the pixel is then assigned to the class for which the probability is the highest. The maximum likelihood decision rule is still one of the most widely used supervised classification algorithms (Jensen, 2005).

The maximum likelihood procedure assumes that the training data statistics for each class in each band are normally distributed (Gaussian). Training data with bi- or n-modal histograms in a single band are not ideal. In such cases the individual modes probably represent unique classes that should be trained upon individually and labeled as separate training classes. This should then produce unimodal, Gaussian training class statistics that fulfill the normal distribution requirement. The computation of an n-dimensional multivariate normal density function for the classes of interested using the equation:

$$p(X|w_i) = \frac{1}{(2\pi)^{\frac{n}{2}}|V_i|^{\frac{1}{2}}} \exp \left[ -\frac{1}{2} (X - M_i)^T V_i^{-1} (X - M_i) \right] \quad (2.1)$$

Where:

$p(X|w_i)$  is the probability density function of class  $w_i$

$|V_i|$  is the determinant of the covariance matrix,

$V_i^{-1}$  is the inverse of the covariance matrix,

$(X - M_i)^T$  is the transpose of the vector  $(X - M_i)$

The mean vectors ( $M_i$ ) and covariance matrix ( $V_i$ ) for each class are estimated from the training data.

If there are  $m$  classes, then  $p(X|w_i)$  is the probability density function associated with the unknown measurement vector  $X$ , given that  $X$  is from a pattern in class  $w_i$ . In this case the maximum likelihood decision rule becomes:

Decide  $X \in w_i$ , if, and only if,

$$p(X|w_i) \cdot p(w_i) \geq p(X|w_j) \cdot p(w_j) \quad (2.2)$$

for all  $i$  and  $j$  out of 1, 2, ...  $m$  possible classes.

Therefore, to classify a pixel in the multispectral remote sensing dataset with an unknown measurement vector  $X$ , a maximum likelihood decision rule computes the product  $p(X|w_i) \cdot p(w_i)$  for each class and assigns the pattern to the class having the largest product. This assumes that some useful information about the prior probabilities of each class  $i$  are known, i.e.  $p(w_i)$  (Jensen, 2005).

Advantage and disadvantage of maximum likelihood classifier is summarized in Table 2.1.

**Table 2.1** Advantage and disadvantage of maximum likelihood decision rule.

Advantages	Disadvantages
<ul style="list-style-type: none"> <li>• The most accurate of the classifiers in the ERDAS IMAGINE system (if the input samples/clusters have a normal distribution), because it takes the most variables into consideration.</li> <li>• Takes the variability of classes into account by using the covariance matrix, as does Mahalanobis distance.</li> </ul>	<ul style="list-style-type: none"> <li>• An extensive equation that takes a long time to compute. The computation time increases with the number of input bands.</li> <li>• Maximum likelihood is parametric, meaning that it relies heavily on a normal distribution of the data in each input band.</li> <li>• Tends to over classify signatures with relatively large values in the covariance matrix.</li> </ul>

**Source:** ERDAS, 2002.



### 2.1.2 Nonparametric classification method

Nonparametric classification method makes no assumption about the probability distribution and is often considered robust because it may work well for a variety of classification, as long as the class signatures are reasonably distinct (Schowengerdt, 1997).

ERDAS (2002) stated that a nonparametric decision rule is not based on statistics; therefore, it is independent of the properties of the data. If a pixel is located within the boundary of a nonparametric signature, then this decision rule assigns the pixel to the signature's class. Basically, a nonparametric decision rule determines whether or not the pixel is located inside of nonparametric signature boundary. The common nonparametric classification methods include level-slice classifier, parallelepiped classifier, minimum distance classifier, nearest neighbor classifier, fuzzy classifier and artificial neural network (ANN). Herein the ANN as a representative of nonparametric classification method is here summarized as below.

Schowengerdt (1997) mentioned that the ANN algorithm is a recently popular nonparametric approach to classification. The decision boundaries by ANN are not fixed by a deterministic rule applied to the prototype training signature, but are determined in an iterative fashion by minimizing an error criterion on the labeling of the training data. In that sense, ANNs are similar to clustering algorithms.

Keiner (1999) stated that ANN can be used for a variety of remote sensing application, including classification, noise reduction, feature tracking, forecasting, and function approximation. Jensen (2005) mentioned that ANN has been used to classify various types of remote sensor data and has in certain instances produces results superior to those of traditional statistics methods. This success can be

attributed to two of the important advantages of neural networks: freedom from normal distribution requirements and ability to adaptively simulate complex and nonlinear pattern given proper topological structures.

The ANN normally contains neurons arranged in three types of layers: (1) an input layer, (2) a hidden layers, and (3) an output layer as shown in Figure 2.1. The hidden layer and the output layer contain processing elements at each node. The input layer nodes, on the other hand, are simply an interface to the input data and do not do any processing. The input patterns are the features used for classification. In the simplest case, they are the multispectral vectors of the training pixels, one band per node. Other features, such as a spatial neighborhood of pixels or multi-temporal spectral vectors, can also be used (Schowengerdt, 1997).

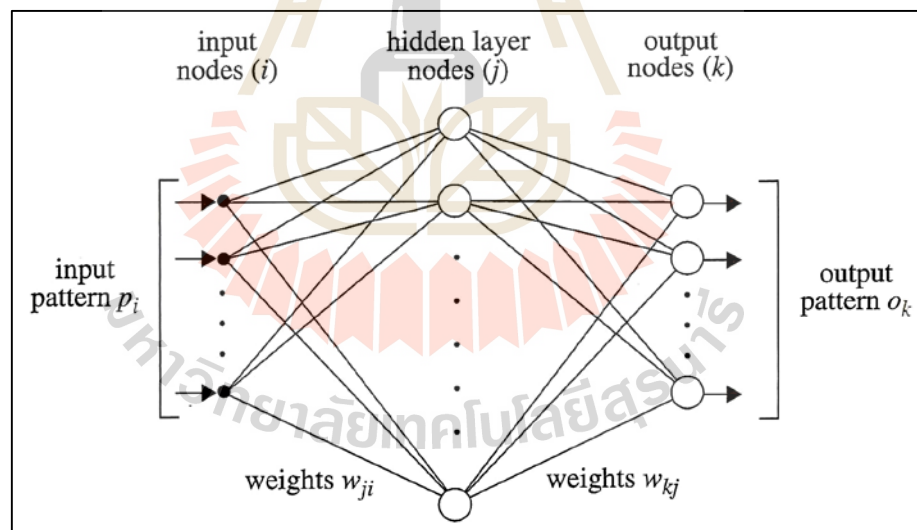


**Figure 2.1** Basic structure of a three layer ANN (Schowengerdt, 1997).

In addition, Jensen (2005) mentioned that ANN requires training and testing (classification) to extract useful information from the remotely sensed and ancillary data like a supervised classification. The neuron in the input layers might be

the multispectral reflectance values plus their textures, surface roughness, terrain elevation, slope, aspect, etc. The use of neurons in the hidden layers enables the simulation of non-linear patterns in the input data. A neuron in the output layers might represent a single thematic map land cover class, e.g., agriculture.

In principle, ANN is defined by neurons, topological structure, and learning rules. The neuron is the fundamental processing unit of an ANN for computation. Each input  $x_i$  is multiplied by the scalar weight  $w_i$  to form  $x_i w_i$ , a term that is sent to the “summing unit” of the processing unit (Figure 2.2). An offset,  $b$ , may be added to the total (Jensen, 2005). The summation output:

$$net = \sum_{i=1}^p (x_i w_i) + b \quad (2.3)$$

It referred to as net input, goes into an activation transfer function  $f$  that produces scaled neuron output  $y$  (between 0 and 1, or -1 to 1) through a transform algorithm. Thus,  $y$  can be calculated as:

$$y = f(net) = \left[ \sum_{i=1}^p (x_i w_i) + b \right] \quad (2.4)$$

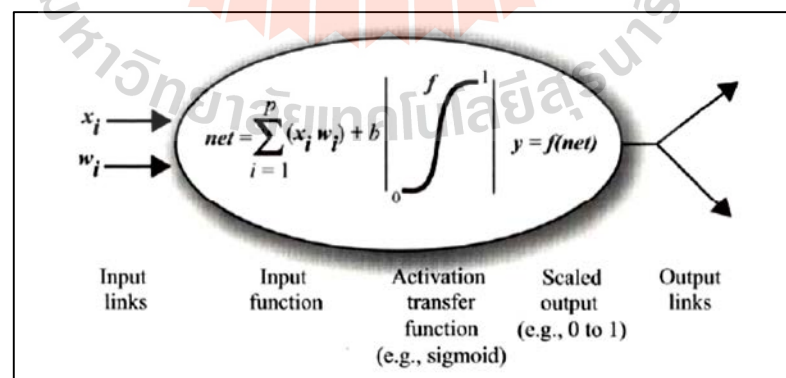


**Figure 2.2** Mathematic model of neuron (Jensen, 2005).

Advantage and disadvantage of ANN is summarized by Jensen (2005) as in Table 2.2.

**Table 2.2** Advantage and disadvantage of ANN.

Advantage	Disadvantage
<ul style="list-style-type: none"> <li>• A single neuron simulates the computation of a multivariate linear regression model.</li> <li>• A neural network makes no a priori assumptions of normal and linear data distribution due to its operation in a nonparametric fashion.</li> <li>• Neural networks are able to learn from existing examples adaptive, which makes the classification objective.</li> <li>• The nonlinear patterns are “learned” from the empirical examples instead of pre-specified” by an analysis based on prior knowledge of the datasets.</li> <li>• The noisy information inevitably included in the examples supplied a trained neural network with the ability to generalized, which makes neural networks robust solutions in the presence of previous unseen, incomplete, or imprecise data.</li> <li>• A neural network can embrace data in all formats as long as the data are converted to a numeric representation.</li> <li>• Neural network are tolerant of noise and missing data and attempt to find the best fit for input patterns.</li> <li>• Neural networks continuously adjust the weights as more training data are provided in a changing environment.</li> </ul>	<ul style="list-style-type: none"> <li>• Despite the excellent performance of neural networks in image classification, it is usually difficult to explain in a comprehensive fashion the process through which a given decision or output has been obtained from a neural network. The rules of image classification and interpretation learned by the neural network are buried in the weights of the neurons of the hidden layers. It is difficult to interpret these weights due to their complex nature. A neural network is often accused of being a black box.</li> <li>• Using neural network, an analyst might find it difficult to gain an understanding of the problem at hand because of the lack of explanatory capability to provide insight into the characteristics of the dataset.</li> <li>• It is difficult to incorporate human expertise to simplify, accelerate, or improve the performance of image classification; a neural network always has to learn from scratch.</li> </ul>

**Source:** Jensen, 2005.

### 2.1.3 Nonmetric classification method

Duda, Hart and Stork (2001) mentioned that nonmetric classification method turned away from description patterns by vectors of real numbers and toward using lists of attributes. Nonmetric algorithms used nominal data for classification by rule-based or synthetic pattern recognition methods. The common nonmetric

classification is rule-based decision tree classifiers (DT) or expert systems. In this study, DT is chosen as representative of nonmetric classification method and it is summarized as below.

Jensen (2005) stated that the best way to conceptualize an expert system is to use a decision-tree-structure where rules and conditions are evaluated in order to test hypotheses. When decision trees are organized with hypotheses, rules, and conditions, each hypothesis may be thought of as the trunk of a tree, each rule a limb of a tree, and each condition a leaf. This is commonly referred as a hierarchical decision-tree classifier.

The DT grows in depth when the hypothesis of one rule is referred to by a condition of another rule. The terminal hypotheses of DT represent the final classes of interest. Intermediate hypotheses may also be flagged as being a class of interest. This may occur when there is an association between classes (ERDAS, 2002). Figure 2.3 presents a single branch of DT. In this example, the rule, which is gentle southern slope, determines the hypothesis, good location. The rule has four conditions depicted on the right side, all of which must be satisfied for the rule to be true. However, the rule may be split if either southern or gentle slope defines the good location hypothesis. While both conditions must still be true to fire a rule, only one rule must be true to satisfy the hypothesis as shown in Figure 2.4.

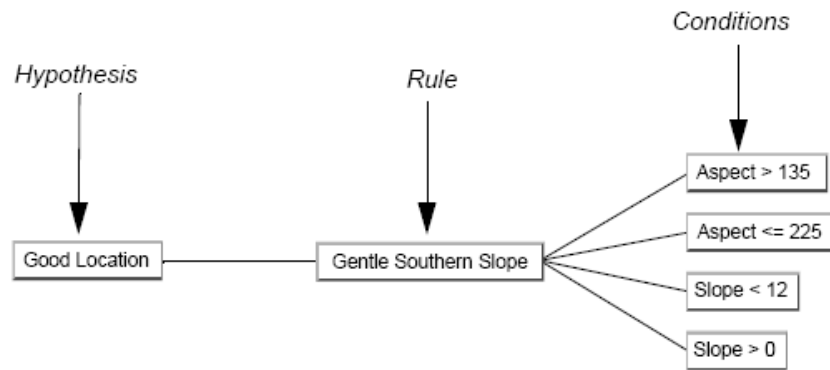


**Figure 2.3** Example of a decision tree branch (ERDAS, 2002).

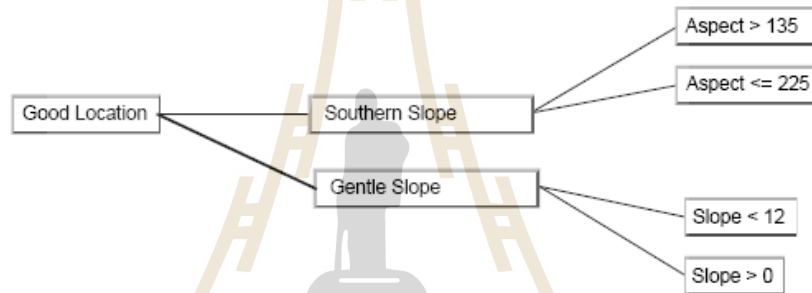


**Figure 2.4** Split rule decision tree branch (ERDAS, 2002).

An expert system comprises two independent components, a domain specific knowledge base and a domain-independent inference engine or control mechanism (Gao, 2009) as shown in Figure 2.5. Advantage and disadvantage of expert system is summarized as shown in Table 2.3.

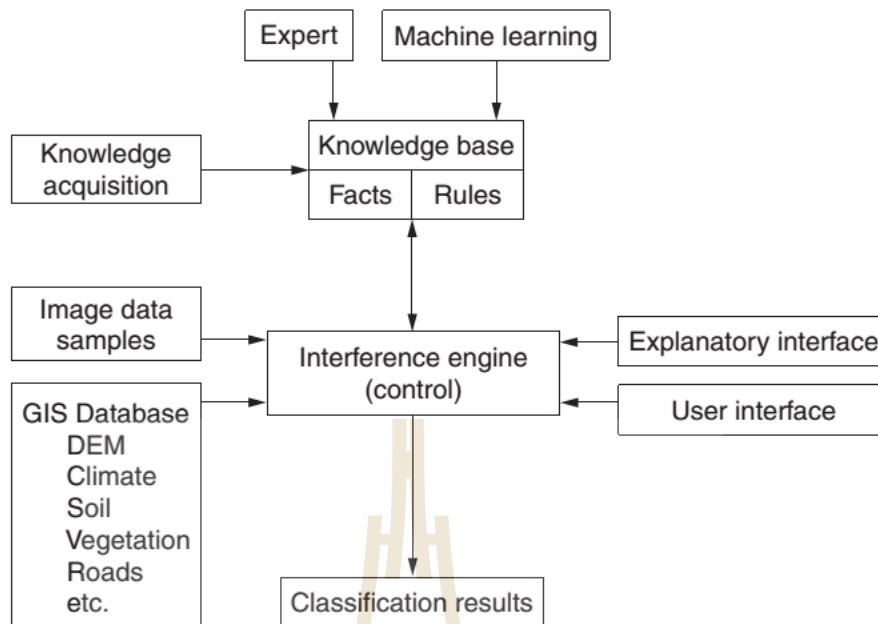


**Figure 2.5** General scheme and components of an expert system for image analysis (Gao, 2009).

**Table 2.3** Advantages and disadvantage of expert system.

Advantage	Disadvantage
<ul style="list-style-type: none"> <li>• Users can evaluate the output of the expert system and work backward to identify how a conclusion was reached.</li> <li>• Expert systems as nonmetric classification algorithm are being used such as decision trees, which make no assumption regarding the distribution of the data.</li> <li>• The decision tree can reveal nonlinear and hierarchical relationships among the input variables and use them to predict class membership.</li> <li>• A large body of evidence demonstrates the ability of machine-learning techniques (particularly decision trees and neural networks) to deal effectively with tasks that involve highly dimensional data.</li> </ul>	<ul style="list-style-type: none"> <li>• The knowledge in a traditional expert system that must be extracted from knowledgeable experts of a domain area may be subjective and incomplete.</li> <li>• Knowledge in an expert system is represented by logical rules made up of binary predicates. Numerical attributes have converted to binary true/false statements, which may cause a large amount of information to be lost in the simplification process.</li> <li>• Most rule-based expert systems fail to generalize a predictable inference if an appropriate match with the perfect rules that must be articulated by experts cannot be obtained.</li> </ul>

**Source:** Jensen, 2005.

## 2.2 Object-Based Image Analysis (OBIA)

Object-oriented classification is patches or segments by used multi-resolution image segmentation process that uses with very high-spatial-resolution imagery. An object can be defined as a grouping of pixels of similar spectral and spatial properties. Thus, applying the object-oriented paradigm to image analysis refers to analyzing the image in object space rather than in pixel space, and objects can be used as the primitives for image classification rather than pixels, which became an area of increasing research interest in the late 1990s, is a contextual segmentation and classification approach that may offer an effective method for overcoming some of the limitations inherent to traditional pixel-based classification of very high resolution (VHR) images. Particularly, the OBIA can overcome within class spectral variation inherent to VHR imagery (Yu, Gong, Clinton, Biging and Shirokauer, 2006). In addition, it can be used to emulate a human interpreter's ability in image interpretation (Blaschke and Strobl, 2001; Blaschke, 2004; Benz et al., 2004; Meinel and Neubert, 2004).

Nussbaum and Menz (2008) stated that OBIA can be compared in a first approximation with visual perception. Thus, a viewer in visual image interpretation consciously recognizes specific shapes and correlations that go beyond the pure grey values and color grades of the image. It perceives typical patterns and associates them with real objects. Apart from pure color information, these patterns result from other features such as texture, shape, size or from the relations between individual objects. A procedure similar to visual interpretation is also aimed at by OBIA in general and the eCognition software used for image analysis in particular.



Nussbaum and Menz (2008) suggested an operational workflow for OBIA using eCognition software as shown in Figure 2.6. Herewith major tasks of OBIA are consist of (a) image segmentation, (b) feature extraction and (c) semantic modelling and classification.

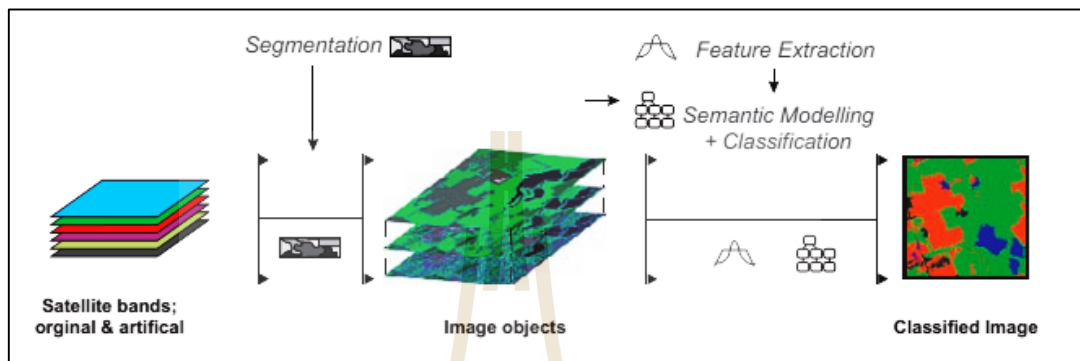


**Figure 2.6** Workflow of object-based image analysis in eCognition.

Under eCognition software, two basic classification methods of OBIA are standard nearest neighbor classifier (SNN) and nearest neighbor classifier with feature space optimization (FSO).

### 2.2.1 Standard nearest neighbor classifier

The standard nearest neighbor classifier is a supervised classification approach whereby for each of the classes require training samples and used to classify all remaining (unknown) objects in the image. The SNN has been used successfully for many classification problems (Wu, 2015). Basically, the distance in the feature space to the nearest sample object of each class is calculated for each image object. Then, the image object is assigned to the class represented by the closest sample object (Definiens, 2007).

### **2.2.2 Nearest neighbor classifier with feature space optimization**

The feature space optimization is an instrument to help you find the combination of features that is particularly suitable for separating classes in conjunction with the SNN. Basically, the feature space optimization compares the samples for selected classes with respect to the features. As a result it finds the combination of features that produces the largest average minimum distance between the samples of the different classes (Definiens, 2007).

To refine the classification further, eCognition software offers an automated feature, the feature space optimization tool, to automatically identify the features which 'best' separate the classes for which samples have been selected. (Wu, 2015).

## **2.3 Literature reviews**

Matinfar, Sarmadian, Panah, and Heck (2007) had conducted comparisons of object-oriented and pixel-based classification of LULC types in arid region of Iran using Landsat 7 ETM+. In this study, land cover types of Kashan test area were analyzed using the minimum distance classification of ILWIS software for PBIA and nearest neighbor classification of eCognition software for OBIA. They concluded that the object-oriented approach gave more accurate results (including higher producer's and user's accuracy for most of the land cover classes) than those achieved by pixel-based classification algorithms.

Cleve, Kelly, Kearns, and Moritz (2008) explored the accuracy of pixel-based and object-based classification methods used for mapping in the wild land–urban interface with free, readily available and high spatial resolution urban imagery, which

was available in many places to municipal and local fire management agencies. This study was conducted in a small community in Napa County, California, USA. Herein, ISODATA (Iterative self-organizing data) of clustering technique was used for PBIA while nearest neighbor classification of eCognition software was applied for OBIA. The results indicated that an object-based classification approach provided a higher accuracy than a pixel-based classification approach when distinguishing between the selected LULC categories.

Dehvari and Heck (2009) had conducted comparisons of PBIA and OBIA classification methods in Griffin Creek, Ontario, Canada. The airborne infrared image was used to produce a map of land cover types using MLC under PBIA and SNN under OBIA. Land cover classes that obtained traditional PBIA approach showed a salt-and-pepper effect having the lowest producer accuracy (59.5%). Overall classification results increased up to 80% in OBIA but still failed to distinguish buildings and creeks. In addition, contours and DEM thematic layers enhanced classification results to a higher level (94%) and increased the producer accuracy for buildings and creek by creating reasonable objects in the segmentation process under OBIA.

Weih and Riggan (2010) had conducted a comparison of an object-based classification with supervised and unsupervised pixel-based classification. Two multi-temporal (leaf-on and leaf-off), medium-spatial resolution SPOT-5 satellite images and a high-spatial resolution color infrared digital orthophoto were used in the analysis. Combinations of these three images were merged to evaluate the relative importance of multi-temporal and multi-spatial imagery to classification accuracy. The object-based classification using all three-image datasets produced the highest overall accuracy (82.0%), while the object-based classification using the high-spatial resolution image

merged with the SPOT-5 leaf-off image had the second highest overall accuracy (78.2%). While these two object-based classifications were statistically significantly different from the other classifications. The presence of the high-spatial resolution imagery had a greater impact on improving overall accuracy than the multi-temporal dataset, especially with the object-based classifications.

Myint, Gober, Brazel, Grossman-Clarke and Weng (2011) conducted per-pixel versus object-based classification of urban land cover extraction using high spatial resolution imagery in the central business district in the city of Phoenix. They employed six different classification procedures with the object-based paradigm that separates spatially and spectrally similar pixels at different scales for various urban land cover. Herewith, classifiers to assign land covers to segmented objects used in the study included membership functions and the nearest neighbor classifier. As results, they found that the object-based classifier achieved a high overall accuracy (90.40%), whereas the most commonly used decision rule, namely maximum likelihood classifier, produced a lower overall accuracy (67.60%). They concluded that the object-based classifier is a significantly better approach than the classical per-pixel classifiers.

Whiteside, Boggs and Maier (2011) had conducted a comparison of object-based and pixel-based classifications for mapping savannas in the tropical north of the Northern Territory of Australia. The object-based approach involved segmentation of image data into objects at multiple scale levels. Objects were assigned classes using training objects and the nearest neighbor supervised and fuzzy classification algorithm. In this study, two objects-based classifications were undertaken using Definiens Developer version 7 software. The first classification was conducted using only the VNIR bands from the ASTER imagery for comparison with the per-pixel classification,

while the second classification incorporated information from the ASTER DEM. Both OBIA involved two sub-processes: (i) segmentation and (ii) classification. The supervised pixel-based classification involved the selection of training areas and a classification using the MLC algorithm. Site-specific accuracy assessment using confusion matrices of both classifications were undertaken based on 256 reference sites. A comparison of the results showed a statistically significant higher overall accuracy of the object-based classification over the pixel-based classification. The incorporation of DEM layer and associated class rules into the object-based classification produced slightly higher accuracies overall and for certain classes. The results indicated that object-based analysis has good potential for extracting land cover information from satellite imagery captured over spatially heterogeneous land covers of tropical Australia.

Duro, Franklin and Dubé (2012) had compared pixel-based and object-based image analysis approaches for classifying broad land cover classes over agricultural landscapes using three supervised machine learning algorithms: decision tree (DT), random forest (RF), and the support vector machine (SVM) in South Saskatchewan River, Saskatchewan, Canada. They found that overall classification accuracies between pixel-based and object-based classifications were not statistically significant ( $p > 0.05$ ) when the same machine learning algorithms were applied. However, there was a statistically significant difference in classification accuracy between maps produced using the DT algorithm compared to maps produced using either RF ( $p = 0.0116$ ) or SVM algorithms ( $p = 0.0067$ ) under object-based image analysis. Meanwhile, there was no statistically significant difference ( $p > 0.05$ ) between the results produced using different classification algorithms under pixel-based image analysis. Classifications

based on RF and SVM algorithms provided a more visually adequate depiction of wetland, riparian, and cropland cover types when compared to DT based classifications, using either object-based or pixel-based image analysis.

Castillejo-González, Peñna-Barragán, Jurado-Expósito, Mesas-Carrascosaa and López-Granados (2014) compared pixel- and object-based techniques for mapping wild oat weed patches in wheat fields using multi-spectral QuickBird satellite imagery for site-specific weed management. The research was conducted at two levels: (1) at the field level, on 11 and 15 individual infested wheat fields in 2006 and 2008, respectively, and (2) on a broader level, by analyzing the entire 2006 and 2008 images. To evaluate the wild oat patches mapping at the field level, both pixel and object-based image analyses were tested with six classification algorithms: Parallelepiped (P), Mahalanobis Distance (MD), Maximum Likelihood (ML), Spectral Angle Mapper (SAM), Support Vector Machine (SVM) and Decision Tree (DT). The results showed that weed patches could be accurately detected with both analyses obtaining global accuracies between 80% and 99% for most of the fields. The MD and SVM classifiers were the most accurate for both the pixel- and object-based images from 2006 and 2008, respectively. In the broad-scale analysis, all of the wheat fields were identified in the imagery using a multiresolution hierarchical segmentation based on two scales. The first segmentation scale was classified using the MD and ML algorithms to discriminate wheat fields from other land uses. Accuracies greater than 85% were obtained for MD and 88% for ML for both imagery. A hierarchical analysis was then performed with the second segmentation scale, increasing the accuracies to 93% and 91% for 2006 and 2008 imagery, respectively. Finally, based on the most accurate results obtained in the field-level study, pixel-based classifications using the MD, ML and SVM algorithms

were applied to the wheat fields identified. The results of these broad-level analyses showed that wild oat patches were accurately discriminated in all the wheat fields present in the entire images with accuracies greater than 91% for all the classifiers tested.

Powers, Hermosilla, Coops and Chen (2015) presented and assessed a geographic object-based image analysis (GEOBIA) approach with high-spatial resolution imagery (SPOT 5) to map industrial disturbances using the oil sands region of Alberta's northeastern boreal forest as a case study. Key components of this study were (i) the development of additional spectral, texture, and geometrical descriptors for characterizing image objects (groups of alike pixels) and their contextual properties, and (ii) the introduction of decision trees with boosting to perform the object-based land cover classification. Results indicated that the approach achieved an overall accuracy of 88%, and that all descriptor groups provided relevant information for the classification. Despite challenges remaining (e.g., distinguishing between spectrally similar classes, or placing discrete boundaries), the approach was able to effectively delineate and classify fine-spatial resolution industrial disturbances.

In summary, an identified data and method and results of the literature review are here again synthesized as summarized in Table 2.4. The finding shows that OBIA method can provide superior result of LULC classification than PBIA method. However, most of input data for comparisons of PBIA and OBIA classification of LULC are very high spatial resolution include aerial photographs, airborne infrared image, QuickBird, ASTER, and SPOT-5 images. In addition, size of study area are mostly small and LULC classification system are simple when they are compared with this research. Therefore, the comparison between PBIA and OBIA for LULC

classification for an optimum method of PBIA and/or OBIA from moderate spatial resolution of free-downloaded Landsat-8 is really challenge in this study.

**Table 2.4** Synthesis of literature reviews.

Author (Title)	Year	Data and method	Result
Matinfar, Sarmadian, Panah and Heck (Comparisons of Object-Oriented and Pixel-Based Classification of Land Use/Land Cover Types Based on Landsat7, ETM+ Spectral Bands (Case Study: Arid Region of Iran))	2007	- Using Landsat 7 ETM+. - Using the minimum distance classification of ILWIS software for PBIA. - Using nearest neighbor classification of eCognition software for OBIA.	The results indicate that the object-oriented approach gave more accurate results than those achieved by pixel-based classification algorithms.
Cleve, Kelly, Kearns and Moritz (Classification of the wild land–urban interface: A comparison of pixel- and object-based classifications using high-resolution aerial photography)	2008	- Using high-resolution aerial photography. - Using ISODATA (Iterative self-organizing data) of clustering technique for PBIA. - Using nearest neighbor classification of eCognition software for OBIA.	The results indicate that an object-based classification approach provides a higher accuracy than a pixel-based classification approach when distinguishing between the selected land-use and land-cover categories.
Dehvari and Heck (Comparison of object-based and pixel based infrared airborne image classification methods using DEM thematic layer)	2009	- Using airborne infrared image. - Using maximum likelihood classification for PBIA. - Using nearest neighbor classification for OBIA.	Land cover classes that obtained pixel-based approach showed a salt-and-pepper effect having the lowest producer accuracy (59.5%). Overall classification results increased up to 80% in object-based approach but still failed to distinguish buildings and creeks. Contours and DEM thematic layers enhanced classification results to a higher level (94%).



**Table 2.4** Synthesis of literature reviews (Continued).

<b>Author (Title)</b>	<b>Year</b>	<b>Data and method</b>	<b>Result</b>
Weih and Riggan (Object-based classification vs. Pixel-based classification: comparative importance of multi-resolution imagery)	2010	<ul style="list-style-type: none"> <li>- Using Two multi-temporal (leaf-on and leaf-off), medium-spatial resolution SPOT-5 satellite images and a high-spatial resolution color infrared digital orthophoto.</li> <li>- Using unsupervised classification for PBIA.</li> <li>- Using supervised classification for OBIA.</li> </ul>	The object-based classification using all three-image datasets produced the highest overall accuracy (82.0%), while the object-based classification using the high-spatial resolution image merged with the SPOT-5 leaf-off image had the second highest overall accuracy (78.2%).
Myint, Gober, Brazel, Grossman-Clarke and Weng (Per-pixel vs. Object-based classification of urban land cover extraction using high spatial resolution imagery)	2011	<ul style="list-style-type: none"> <li>- Using QuickBird image data.</li> <li>- Using the decision rule and maximum likelihood classifier for PBIA.</li> <li>- Using membership functions and the nearest neighbor classifier for OBIA.</li> </ul>	The results indicate that the object-based classifier is a significantly better approach than the classical per-pixel classifiers.
Whiteside, Boggs and Maier (Comparing object-based and pixel-based classifications for mapping savannas)	2011	<ul style="list-style-type: none"> <li>- Using the ASTER imagery.</li> <li>- Using the maximum likelihood classifier algorithm for PBIA.</li> <li>- Using the nearest neighbor supervised and fuzzy classification algorithms for OBIA.</li> </ul>	The results indicated that object-based analysis has good potential for extracting land cover information from satellite imagery captured over spatially heterogeneous land covers of tropical Australia.
Duro, Franklin and Dubé (A comparison of pixel-based and object-based image analysis with selected machine learning algorithms for the classification of agricultural landscapes using SPOT-5 HRG imagery)	2012	<ul style="list-style-type: none"> <li>- Using SPOT-5 HRG imagery</li> <li>- Using three supervised machine learning algorithms: decision tree (DT), random forest (RF), and the support vector machine (SVM) for PBIA and OBIA.</li> </ul>	The results indicated that overall classification accuracies between pixel-based and object-based classifications were not statistically significant ( $p > 0.05$ ) when the same machine learning algorithms were applied.

**Table 2.4** Synthesis of literature reviews (Continued).

Author (Title)	Year	Data and method	Result
Castillejo-González, Peña-Barragán, Jurado-Expósito, Mesas-Carrascosaa and López-Granados (Evaluation of pixel- and object-based approaches for mapping wild oat ( <i>Avena sterilis</i> ) weed patches in wheat fields using QuickBird imagery for site-specific management)	2014	<ul style="list-style-type: none"> <li>- Using multi-spectral QuickBird satellite imagery.</li> <li>- Using six classification algorithms: Parallelepiped (P), Mahalanobis Distance (MD), Maximum Likelihood (ML), Spectral Angle Mapper (SAM), Support Vector Machine (SVM) and Decision Tree (DT) for PBI and OBI.</li> </ul>	The results of these broad-level analyses showed that wild oat patches were accurately discriminated in all the wheat fields present in the entire images with accuracies greater than 91% for all the classifiers tested.
Powers, Hermosilla, Coops and Chen (Remote sensing and object-based techniques for mapping fine-scale industrial disturbances)	2015	<ul style="list-style-type: none"> <li>- Using high-spatial resolution imagery (SPOT 5).</li> <li>- Using geographic object-based image analysis (GEOBIA).</li> </ul>	Results indicated that the approach achieved an overall accuracy of 88%, and that all descriptor groups provided relevant information for the classification. Despite challenges remaining, the approach was able to effectively delineate and classify fine-spatial resolution industrial disturbances.

## **CHAPTER III**

### **RESEARCH METHODOLOGY**

The research methodology framework consists of three major components include (1) data collection and preparation (2) LULC classification under PBIA and OBIA and (3) thematic LULC accuracy assessment and the best practical method for LULC classification under PBIA and OBIA (Figure 3.1). Details of each component with major tasks are separately described in the following sections.

#### **3.1 Data collection and preparation**

Landsat 8, Path 128 Row 50, acquired date 15 December 2015 was collected by downloading from USGS website ([www.earthexplorer.usgs.gov](http://www.earthexplorer.usgs.gov)). The Landsat 8 satellite images have every 16 days of the entire Earth. Landsat 8 data products are all standard Level-1 product with terrain correction (USGS, 2015) and its specifications is summarized in Table 3.1. Landsat 8 measures different ranges of frequencies along the electromagnetic spectrum with 11 bands as shown in Table 3.2 and Figure 3.2.

After that Landsat 8 data were processed pan-sharpening image to increase spatial and spectral resolutions of image using the selected methods include (1) MIHS, (2) WT, (3) HPF, (4) EF, and (5) GS. The derived results were then identified an optimum pan-sharpening image for LULC classification using the Universal Image Quality Index (UIQI) of Wang and Bovik (2002) as:

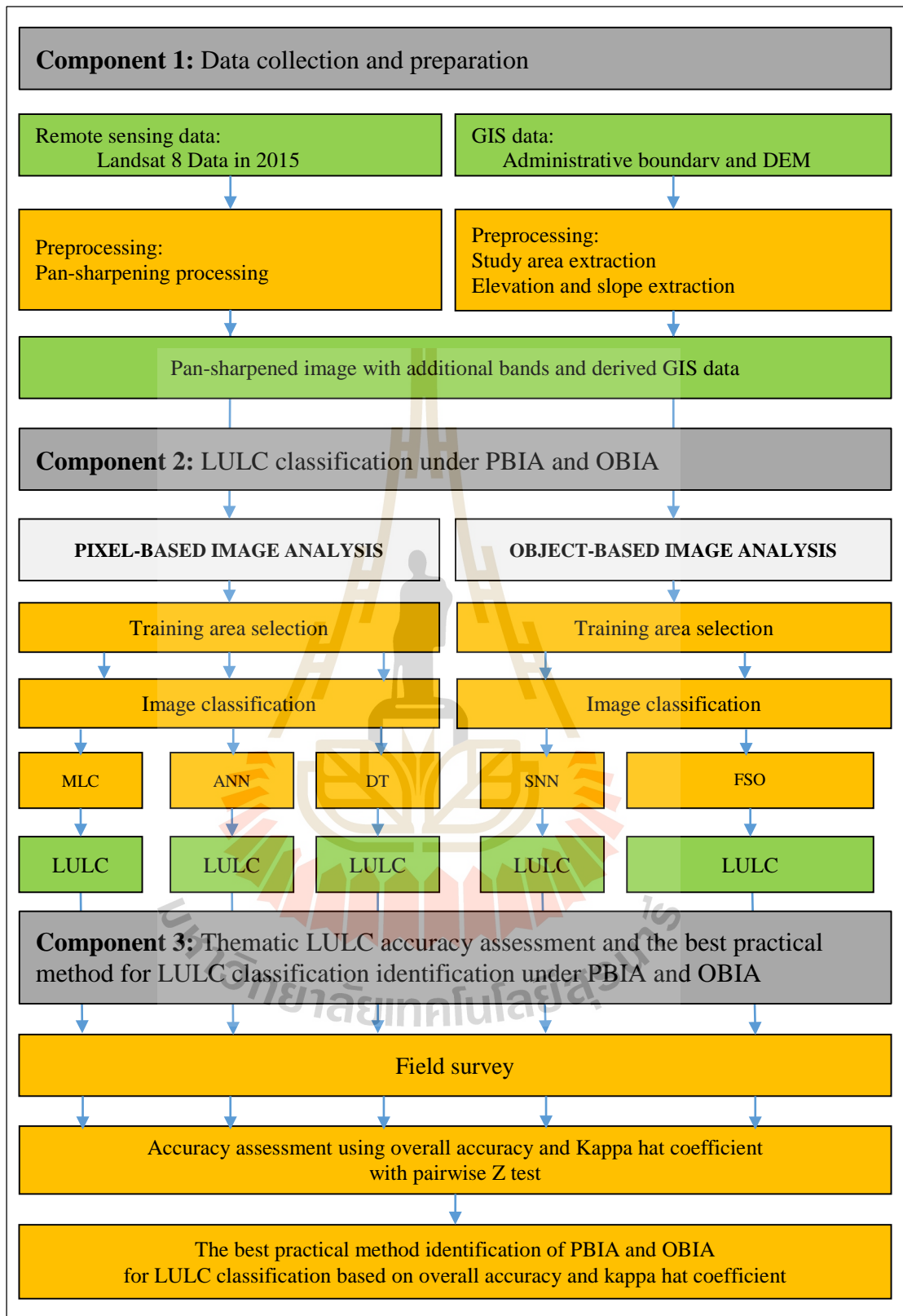


**Figure 3.1** A Workflow of research methodology framework.

$$Q = \frac{\sigma_{xy}}{\sigma_x \sigma_y} * \frac{2\bar{x}\bar{y}}{(\bar{x}^2) + (\bar{y}^2)} * \frac{2\sigma_x \sigma_y}{\sigma_x^2 + \sigma_y^2} \quad (3.1)$$

Herewith x is pixel value of original image and y is test image, where

$$\bar{x} = \frac{1}{N} \sum_{i=1}^N x_i,$$

$$\bar{y} = \frac{1}{N} \sum_{i=1}^N y_i,$$

$$\sigma_x^2 = \frac{1}{N-1} \sum_{i=1}^N (x_i - \bar{x})^2,$$

$$\sigma_y^2 = \frac{1}{N-1} \sum_{i=1}^N (y_i - \bar{y})^2,$$

$$\sigma_{xy} = \frac{1}{N-1} \sum_{i=1}^N (x_i - \bar{x})(y_i - \bar{y})$$

In addition, the derived pan-sharpened image was used to create additional spectral bands included NDVI, MNDWI and NDBI using following equations:

$$NDVI = \frac{NIR-RED}{NIR+RED} \quad (3.2)$$

$$MNDWI = \frac{GREEN-SWIR}{GREEN+SWIR} \quad (3.3)$$

$$NDBI = \frac{SWIR-NIR}{SWIR+NIR} \quad (3.4)$$

Where:

*GREEN* is Brightness value of Band 3 of Landsat-8;

*RED* is Brightness value of Band 4 of Landsat-8;

*NIR* is Brightness value of Band 5 of Landsat-8;

*SWIR* is Brightness value of Band 6 of Landsat-8.

Meanwhile GIS data consisted of administrative boundary and DEM were used to extract study area and elevation and slope, respectively.

**Table 3.1** Specification of Landsat 8 products.

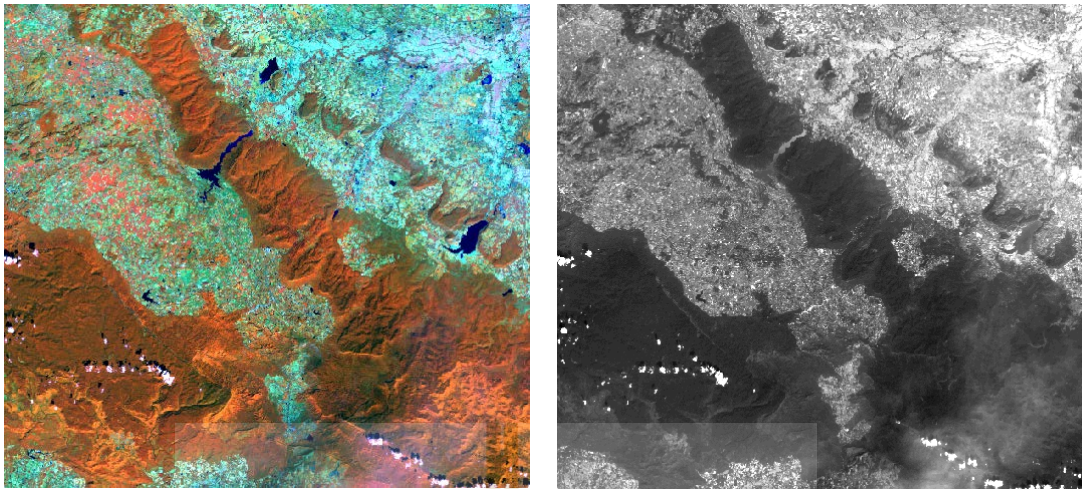
<b>Processing</b>	Level 1 T- Terrain Corrected
<b>Pixel Size</b>	OLI multispectral bands 1-7, 9: 30-meters OLI panchromatic band 8: 15-meters TIRS bands 10-11: collected at 100 meters but resampled to 30 meters to match OLI multispectral bands
<b>Data Characteristics</b>	GeoTIFF data format Cubic Convolution (CC) resampling North Up (MAP) orientation Universal Transverse Mercator (UTM) map projection (Polar Stereographic projection for scenes with a center latitude greater than or equal to -63.0 degrees) World Geodetic System (WGS) 84 datum 12 meter circular error, 90% confidence global accuracy for OLI 12 meter circular error, 90% confidence global accuracy for OLI 41 meter circular error, 90% confidence global accuracy for TIRS 16-bit pixel values
<b>Data Delivery</b>	.tar.gz compressed file via HTTP Download
<b>File size</b>	Approximately 1 GB (compressed), approximately 2 GB (uncompressed)

**Source:** USGS, www, 2015.

**Table 3.2** Sensors and number band of Landsat 8.

Sensor	Bands	Wavelength ( $\mu\text{m}$ )	Resolution (m)
Operational Land Imager (OLI)	Band 1 - Coastal aerosol	0.43 - 0.45	30
	Band 2 - Blue	0.45 - 0.51	30
	Band 3 - Green	0.53 - 0.59	30
	Band 4 - Red	0.64 - 0.67	30
	Band 5 - Near Infrared (NIR)	0.85 - 0.88	30
	Band 6 - SWIR 1	1.57 - 1.65	30
	Band 7 - SWIR 2	2.11 - 2.29	30
	Band 8 - Panchromatic	0.50 - 0.68	15
	Band 9 - Cirrus	1.36 - 1.38	30
Thermal Infrared Sensor (TIRS)	Band 10 - Thermal Infrared (TIRS) 1	10.60 - 11.19	100 * (30)
	Band 11 - Thermal Infrared (TIRS) 2	11.50 - 12.51	100 * (30)

**Source:** USGS, www, 2015.



(a) Multispectral band 2-7  
(Band 5, 6, 4: RGB)

(b) Panchromatic band 8

**Figure 3.2** Landsat 8 data acquired date 15 December 2015.

### 3.2 LULC classification under PBIA and OBIA

Representative of classification method of PBIA and OBIA were here applied to classify LULC data based on the defined training areas. Herein MLC of parametric classification method, ANN of nonparametric classification method and DT classifier of nonmetric classification method were used to classify LULC under PBIA. Meanwhile SNN classifier and NN classifier with feature space optimization were applied to classify LULC under OBIA.

In this study, the derived pan-sharpened image of Landsat-8 in 2015 (Band 2, 3, 4, 5, 6 and 7) based on optimum pan-sharpening method was here used as basic input dataset of PBIA and OBIA. Meanwhile additional bands of spectral indices and physical data were systematically assigned as additional band for LULC classification with various methods under PBIA and OBIA.

The LULC classification system, which was modified from standard land use classification system of LDD, consisted of (1) urban and built-up area, (2) paddy field,

(3) cassava, (4) maize, (5) sugarcane, (6) orchard and perennial trees, (7) forest area, (8) water bodies, and (9) miscellaneous land.

### 3.3 Thematic LULC accuracy assessment and the best practical method for LULC classification under PBIA and OBIA

The derived thematic LULC maps from five selected methods of PBIA and OBIA were assessed accuracy using overall accuracy with producer's accuracy and user's accuracy and kappa analysis by field survey in 2017 according to error matrix as shown in Table 3.3.

**Table 3.3** The error matrix.

Class	Ground reference test information				Row total	
	1	2	3	k		
Remote sensing classification	1	$n_{1,1}$	$n_{1,2}$	$n_{1,3}$	$n_{1,k}$	$n_{1+}$
	2	$n_{2,1}$	$n_{2,2}$	$n_{2,3}$	$n_{2,k}$	$n_{2+}$
	3	$n_{3,1}$	$n_{3,2}$	$n_{3,3}$	$n_{3,k}$	$n_{3+}$
	4	$n_{k,1}$	$n_{k,2}$	$n_{k,3}$	$n_{k,k}$	$n_{k+}$
Column total	$n_{+1}$	$n_{+2}$	$n_{+3}$	$n_{+k}$	$N$	

The formula for calculation of accuracy values (Congalton and Green, 1999) are as follows:

$$\text{Overall accuracy} = \frac{\sum_{i=1}^k n_{ii}}{n} \quad (3.5)$$

$$\text{Producer's accuracy } j = \frac{n_{jj}}{n_{+j}} \quad (3.6)$$

$$\text{User's accuracy } i = \frac{n_{ii}}{n_{+i}} \quad (3.7)$$

$$\text{Khat} = \frac{N \sum_{i=1}^k n_{ii} - \sum_{i=1}^k (n_{i+} \times n_{+i})}{N^2 - \sum_{i=1}^k (n_{i+} \times n_{+i})} \quad (3.8)$$



Where:

$k$  is the number of rows ( land-cover classes) in the matrix

$n_{ii}$  is the number of the observation in row  $i$  and column  $i$

$n_{i+}$  is the marginal totals for row  $i$

$n_{+i}$  is the marginal totals for column  $i$

$N$  is the total number of observations.

In this study, number of random stratified sampling points was calculated based on multinomial distribution theory (Congalton and Green, 1999) as:

$$N = \frac{B}{4b_i^2} \quad (3.9)$$

Where:

$B$  is the upper  $(\alpha/k) \times 100$  percentile of the chi square ( $\chi^2$ ) distribution with 1 degree of freedom, and

$b_i$  is the desired precision (e.g., 5%) for the class.

In addition, pairwise Z test was examined to identify the significant different of accuracy based on kappa hat coefficient values among various methods (Congalton and Green, 2009) as:

$$Z = \frac{|Khat_1 - Khat_2|}{\sqrt{\widehat{var}(Khat_1) + \widehat{var}(Khat_2)}} \quad (3.10)$$

and variance of KHAT is calculated by:

$$\widehat{var}(\widehat{K}) = \frac{1}{n} \left\{ \frac{\theta_1(1-\theta_1)}{(1-\theta_2)^2} + \frac{2(1-\theta_1)(2\theta_1\theta_2-\theta_3)}{(1-\theta_2)^3} + \frac{(1-\theta_1)^2(\theta_4-4\theta_2)^2}{(1-\theta_2)^4} \right\} \quad (3.11)$$

When:

$$\theta_1 = \frac{1}{n^2} \sum_{i=1}^k n_{ii}$$

$$\theta_2 = \frac{1}{n^2} \sum_{i=1}^k n_{i+} n_{+i}$$

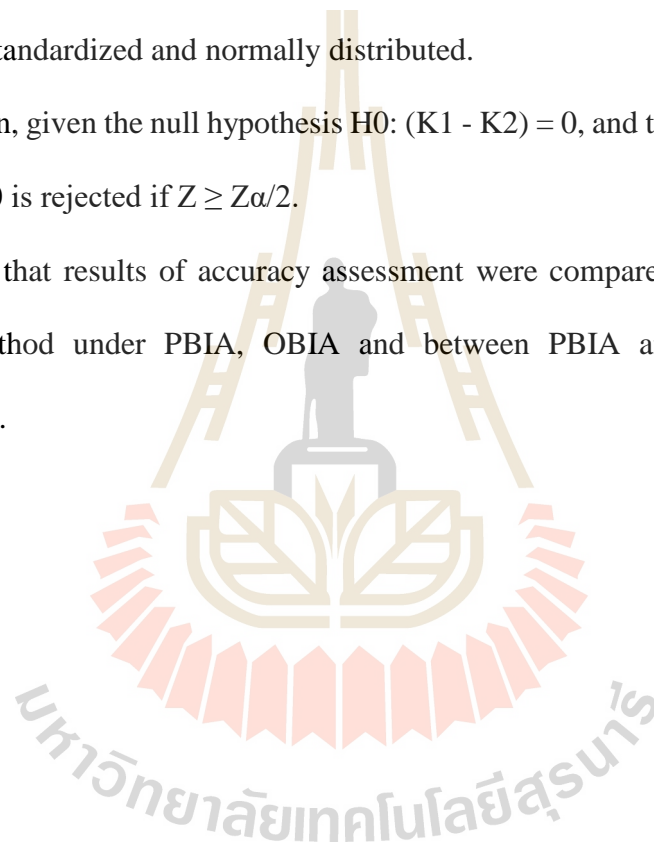
$$\theta_3 = \frac{1}{n^2} \sum_{i=1}^k n_{ii} (n_{i+} n_{+i})$$

$$\theta_4 = \frac{1}{n^3} \sum_{i=1}^k \sum_{j=1}^k n_{ij} (n_{j+} n_{+i})^2$$

Z is standardized and normally distributed.

Herein, given the null hypothesis  $H_0: (K1 - K2) = 0$ , and the alternative  $H_1: (K1 - K2) \neq 0$ ,  $H_0$  is rejected if  $Z \geq Z_{\alpha/2}$ .

After that results of accuracy assessment were compared to identify the best practical method under PBIA, OBIA and between PBIA and OBIA for LULC classification.



# **CHAPTER IV**

## **PREPROCESSING OF REMOTE SENSING**

### **AND GIS DATA**

Results of six major tasks of preprocessing of remote sensing data for PBIA and OBIA including (1) pan-sharpening processing, (2) optimum pan-sharpening method identification using UIQI, (3) Additional spectral band generation, (4) elevation and slope extraction, and (5) preparation of image dataset for PBIA and OBIA are described and discussed in this chapter.

#### **4.1 Pan-sharpening processing**

Landsat 8 data (multispectral and panchromatic bands) acquiring in 2015 were applied to process pan-sharpening image using the selected methods including (1) MIHS, (2) WT, (3) HPF, (4) EF, and (5) GS for PBIA and OBIA and its result is displayed as color composite image in Figures 4.1 to 4.5, respectively. The basic statistical data of six pan-sharpened image is summarized in Tables 4.1 to 4.5.

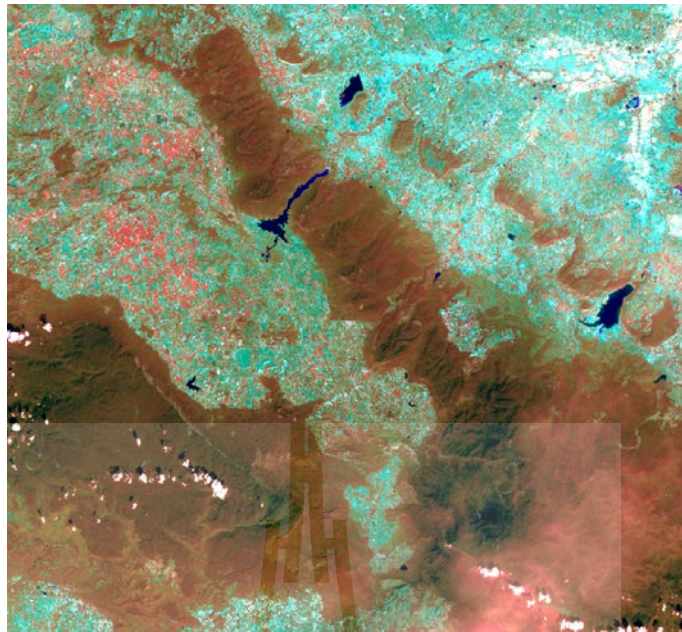


**Figure 4.1** False color composite image of pan-sharpened image of modified IHS transformation: Band 5, 6 and 4 (RGB).

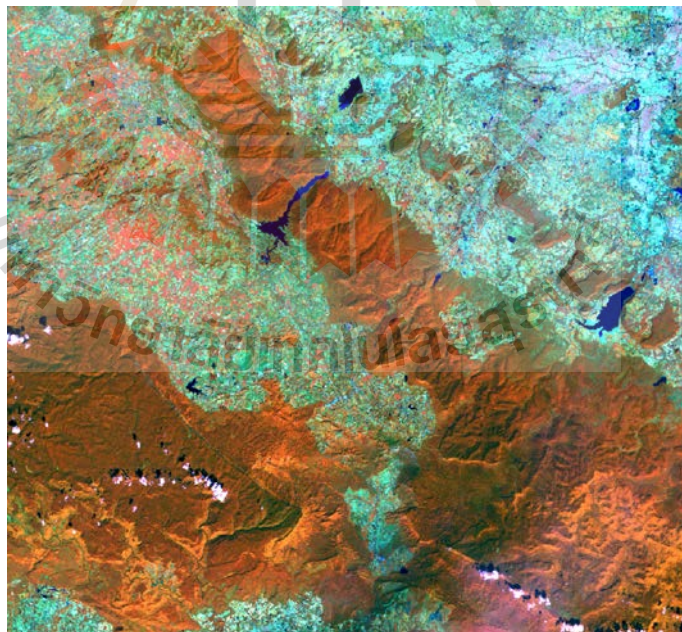


**Figure 4.2** False color composite image of pan-sharpened image of wavelet fusion: Band 5, 6 and 4 (RGB).

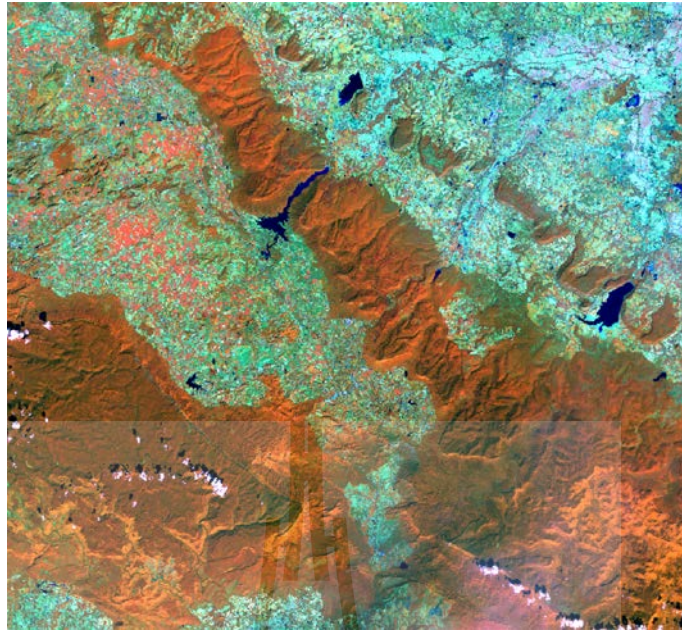


**Figure 4.3** False color composite image of pan-sharpened image of high pass filtering: Band 5, 6 and 4 (RGB).

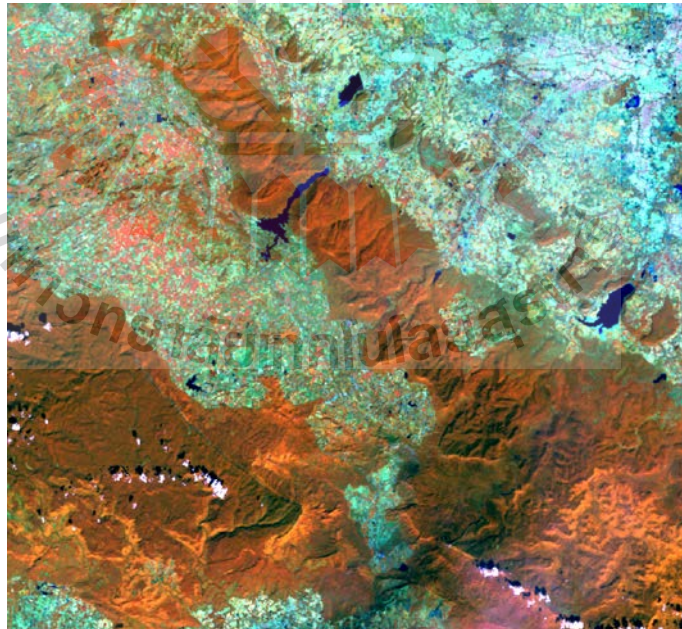


**Figure 4.4** False color composite image of pan-sharpened image of Ehlers fusion: Band 5, 6 and 4 (RGB).

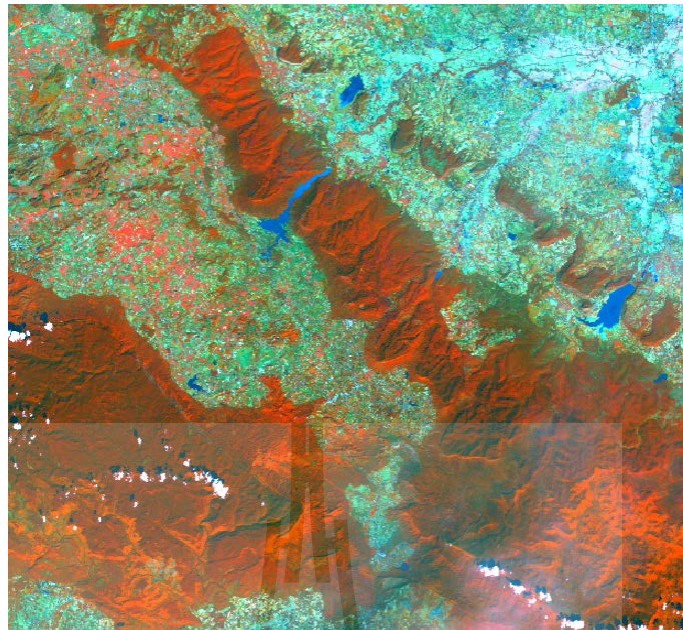


**Figure 4.5** False color composite image of pan-sharpened image of Gram-Schmidt pan-sharpening: Band 5, 6 and 4 (RGB).

**Table 4.1** Basic statistical data of pan-sharpened image with MIHS.

	Minimum	Maximum	Mean	Std. Deviation	Variance
<b>Band 2</b>	0	254	9.011	5.97	35.68
<b>Band 3</b>	0	254	12.352	6.99	48.85
<b>Band 4</b>	0	254	12.878	9.63	92.72
<b>Band 5</b>	0	255	62.230	11.58	134.17
<b>Band 6</b>	0	255	52.594	22.40	501.67
<b>Band 7</b>	0	145	18.536	12.12	146.77

**Table 4.2** Basic statistical data of pan-sharpened image with WT.

	Minimum	Maximum	Mean	Std. Deviation	Variance
<b>Band 2</b>	0	252	8.447	6.07	36.88
<b>Band 3</b>	0	251	11.835	77.13	5948.27
<b>Band 4</b>	0	250	12.244	9.84	96.88
<b>Band 5</b>	0	253	62.352	12.48	155.75
<b>Band 6</b>	0	254	51.377	21.76	473.28
<b>Band 7</b>	0	255	17.510	12.09	146.05

**Table 4.3** Basic statistical data of pan-sharpened image with HPF.

	Minimum	Maximum	Mean	Std. Deviation	Variance
<b>Band 2</b>	0	252	8.630	6.04	36.51
<b>Band 3</b>	0	253	12.061	7.09	50.31
<b>Band 4</b>	0	255	12.570	9.81	96.16
<b>Band 5</b>	0	255	62.484	12.52	156.63
<b>Band 6</b>	0	255	52.141	21.77	473.72
<b>Band 7</b>	0	237	17.960	12.06	145.35

**Table 4.4** Basic statistical data of pan-sharpened image with EF.

	Minimum	Maximum	Mean	Std. Deviation	Variance
<b>Band 2</b>	0	255	8.272	6.16	37.88
<b>Band 3</b>	0	254	11.546	7.24	52.45
<b>Band 4</b>	0	254	12.115	9.91	98.17
<b>Band 5</b>	0	255	61.879	12.34	152.15
<b>Band 6</b>	0	255	51.826	21.99	483.34
<b>Band 7</b>	0	229	24.184	16.18	261.73

**Table 4.5** Basic statistical data of pan-sharpened image with GS.

	Minimum	Maximum	Mean	Std. Deviation	Variance
<b>Band 2</b>	0	255	9.129	6.92	47.89
<b>Band 3</b>	0	255	12.556	8.03	64.40
<b>Band 4</b>	0	255	13.080	10.92	119.25
<b>Band 5</b>	8	255	62.989	11.59	134.24
<b>Band 6</b>	0	255	52.627	20.64	425.97
<b>Band 7</b>	0	245	18.430	12.10	146.43

## 4.2 Optimum pan-sharpening method identification using UIQI

The UIQI of Wang and Bovik (2002) was here applied to identify the optimum pan-sharpening method using Eq. 3.1 as mentioned Chapter III. In fact the domain value of UIQI varies between 0 and 1. In this study, UIQI were calculated using Model Builder module under ERDAS Imagine software as shown in Figure 4.6.

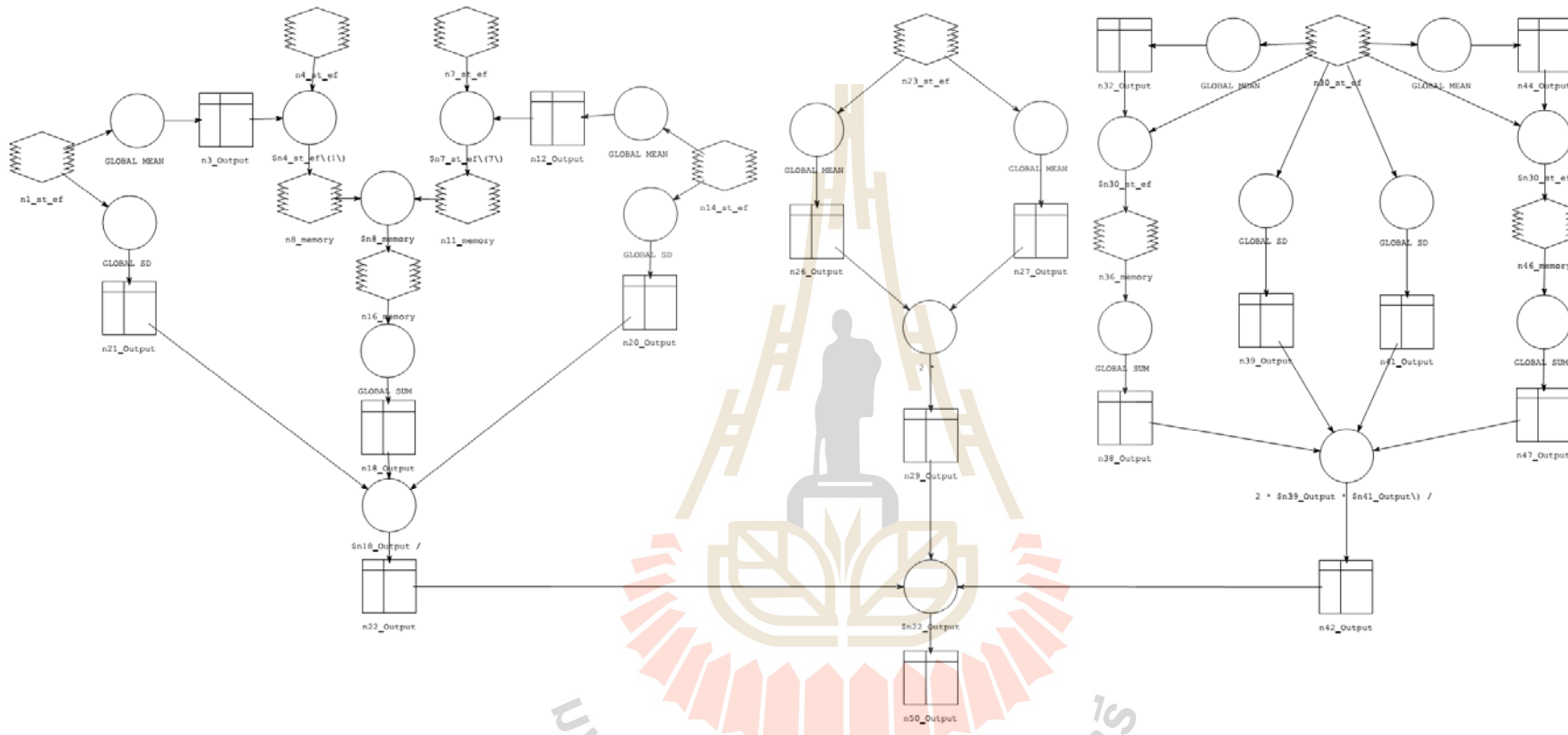


**Figure 4.6** Universal Image Quality Index Model.



The average value of UIQI of the pan-sharpened images of Landsat 8 data in 2015 is presented in Table 4.6. It reveals that WT method shows the best result with value of 0.95904 and followed by HPF, EF, GS and MIHST with value of 0.95090, 0.93230, 0.89788 and 0.87619, respectively. In general, it can be assumed that WT method provides the best results of spectral authenticity. However, due to its poor performance in the visual test, this method is not be taken into consideration for PBI and OBI. The HPF represents a good alternative for the sharpening of Landsat 8 data in this study. In the quality estimate given above, the average UIQI value of this method is only about 0.00814 lower than the WT method. Moreover, the HPF method makes the sharpest optical impression. It is also decisive that the edges of LULC classes are retained thus making it easier to identify them as separate objects (Figure 4.7). Consequently, the pan-sharpened Landsat 8 satellite images by HPF is here selected as the data basis for PBI and OBI.

**Table 4.6** Comparison of the image quality from different pan-sharpening methods for Landsat 8 data of 2015 based on average UIQI value.

Band	Q and Q-average of various pan-sharpening methods				
	MIHS	WT	HPF	EF	GS
2	0.95543	0.96325	0.95778	0.95606	0.92171
3	0.94582	0.95670	0.95632	0.94784	0.90828
4	0.96401	0.94954	0.95443	0.96363	0.90203
5	0.55387	0.99737	0.93639	0.86368	0.89708
6	0.89358	0.94328	0.95019	0.95861	0.87532
7	0.94440	0.94410	0.95029	0.90399	0.88285
<b>Sum</b>	<b>5.25711</b>	<b>5.75424</b>	<b>5.70541</b>	<b>5.59381</b>	<b>5.38727</b>
<b>UIQI-average</b>	<b>0.87619</b>	<b>0.95904</b>	<b>0.95090</b>	<b>0.93230</b>	<b>0.89788</b>
<b>Ranking</b>	<b>5</b>	<b>1</b>	<b>2</b>	<b>3</b>	<b>4</b>

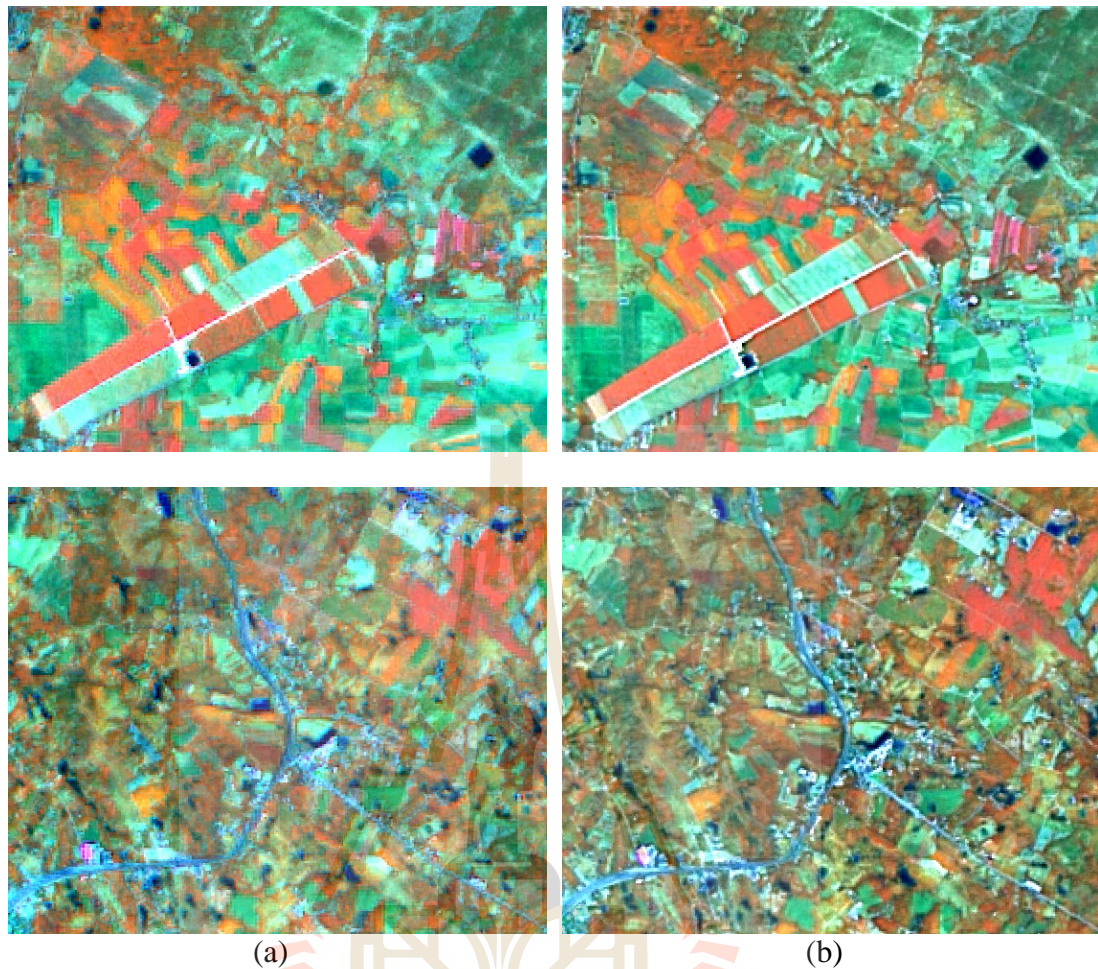


**Figure 4.7** Comparison of color composite of pan-sharpened image (Band 5, 6, 4: RGB) for visual test: (a) WT and (b) HPF methods.

### 4.3 Additional spectral band generation

The derived pan-sharpened image of Landsat 8 was used to generate additional spectral bands for LULC classification included NDVI, MNDWI and NDBI as results shown in Figures 4.8 to 4.10, respectively.

As a result, NDVI that was generated using Eq. 3.2 and it can be assumed that vegetation areas have high NDVI values and appears as bright gray tones in the image. In contrast, MNDWI that was generated using Eq. 3.3 represents degree of water

availability. Meanwhile, NDBI that was generated using Eq. 3.4 represents urban and built-up features.

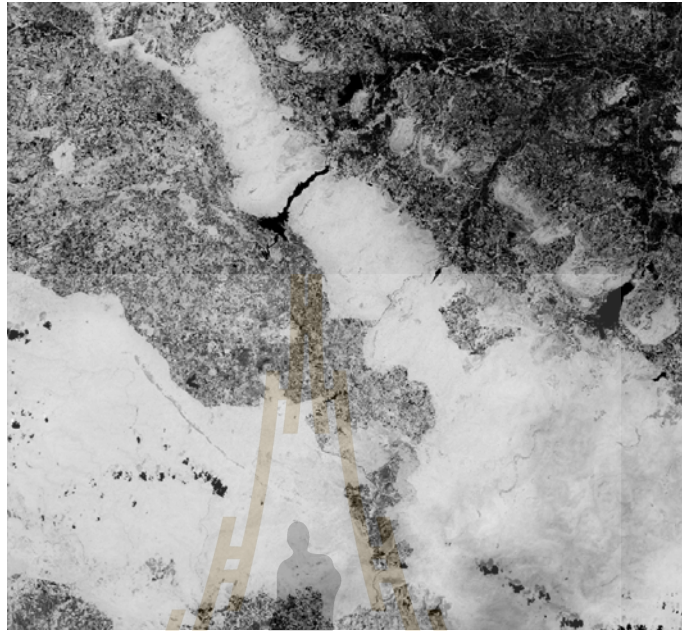


**Figure 4.8** Normalized Difference Vegetation Index (NDVI) image.

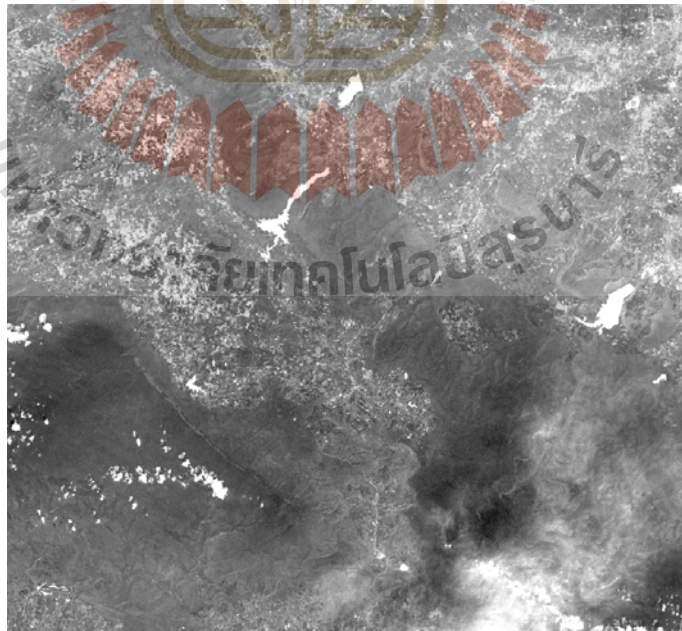


**Figure 4.9** Modified Normalized Difference Water Index (MNDWI) image.

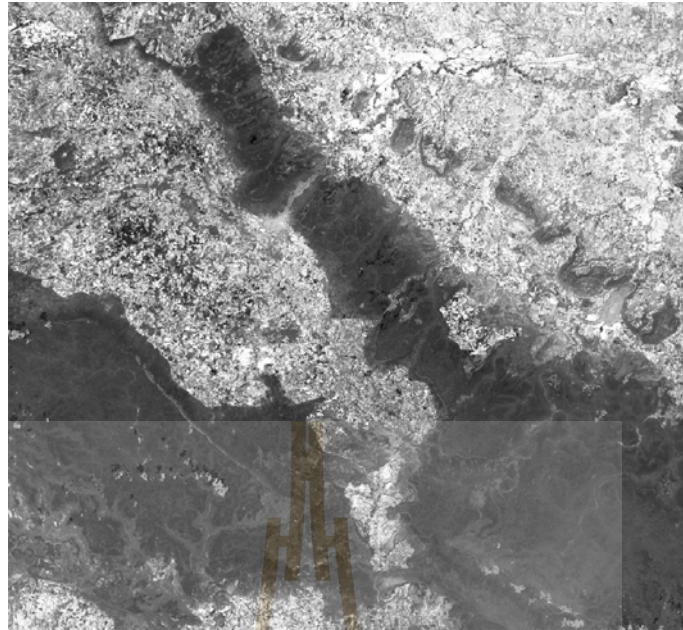


**Figure 4.10** Normalized Difference Built-up Index (NDBI) image.

#### **4.4 Elevation and slope extraction**

Elevation and slope data that represents physical factor on distribution of LULC classes were here extracted from DEM of STRM 1 arc-second from earthexplorer.usgs.gov website with cell size of 15 x 15 m as results shown in Figure 4.11 and Figure 4.12, respectively. The extracted elevation and slope were here further reclassify as thematic classes based on standard classification of LDD (2009) as shown in Figures 4.13 to 4.14, respectively. Area and percentage of elevation and slope in the study area is summarized in Tables 4.7 to 4.8, respectively.

As results, it reveals that most of the study area situates between 350 and 750 m above mean sea level and covers area of 828.96 km<sup>2</sup> or 78.63% of the total area. The top three dominant topography of the study area are undulation, rolling and slightly undulating and cover area of 331.13 km<sup>2</sup>, 204.96 km<sup>2</sup> and 199.10 km<sup>2</sup> or 31.41%, 19.44%, and 18.88% of the total area.

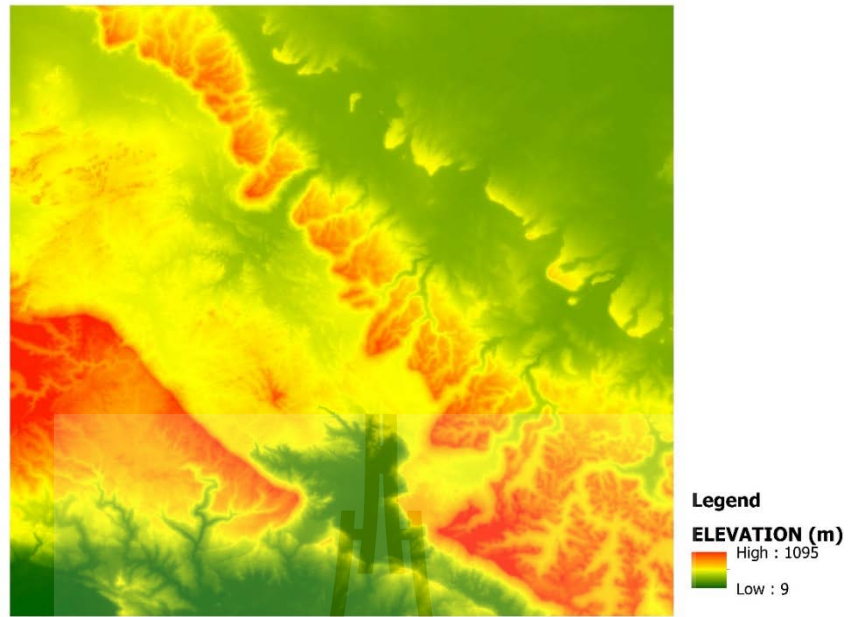


Figure 4.11 Elevation data.

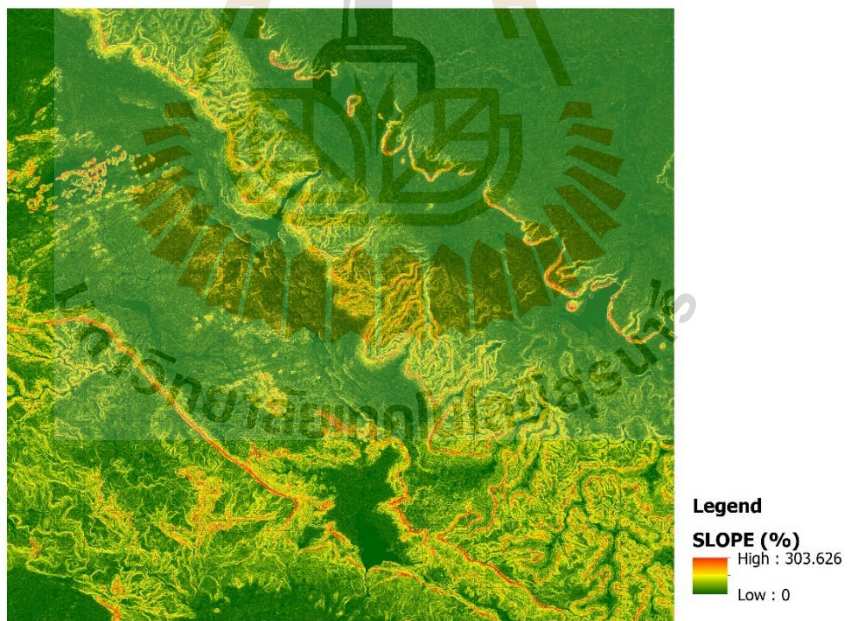
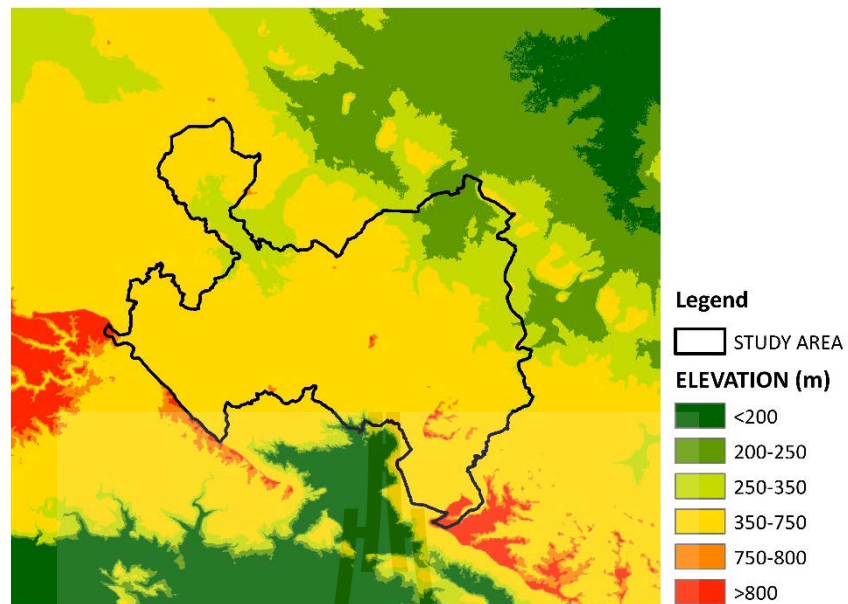
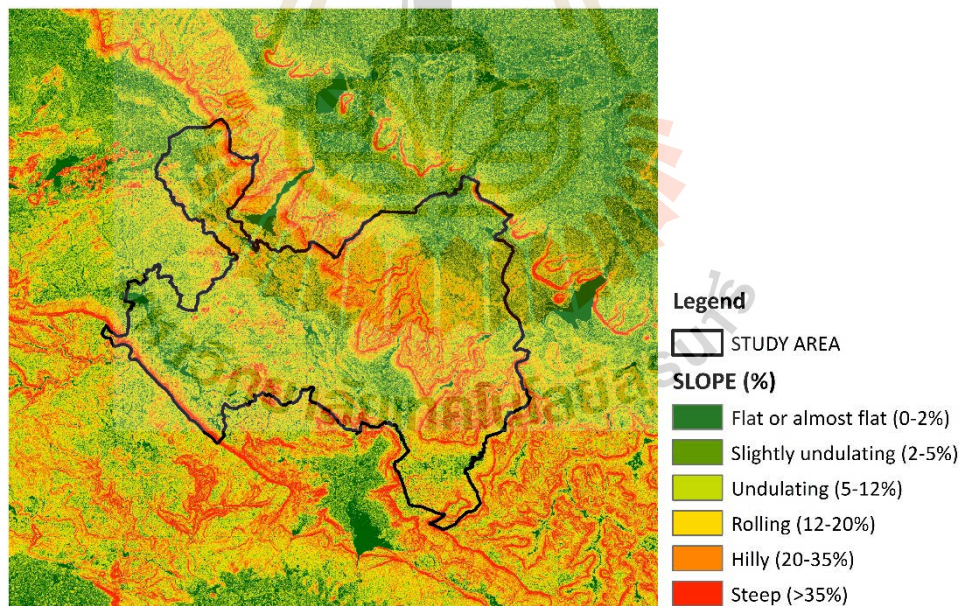


Figure 4.12 Slope data.



**Figure 4.13** Distribution of elevation classification.



**Figure 4.14** Distribution of slope classification.

**Table 4.7** Area and percentage of elevation classification in the study area.

No	Elevation (m)	Area (sq. km)	Percentage
1	< 200	1.00	0.09
2	200-250	51.78	4.91
3	250-350	152.93	14.51
4	350-750	828.96	78.63
5	750-800	9.80	0.93
6	> 800	9.83	0.93
<b>Total</b>		<b>1,054.30</b>	<b>100.00</b>

**Table 4.8** Area and percentage of slope classification in the study area.

No	Slope (%)	Topography	Area (sq. km)	Percentage
1	0-2	Flat or almost flat	94.27	8.94
2	2-5	Slightly undulating	199.10	18.88
3	5-12	Undulating	331.13	31.41
4	12-20	Rolling	204.96	19.44
5	20-35	Hilly	158.72	15.05
6	>35	Steep	66.12	6.27
<b>Total</b>			<b>1,054.30</b>	<b>100.00</b>

#### 4.5 Preparation of image dataset for PBIA and OBIA

The derived pan-sharpened image of Landsat-8 in 2015 (Band 2, 3, 4, 5, 6 and 7) based on HPF method were here used as basic input dataset of PBIA and OBIA. Meanwhile spectral indices (NDVI, MNDWI and NDBI) and physical data (elevation and slope) were systematically assigned as additional bands for LULC classification with various classification methods of PBIA and OBIA datasets as follows:

#### 4.5.1 Dataset of PBIA

For MLC classification of parametric approach and ANN classification of nonparametric approach under PBIA, two datasets were assigned for LULC classification included:

(1) Six bands of pan-sharpened Landsat-8 images (Band 2, 3, 4, 5, 6 and 7), and

(2) Nine bands of six pan-sharpened Landsat-8 images (Band 2, 3, 4, 5, 6 and 7) and three spectral index bands (NDVI, MNDWI and NDBI).

In case of ANN classification, two datasets of six and nine bands were also applied to examine the performance of learning rate of ANN at 0.1 and 0.2 for LULC classification.

Meanwhile, for DT classification of nonmetric approach under PBIA, three datasets were applied for LULC classification included:

(1) Six bands of pan-sharpened Landsat-8 images (Band 2, 3, 4, 5, 6 and 7);

(2) Nine bands of six pan-sharpened Landsat-8 images (Band 2, 3, 4, 5, 6 and 7) and three spectral index bands (NDVI, MNDWI and NDBI); and

(3) Eleven bands of six pan-sharpened Landsat-8 images (Band 2, 3, 4, 5, 6 and 7), three spectral index bands (NDVI, MNDWI and NDBI) and two physical bands (elevation and slope).



#### 4.5.2 Dataset of OBIA

Like DT classification under PBIA, three datasets of pan-sharpened Landsat-8 images and additional bands included: (1) six bands of pan-sharpened Landsat-8 images (Band 2, 3, 4, 5, 6 and 7); (2) nine bands of six pan-sharpened Landsat-8 images (Band 2, 3, 4, 5, 6 and 7) and three spectral index bands (NDVI, MNDWI and NDBI); and (3) eleven bands of six pan-sharpened Landsat-8 images (Band 2, 3, 4, 5, 6 and 7), three spectral index bands (NDVI, MNDWI and NDBI) and two physical bands (elevation and slope) were applied for LULC classification with SNN.

Meanwhile, six bands of pan-sharpened Landsat-8 images (Band 2, 3, 4, 5, 6 and 7) were used as basic data for feature selection under FSO with 5 combinations as follows:

- (1) Brightness, Mean value of Band 2-7, and Max. Diff.;
- (2) Brightness, Mean value of Band 2-7, Max. Diff., and Standard deviation of Band 2-7;
- (3) Brightness, Mean value of Band 2-7, Max. Diff., Standard deviation of Band 2-7, and Ratio of Band 2-7;
- (4) Brightness, Mean value of Band 2-7, Max. Diff., Standard deviation of Band 2-7, Ratio of Band 2-7, NDVI, MNDWI, and NDBI;
- (5) Brightness, Mean value of Band 2-7, Max. Diff., Standard deviation of Band 2-7, Ratio of Band 2-7, NDVI, MNDWI, NDBI, and gray level co-occurrence matrices (GLCM) of texture data (angular second moment, contrast, correlation, entropy and homogeneity).

## **CHAPTER V**

### **PIXEL-BASED IMAGE ANALYSIS**

Results of the representative parametric classification method: maximum likelihood classifier (MLC), nonparametric classification method: artificial neural network (ANN), and nonmetric: decision tree classification (DT) under pixel-based image analysis (PBIA) are here reported and discussed under this chapter.

#### **5.1 LULC classification of MLC**

Two datasets of pan-sharpened Landsat-8 and additional layers included (1) six bands of pan-sharpened Landsat-8 (Band 2, 3, 4, 5, 6 and 7) and (2) nine bands of six original pan-sharpened Landsat-8 images (Band 2, 3, 4, 5, 6 and 7) and three spectral index bands (NDVI, MNDWI and NDBI) were here applied to extract LULC based on the common training areas in the study area under ERDAS Imagine software. Figure 5.1 displays examples of training areas of LULC classes including (a) urban and built-up area, (b) paddy field, (c) cassava, (d) maize, (e) sugarcane, (f) orchard and perennial trees, (g) forest area, (h) water bodies and (i) miscellaneous land. Result of both datasets are separately described and discussed in the following sections.

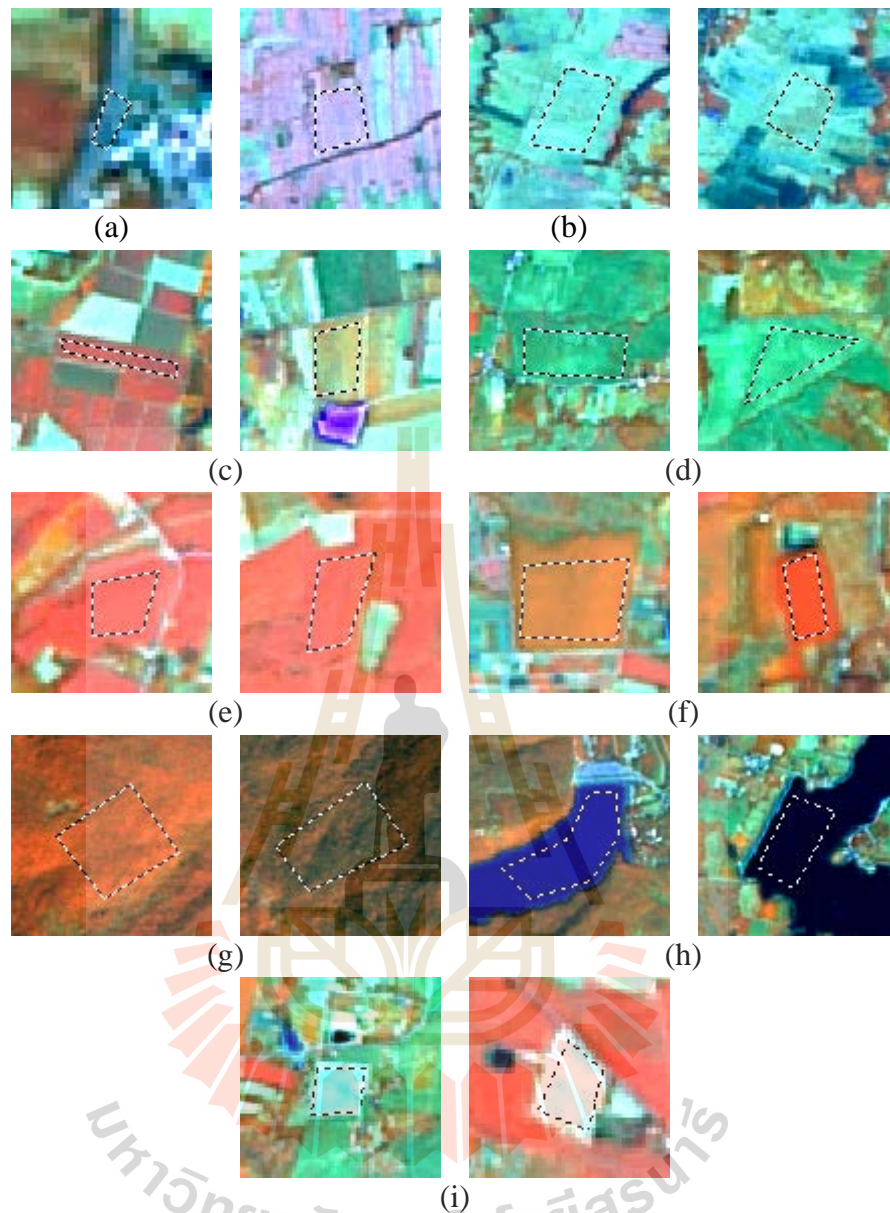


**Figure 5.1** Examples of training areas of 9 LULC classes for MLC: (a) urban and built-up area, (b) paddy field, (c) cassava, (d) maize, (e) sugarcane, (f) orchard and perennial trees, (g) forest area, (h) water bodies and (i) miscellaneous land.

### 5.1.1 LULC classification of MLC with six bands

The result of LULC classification using MLC with six multispectral bands of pan-sharpened image of Landsat-8 is summarized in Table 5.1 and distribution of LULC data is displayed in Figure 5.2.

**Table 5.1** Area and percentage of final LULC classification of MLC with 6 bands.

No.	LULC class	Area in sq.km	Percent
1	Urban and built-up area	35.88	3.40
2	Paddy field	22.74	2.16
3	Cassava	128.02	12.14
4	Maize	182.54	17.31
5	Sugarcane	8.02	0.76
6	Orchard and perennial trees	37.84	3.59
7	Forest area	590.34	55.99
8	Water bodies	1.30	0.12
9	Miscellaneous land	47.61	4.52
<b>Total</b>		<b>1,054.30</b>	<b>100.00</b>

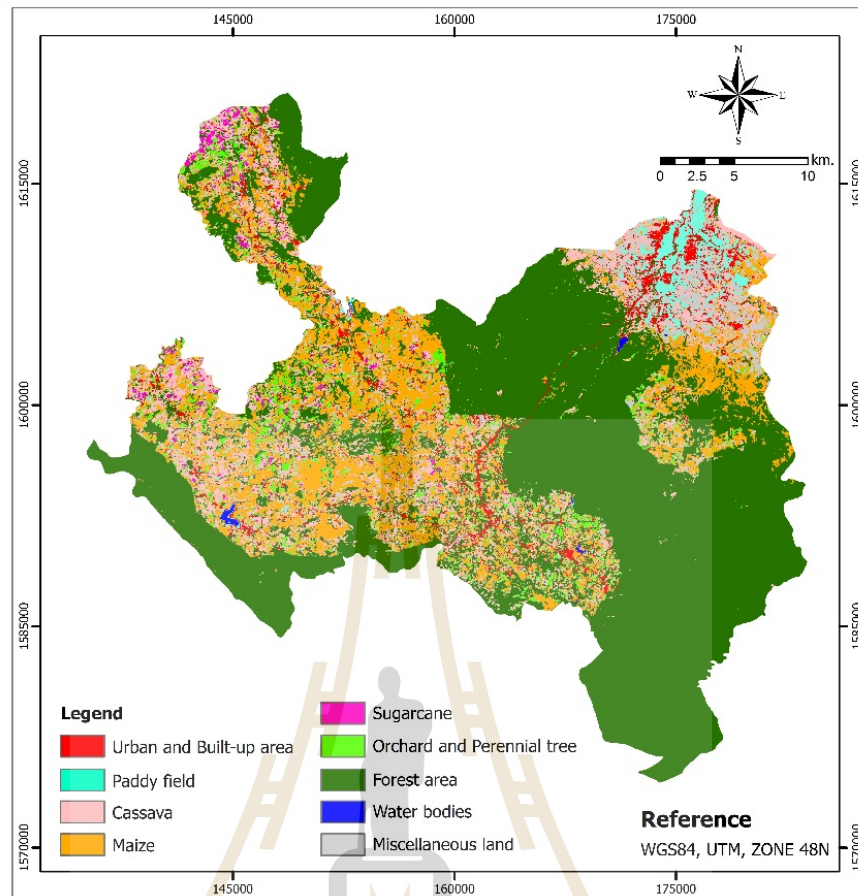


**Figure 5.2** LULC classification of 2015 of maximum likelihood classifier with 6 bands.

As results, top three dominant LULC classes in the study area are forest area, maize, and cassava and cover area of 590.34 km<sup>2</sup>, 182.54 km<sup>2</sup> and 128.02 km<sup>2</sup> or 55.99%, 17.31% and 12.14% of the total study area, respectively.

In addition, the classified LULC map was further performed accuracy assessment using 193 sample points with stratified random sampling by field survey in 2017 (Figure 5.3). Error matrix form for LULC accuracy assessment is displayed in Table 5.2. It reveals that overall accuracy is 82.90% and Kappa hat coefficient is 78.00%. Meanwhile producer's accuracy of LULC classes varies between 37.50% for orchard and perennial trees and 100.00% for paddy field and maize while user's

accuracy of LULC classes varies between 27.27% for orchard and perennial trees and 100.00% for water bodies. Based on Fitzpatrick-Lins (1981), Kappa hat coefficient between 40-80% represents moderate agreement or accuracy between the predicted map and the reference map.

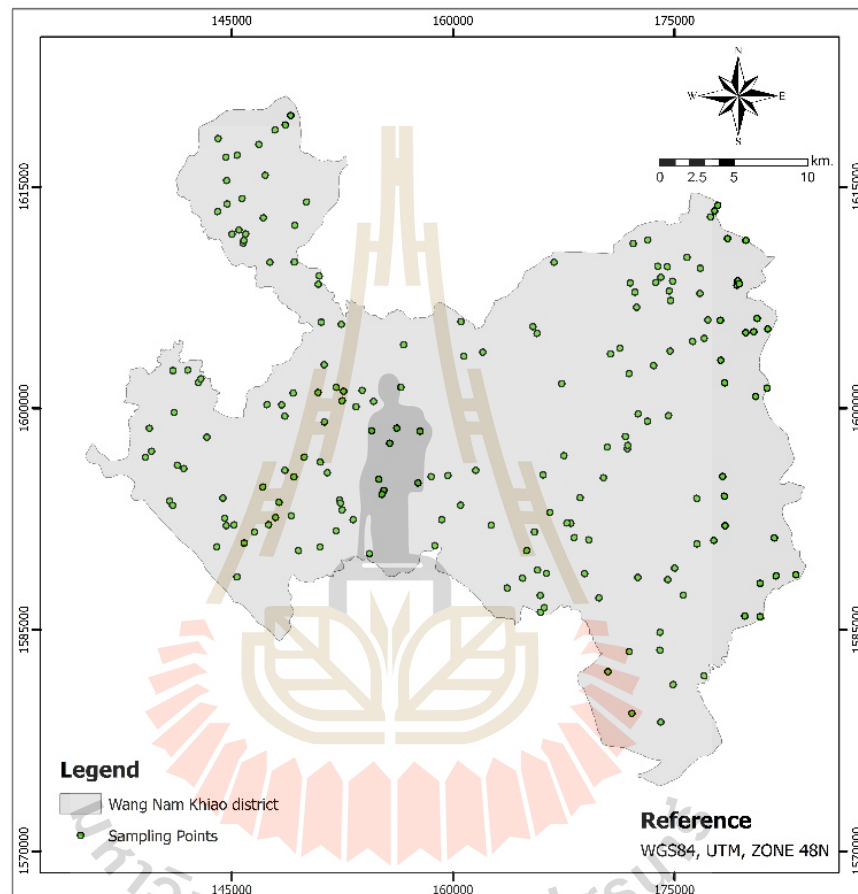


**Figure 5.3** Distribution of 193 sampling points for accuracy assessment.

**Table 5.2** Error matrix and accuracy assessment of LULC classification of MLC with 6 bands.

Classified LULC class	Reference data									Row Total
	UB	PD	CV	MA	SU	OP	FA	WB	ML	
Urban and built-up area (UB)	7		1							8
Paddy field (PD)		5						5	2	12
Cassava (CV)			5		3	1	1			10
Maize (MA)				20			1		4	25
Sugarcane (SU)			1		10	1				12
Orchard and perennial trees (OP)			4		4	3				11
Forest area (FA)						3	75			78
Water bodies (WB)								4		4
Miscellaneous land (ML)	1							1	31	33
<b>Column Total</b>	<b>8</b>	<b>5</b>	<b>11</b>	<b>20</b>	<b>17</b>	<b>8</b>	<b>77</b>	<b>10</b>	<b>37</b>	<b>193</b>
<b>Producer's accuracy (%)</b>	87.50	100	45.40	100	58.80	37.50	97.40	40.00	83.78	
<b>User's accuracy (%)</b>	87.50	41.67	50.00	80.00	83.33	27.27	96.15	100	93.94	
<b>Overall accuracy (%)</b>	<b>82.90</b>									
<b>Kappa hat coefficient (%)</b>	<b>78.00</b>									

### 5.1.2 LULC classification of MLC with nine bands

The result of LULC classification using MLC with nine bands of six multispectral bands and three spectral indices of pan-sharpened image of Landsat-8 is summarized in Table 5.3 and distribution of LULC data is displayed in Figure 5.4.

Like the previous results of MLC, top three dominant LULC classes are forest area, cassava and maize cover area of 586.80 km<sup>2</sup>, 192.00 km<sup>2</sup> and 152.61 km<sup>2</sup> or 55.66%, 18.21% and 14.47% of the total study area, respectively.

**Table 5.3** Area and percentage of final LULC classification of MLC with 9 bands.

No.	LULC class	Area in sq.km	Percent
1	Urban and built-up area	25.92	2.46
2	Paddy field	24.38	2.31
3	Cassava	192.00	18.21
4	Maize	152.61	14.47
5	Sugarcane	5.44	0.52
6	Orchard and perennial trees	25.67	2.43
7	Forest area	586.80	55.66
8	Water bodies	2.27	0.22
9	Miscellaneous land	39.21	3.72
<b>Total</b>		<b>1,054.30</b>	<b>100.00</b>

In addition, the classified LULC map was further performed accuracy assessment with 193 sample points by field survey in 2017 (See Figure 5.3). Error matrix form for LULC accuracy assessment is displayed in Table 5.4. It reveals that overall accuracy is 86.01% and Kappa hat coefficient is 81.93%. Meanwhile producer's accuracy of LULC classes varies between 37.50% for orchard and perennial trees and 100.00% for paddy field and maize while user's accuracy of LULC classes varies between 27.27% for orchard and perennial trees and 100.00% for urban and built-up area and water bodies. Based on Fitzpatrick-Lins (1981), Kappa hat coefficient more than 80 percent represents strong agreement or accuracy between the predicted map and the reference map



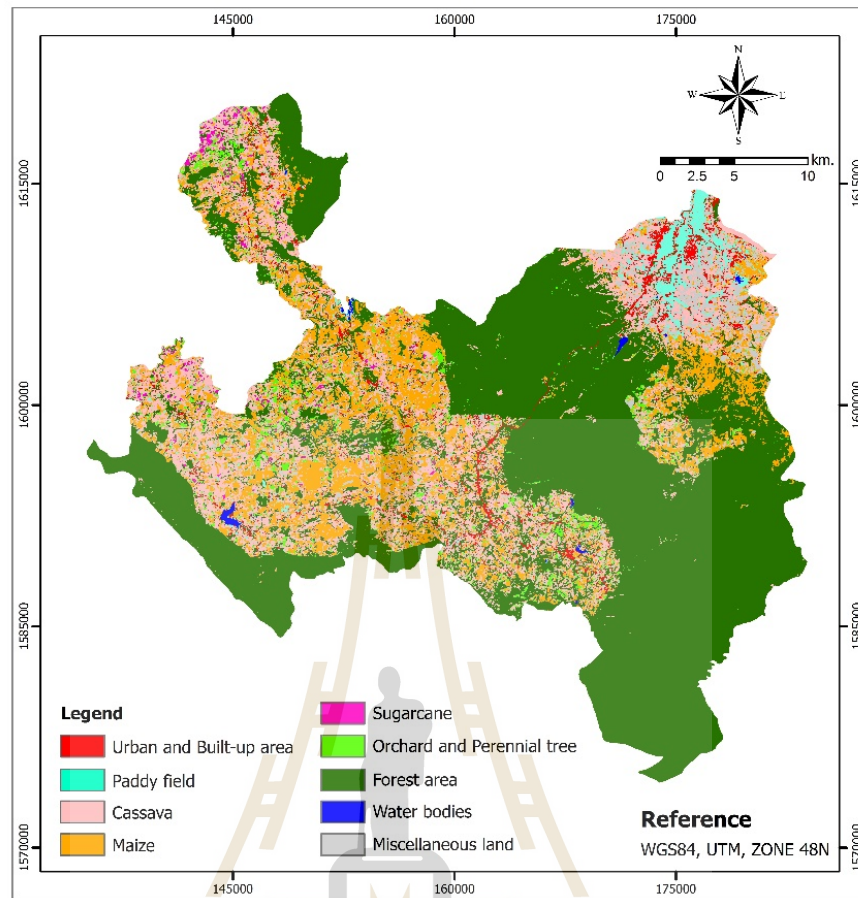


**Figure 5.4** LULC classification of 2015 of MLC with 9 bands.

**Table 5.4** Error matrix and accuracy assessment of LULC classification of MLC with 9 bands.

Classified LULC class	Reference data									Row Total
	UB	PD	CV	MA	SU	OP	FA	WB	ML	
Urban and built-up area (UB)	7									7
Paddy field (PD)		5						2		7
Cassava (CV)			7		3	1	1			12
Maize (MA)				20					5	25
Sugarcane (SU)			1		9	1				11
Orchard and perennial trees (OP)			3		5	3				11
Forest area (FA)						3	76			79
Water bodies (WB)								7		7
Miscellaneous land (ML)	1							1	32	34
<b>Column Total</b>	<b>8</b>	<b>5</b>	<b>11</b>	<b>20</b>	<b>17</b>	<b>8</b>	<b>77</b>	<b>10</b>	<b>37</b>	<b>193</b>
<b>Producer's accuracy (%)</b>	87.50	100	63.64	100	52.94	37.50	98.70	70.00	86.49	
<b>User's accuracy (%)</b>	100	71.43	58.33	80.00	81.82	27.27	96.20	100	94.12	
<b>Overall accuracy (%)</b>	<b>86.01</b>									
<b>Kappa hat coefficient (%)</b>	<b>81.93</b>									

## Discussion

As results of LULC classification of MLC from both datasets, it was found that area of LULC classes from both datasets are similar except cassava and maize as shown in Figure 5.5. Area of cassava from MLC with nine bands is higher than MLC with six bands while area of maize from MLC with nine bands is lower than MLC with six bands. This results shows influence of additional three spectral indices on different LULC classes when they are applied on LULC classification with MLC.

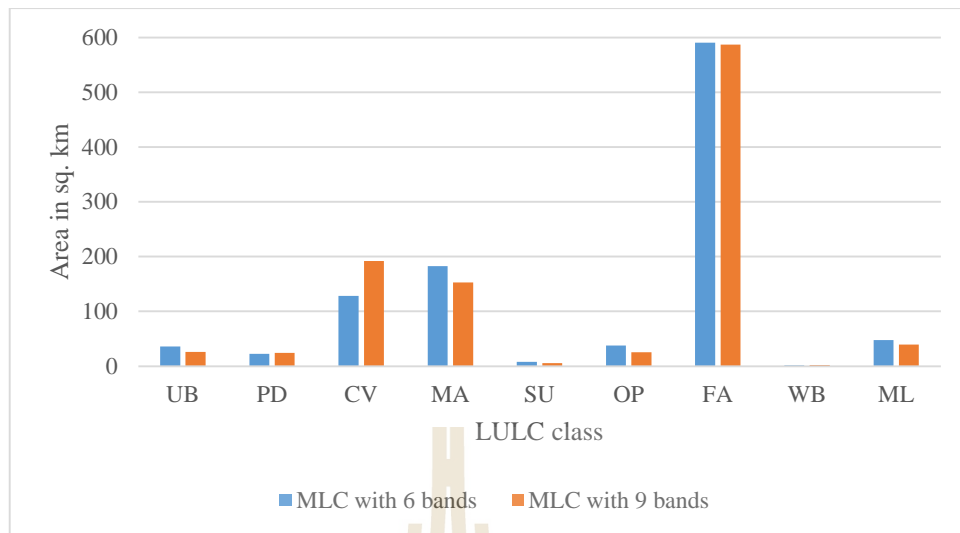


**Figure 5.5** Comparison area of LULC classification of MLC.

In addition, it can be observed that overall accuracy and Kappa hat coefficient of LULC classification map of MLC with nine bands are higher than LULC classification map of MLC with six bands. Likewise producer's accuracy and user's accuracy of LULC classes of MLC with nine bands is higher than six bands as shown in Figure 5.6.

Thus, it can be here concluded that LULC classification of MLC with multispectral band and addition spectral indices with totally nine bands is more suitable than only six bands of multispectral data. This finding was mentioned by many researchers include Skidmore, Turner, Brinkhof, and Knowles, (1997); Qiu and Jensen, (2004); and Stow, Coulter, Kaiser, Hope, Service, Schutte, and Walters, (2003).

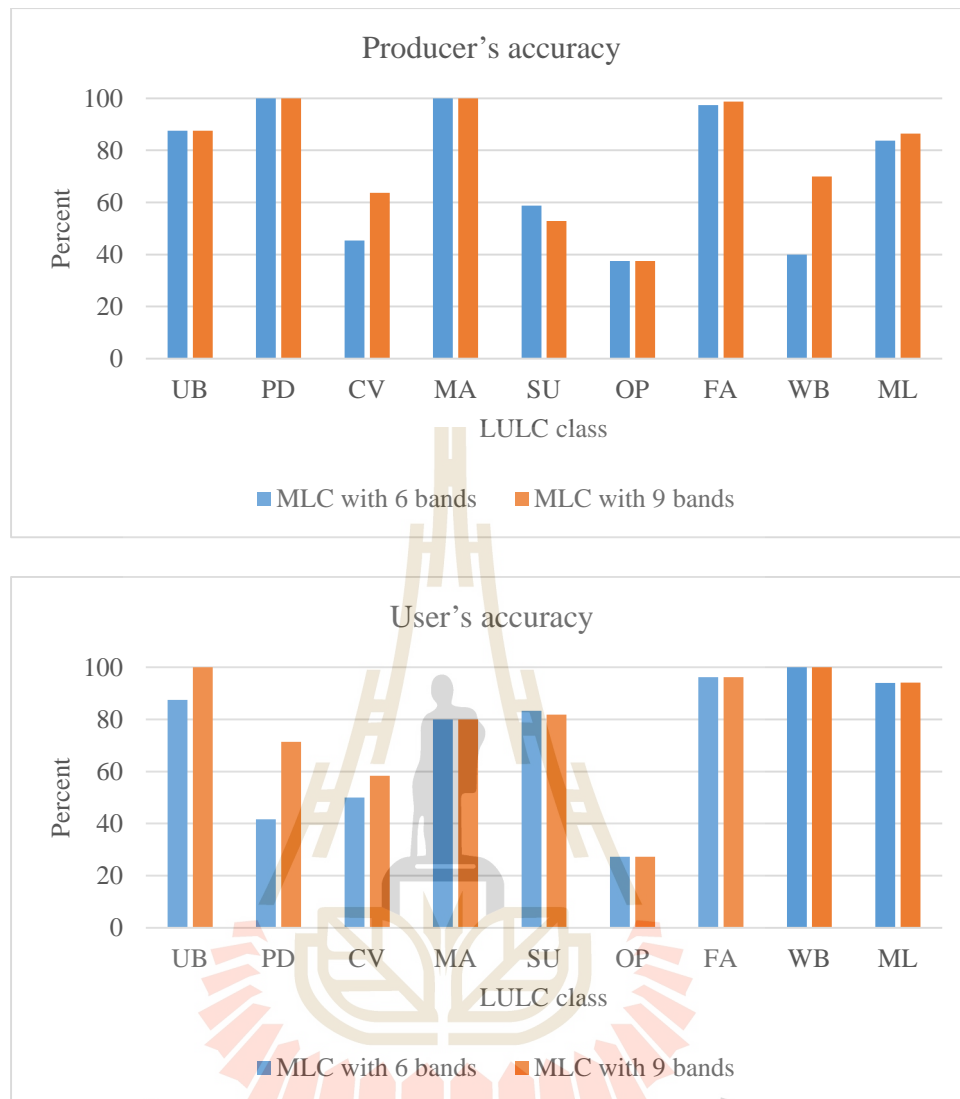


**Figure 5.6** Comparison of producer's accuracy and user's accuracy of MLC with six and nine bands.

However, the pairwise Z test of MLC with two datasets based on Kappa hat analysis shows that the accuracy of both LULC classification of MLC with six and nine bands are not significantly different at the 80% confidence level since the Z-value is less than Chi square values at various confidence levels as shown in Table 5.5. This finding suggests that if operation time is considered, it should apply six bands dataset

instead of nine bands because their Kappa hat coefficients are not significantly different.

**Table 5.5** Pairwise Z test of Kappa hat coefficient value for LULC classification of MLC with six and nine bands.

Pairwise Z test	Kappa hat	Variance	Z-Statistic	Confidential level of critical value			
				80%	90%	95%	100%
MLC with six bands	0.78005	0.00109	<b>0.86554</b>	<b>1.28</b>	<b>1.65</b>	<b>1.96</b>	<b>2.58</b>
MLC with nine bands	0.81931	0.00097					

## 5.2 LULC classification of ANN

Two datasets of pan-sharpened Landsat-8 and additional layers include (1) six bands of pan-sharpened Landsat-8 (Band 2, 3, 4, 5, 6 and 7) and (2) nine bands of six multispectral of pan-sharpened Landsat-8 images (Band 2, 3, 4, 5, 6 and 7) and three spectral index bands (NDVI, MNDWI and NDBI) were here applied to extract LULC using the common training areas of MLC as points under RSI ENVI software. Figure 5.7 displays examples of training areas of LULC classes for ANN. In addition, configuration of ANN operation with learning rate of 0.1 and 0.2 was here applied with two datasets as follows:

Activation function: Logistic,

Training Threshold Contribution: 0.9,

Learning Rate: 0.1 and 0.2,

Training Momentum: 0.9,

Training RMS Exit Criteria: 0.1,

Number of Hidden Layers: 1,

Number of Training Iterations: 10000,

Result of LULC classification of ANN from two datasets with learning rate of 0.1 and 0.2 are separately described in the following sections.

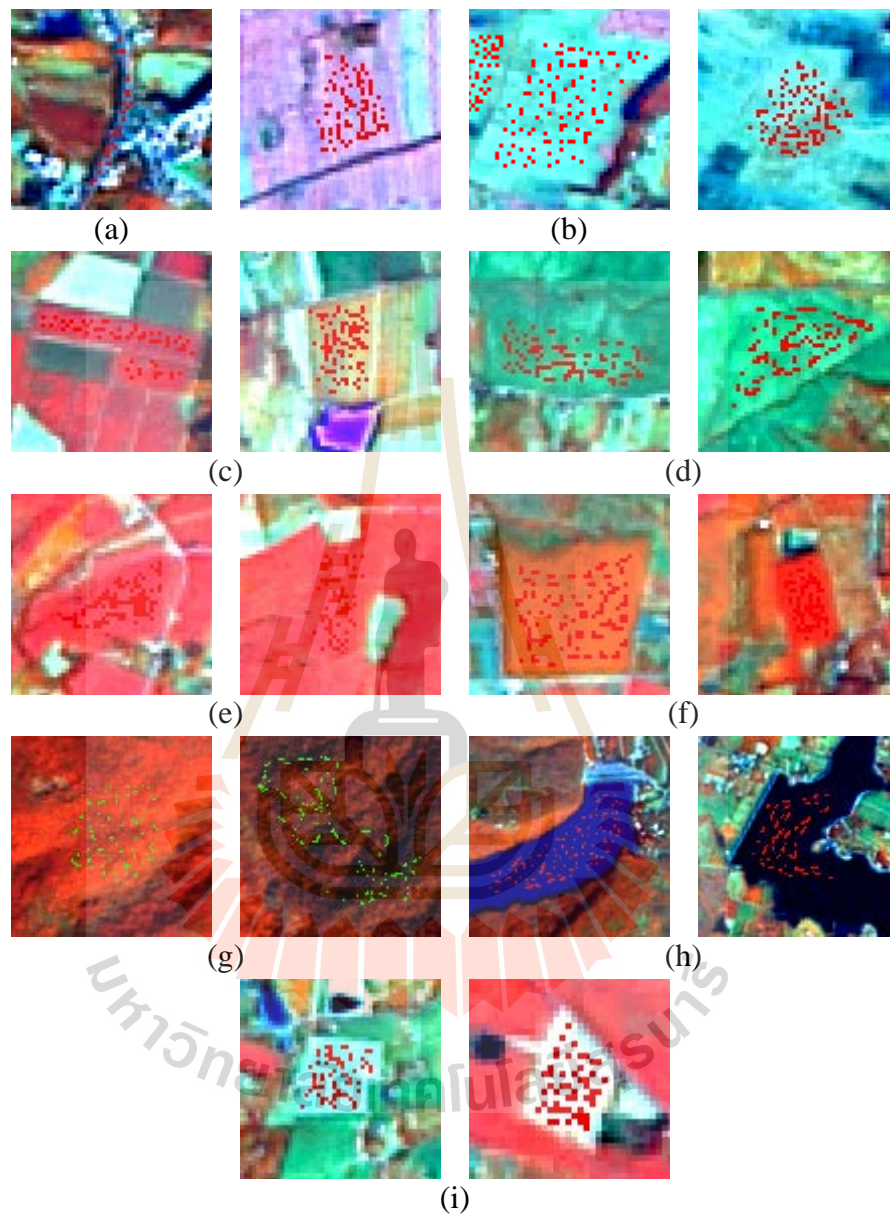


**Figure 5.7** Example training areas of 9 LULC classes for ANN: (a) urban and built-up area, (b) paddy field, (c) cassava, (d) maize, (e) sugarcane, (f) orchard and perennial trees, (g) forest area, (h) water bodies and (i) miscellaneous land.

### 5.2.1 LULC classification of ANN at learning rate of 0.1 with six bands

The result of LULC classification of ANN at learning rate of 0.1 with six multispectral bands of pan-sharpened image of Landsat-8 is summarized in Table 5.6 and distribution of LULC data is displayed in Figure 5.8. Top three dominant LULC classes are forest area, maize, and cassava and cover area of 659.68 km<sup>2</sup>, 171.89 km<sup>2</sup> and 72.25 km<sup>2</sup> or 62.57%, 16.30% and 6.85% of the total study area, respectively.

**Table 5.6** Area and percentage of final LULC classification of ANN at learning rate of 0.1 with six bands.

No.	LULC class	Area in sq.km	Percent
1	Urban and built-up area	4.73	0.45
2	Paddy field	59.70	5.66
3	Cassava	72.25	6.85
4	Maize	171.89	16.30
5	Sugarcane	2.40	0.23
6	Orchard and perennial trees	53.86	5.11
7	Forest area	659.68	62.57
8	Water bodies	5.56	0.53
9	Miscellaneous land	24.23	2.30
<b>Total</b>		<b>1,054.30</b>	<b>100.00</b>

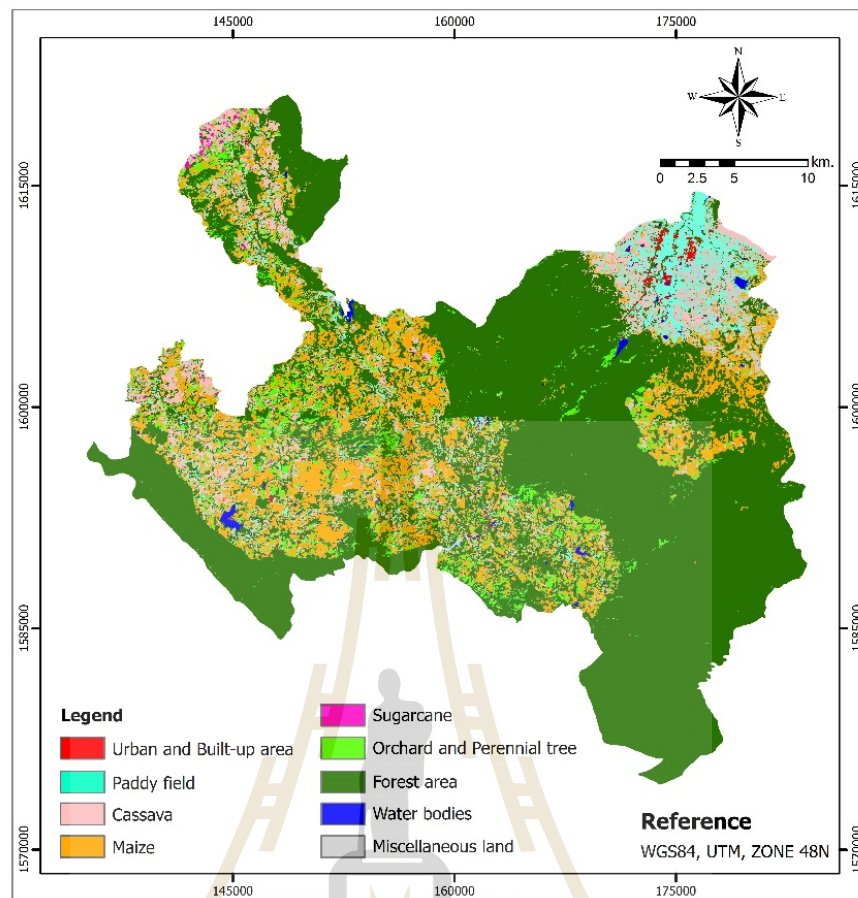


**Figure 5.8** LULC classification of 2015 of ANN at learning rate of 0.1 with six bands.

In addition, the classified LULC map was further performed accuracy assessment with 193 sample points by field survey in 2017 (See Figure 5.3). Error matrix form for LULC accuracy assessment is displayed in Table 5.7. It reveals that overall accuracy is 80.83% and Kappa hat coefficient is 75.48%. Meanwhile producer's accuracy of LULC classes varies between 25.00% for urban and built-up area and 100.00% for paddy field and maize while user's accuracy of LULC classes varies between 38.46% for paddy field and Orchard and perennial trees and 100.00% for sugarcane. Based on Fitzpatrick-Lins (1981), Kappa hat coefficient between 40-80



percent represents moderate agreement or accuracy between the predicted map and the reference map.

**Table 5.7** Error matrix and accuracy assessment of LULC classification of ANN at learning rate of 0.1 with six bands.

Classified LULC class	Reference data									Row Total
	UB	PD	CV	MA	SU	OP	FA	WB	ML	
Urban and built-up area (UB)	2		1							3
Paddy field (PD)	5	5							3	13
Cassava (CV)			6		7		1			14
Maize (MA)			1	20			1		5	27
Sugarcane (SU)					6					6
Orchard and perennial trees (OP)			3		4	5	1			13
Forest area (FA)						3	74			77
Water bodies (WB)	1							9		10
Miscellaneous land (ML)								1	29	30
<b>Column Total</b>	<b>8</b>	<b>5</b>	<b>11</b>	<b>20</b>	<b>17</b>	<b>8</b>	<b>77</b>	<b>10</b>	<b>37</b>	<b>193</b>
<b>Producer's accuracy (%)</b>	25.00	100	54.55	100	35.29	62.50	96.10	90.00	78.38	
<b>User's accuracy (%)</b>	66.67	38.46	42.86	74.07	100	38.46	96.10	90.00	96.67	
<b>Overall accuracy (%)</b>	<b>80.83</b>									
<b>Kappa hat coefficient (%)</b>	<b>75.48</b>									

### 5.2.2 LULC classification of ANN at learning rate of 0.2 with six bands

The result of LULC classification of ANN at learning rate of 0.2 with six multispectral bands of pan-sharpened image of Landsat-8 is summarized in Table 5.8 and distribution of LULC data is displayed in Figure 5.9. Top three dominant LULC classes are forest area, maize, and orchard and perennial trees and cover area of 647.93 km<sup>2</sup>, 199.86 km<sup>2</sup> and 68.69 km<sup>2</sup> or 61.46%, 18.96% and 6.52% of the total study area, respectively.

**Table 5.8** Area and percentage of final LULC classification of ANN at learning rate of 0.2 with six bands.

No.	LULC class	Area in sq.km	Percent
1	Urban and built-up area	2.81	0.27
2	Paddy field	54.85	5.20
3	Cassava	40.62	3.85
4	Maize	199.86	18.96
5	Sugarcane	7.78	0.74
6	Orchard and perennial trees	68.69	6.52
7	Forest area	647.93	61.46
8	Water bodies	11.96	1.13
9	Miscellaneous land	19.80	1.88
<b>Total</b>		<b>1,054.30</b>	<b>100.00</b>

In addition, the classified LULC map was further performed accuracy assessment with 193 sample points by field survey in 2017 (See Figure 5.3). Error matrix form for LULC accuracy assessment is displayed in Table 5.9. It reveals that overall accuracy is 80.31% and Kappa hat coefficient is 74.81%. Meanwhile producer's accuracy of LULC classes varies between 12.50% for urban and built-up area and 100.00% for paddy field and maize while user's accuracy of LULC classes varies between 38.46% for paddy field and Orchard and perennial trees and 100.00% for urban and built-up area and water bodies. Based on Fitzpatrick-Lins (1981), Kappa hat coefficient between 40-80 percent represents moderate agreement or accuracy between the predicted map and the reference map.

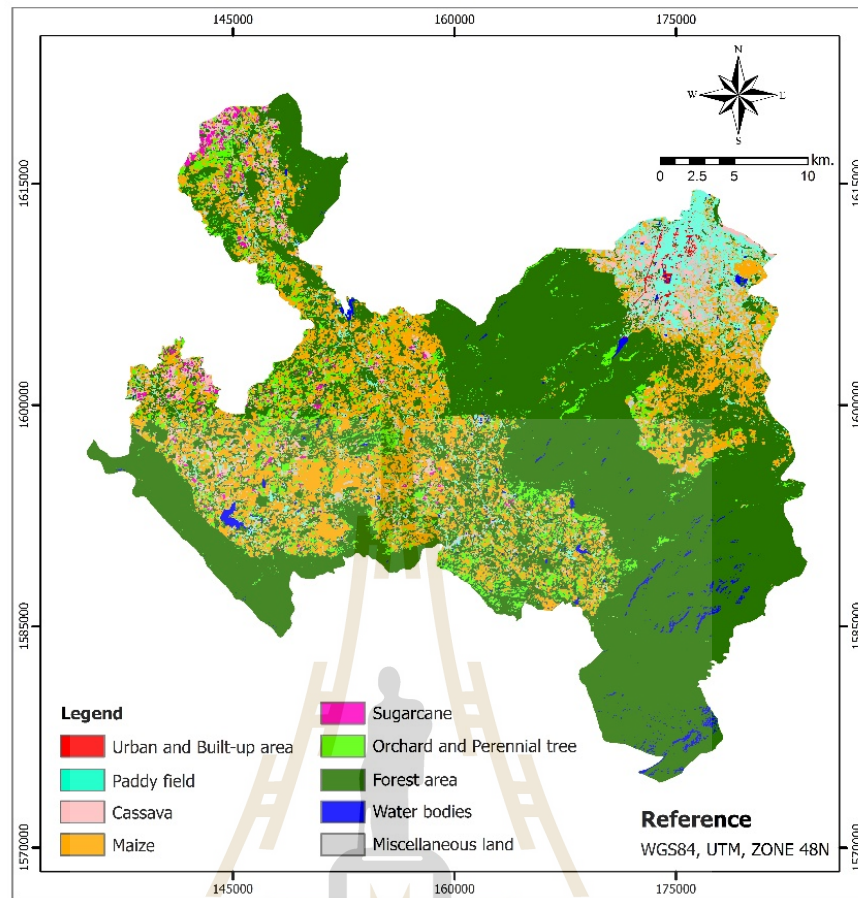


**Figure 5.9** LULC classification of 2015 of ANN at learning rate of 0.2 with 6 bands.

**Table 5.9** Error matrix and accuracy assessment of LULC classification of ANN at learning rate of 0.2 with six bands.

Classified LULC class	Reference data									Row Total
	UB	PD	CV	MA	SU	OP	FA	WB	ML	
Urban and built-up area (UB)	1									1
Paddy field (PD)	7	5							1	13
Cassava (CV)			6		1				2	9
Maize (MA)				20			1		10	31
Sugarcane (SU)			1		13	1				15
Orchard and perennial trees (OP)			3		2	5	3			13
Forest area (FA)			1		1	2	73		1	78
Water bodies (WB)								9		9
Miscellaneous land (ML)								1	23	24
<b>Column Total</b>	<b>8</b>	<b>5</b>	<b>11</b>	<b>20</b>	<b>17</b>	<b>8</b>	<b>77</b>	<b>10</b>	<b>37</b>	<b>193</b>
<b>Producer's accuracy (%)</b>	12.50	100	54.55	100	76.47	62.50	94.81	90.00	62.16	
<b>User's accuracy (%)</b>	100	38.46	66.67	64.52	86.67	38.46	93.59	100	95.83	
<b>Overall accuracy (%)</b>	<b>80.31</b>									
<b>Kappa hat coefficient (%)</b>	<b>74.81</b>									

## Discussion

As results of LULC classification of ANN from six bands with two different learning rate (0.1 and 0.2), it can be observed that area of LULC classes from both different learning rates are similar except cassava and maize as shown in Figure 5.10. Area of cassava from ANN with learning rate of 0.1 is higher than ANN with learning rate of 0.2 while area of maize from ANN learning rate of 0.1 is lower than ANN learning rate of 0.2. The finding shows effect of learning rate of ANN on LULC classification.

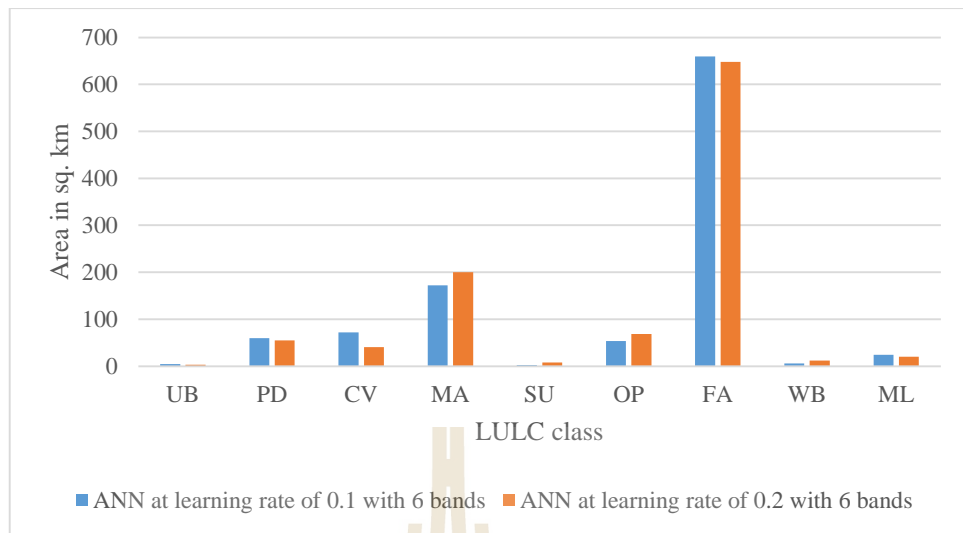


**Figure 5.10** Comparison area of LULC classification of ANN from six bands with different learning rates (0.1 and 0.2).

In addition, overall accuracy and Kappa hat coefficient of LULC classification map of ANN from six bands with learning rate of 0.1 is slightly higher than LULC classification map of ANN from six bands with learning rate of 0.2. Likewise, most of producer's accuracy and user's accuracy of LULC classes of ANN from six bands with learning rate of 0.1 are higher than ANN from six bands with learning rate of 0.2 as shown in Figure 5.11. Thus, it can concluded that LULC classification of ANN using six bands with learning rate of 0.1 provides higher accuracy than six bands with learning rate of 0.2. This finding is consistent with the previous work of Tessawat (2011) who found that ANN with learning rate of 0.1 provided the highest accuracy for LULC classification among three different learning rates (0.1, 0.2, and 0.3).

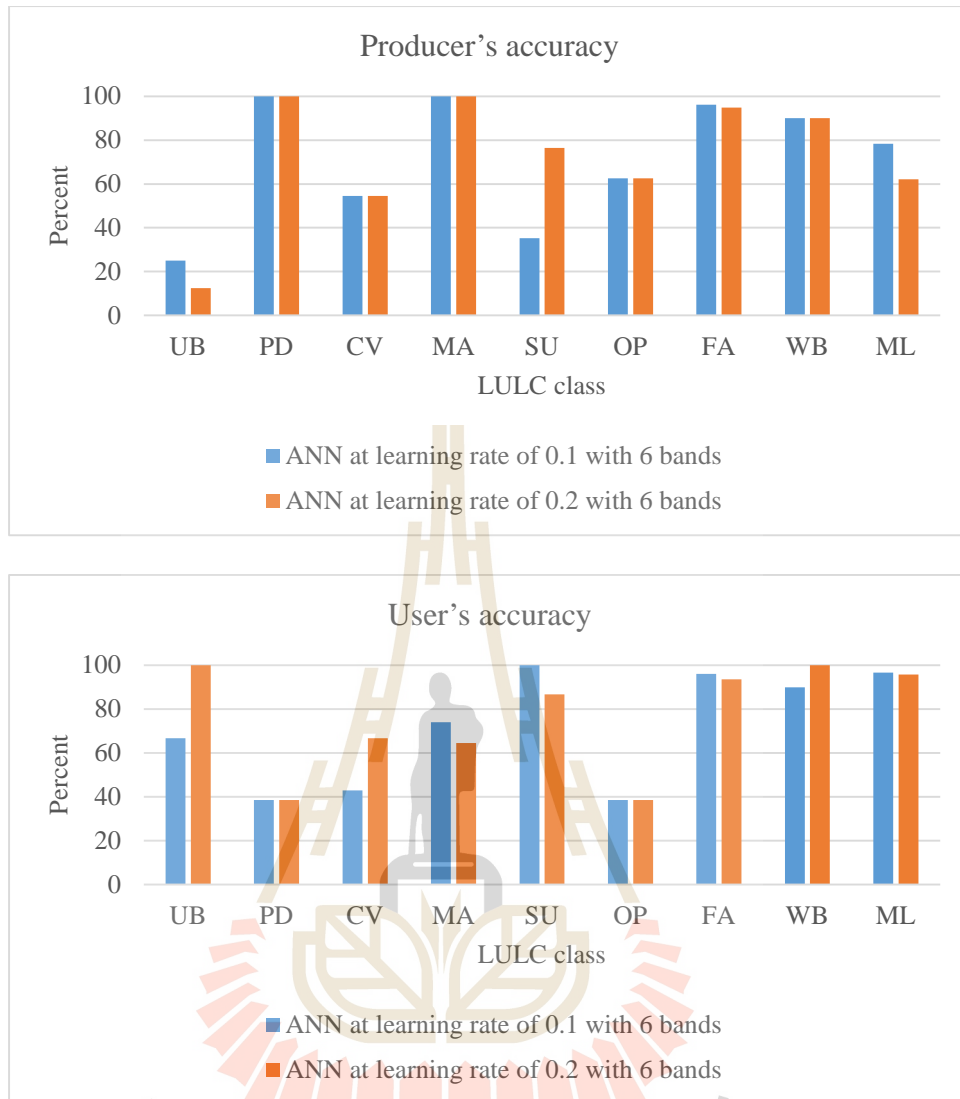


**Figure 5.11** Comparison of producer's accuracy and user's accuracy of LULC classes of ANN from six bands with different learning rates.

However, the pairwise Z test of ANN from six bands dataset with learning rate of 0.1 and 0.2 based on Kappa hat analysis shows that accuracy of LULC classification maps of ANN from six bands dataset with different rates are not significantly different at the 80% confidence level as shown in Table 5.10.

**Table 5.10** Pairwise Z test of Kappa hat coefficient value for LULC classification of ANN from six bands dataset with different learning rate.

Pairwise Z test	Kappa hat	Variance	Z-Statistic	Confidential level of critical value			
				80%	90%	95%	100%
ANN at learning rate of 0.1 with six bands	0.75478	0.00116	<b>0.13654</b>	<b>1.28</b>	<b>1.65</b>	<b>1.96</b>	<b>2.58</b>
ANN at learning rate of 0.2 with six bands	0.74809	0.00124					

### 5.2.3 LULC classification of ANN at learning rate of 0.1 with nine bands

The result of LULC classification of ANN at learning rate of 0.1 with nine bands of six multispectral bands and three spectral indices of pan-sharpened image of Landsat-8 is summarized in Table 5.11 and distribution of LULC data is displayed in Figure 5.12. Top three dominant LULC classes are forest area, maize, and paddy field and cover area of 544.68 km<sup>2</sup>, 266.21 km<sup>2</sup> and 91.53 km<sup>2</sup> or 51.66%, 25.25% and 8.68% of the total study area, respectively.

**Table 5.11** Area and percentage of final LULC classification of ANN at learning rate of 0.1 with nine bands.

No.	LULC class	Area in sq.km	Percent
1	Urban and built-up area	6.82	0.65
2	Paddy field	91.53	8.68
3	Cassava	42.70	4.05
4	Maize	266.21	25.25
5	Sugarcane	4.32	0.41
6	Orchard and perennial trees	75.82	7.19
7	Forest area	544.68	51.66
8	Water bodies	2.25	0.21
9	Miscellaneous land	19.96	1.89
<b>Total</b>		<b>1,054.30</b>	<b>100.00</b>

In addition, the classified LULC map was further performed accuracy assessment with 193 sample points by field survey in 2017 (See Figure 5.3). Error matrix form for LULC accuracy assessment is displayed in Table 5.12. It reveals that overall accuracy is 76.17% and Kappa hat coefficient is 70.02%. Meanwhile producer's accuracy of LULC classes varies between 50.00% for urban and built-up area and 100.00% for paddy field and maize while user's accuracy of LULC classes varies between 26.32% for orchard and perennial trees and 100.00% for urban and built-up area and water bodies. Based on Fitzpatrick-Lins (1981), Kappa hat coefficient between 40-80 percent represents moderate agreement or accuracy between the predicted map and the reference map.

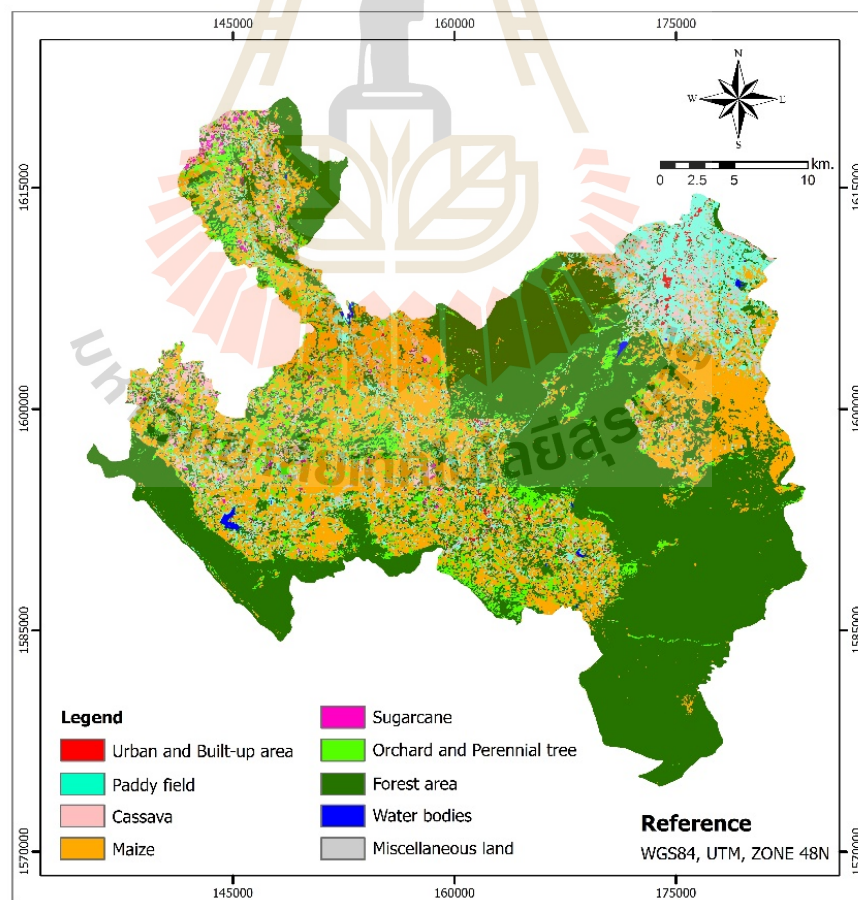


**Figure 5.12** LULC classification of 2015 of ANN at learning rate of 0.1 with 9 bands.



**Table 5.12** Error matrix and accuracy assessment of LULC classification of ANN at learning rate of 0.1 with nine bands.

Classified LULC class	Reference data									Row Total
	UB	PD	CV	MA	SU	OP	FA	WB	ML	
Urban and built-up area (UB)	4									4
Paddy field (PD)	4	5							6	15
Cassava (CV)			6		5					11
Maize (MA)			1	20			4		4	29
Sugarcane (SU)			1		9					10
Orchard and perennial trees (OP)			3		2	5	8		1	19
Forest area (FA)					1	3	65	1	1	71
Water bodies (WB)								8		8
Miscellaneous land (ML)								1	25	26
<b>Column Total</b>	<b>8</b>	<b>5</b>	<b>11</b>	<b>20</b>	<b>17</b>	<b>8</b>	<b>77</b>	<b>10</b>	<b>37</b>	<b>193</b>
<b>Producer's accuracy (%)</b>	50.00	100	54.55	100	52.94	62.50	84.42	80.00	67.57	
<b>User's accuracy (%)</b>	100	33.33	54.55	68.97	90.00	26.32	91.55	100	96.15	
<b>Overall accuracy (%)</b>	<b>76.17</b>									
<b>Kappa hat coefficient (%)</b>	<b>70.02</b>									

#### 5.2.4 LULC classification of ANN at learning rate of 0.2 with nine bands

The result of LULC classification of ANN at learning rate of 0.2 with nine bands of six multispectral bands and spectral indices of pan-sharpened image of Landsat-8 is summarized in Table 5.13 and distribution of LULC data is displayed in Figure 5.13. Top three dominant LULC classes are forest area, maize, and cassava and cover area of 553.57 km<sup>2</sup>, 208.84 km<sup>2</sup> and 114.11 km<sup>2</sup> or 52.51%, 19.81% and 10.82% of the total study area, respectively.

**Table 5.13** Area and percentage of final LULC classification of ANN at learning rate of 0.2 with 9 bands.

No.	LULC class	Area in sq.km	Percent
1	Urban and built-up area	32.03	3.04
2	Paddy field	69.72	6.61
3	Cassava	114.11	10.82
4	Maize	208.84	19.81
5	Sugarcane	4.77	0.45
6	Orchard and perennial trees	48.96	4.64
7	Forest area	553.57	52.51
8	Water bodies	1.95	0.18
9	Miscellaneous land	20.36	1.93
<b>Total</b>		<b>1,054.30</b>	<b>100.00</b>

In addition, the classified LULC map was further performed accuracy assessment with 193 sample points by field survey in 2017 (See Figure 5.3). Error matrix form for LULC accuracy assessment is displayed in Table 5.14. It reveals that overall accuracy is 75.13% and Kappa hat coefficient is 68.30%. Meanwhile producer's accuracy of LULC classes varies between 37.50% for orchard and perennial trees and 100.00% for maize while user's accuracy of LULC classes varies between 25.00% for orchard and perennial trees and 100.00% for urban and built-up area and water bodies. Based on Fitzpatrick-Lins (1981), Kappa hat coefficient between 40-80 percent represents moderate agreement or accuracy between the predicted map and the reference map.

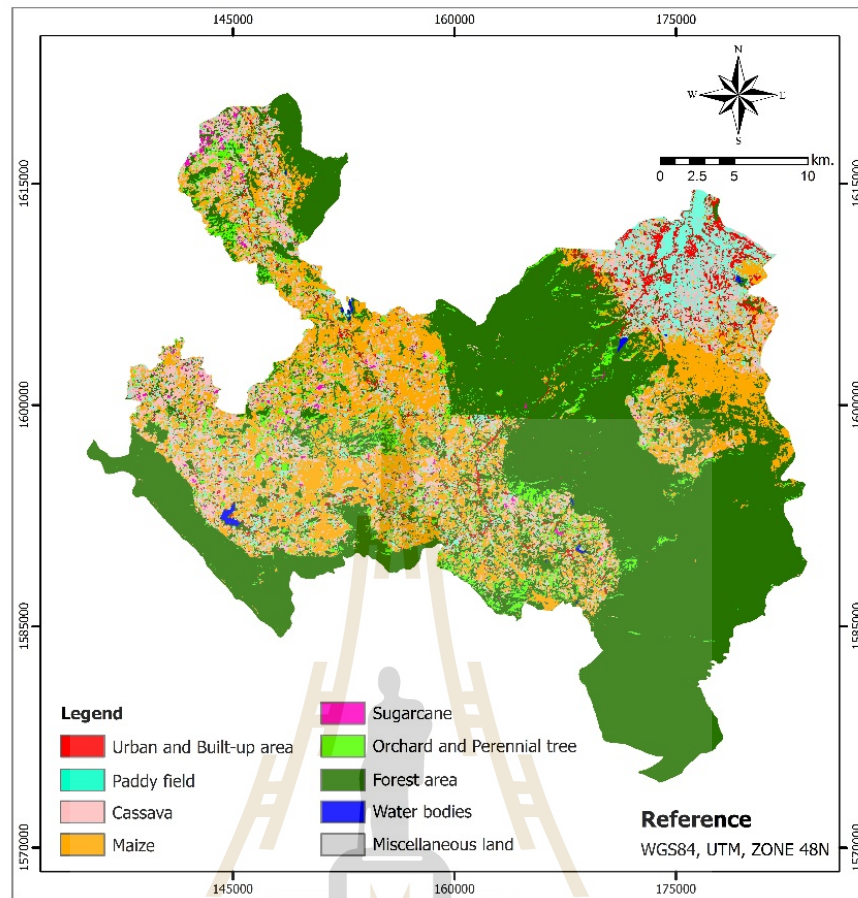


**Figure 5.13** LULC classification of 2015 of ANN at learning rate of 0.2 with 9 bands.

**Table 5.14** Error matrix and accuracy assessment of LULC classification of ANN at learning rate of 0.2 with nine bands.

Classified LULC class	Reference data									Row Total
	UB	PD	CV	MA	SU	OP	FA	WB	ML	
Urban and built-up area (UB)	4									4
Paddy field (PD)	4	4							4	12
Cassava (CV)			8		3	1	1			13
Maize (MA)				20			5		7	32
Sugarcane (SU)			1		9	1				11
Orchard and perennial trees (OP)			2		1	3	6			12
Forest area (FA)					4	3	65	3		75
Water bodies (WB)								6		6
Miscellaneous land (ML)		1						1	26	28
<b>Column Total</b>	<b>8</b>	<b>5</b>	<b>11</b>	<b>20</b>	<b>17</b>	<b>8</b>	<b>77</b>	<b>10</b>	<b>37</b>	<b>193</b>
<b>Producer's accuracy (%)</b>	50.00	80.00	72.73	100	52.94	37.50	84.42	60.00	70.27	
<b>User's accuracy (%)</b>	100	33.33	61.54	62.50	81.82	25.00	86.67	100	92.86	
<b>Overall accuracy (%)</b>	<b>75.13</b>									
<b>Kappa hat coefficient (%)</b>	<b>68.30</b>									

## Discussion

As results of LULC classification of ANN from nine bands with both different learning rates (0.1 and 0.2), it can be observed that area of LULC classes from both different learning rate are rather different except sugarcane and miscellaneous land as shown in Figure 5.14.

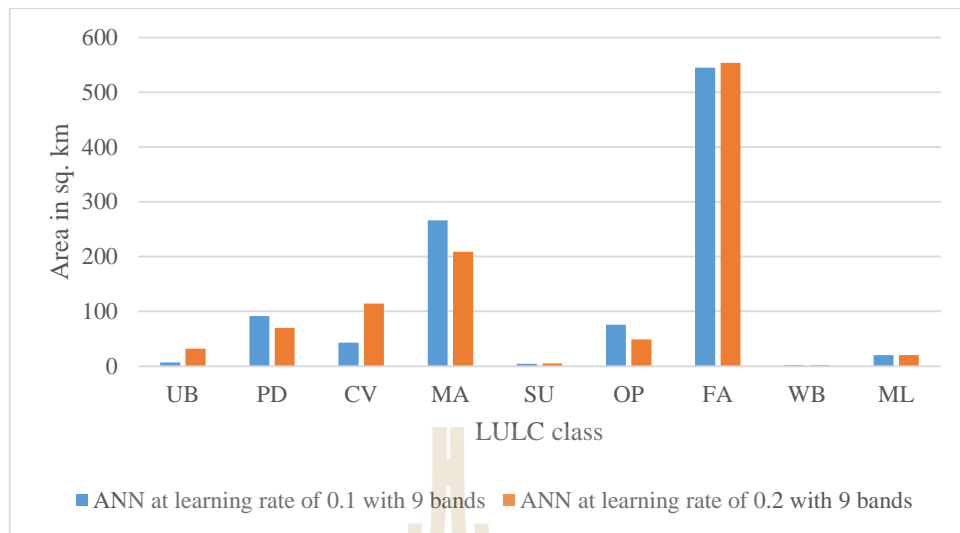


**Figure 5.14** Comparison area of LULC classification of ANN from nine bands with different learning rates (0.1 and 0.2).

In addition, overall accuracy and Kappa hat coefficient of LULC classification map of ANN from nine bands with learning rate 0.1 is slightly higher than LULC classification map of ANN from nine bands with learning rate 0.2. Producer's accuracy and user's accuracy of LULC classes of ANN from nine bands with learning rate of 0.1 and 0.2 are rather different as shown in Figure 5.15. Thus, it can be here concluded that ANN at learning rate of 0.1 with nine bands can provide better accuracy than ANN at learning rate of 0.2 with nine bands.

However, the pairwise Z test of ANN from nine bands dataset with learning rate of 0.1 and 0.2 based on Kappa hat analysis shows that accuracy of LULC classification maps of ANN from nine bands dataset with different rates are not significantly different at the 80% confidence level as shown in Table 5.15.

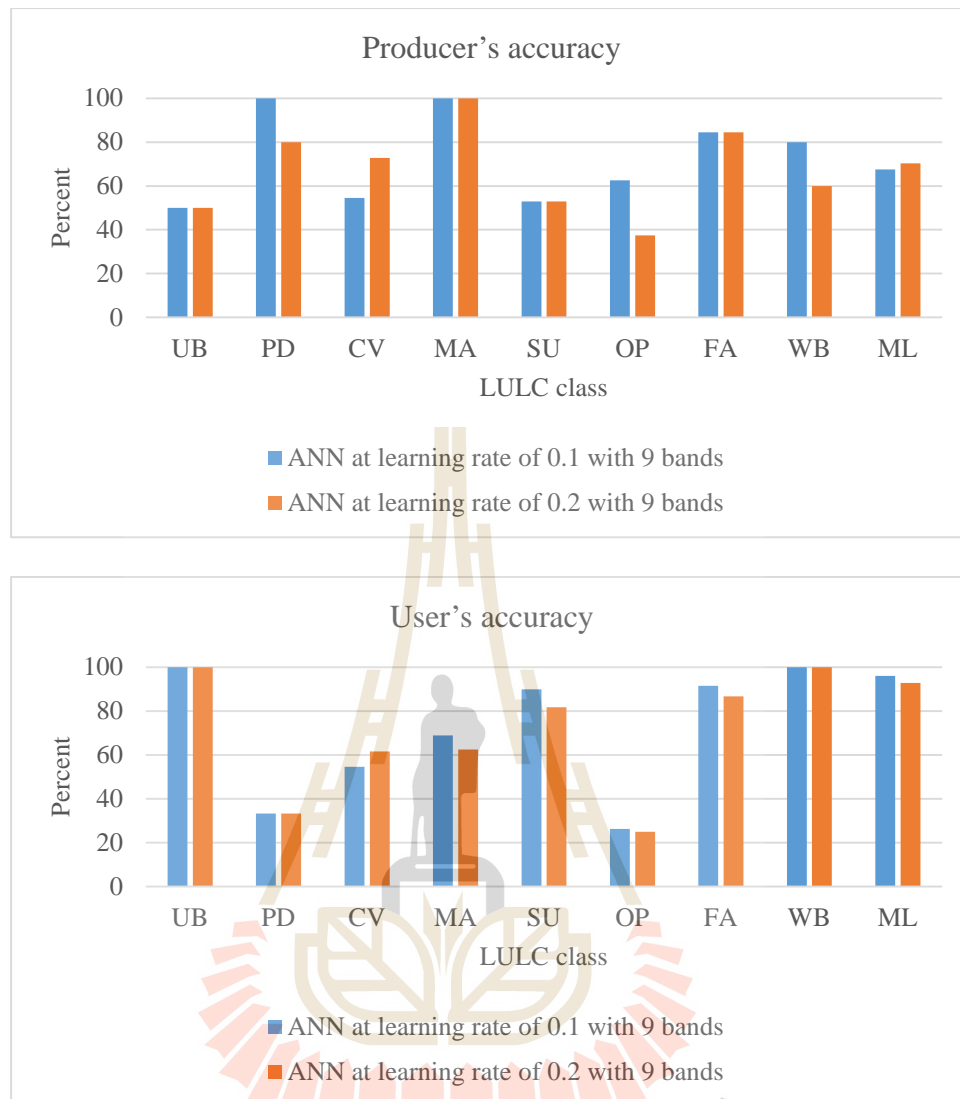


**Figure 5.15** Comparison of producer's accuracy and user's accuracy of LULC classes of ANN from nine bands with different learning rates.

**Table 5.15** Pairwise Z test of Kappa hat coefficient value for LULC classification of ANN from nine bands dataset with different learning rate.

Pairwise Z test	Kappa hat	Variance	Z-Statistic	Confidential level of critical value			
				80%	90%	95%	100%
ANN at learning rate of 0.1 with nine bands	0.70017	0.00137	<b>0.32056</b>	<b>1.28</b>	<b>1.65</b>	<b>1.96</b>	<b>2.58</b>
ANN at learning rate of 0.2 with nine bands	0.68296	0.00151					

Furthermore, the pairwise Z test of LULC classification using ANN with learning rate of 0.1 and 0.2 and two different datasets (six and nine bands) were examined based on Kappa hat analysis. It was found that accuracy of LULC classification maps of ANN at learning rate at 0.1 or 0.2 with two different datasets (six and nine bands) are not significantly different at the 80% confidence level as shown in Table 5.16. Like MLC method, this finding suggests that it should apply six bands dataset for reducing operation time for LULC classification.

Additionally, Kappa hat coefficient of LULC classification using ANN at learning rate of 0.1 with six bands (75.48%) is higher than Kappa hat coefficient of nine bands (70.02%). Likewise, Kappa hat coefficient of LULC classification using ANN at learning rate at 0.2 with six bands (74.81%) is higher than Kappa hat coefficient of nine bands (68.30%). As a result, it infers that additional spectral bands (NDVI, MNDWI, and NDBI) under nine bands dataset do not improve accuracy of LULC classification using ANN at learning rate of 0.1 or 0.2. This finding is adverse with the MLC as mentioned in Section 5.1.

In summary, it can be here concluded that ANN at learning rate of 0.1 with six bands of pan-sharpened Landsat-8 data is the most suitable for LULC classification using ANN method under PBIA.

**Table 5.16** Pairwise Z test of Kappa hat coefficient value for LULC classification of ANN at learning rate at 0.1 and 0.2 with two different datasets (six and nine bands).

Pairwise Z test	Kappa hat	Variance	Z-Statistic	Confidential level of critical value			
				80%	90%	95%	100%
ANN at learning rate of 0.1 with six bands	0.75478	0.00116	<b>1.07680</b>	<b>1.28</b>	<b>1.65</b>	<b>1.96</b>	<b>2.58</b>
ANN at learning rate of 0.1 with nine bands	0.70017	0.00141					
ANN at learning rate of 0.2 with six bands	0.74809	0.00121	<b>1.24863</b>	<b>1.28</b>	<b>1.65</b>	<b>1.96</b>	<b>2.58</b>
ANN at learning rate of 0.2 with nine bands	0.68296	0.00151					

### 5.3 LULC classification of DT

Three datasets of pan-sharpened Landsat-8 and additional layers include (1) six bands of pan-sharpened Landsat-8 band (Band 2, 3, 4, 5, 6 and 7); (2) nine bands of six original pan-sharpened Landsat-8 image (Band 2, 3, 4, 5, 6 and 7) and three spectral index bands (NDVI, MNDWI and NDBI); and (3) eleven bands of six original pan-sharpened Landsat-8 image (Band 2, 3, 4, 5, 6 and 7), three spectral index bands (NDVI, MNDWI and NDBI) and two physical data (elevation and slope) were here applied to extract LULC using the common training areas of MLC. In practice, ASCII file of training area include LULC class and independent variables (Landsat data, spectral indices, and physical data) are export into SPSS statistical software to construct tree using CRT algorithm with 100% samples and with splitting samples into 60% and 40% for modelling and testing. Result of three different datasets with two methods for construction decision tree are separately described and discussed in the following sections.



### 5.3.1 LULC classification of DT without splitting samples with six bands

Summary of DT construction without splitting samples with six bands is summarized in Table 5.17 while binary decision tree structure is displayed in Figure 5.16. It reveals that the final criteria of decision tree for LULC classification applies all six bands. The decision tree consists of 155 nodes that includes 78 with tree depth of 15. This binary decision tree is further applied to classify LULC classes under Knowledge Engineer module of Expert System under ERDAS Imagine software.

**Table 5.17** Model summary of DT without splitting samples with six bands: specifications and results.

<b>Specifications</b>	Growing Method	CRT
	Dependent Variable	CLASS
	Independent Variables	BLUE, GREEN, RED, NIR, SWIR1, SWIR2
	Validation	None
	Maximum Tree Depth	15
	Minimum Cases in Parent Node	10
	Minimum Cases in Child Node	5
<b>Results</b>	Independent Variables Included	BLUE, GREEN, RED, NIR, SWIR1, SWIR2
	Number of Nodes	155
	Number of Terminal Nodes	78
	Depth	15



According to accuracy assessment of the model based on training data as model-based inference statistics, the derived decision tree provides overall accuracy of 99.00% (Table 5.18). Basically, model-based inference statistic is not concerned with the accuracy of the thematic map. It is concerned with estimating the error of model that generates the thematic map. Model-based inference can provide the user with a quantitative assessment of each classification decision (Stehman, 2000, 2001). The accuracy of the derived optimum model for LULC classification varies between 57.60% for urban and built-up area and 100% for water bodies.

**Table 5.18** Accuracy assessment of the model based on training data as model-based inference statistics.

Observed	Predicted									Percent Correct
	CV	FA	MA	ML	OP	PD	SU	UB	WB	
Cassava (CV)	980	76	3	0	3	0	2	0	0	92.10%
Forest area (FA)	33	23718	0	0	29	0	0	0	0	99.70%
Maize (MA)	0	0	1780	6	0	8	0	0	0	99.20%
Miscellaneous land (ML)	0	0	14	941	0	13	0	0	0	97.20%
Orchard and perennial trees (OP)	0	161	0	0	1270	0	9	0	0	88.20%
Paddy field (PD)	0	0	5	6	0	2081	0	5	0	99.20%
Sugarcane (SU)	6	7	0	0	5	0	1372	0	0	98.70%
Urban and built-up area (UB)	2	1	0	0	0	11	0	19	0	57.60%
Water bodies (WB)	0	0	0	0	0	0	0	0	8296	100%
<b>Overall Percentage</b>	<b>2.50%</b>	<b>58.60%</b>	<b>4.40%</b>	<b>2.30%</b>	<b>3.20%</b>	<b>5.20%</b>	<b>3.40%</b>	<b>0.10%</b>	<b>20.30%</b>	<b>99.00%</b>

The result of LULC classification of DT without splitting samples with six bands is summarized in Table 5.19 and distribution of LULC data is displayed in Figure 5.17. Top three dominant LULC classes are forest area, maize, and cassava and cover area of 695.13 km<sup>2</sup>, 162.09 km<sup>2</sup> and 108.37 km<sup>2</sup> or 65.93%, 15.37% and 10.28% of the total study area, respectively.

In addition, the classified LULC map was further performed accuracy assessment with 193 sample points by field survey in 2017 (See Figure 5.3). Error matrix form for LULC accuracy assessment is displayed in Table 5.20. It reveals that overall accuracy is 82.38% and Kappa hat coefficient is 77.02%. Meanwhile producer's accuracy of LULC classes varies between 0.00% for urban and built-up area and 100.00% for paddy field, maize, and forest area while user's accuracy of LULC classes varies between 0% for urban and built-up area and 100.00% for water bodies. Based on Fitzpatrick-Lins (1981), Kappa hat coefficient between 40-80 percent represents moderate agreement or accuracy between the predicted map and the reference map.

**Table 5.19** Area and percentage of final LULC classification of DT without splitting samples with six bands.

No.	LULC class	Area in sq.km	Percent
1	Urban and built-up area	0.76	0.07
2	Paddy field	46.35	4.40
3	Cassava	108.37	10.28
4	Maize	162.09	15.37
5	Sugarcane	4.65	0.44
6	Orchard and perennial trees	13.64	1.29
7	Forest area	695.13	65.93
8	Water bodies	3.29	0.31
9	Miscellaneous land	20.02	1.90
<b>Total</b>		<b>1,054.30</b>	<b>100.00</b>

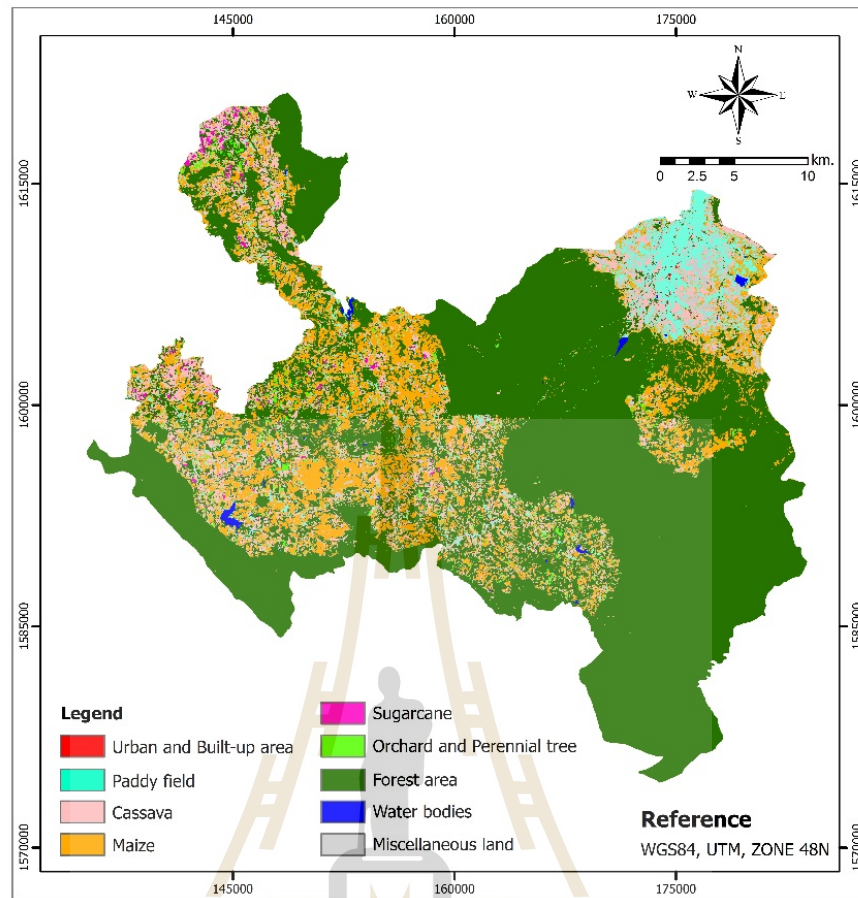


**Figure 5.17** LULC classification of 2015 of DT without splitting samples with six bands.

**Table 5.20** Error matrix and accuracy assessment of LULC classification of DT without splitting samples with six bands.

Classified LULC class	Reference data									Row Total
	UB	PD	CV	MA	SU	OP	FA	WB	ML	
Urban and built-up area (UB)	0									0
Paddy field (PD)	7	5							1	13
Cassava (CV)			7		4					11
Maize (MA)				20					5	25
Sugarcane (SU)			1		7	1				9
Orchard and perennial trees (OP)			2		4	3				9
Forest area (FA)			1		2	4	77			84
Water bodies (WB)								9		9
Miscellaneous land (ML)	1							1	31	33
<b>Column Total</b>	<b>8</b>	<b>5</b>	<b>11</b>	<b>20</b>	<b>17</b>	<b>8</b>	<b>77</b>	<b>10</b>	<b>37</b>	<b>193</b>
<b>Producer's accuracy (%)</b>	0	100	63.64	100	41.18	37.50	100	90.00	83.78	
<b>User's accuracy (%)</b>	0	38.46	63.64	80.00	77.78	33.33	91.67	100	93.94	
<b>Overall accuracy (%)</b>	<b>82.38</b>									
<b>Kappa hat coefficient (%)</b>	<b>77.02</b>									

### 5.3.2 LULC classification of DT without splitting samples with nine bands

Summary of DT construction without splitting samples with nine bands is summarized in Table 5.21 while binary decision tree structure is displayed in Figure 5.18. It reveals that the final criteria of decision tree for LULC classification applies all nine bands. The decision tree consists of 175 nodes that includes 88 with tree depth of 15. This binary decision tree is further applied to classify LULC classes under Knowledge Engineer module of Expert System under ERDAS Imagine software.

**Table 5.21** Model summary of DT without splitting samples with nine bands: specifications and results.

<b>Specifications</b>	Growing Method	CRT
	Dependent Variable	CLASS
	Independent Variables	BLUE, GREEN, RED, NIR, SWIR1, SWIR2, NDVI, MNDWI, NDBI
	Validation	None
	Maximum Tree Depth	15
	Minimum Cases in Parent Node	10
	Minimum Cases in Child Node	5
<b>Results</b>	Independent Variables Included	BLUE, GREEN, RED, NIR, SWIR1, SWIR2, NDVI, MNDWI, NDBI
	Number of Nodes	175
	Number of Terminal Nodes	88
	Depth	15

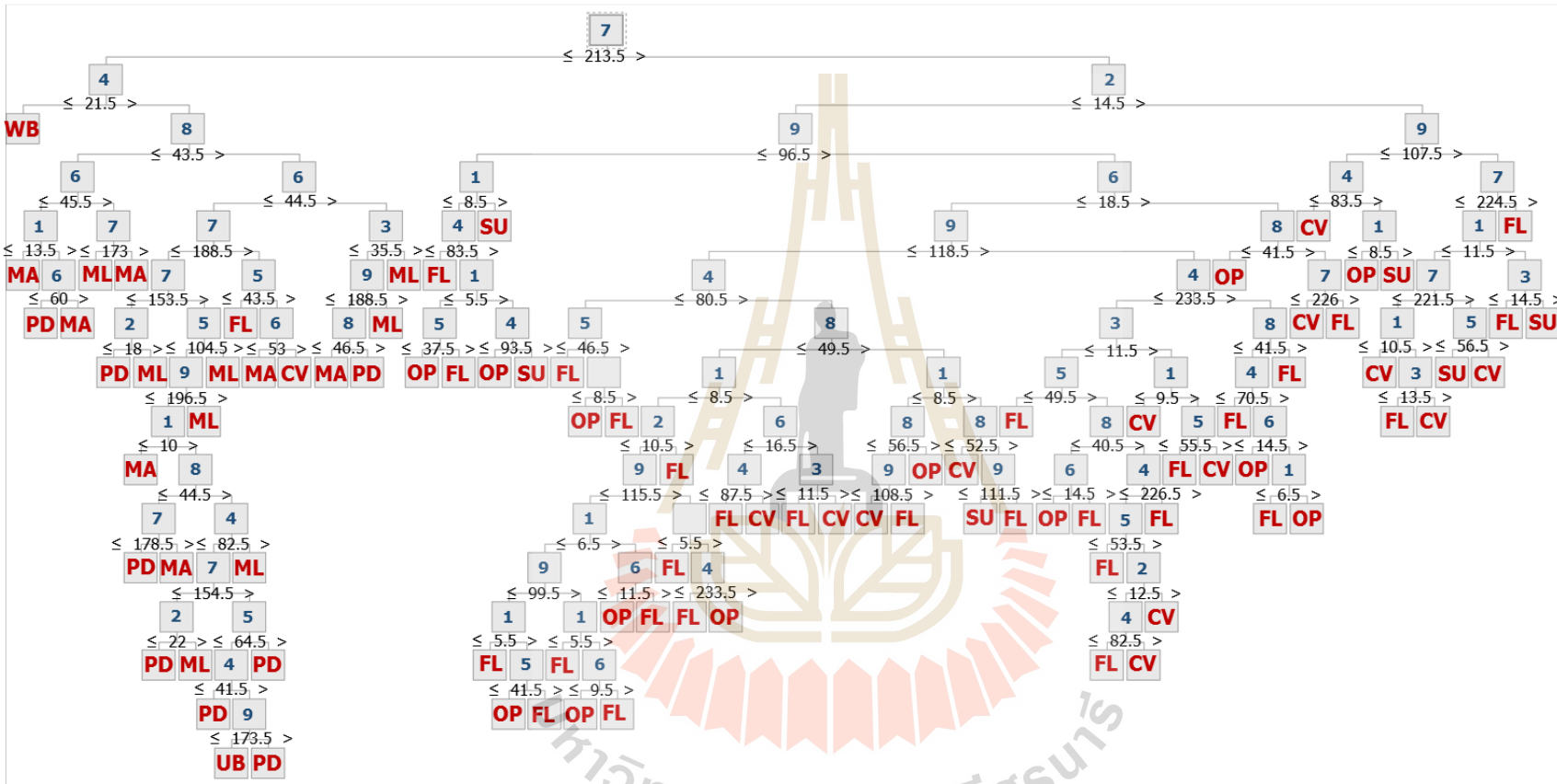


Figure 5.18 Binary decision tree structure for LULC classification without splitting samples with nine bands.



According to accuracy assessment of the model based on training data as model-based inference statistics, the derived decision tree provides overall accuracy of 99.20% (Table 5.22). The accuracy of the derived optimum model for LULC classification varies between 81.80% for urban and built-up area and 100% for water bodies.

**Table 5.22** Accuracy assessment of the model based on training data as model-based inference statistics.

Observed	Predicted									Percent Correct
	CV	FA	MA	ML	OP	PD	SU	UB	WB	
Cassava (CV)	1014	42	2	0	2	0	4	0	0	95.30%
Forest area (FA)	7	23738	0	0	34	0	1	0	0	99.80%
Maize (MA)	1	0	1783	0	0	10	0	0	0	99.40%
Miscellaneous land (ML)	1	0	11	928	0	28	0	0	0	95.90%
Orchard and perennial trees (OP)	1	120	0	0	1308	0	11	0	0	90.80%
Paddy field (PD)	2	0	9	8	0	2066	0	12	0	98.50%
Sugarcane (SU)	2	0	0	0	5	0	1383	0	0	99.50%
Urban and built-up area (UB)	0	1	0	0	0	5	0	27	0	81.80%
Water bodies (WB)	0	0	0	0	0	0	0	0	8296	100%
<b>Overall Percentage</b>	<b>2.50%</b>	<b>58.50%</b>	<b>4.40%</b>	<b>2.30%</b>	<b>3.30%</b>	<b>5.20%</b>	<b>3.40%</b>	<b>0.10%</b>	<b>20.30%</b>	<b>99.20%</b>

The result of LULC classification of DT without splitting samples with nine bands is summarized in Table 5.23 and distribution of LULC data is displayed in Figure 5.19. Top three dominant LULC classes are forest area, maize, and cassava and cover area of 666.40 km<sup>2</sup>, 152.83 km<sup>2</sup> and 141.96 km<sup>2</sup> or 63.21%, 14.50% and 13.46% of the total study area, respectively.

**Table 5.23** Area and percentage of final LULC classification of DT without splitting samples with nine bands.

No.	LULC class	Area in sq.km	Percent
1	Urban and built-up area	2.88	0.27
2	Paddy field	52.86	5.01
3	Cassava	141.96	13.46
4	Maize	152.83	14.50
5	Sugarcane	6.50	0.62
6	Orchard and perennial trees	14.84	1.41
7	Forest area	666.40	63.21
8	Water bodies	3.38	0.32
9	Miscellaneous land	12.65	1.20
<b>Total</b>		<b>1,054.30</b>	<b>100.00</b>

In addition, the classified LULC map was further performed accuracy assessment with 193 sample points by field survey in 2017 (See Figure 5.3). Error matrix form for LULC accuracy assessment is displayed in Table 5.24. It reveals that overall accuracy is 80.31% and Kappa hat coefficient is 74.66%. Meanwhile producer's accuracy of LULC classes varies between 12.50% for urban and built-up area and 100.00% for paddy field and maize while user's accuracy of LULC classes varies between 22.22% for orchards and perennial trees and 100.00% for urban and built-up area and water bodies. Based on Fitzpatrick-Lins (1981), Kappa hat coefficient between 40-80 percent represents moderate agreement or accuracy between the predicted map and the reference map.

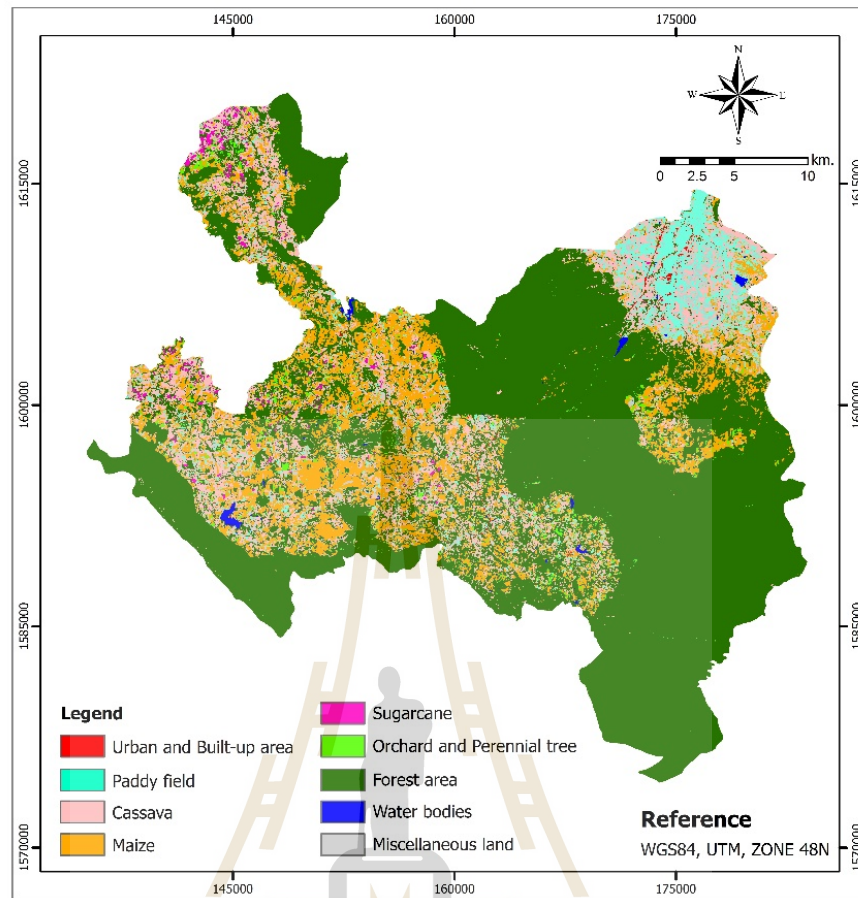


**Figure 5.19** LULC classification of 2015 of DT without splitting samples with nine bands.

**Table 5.24** Error matrix and accuracy assessment of LULC classification of DT without splitting samples with nine bands.

Classified LULC class	Reference data									Row Total
	UB	PD	CV	MA	SU	OP	FA	WB	ML	
Urban and built-up area (UB)	1									1
Paddy field (PD)	6	5							8	19
Cassava (CV)			6		1		1			8
Maize (MA)				20					5	25
Sugarcane (SU)			1		13	1				15
Orchard and perennial trees (OP)			3		3	2	1			9
Forest area (FA)			1			5	75			81
Water bodies (WB)								9		9
Miscellaneous land (ML)	1							1	24	26
<b>Column Total</b>	<b>8</b>	<b>5</b>	<b>11</b>	<b>20</b>	<b>17</b>	<b>8</b>	<b>77</b>	<b>10</b>	<b>37</b>	<b>193</b>
<b>Producer's accuracy (%)</b>	12.50	100	54.55	100	76.47	25.00	97.40	90.00	64.86	
<b>User's accuracy (%)</b>	100	26.32	75.00	80.00	86.67	22.22	92.59	100	92.31	
<b>Overall accuracy (%)</b>	<b>80.31</b>									
<b>Kappa hat coefficient (%)</b>	<b>74.66</b>									

### 5.3.3 LULC classification of DT without splitting samples with eleven bands

Summary of DT construction without splitting samples with eleven bands is summarized in Table 5.25 while binary decision tree structure is displayed in Figure 5.20. It reveals that the final criteria of decision tree for LULC classification applies all eleven bands. The decision tree consists of 101 nodes that includes 55 with tree depth of 11. This binary decision tree is further applied to classify LULC classes under Knowledge Engineer module of Expert System under ERDAS Imagine software.

**Table 5.25** Model summary of DT without splitting samples with eleven bands: specifications and results.

<b>Specifications</b>	Growing Method	CRT
	Dependent Variable	CLASS
	Independent Variables	BLUE, GREEN, RED, NIR, SWIR1, SWIR2, NDVI, MNDWI, NDBI, SLOPE, ELEVATION
	Validation	None
	Maximum Tree Depth	15
	Minimum Cases in Parent Node	10
	Minimum Cases in Child Node	5
	<b>Results</b>	Independent Variables Included
Number of Nodes		101
Number of Terminal Nodes		51
Depth		11



According to accuracy assessment of the model based on training data as model-based inference statistics, the derived decision tree provides overall accuracy of 99.50% (Table 5.26). The accuracy of the derived optimum model for LULC classification varies between 94.00% for Orchard and perennial trees and 100% for paddy field and water bodies.

**Table 5.26** Accuracy assessment of the model based on training data as model-based inference statistics.

Observed	Predicted									Percent Correct
	CV	FA	MA	ML	OP	PD	SU	UB	WB	
Cassava (CV)	1037	27	0	0	0	0	0	0	0	97.50%
Forest area (FA)	9	23727	0	0	40	0	4	0	0	99.80%
Maize (MA)	3	0	1789	2	0	0	0	0	0	99.70%
Miscellaneous land (ML)	3	0	16	949	0	0	0	0	0	98.00%
Orchard and perennial trees (OP)	1	71	0	0	1354	0	14	0	0	94.00%
Paddy field (PD)	1	0	0	0	0	2096	0	0	0	100%
Sugarcane (SU)	3	8	0	0	4	0	1375	0	0	98.90%
Urban and built-up area (UB)	0	0	0	1	0	0	0	32	0	97.00%
Water bodies (WB)	0	0	0	0	0	0	0	0	8296	100%
<b>Overall Percentage</b>	<b>2.60%</b>	<b>58.30%</b>	<b>4.40%</b>	<b>2.30%</b>	<b>3.40%</b>	<b>5.10%</b>	<b>3.40%</b>	<b>0.10%</b>	<b>20.30%</b>	<b>99.50%</b>

The result of LULC classification of DT without splitting samples with eleven bands is summarized in Table 5.27 and distribution of LULC data is displayed in Figure 5.21. Top three dominant LULC classes are forest area, cassava and maize and cover area of 657.38 km<sup>2</sup>, 198.78 km<sup>2</sup> and 114.77 km<sup>2</sup> or 62.35%, 18.85% and 10.89% of the total study area, respectively.

**Table 5.27** Area and percentage of final LULC classification of DT without splitting samples with eleven bands.

No.	LULC class	Area in sq.km	Percent
1	Urban and built-up area	8.94	0.85
2	Paddy field	31.42	2.98
3	Cassava	198.78	18.85
4	Maize	114.77	10.89
5	Sugarcane	4.81	0.46
6	Orchard and perennial trees	16.84	1.60
7	Forest area	657.38	62.35
8	Water bodies	3.25	0.31
9	Miscellaneous land	18.11	1.72
<b>Total</b>		<b>1,054.30</b>	<b>100.00</b>

In addition, the classified LULC map was further performed accuracy assessment with 193 sample points by field survey in 2017 (See Figure 5.3). Error matrix form for LULC accuracy assessment is displayed in Table 5.28. It reveals that overall accuracy is 79.27% and Kappa hat coefficient is 73.13%. Meanwhile producer's accuracy of LULC classes varies between 25.00% for orchards and perennial trees and 100.00% for paddy field and maize while user's accuracy of LULC classes varies between 25.00% for orchards and perennial trees and 100.00% for water bodies. Based on Fitzpatrick-Lins (1981), Kappa hat coefficient between 40-80 percent represents moderate agreement or accuracy between the predicted map and the reference map.



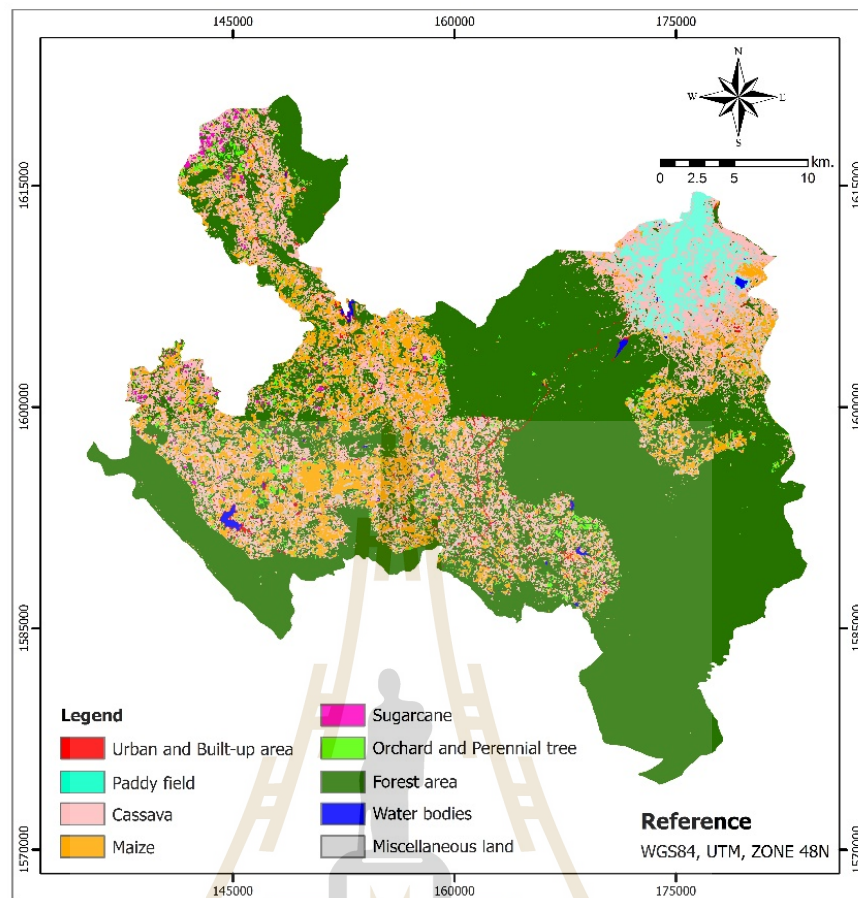


**Figure 5.21** LULC classification of 2015 of DT without splitting samples with eleven bands.

**Table 5.28** Error matrix and accuracy assessment of LULC classification of DT without splitting samples with eleven bands.

Classified LULC class	Reference data									Row Total
	UB	PD	CV	MA	SU	OP	FA	WB	ML	
Urban and built-up area (UB)	3						1			4
Paddy field (PD)	2	5							5	12
Cassava (CV)	1		6		7					14
Maize (MA)				20					6	26
Sugarcane (SU)			1		6	1				8
Orchard and perennial trees (OP)			4		2	2				8
Forest area (FA)					2	5	76			83
Water bodies (WB)								9		9
Miscellaneous land (ML)	2							1	26	29
<b>Column Total</b>	<b>8</b>	<b>5</b>	<b>11</b>	<b>20</b>	<b>17</b>	<b>8</b>	<b>77</b>	<b>10</b>	<b>37</b>	<b>193</b>
<b>Producer's accuracy (%)</b>	37.50	100	54.55	100	35.29	25.00	98.70	90.00	70.27	
<b>User's accuracy (%)</b>	75.00	41.67	42.86	76.92	75.00	25.00	91.57	100	89.66	
<b>Overall accuracy (%)</b>	<b>79.27</b>									
<b>Kappa hat coefficient (%)</b>	<b>73.13</b>									

## Discussion

As results of LULC classification of DT without splitting samples from six, nine, and eleven bands, it can be observed that area of LULC classes from three dataset are quite different as shown in Figure 5.22. In addition, producer's accuracy and user's accuracy of LULC classes of DT without splitting samples from three datasets are rather different as shown in Figure 5.23.

Overall accuracy and Kappa hat coefficient of LULC classification map of DT without splitting samples from six bands provides the best performance. Thus, it can be here concluded that DT without splitting samples from six bands of pan-sharpened Landsat-8 data is the most suitable for LULC classification using DT method without splitting samples under PBIA.

However, the pairwise Z test of DT from three datasets without splitting samples based on Kappa hat analysis shows that accuracy of LULC classification maps are not significantly different at the 80% confidence level as shown in Table 5.29.

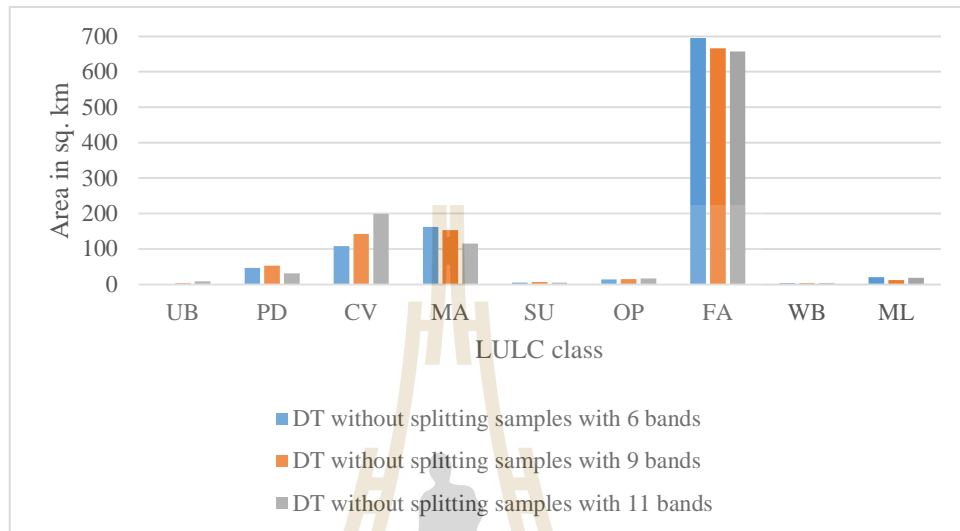


**Figure 5.22** Comparison area of LULC classification of DT without splitting samples.



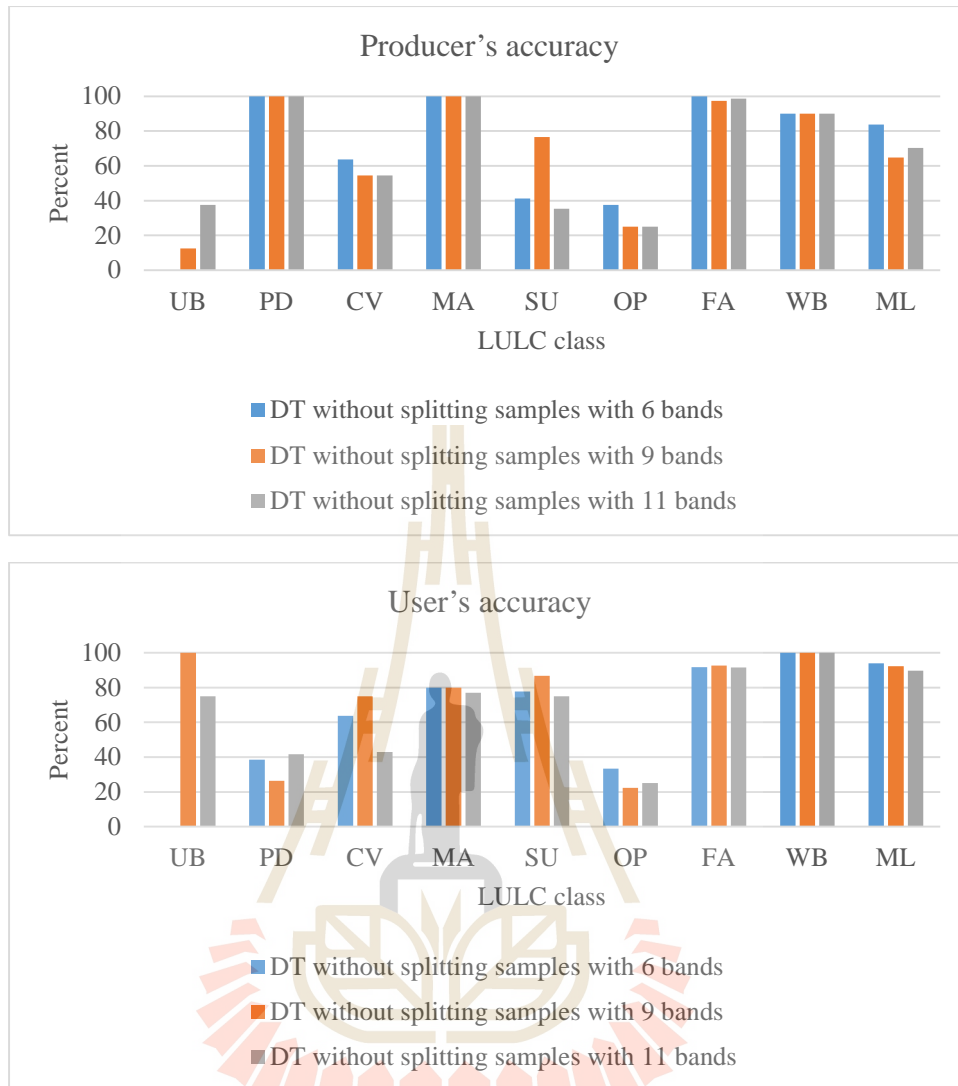


**Figure 5.23** Comparison of producer's accuracy and user's accuracy of LULC classes of DT without splitting samples from six, nine, and eleven bands.

**Table 5.29** Pairwise Z test of Kappa hat coefficient value for LULC extraction in DT without splitting samples.

Pairwise Z test	Kappa hat	Variance	Z-Statistic	Confidential level of critical value			
				80%	90%	95%	100%
DT without splitting samples with six bands	0.77023	0.00113					
DT without splitting samples with nine bands	0.74660	0.00124	<b>0.48576</b>	<b>1.28</b>	<b>1.65</b>	<b>1.96</b>	<b>2.58</b>
DT without splitting samples with six bands	0.77023	0.00113					
DT without splitting samples with eleven bands	0.73128	0.00129	<b>0.79137</b>	<b>1.28</b>	<b>1.65</b>	<b>1.96</b>	<b>2.58</b>
DT without splitting samples with nine bands	0.74660	0.00120					
DT without splitting samples with eleven bands	0.73128	0.00129	<b>0.30662</b>	<b>1.28</b>	<b>1.65</b>	<b>1.96</b>	<b>2.58</b>

#### 5.3.4 LULC classification of DT with splitting samples with six bands

Summary of DT construction with splitting samples with six bands is summarized in Table 5.30 while binary decision tree structure is displayed in Figure 5.24. It reveals that the final criteria of decision tree for LULC classification applies all six bands. The decision tree consists of 135 nodes that includes 68 with tree depth of 15. This binary decision tree is further applied to classify LULC classes under Knowledge Engineer module of Expert System under ERDAS Imagine software.

**Table 5.30** Model summary of DT with splitting samples with six bands: specifications and results.

<b>Specifications</b>	Growing Method	CRT
	Dependent Variable	CLASS
	Independent Variables	BLUE, GREEN, RED, NIR, SWIR1, SWIR2
	Validation	Split Sample
	Maximum Tree Depth	15
	Minimum Cases in Parent Node	10
	Minimum Cases in Child Node	5
<b>Results</b>	Independent Variables Included	BLUE, GREEN, RED, NIR, SWIR1, SWIR2
	Number of Nodes	135
	Number of Terminal Nodes	68
	Depth	15



According to accuracy assessment of the model based on training data as model-based inference statistics, the derived decision tree provides overall accuracy of 98.90% from training data and 98.70% from testing data (Table 5.31).

**Table 5.31** Accuracy assessment of the model based on training data as model-based inference statistics.

Sample	Observed	Predicted									Percent Correct
		CV	FA	MA	ML	OP	PD	SU	UB	WB	
<b>Training</b>	Cassava (CV)	608	40	2	0	2	0	0	0	0	93.30%
	Forest area (FA)	12	14233	0	0	10	0	1	0	0	99.80%
	Maize (MA)	0	0	1054	6	0	6	0	0	0	98.90%
	Miscellaneous land (ML)	0	0	9	575	0	5	0	0	0	97.60%
	Orchard and perennial trees (OP)	0	117	0	0	717	0	13	0	0	84.70%
	Paddy field (PD)	0	0	9	9	0	1276	0	1	0	98.50%
	Sugarcane (SU)	1	6	0	0	5	0	814	0	0	98.50%
	Urban and built-up area (UB)	1	0	0	0	0	5	0	9	0	60.00%
	Water bodies (WB)	0	0	0	0	0	0	0	0	5069	100%
	<b>Overall Percentage</b>	<b>2.50%</b>	<b>58.50%</b>	<b>4.40%</b>	<b>2.40%</b>	<b>3.00%</b>	<b>5.20%</b>	<b>3.40%</b>	<b>0.00%</b>	<b>20.60%</b>	<b>98.90%</b>
<b>Test</b>	Cassava (CV)	371	36	3	0	1	0	1	0	0	90.00%
	Forest area (FA)	12	9505	0	0	7	0	0	0	0	99.80%
	Maize (MA)	0	0	720	7	0	1	0	0	0	98.90%
	Miscellaneous land (ML)	1	0	5	369	0	4	0	0	0	97.40%
	Orchard and perennial trees (OP)	0	90	0	0	489	0	14	0	0	82.50%
	Paddy field (PD)	0	0	4	6	0	789	0	3	0	98.40%
	Sugarcane (SU)	6	1	0	0	5	0	552	0	0	97.90%
	Urban and built-up area (UB)	1	1	0	0	0	7	0	9	0	50.00%
	Water bodies (WB)	0	0	0	0	0	0	0	0	3227	100%
	<b>Overall Percentage</b>	<b>2.40%</b>	<b>59.30%</b>	<b>4.50%</b>	<b>2.40%</b>	<b>3.10%</b>	<b>4.90%</b>	<b>3.50%</b>	<b>0.10%</b>	<b>19.90%</b>	<b>98.70%</b>

The result of LULC classification of DT with splitting samples with six bands is summarized in Table 5.32 and distribution of LULC data is displayed in Figure 5.25. Top three dominant LULC classes are forest area, maize, and cassava and cover area of 695.41 km<sup>2</sup>, 169.65 km<sup>2</sup> and 104.86 km<sup>2</sup> or 65.96%, 16.09% and 9.95% of the total study area, respectively.



**Table 5.32** Area and percentage of final LULC classification of DT with splitting samples with six bands.

No.	LULC class	Area in sq.km	Percent
1	Urban and built-up area	0.53	0.05
2	Paddy field	39.53	3.75
3	Cassava	104.86	9.95
4	Maize	169.65	16.09
5	Sugarcane	4.64	0.44
6	Orchard and perennial trees	14.02	1.33
7	Forest area	695.41	65.96
8	Water bodies	3.31	0.31
9	Miscellaneous land	22.35	2.12
<b>Total</b>		<b>1,054.30</b>	<b>100.00</b>

In addition, the classified LULC map was further performed accuracy assessment with 193 sample points by field survey in 2017 (See Figure 5.3). Error matrix form for LULC accuracy assessment is displayed in Table 5.33. It reveals that overall accuracy is 81.87% and Kappa hat coefficient is 76.23%. Meanwhile producer's accuracy of LULC classes varies between 0.00% for urban and built-up area and 100.00% for paddy field, maize, and forest area while user's accuracy of LULC classes varies between 0% for urban and built-up area and 100.00% for water bodies. Based on Fitzpatrick-Lins (1981), Kappa hat coefficient between 40-80 percent represents moderate agreement or accuracy between the predicted map and the reference map.

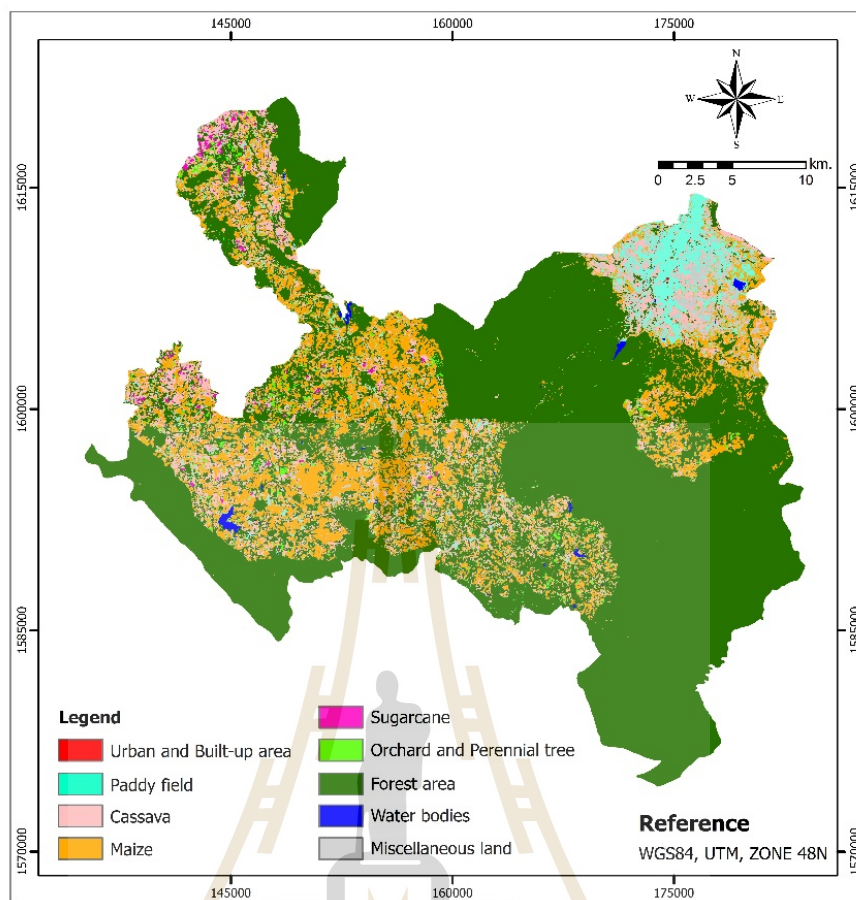


**Figure 5.25** LULC classification of 2015 of DT with splitting samples with six bands.

**Table 5.33** Error matrix and accuracy assessment of LULC classification of DT with splitting samples with six bands.

Classified LULC class	Reference data									Row Total
	UB	PD	CV	MA	SU	OP	FA	WB	ML	
Urban and built-up area (UB)	0									0
Paddy field (PD)	7	5							1	13
Cassava (CV)			7		4					11
Maize (MA)				20					5	25
Sugarcane (SU)			1		7	1				9
Orchard and perennial trees (OP)			2		3	2				7
Forest area (FA)			1		3	5	77			86
Water bodies (WB)								9		9
Miscellaneous land (ML)	1							1	31	33
<b>Column Total</b>	<b>8</b>	<b>5</b>	<b>11</b>	<b>20</b>	<b>17</b>	<b>8</b>	<b>77</b>	<b>10</b>	<b>37</b>	<b>193</b>
<b>Producer's accuracy (%)</b>	0	100	63.64	100	41.18	25.00	100	90.00	83.78	
<b>User's accuracy (%)</b>	0	38.00	63.64	80.00	77.78	28.57	89.53	100	93.94	
<b>Overall accuracy (%)</b>	<b>81.87</b>									
<b>Kappa hat coefficient (%)</b>	<b>76.23</b>									

### 5.3.5 LULC classification of DT with splitting samples with nine bands

Summary of DT construction with splitting samples with nine bands is summarized in Table 5.34 while binary decision tree structure is displayed in Figure 5.26. It reveals that the final criteria of decision tree for LULC classification applies all nine bands. The decision tree consists of 175 nodes that includes 88 with tree depth of 15. This binary decision tree is further applied to classify LULC classes under Knowledge Engineer module of Expert System under ERDAS Imagine software.

**Table 5.34** Model summary of DT with splitting samples with nine bands: specifications and results.

<b>Specifications</b>	Growing Method	CRT
	Dependent Variable	CLASS
	Independent Variables	BLUE, GREEN, RED, NIR, SWIR1, SWIR2, NDVI, MNDWI, NDBI
	Validation	Split Sample
	Maximum Tree Depth	15
	Minimum Cases in Parent Node	5
	Minimum Cases in Child Node	1
<b>Results</b>	Independent Variables Included	BLUE, GREEN, RED, NIR, SWIR1, SWIR2, NDVI, MNDWI, NDBI
	Number of Nodes	175
	Number of Terminal Nodes	88
	Depth	15

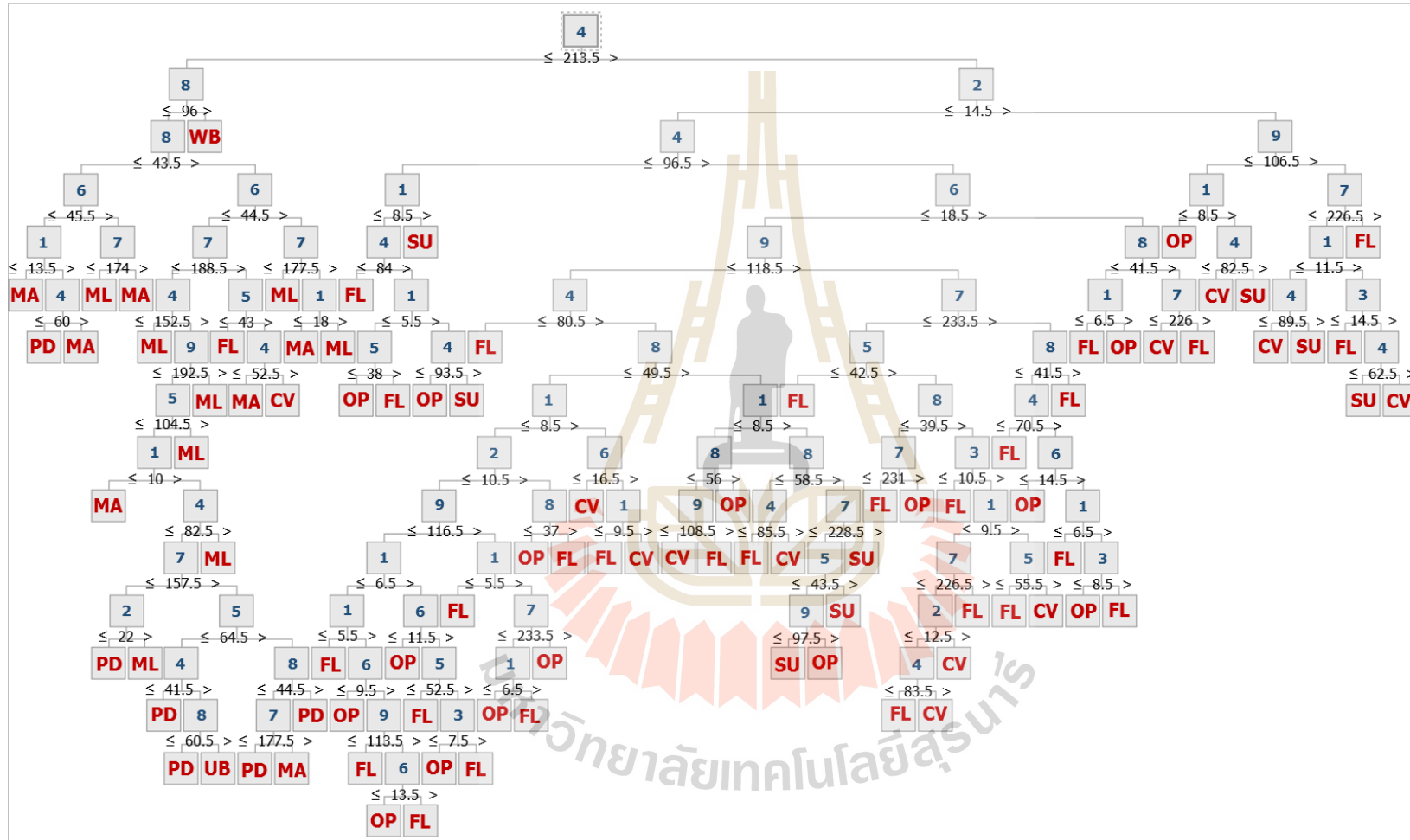


Figure 5.26 Binary decision tree structure for LULC classification with splitting samples with nine bands.

According to accuracy assessment of the model based on training data as model-based inference statistics, the derived decision tree provides overall accuracy of 99.30% of training data and 98.90% from testing data (Table 5.35).

**Table 5.35** Accuracy assessment of the model based on training data as model-based inference statistics.

Sample	Observed	Predicted									Percent Correct
		CV	FA	MA	ML	OP	PD	SU	UB	WB	
<b>Training</b>	Cassava (CV)	605	20	0	0	0	0	0	0	0	96.80%
	Forest area (FA)	14	14338	0	0	17	0	0	0	0	99.80%
	Maize (MA)	0	0	1071	2	0	2	0	0	0	99.60%
	Miscellaneous land (ML)	1	0	5	576	0	9	0	0	0	97.50%
	Orchard and perennial trees (OP)	2	62	0	0	810	0	2	0	0	92.50%
	Paddy field (PD)	1	0	4	9	0	1234	0	4	0	98.60%
	Sugarcane (SU)	2	0	0	0	3	0	834	0	0	99.40%
	Urban and built-up area (UB)	0	1	0	0	0	4	0	21	0	80.80%
	Water bodies (WB)	0	0	0	0	0	0	0	0	4985	100%
	<b>Overall Percentage</b>	<b>2.50%</b>	<b>58.50%</b>	<b>4.40%</b>	<b>2.40%</b>	<b>3.40%</b>	<b>5.10%</b>	<b>3.40%</b>	<b>0.10%</b>	<b>20.20%</b>	<b>99.30%</b>
<b>Test</b>	Cassava (CV)	407	21	2	0	2	0	7	0	0	92.70%
	Forest area (FA)	6	9380	0	0	24	0	1	0	0	99.70%
	Maize (MA)	1	0	711	2	0	5	0	0	0	98.90%
	Miscellaneous land (ML)	0	0	6	362	0	9	0	0	0	96.00%
	Orchard and perennial trees (OP)	0	56	0	0	506	0	2	0	0	89.70%
	Paddy field (PD)	1	0	6	12	0	820	0	6	0	97.00%
	Sugarcane (SU)	8	0	0	0	6	0	537	0	0	97.50%
	Urban and built-up area (UB)	0	0	0	0	0	3	0	4	0	57.10%
	Water bodies (WB)	0	0	0	0	0	0	0	0	3311	100%
	<b>Overall Percentage</b>	<b>2.60%</b>	<b>58.30%</b>	<b>4.50%</b>	<b>2.30%</b>	<b>3.30%</b>	<b>5.20%</b>	<b>3.40%</b>	<b>0.10%</b>	<b>20.40%</b>	<b>98.90%</b>

The result of LULC classification of DT with splitting samples with six bands is summarized in Table 5.36 and distribution of LULC data is displayed in Figure 5.27. Top three dominant LULC classes are forest area, maize, and cassava and cover

area of 671.76 km<sup>2</sup>, 148.26 km<sup>2</sup> and 145.83 km<sup>2</sup> or 63.72%, 14.06% and 13.83% of the total study area, respectively.

**Table 5.36** Area and percentage of final LULC classification of DT with splitting samples with nine bands.

No.	LULC class	Area in sq.km	Percent
1	Urban and built-up area	1.50	0.14
2	Paddy field	47.06	4.46
3	Cassava	145.83	13.83
4	Maize	148.26	14.06
5	Sugarcane	4.23	0.40
6	Orchard and perennial trees	12.72	1.21
7	Forest area	671.76	63.72
8	Water bodies	3.53	0.33
9	Miscellaneous land	19.42	1.84
<b>Total</b>		<b>1,054.30</b>	<b>100.00</b>

In addition, the classified LULC map was further performed accuracy assessment with 193 sample points by field survey in 2017 (See Figure 5.3). Error matrix form for LULC accuracy assessment is displayed in Table 5.37. It reveals that overall accuracy is 79.79% and Kappa hat coefficient is 73.77%. Meanwhile producer's accuracy of LULC classes varies between 0% for urban and built-up area and 100.00% for paddy field and maize while user's accuracy of LULC classes varies between 0% for urban and built-up area and 100.00% for water bodies. Based on Fitzpatrick-Lins (1981), Kappa hat coefficient between 40-80 percent represents moderate agreement or accuracy between the predicted map and the reference map.

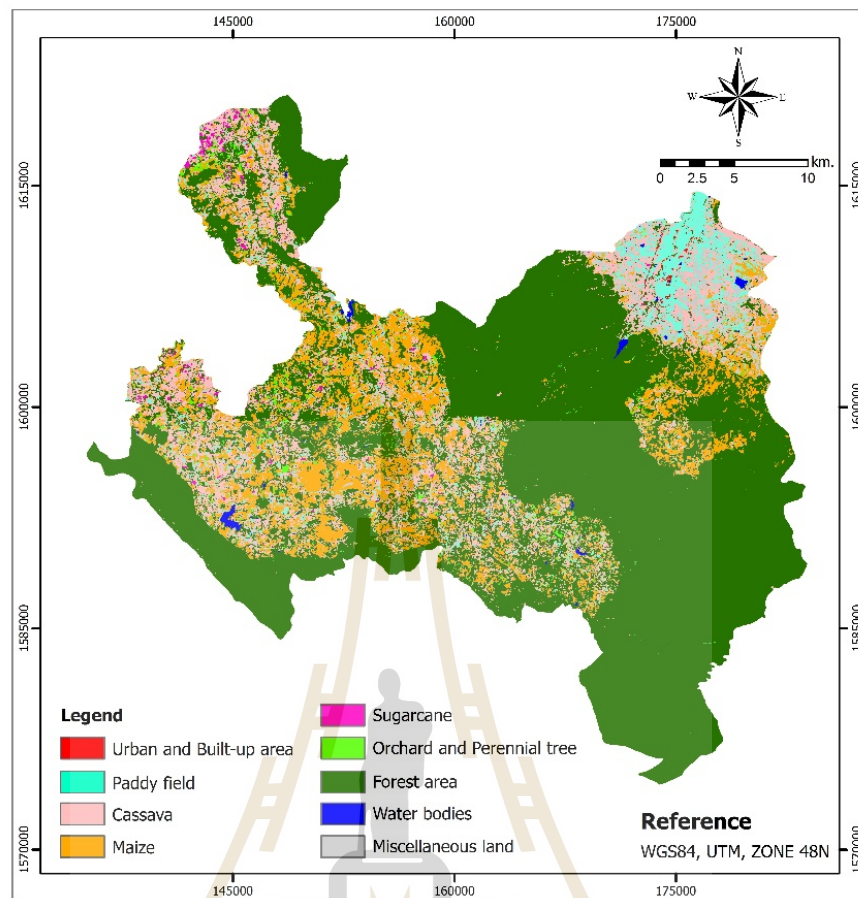


**Figure 5.27** LULC classification of 2015 of DT with splitting samples with nine bands.



**Table 5.37** Error matrix and accuracy assessment of LULC classification of DT with splitting samples with nine bands.

Classified LULC class	Reference data									Row Total
	UB	PD	CV	MA	SU	OP	FA	WB	ML	
Urban and built-up area (UB)	0									0
Paddy field (PD)	7	5							3	15
Cassava (CV)			6		6		1			13
Maize (MA)				20					6	26
Sugarcane (SU)			1		8	1				10
Orchard and perennial trees (OP)			2		3	2				7
Forest area (FA)			2			5	76			83
Water bodies (WB)								9		9
Miscellaneous land (ML)	1							1	28	30
<b>Column Total</b>	<b>8</b>	<b>5</b>	<b>11</b>	<b>20</b>	<b>17</b>	<b>8</b>	<b>77</b>	<b>10</b>	<b>37</b>	<b>193</b>
<b>Producer's accuracy (%)</b>	0	100	54.55	100	47.06	25.00	98.70	90.00	75.68	
<b>User's accuracy (%)</b>	0	33.33	46.15	76.92	80.00	28.57	91.57	100	93.33	
<b>Overall accuracy (%)</b>	<b>79.79</b>									
<b>Kappa hat coefficient (%)</b>	<b>73.77</b>									

### 5.3.6 LULC classification of DT with splitting samples with eleven bands

Summary of DT construction with splitting samples with eleven bands is summarized in Table 5.38 while binary decision tree structure is displayed in Figure 5.28. It reveals that the final criteria of decision tree for LULC classification applies all eleven bands. The decision tree consists of 87 nodes that includes 44 with tree depth of 11. This binary decision tree is further applied to classify LULC classes under Knowledge Engineer module of Expert System under ERDAS Imagine software.

**Table 5.38** Model summary of DT without splitting samples with eleven bands: specifications and results.

Specifications	Growing Method	CRT
	Dependent Variable	CLASS
	Independent Variables	BLUE, GREEN, RED, NIR, SWIR1, SWIR2, NDVI, MNDWI, NDBI, SLOPE, ELEVATION
	Validation	Split Sample
	Maximum Tree Depth	15
	Minimum Cases in Parent Node	10
	Minimum Cases in Child Node	5
	Results	Independent Variables Included
Number of Nodes		87
Number of Terminal Nodes		44
Depth		11

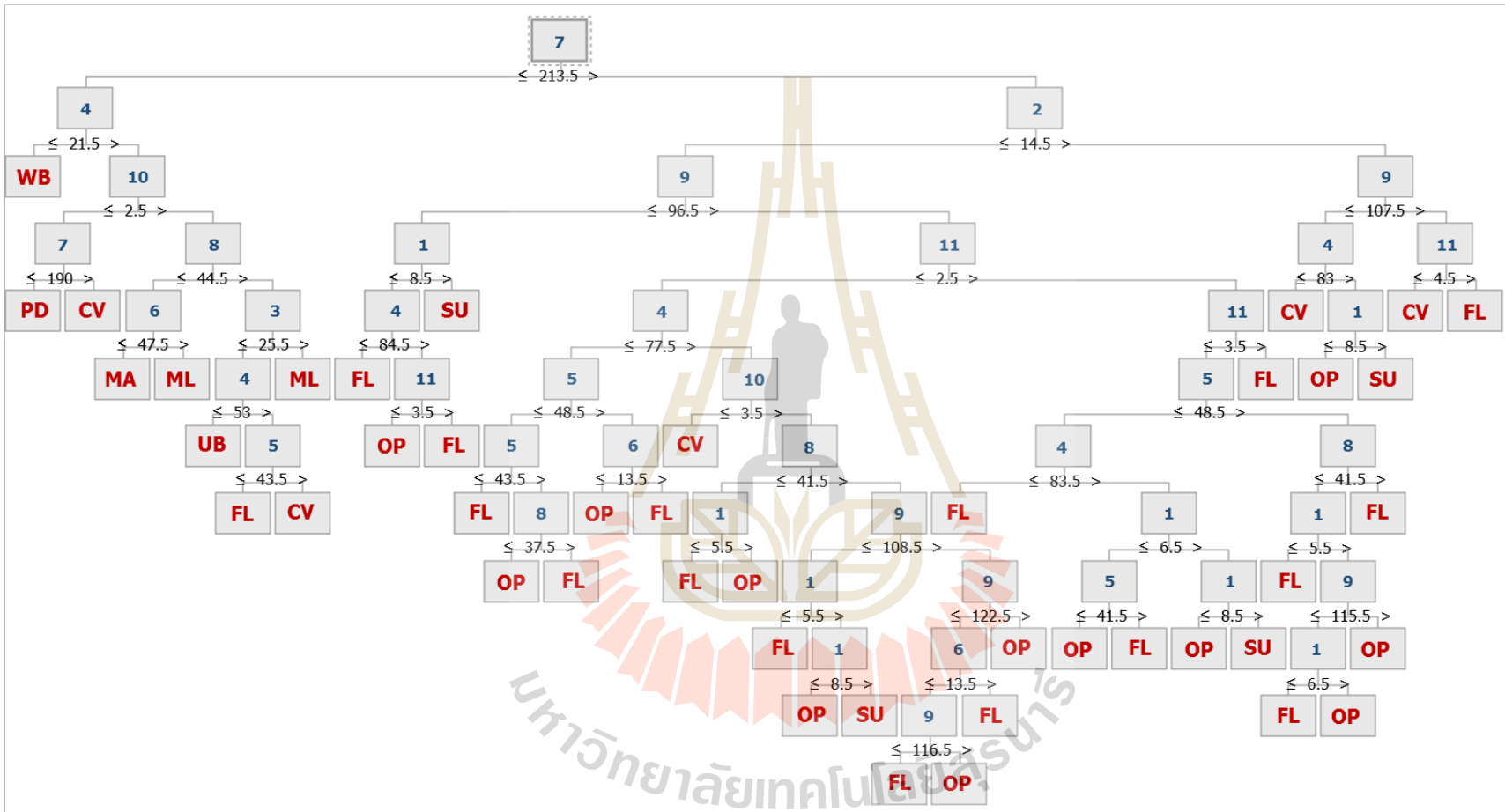


Figure 5.28 Binary decision tree structure for LULC classification with splitting samples with eleven bands.

According to accuracy assessment of the model based on training data as model-based inference statistics, the derived decision tree provides overall accuracy of 99.40% from training data and 99.20% from testing data (Table 5.39).

**Table 5.39** Accuracy assessment of the model based on training data as model-based inference statistics.

Sample	Observed	Predicted									Percent Correct
		CV	FA	MA	ML	OP	PD	SU	UB	WB	
<b>Training</b>	Cassava (CV)	627	17	4	0	0	0	0	0	0	96.80%
	Forest area (FA)	5	14238	0	0	25	0	0	0	0	99.80%
	Maize (MA)	0	0	1072	3	0	0	0	4	0	99.40%
	Miscellaneous land (ML)	0	0	14	553	0	0	0	0	0	97.50%
	Orchard and perennial trees (OP)	1	46	0	0	828	0	5	0	0	94.10%
	Paddy field (PD)	0	0	0	0	0	1207	0	0	0	100%
	Sugarcane (SU)	5	4	0	0	5	0	828	0	0	98.30%
	Urban and built-up area (UB)	0	0	0	2	0	0	0	23	0	92.00%
	Water bodies (WB)	0	0	0	0	0	0	0	0	4991	100%
	<b>Overall Percentage</b>	<b>2.60%</b>	<b>58.40%</b>	<b>4.40%</b>	<b>2.30%</b>	<b>3.50%</b>	<b>4.90%</b>	<b>3.40%</b>	<b>0.10%</b>	<b>20.40%</b>	<b>99.40%</b>
<b>Test</b>	Cassava (CV)	395	18	3	0	0	0	0	0	0	95.00%
	Forest area (FA)	3	9491	0	0	18	0	0	0	0	99.80%
	Maize (MA)	0	0	705	4	0	0	0	6	0	98.60%
	Miscellaneous land (ML)	0	0	10	391	0	0	0	0	0	97.50%
	Orchard and perennial trees (OP)	0	39	0	0	517	0	4	0	0	92.30%
	Paddy field (PD)	1	0	0	0	0	889	0	0	0	99.90%
	Sugarcane (SU)	10	5	0	0	3	0	530	0	0	96.70%
	Urban and built-up area (UB)	0	0	0	1	0	0	0	7	0	87.50%
	Water bodies (WB)	0	0	0	0	0	0	0	0	3305	100%
	<b>Overall Percentage</b>	<b>2.50%</b>	<b>58.40%</b>	<b>4.40%</b>	<b>2.40%</b>	<b>3.30%</b>	<b>5.40%</b>	<b>3.30%</b>	<b>0.10%</b>	<b>20.20%</b>	<b>99.20%</b>

The result of LULC classification of DT without splitting samples with eleven bands is summarized in Table 5.40 and distribution of LULC data is displayed in Figure 5.29. Top three dominant LULC classes are forest area, maize, and cassava

and cover area of 681.94 km<sup>2</sup>, 151.29 km<sup>2</sup> and 120.91 km<sup>2</sup> or 64.68%, 14.35% and 11.47% of the total study area, respectively.

**Table 5.40** Area and percentage of final LULC classification of DT with splitting samples with eleven bands.

No.	LULC class	Area in sq.km	Percent
1	Urban and built-up area	22.04	2.09
2	Paddy field	31.44	2.98
3	Cassava	120.91	11.47
4	Maize	151.29	14.35
5	Sugarcane	3.99	0.38
6	Orchard and perennial trees	11.62	1.10
7	Forest area	681.94	64.68
8	Water bodies	3.20	0.30
9	Miscellaneous land	27.87	2.64
<b>Total</b>		<b>1,054.30</b>	<b>100.00</b>

In addition, the classified LULC map was further performed accuracy assessment with 193 sample points by field survey in 2017 (See Figure 5.3). Error matrix form for LULC accuracy assessment is displayed in Table 5.41. It reveals that overall accuracy is 79.27% and Kappa hat coefficient is 72.93%. Meanwhile producer's accuracy of LULC classes varies between 25.00% for urban and built-up area and orchard and perennial trees and 100.00% for paddy field and maize while user's accuracy of LULC classes varies between 33.33% for orchards and perennial trees and 100.00% for water bodies. Based on Fitzpatrick-Lins (1981), Kappa hat coefficient between 40-80 percent represents moderate agreement or accuracy between the predicted map and the reference map.

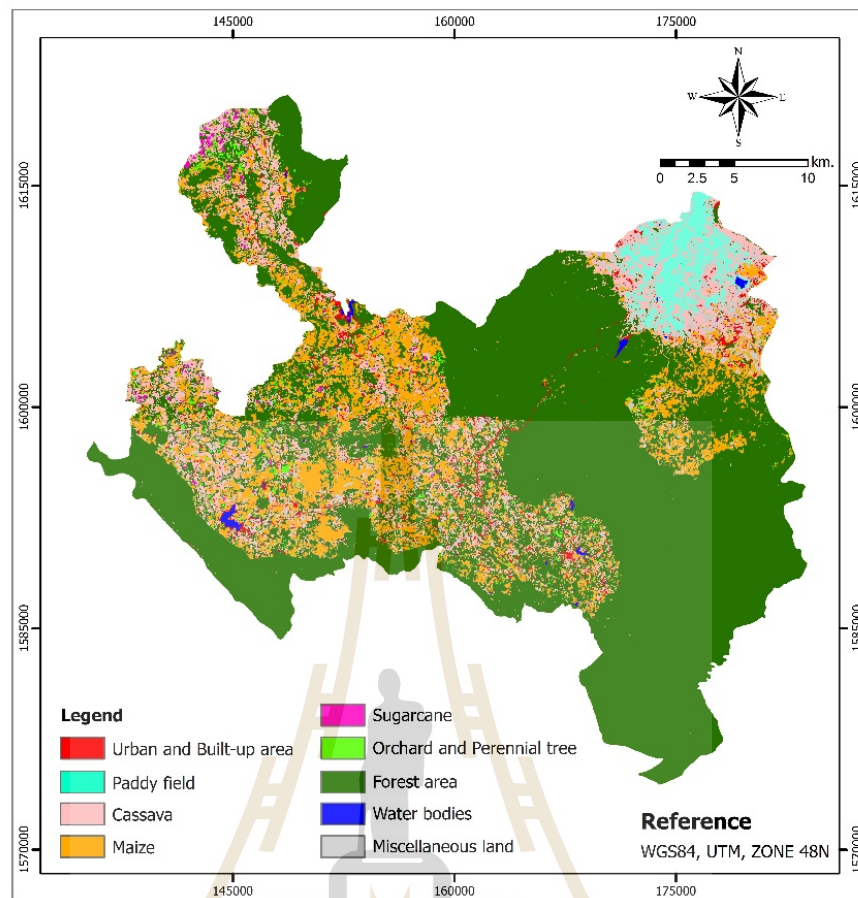


**Figure 5.29** LULC classification of 2015 of DT with splitting samples with eleven bands.

**Table 5.41** Error matrix and accuracy assessment of LULC classification of DT with splitting samples with eleven bands.

Classified LULC class	Reference data									Row Total
	UB	PD	CV	MA	SU	OP	FA	WB	ML	
Urban and built-up area (UB)	2						1		1	4
Paddy field (PD)	2	5								12
Cassava (CV)			6		6					12
Maize (MA)			1	20					4	25
Sugarcane (SU)			1		6	1				8
Orchard and perennial trees (OP)			2		2	2				6
Forest area (FA)			1		3	5	76			85
Water bodies (WB)								9		9
Miscellaneous land (ML)	4							1	27	32
<b>Column Total</b>	<b>8</b>	<b>5</b>	<b>11</b>	<b>20</b>	<b>17</b>	<b>8</b>	<b>77</b>	<b>10</b>	<b>37</b>	<b>193</b>
<b>Producer's accuracy (%)</b>	25.00	100	54.55	100	35.29	25.00	98.70	90.00	72.97	
<b>User's accuracy (%)</b>	50.00	41.67	50.00	80.00	75.00	33.33	89.41	100	84.38	
<b>Overall accuracy (%)</b>	<b>79.27</b>									
<b>Kappa hat coefficient (%)</b>	<b>72.93</b>									

## Discussion

As results of LULC classification of DT with splitting samples from six, nine, and eleven bands, it can be observed that area of LULC classes from three dataset are similar as shown in Figure 5.30.

Overall accuracy and Kappa hat coefficient of LULC classification map of DT with splitting samples from six bands also provides the best performance. Producer's accuracy and user's accuracy of LULC classes of DT without splitting samples from three datasets are rather different as shown in Figure 5.31.

However, the pairwise Z test of DT from three datasets with splitting samples based on Kappa hat analysis show that accuracy of LULC classification maps are not significantly different at the 80% confidence level as shown in Table 5.42.

Additionally, it can be here concluded that DT with splitting samples from six bands is the most suitable for LULC classification using DT method under PBI.

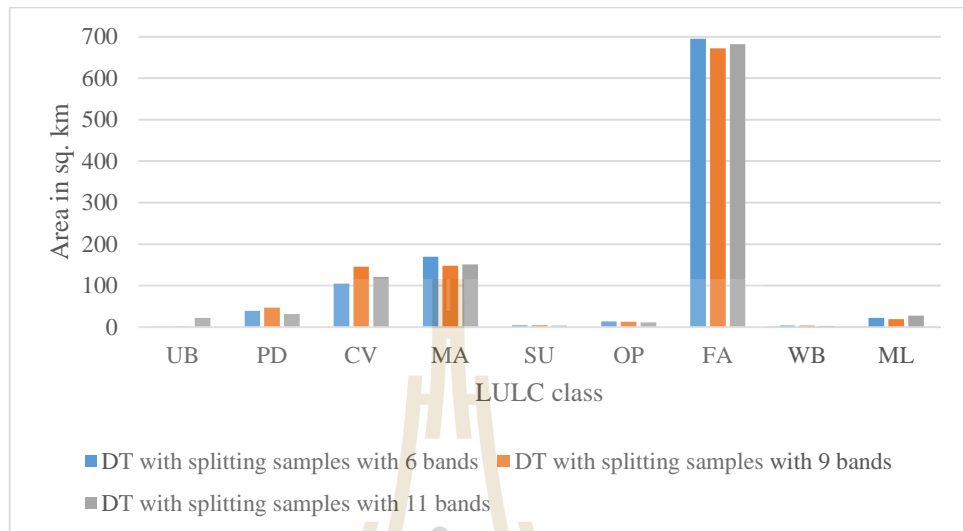


**Figure 5.30** Comparison area of LULC classification of DT with splitting samples from six, nine, and eleven bands.



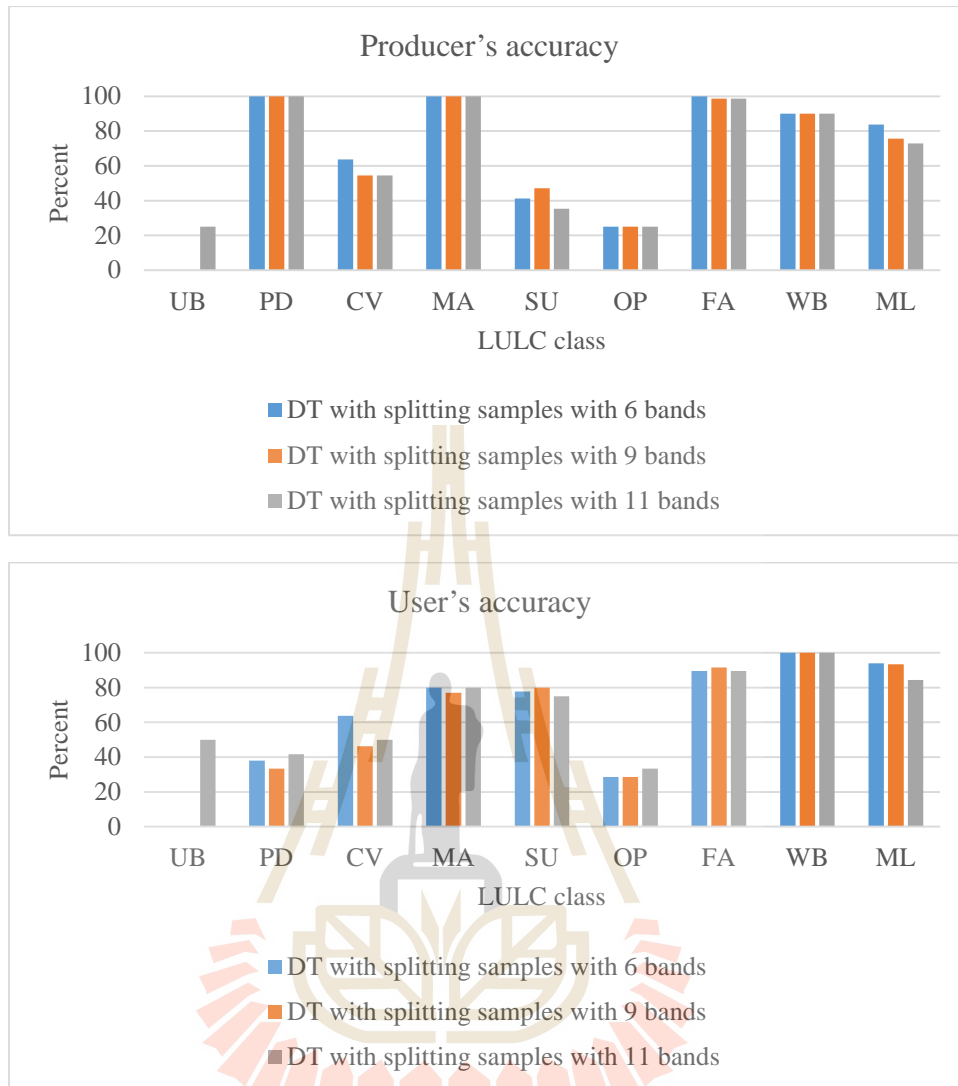


**Figure 5.31** Comparison of producer's accuracy and user's accuracy of LULC classes of DT with splitting samples from six, nine, and eleven bands.

**Table 5.42** Pairwise Z test of Kappa hat coefficient value for LULC extraction in DT with splitting samples from three datasets.

Pairwise Z test	Kappa hat	Variance	Z-Statistic	Confidential level of critical value			
				80%	90%	95%	100%
LULC data of DT with splitting samples with six bands	0.76232	0.00117	<b>0.49972</b>	<b>1.28</b>	<b>1.65</b>	<b>1.96</b>	<b>2.58</b>
DT with splitting samples with nine bands	0.73768	0.00126					
DT with splitting samples with six bands	0.76232	0.00117	<b>0.66115</b>	<b>1.28</b>	<b>1.65</b>	<b>1.96</b>	<b>2.58</b>
DT with splitting samples with eleven bands	0.72933	0.00132					
DT with splitting samples with nine bands	0.73768	0.00123	<b>0.16544</b>	<b>1.28</b>	<b>1.65</b>	<b>1.96</b>	<b>2.58</b>
DT with splitting samples with eleven bands	0.72933	0.00132					

Furthermore, overall accuracy and Kappa hat coefficient of LULC classification map of DT with and without splitting samples for decision tree construction in each dataset (six, nine, eleven bands) are compared to identify the most suitable DT method for LULC classification. It reveals that DT without splitting sample for decision tree construction of six bands provides the highest accuracy for LULC classification as shown in Figure 5.32. Producer's accuracy and user's accuracy of LULC classes of DT with and without splitting samples of three different bands are rather different as shown in Figure 5.33. It can be here concluded that DT without splitting samples from six bands of pan-sharpened Landsat-8 data is the most suitable for LULC classification using DT method without splitting samples under PBIA.

However, the pairwise Z test of DT from with and without splitting samples of six, nine, and eleven bands based on Kappa hat coefficient and their error matrices

reveals that accuracy of LULC classification maps of DT with and without splitting samples of three different datasets are not significantly different at the 80% confidence level as shown in Table 5.43. This finding implies that the most effective dataset for LULC classification of DT with and without splitting samples is six bands dataset.

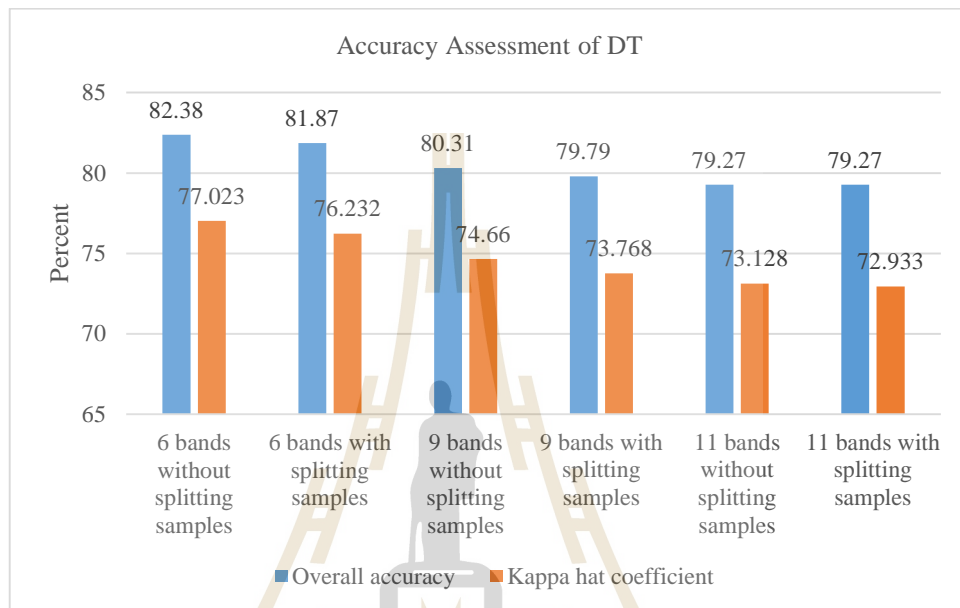


**Figure 5.32** Accuracy assessment of DT classification with and without splitting sample for decision tree construction in each dataset (six, nine, eleven bands).

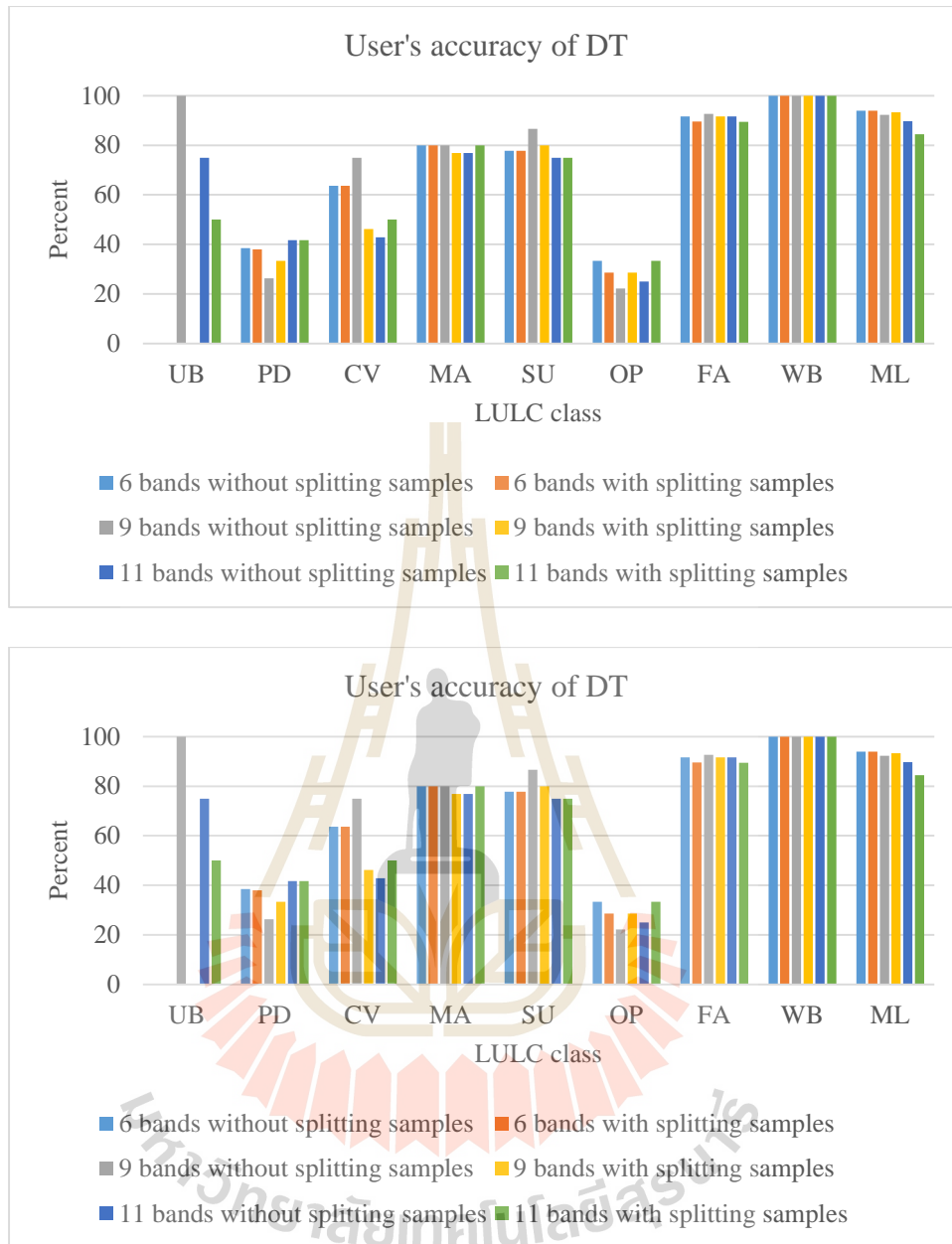


**Figure 5.33** Comparison of producer's accuracy and user's accuracy of LULC classes of DT classification with and without splitting sample for decision tree construction in each dataset (six, nine, eleven bands).

**Table 5.43** Pairwise Z test of Kappa hat coefficient value for LULC extraction in DT with splitting samples.

Pairwise Z test	Kappa hat	Variance	Z-Statistic	Confidential level of critical value			
				80%	90%	95%	100%
DT without splitting samples with six bands	0.77023	0.00113	<b>0.16377</b>	<b>1.28</b>	<b>1.65</b>	<b>1.96</b>	<b>2.58</b>
DT with splitting samples with six bands	0.76232	0.00120					
DT without splitting samples with nine bands	0.74660	0.00120	<b>0.17957</b>	<b>1.28</b>	<b>1.65</b>	<b>1.96</b>	<b>2.58</b>
DT with splitting samples with nine bands	0.73768	0.00126					
DT without splitting samples with eleven bands	0.73128	0.00125	<b>0.03844</b>	<b>1.28</b>	<b>1.65</b>	<b>1.96</b>	<b>2.58</b>
DT with splitting samples with eleven bands	0.72933	0.00132					

## **CHAPTER VI**

### **OBJECT-BASED IMAGE ANALYSIS**

Results of the representative object-based classification method: standard nearest neighbor classifier (SNN) and nearest neighbor classifier with feature space optimization (FSO) under object-based image analysis (OBIA) are here reported and discussed under this chapter.

#### **6.1 LULC classification of SNN**

Three datasets of pan-sharpened Landsat-8 and additional bands included (1) six pan-sharpened Landsat-8 bands (Band 2, 3, 4, 5, 6 and 7); (2) nine bands of six pan-sharpened Landsat-8 bands (Band 2, 3, 4, 5, 6 and 7) and three spectral bands (NDVI, MNDWI and NDBI); and (3) eleven bands of six pan-sharpened Landsat-8 bands (Band 2, 3, 4, 5, 6 and 7), three spectral bands (NDVI, MNDWI and NDBI) and two physical data (elevation and slope) were here applied to extract LULC using SNN method under OBIA of the eCognition software. In practice, images of each dataset are firstly segmented using multiresolution segmentation method with specific scale and weight of spectral, shape, compactness and smoothness, then image object samples of each LULC class were collected and applied for LULC classification using SNN method.

Figure 6.1 displays segmented image as image objects using multiresolution segmentation with the scale factor of 15 and color parameter of 0.9 and compactness of

0.5. Summary of image segmentation and its parameter and number of image objects of three datasets for LULC classification with SNN is presented in Table 6.1.

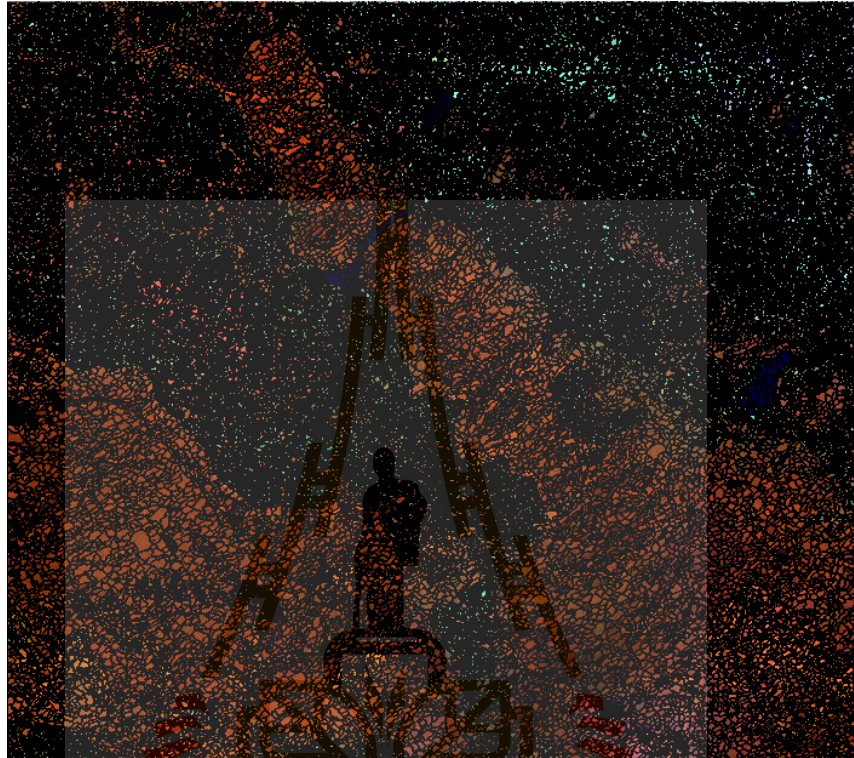


**Figure 6.1** Image segmentation as image objects using multiresolution segmentation with the scale factor of 15, color parameter of 0.9 and compactness of 0.5.

**Table 6.1** Parameter setting of multiresolution segmentation and number of the derived image objects of three datasets for LULC classification with SNN.

Number of bands	Scale	Color weight	Shape weight = 0.1		Number of image objects
			Compactness	Smoothness	
6 bands	15	0.9	0.5	0.5	71,231
9 bands	15	0.9	0.5	0.5	78,106
11 bands	15	0.9	0.5	0.5	67,819

Meanwhile, Figure 6.2 displays an example of image object samples as training areas of each LULC classes. These training areas of SNN were also applied to nearest neighbor classifier with feature space optimization (FSO). The standard features that were applied for LULC classification with SNN of each dataset in this study is summarized in Table 6.2





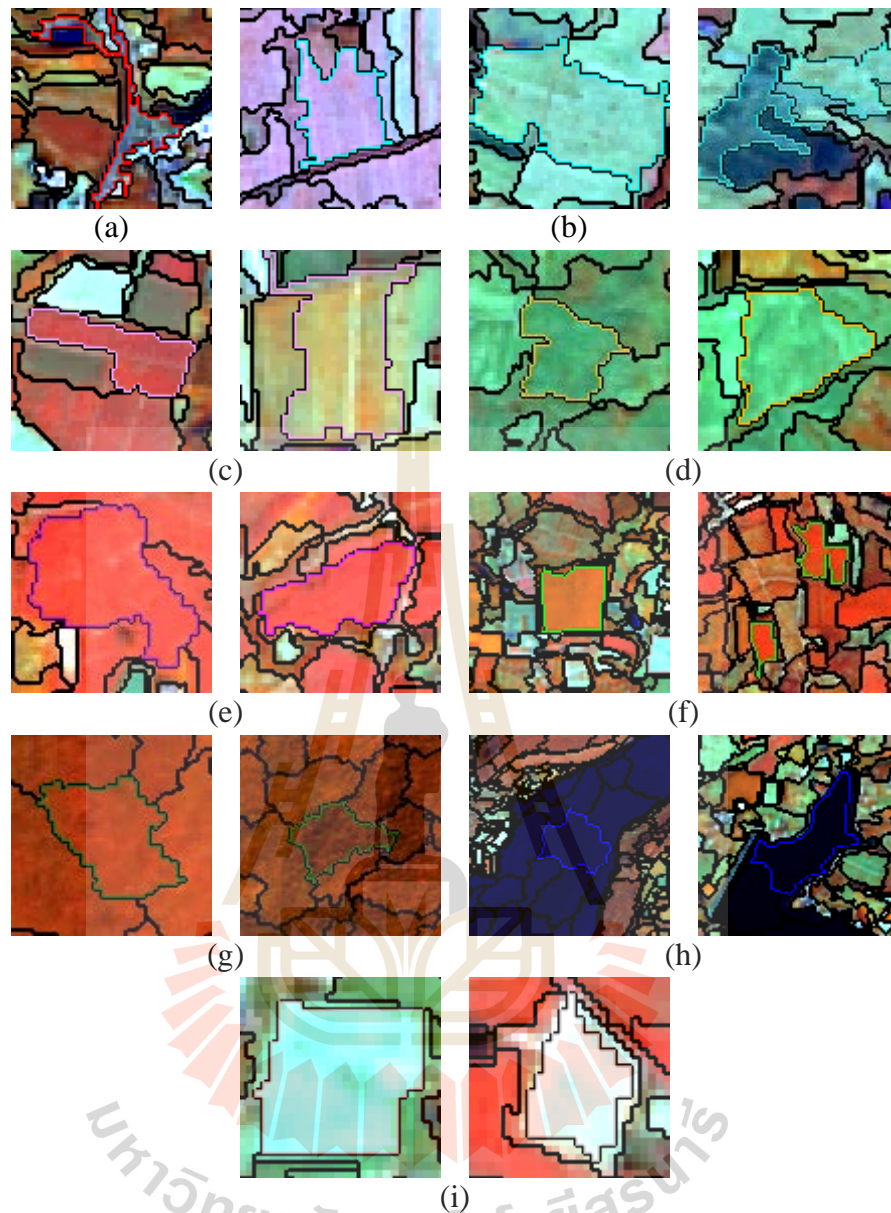


**Figure 6.2** Training areas of 9 LULC classes for SNN and FSO methods: (a) urban and built-up area, (b) paddy field, (c) cassava, (d) maize, (e) sugarcane, (f) orchard and perennial trees, (g) forest area, (h) water bodies and (i) miscellaneous land.

**Table 6.2** List of features of SNN with three different dataset.

No	Dataset		
	Six bands	Nine bands	Eleven bands
1	Brightness	Brightness	Brightness
2	Mean layer 1 (Band 2)	Mean layer 1 (Band 2)	Mean layer 1 (Band 2)
3	Mean layer 2 (Band 3)	Mean layer 2 (Band 3)	Mean layer 2 (Band 3)
4	Mean layer 3 (Band 4)	Mean layer 3 (Band 4)	Mean layer 3 (Band 4)
5	Mean layer 4 (Band 5)	Mean layer 4 (Band 5)	Mean layer 4 (Band 5)
6	Mean layer 5 (Band 6)	Mean layer 5 (Band 6)	Mean layer 5 (Band 6)
7	Mean layer 6 (Band 7)	Mean layer 6 (Band 7)	Mean layer 6 (Band 7)
8	Max. Diff.	Mean layer 7 (NDVI)	Mean layer 7 (NDVI)
9	Std. deviation 1 (Band 2)	Mean layer 8 (MNDWI)	Mean layer 8 (MNDWI)
10	Std. deviation 2 (Band 3)	Mean layer 9 (NDBI)	Mean layer 9 (NDBI)
11	Std. deviation 3 (Band 4)	Max. Diff.	Mean layer 10 (ELEVATION)
12	Std. deviation 4 (Band 5)	Std. deviation 1 (Band 2)	Mean layer 11 (SLOPE)
13	Std. deviation 5 (Band 6)	Std. deviation 2 (Band 3)	Max. Diff.
14	Std. deviation 6 (Band 7)	Std. deviation 3 (Band 4)	Std. deviation 1 (Band 2)
15	Ratio 1 (Band 2)	Std. deviation 4 (Band 5)	Std. deviation 2 (Band 3)
16	Ratio 2 (Band 3)	Std. deviation 5 (Band 6)	Std. deviation 3 (Band 4)
17	Ratio 3 (Band 4)	Std. deviation 6 (Band 7)	Std. deviation 4 (Band 5)
18	Ratio 4 (Band 5)	Std. deviation 7 (NDVI)	Std. deviation 5 (Band 6)
19	Ratio 5 (Band 6)	Std. deviation 8 (MNDWI)	Std. deviation 6 (Band 7)
20	Ratio 6 (Band 7)	Std. deviation 9 (NDBI)	Std. deviation 7 (NDVI)
21		Ratio 1 (Band 2)	Std. deviation 8 (MNDWI)
22		Ratio 2 (Band 3)	Std. deviation 9 (NDBI)
23		Ratio 3 (Band 4)	Std. deviation 10 (ELEVATION)
24		Ratio 4 (Band 5)	Std. deviation 11 (SLOPE)
25		Ratio 5 (Band 6)	Ratio 1 (Band 2)
26		Ratio 6 (Band 7)	Ratio 2 (Band 3)
27		Ratio 7 (NDVI)	Ratio 3 (Band 4)
28		Ratio 8 (MNDWI)	Ratio 4 (Band 5)
29		Ratio 9 (NDBI)	Ratio 5 (Band 6)
30			Ratio 6 (Band 7)
31			Ratio 7 (NDVI)
32			Ratio 8 (MNDWI)
33			Ratio 9 (NDBI)
34			Ratio 10 (ELEVATION)
35			Ratio 11 (SLOPE)

### 6.1.1 LULC classification of SNN with six bands

The result of LULC classification using SNN with six bands is summarized in Table 6.3 and distribution of LULC data is displayed in Figure 6.3.

**Table 6.3** Area and percentage of final LULC classification of SNN with six bands.

No.	LULC class	Area in sq.km	Percent
0	Unclassified	2.52	0.24
1	Urban and built-up area	80.49	7.63
2	Paddy field	13.46	1.28
3	Cassava	156.05	14.80
4	Maize	120.35	11.42
5	Sugarcane	3.76	0.36
6	Orchard and perennial trees	5.10	0.48
7	Forest area	618.32	58.65
8	Water bodies	2.25	0.21
9	Miscellaneous land	52.00	4.93
<b>Total</b>		<b>1,054.30</b>	<b>100.00</b>

As results, top three dominant LULC classes in the study area are forest area, cassava and maize and cover area of 618.32 km<sup>2</sup>, 156.05 km<sup>2</sup> and 120.35 km<sup>2</sup> or 58.65%, 14.80% and 11.42% of the total study area, respectively.

In addition, the classified LULC map was further performed accuracy assessment with 193 sample points by field survey in 2017 (See Figure 5.3). Error matrix form for LULC accuracy assessment is displayed in Table 6.4. It reveals that overall accuracy is 77.72% and Kappa hat coefficient is 70.74%. Meanwhile producer's accuracy of LULC classes varies between 25.00% for orchard and perennial trees and 100.00% for paddy field while user's accuracy of LULC classes varies between 31.25% for cassava and 100.00% for water bodies. Based on Fitzpatrick-Lins (1981), Kappa

hat coefficient between 40-80% represents moderate agreement or accuracy between the predicted map and the reference map.

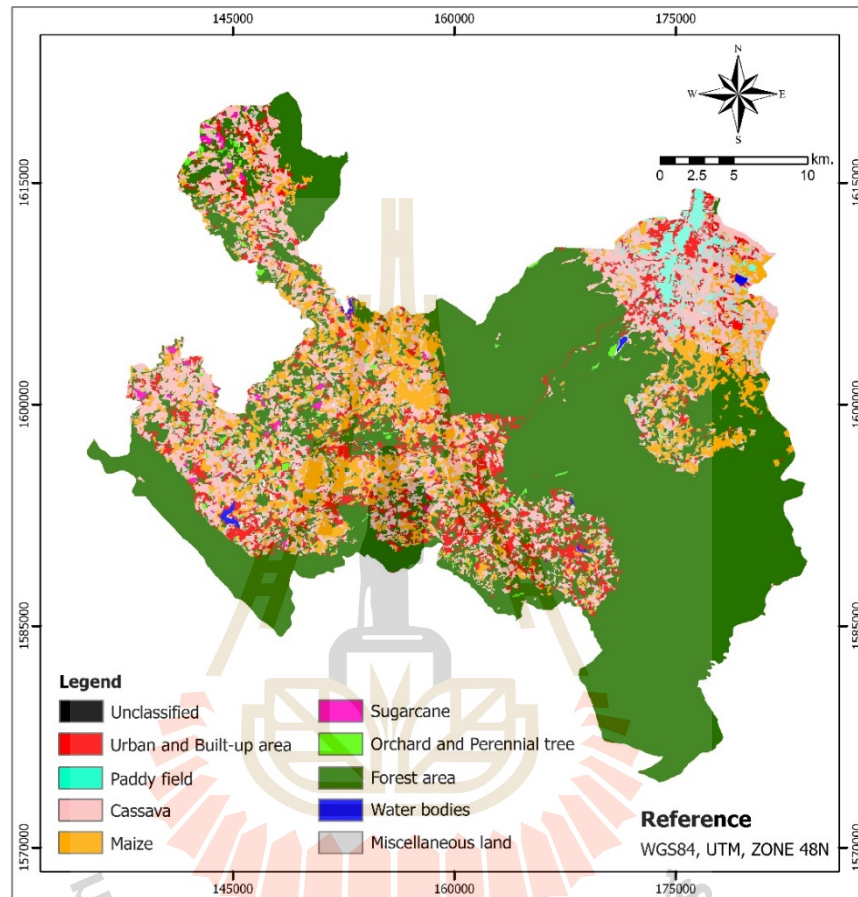


**Figure 6.3** LULC classification of 2015 of SNN with six bands.

**Table 6.4** Error matrix and accuracy assessment of LULC classification of SNN with six bands.

Classified LULC class	Reference data										Row Total
	UC	UB	PD	CV	MA	SU	OP	FA	WB	ML	
Unclassified (UC)	0	1							2	1	4
Urban and built-up area (UB)		6		1							7
Paddy field (PD)			5							1	6
Cassava (CV)				5	1	5	1	3		1	16
Maize (MA)				1	18			1		2	22
Sugarcane (SU)				1		3	1				5
Orchard and perennial trees (OP)						1	2	1			4
Forest area (FA)				3		8	4	72			87
Water bodies (WB)									7		7
Miscellaneous land (ML)		1			1				1	32	35
<b>Column Total</b>	<b>0</b>	<b>8</b>	<b>5</b>	<b>11</b>	<b>20</b>	<b>17</b>	<b>8</b>	<b>77</b>	<b>10</b>	<b>37</b>	<b>193</b>
<b>Producer's accuracy (%)</b>	0	75.00	100	45.45	90.00	17.65	25.00	93.51	70.00	86.49	
<b>User's accuracy (%)</b>	0	85.71	83.33	31.25	81.82	60.00	50.00	82.76	100	91.43	
<b>Overall accuracy (%)</b>	<b>77.72</b>										
<b>Kappa hat coefficient (%)</b>	<b>70.74</b>										

### 6.1.2 LULC classification of SNN with nine bands

The result of LULC classification using SNN with nine bands is summarized in Table 6.5 and distribution of LULC data is displayed in Figure 6.4.

**Table 6.5** Area and percentage of final LULC classification of SNN with nine bands.

No.	LULC class	Area in sq.km	Percent
0	Unclassified	3.20	0.30
1	Urban and built-up area	59.20	5.61
2	Paddy field	16.81	1.59
3	Cassava	194.79	18.48
4	Maize	118.39	11.23
5	Sugarcane	5.07	0.48
6	Orchard and perennial trees	6.30	0.60
7	Forest area	617.15	58.54
8	Water bodies	2.87	0.27
9	Miscellaneous land	30.52	2.89
<b>Total</b>		<b>1,054.30</b>	<b>100.00</b>

As results, top three dominant LULC classes in the study area are forest area, maize, and cassava and cover area of 617.15 km<sup>2</sup>, 194.79 km<sup>2</sup> and 118.39 km<sup>2</sup> or 58.54%, 18.48% and 11.23% of the total study area, respectively.

In addition, the classified LULC map was further performed accuracy assessment with 193 sample points by field survey in 2017 (See Figure 5.3). Error matrix form for LULC accuracy assessment is displayed in Table 6.6. It reveals that overall accuracy is 78.24% and Kappa hat coefficient is 71.83%. Meanwhile producer's accuracy of LULC classes varies between 25.00% for orchard and perennial trees and 96.10% for forest area while user's accuracy of LULC classes varies between 33.33% for orchard and perennial trees and 100.00% for water bodies.

Based on Fitzpatrick-Lins (1981), Kappa hat coefficient between 40-80% represents moderate agreement or accuracy between the predicted map and the reference map.

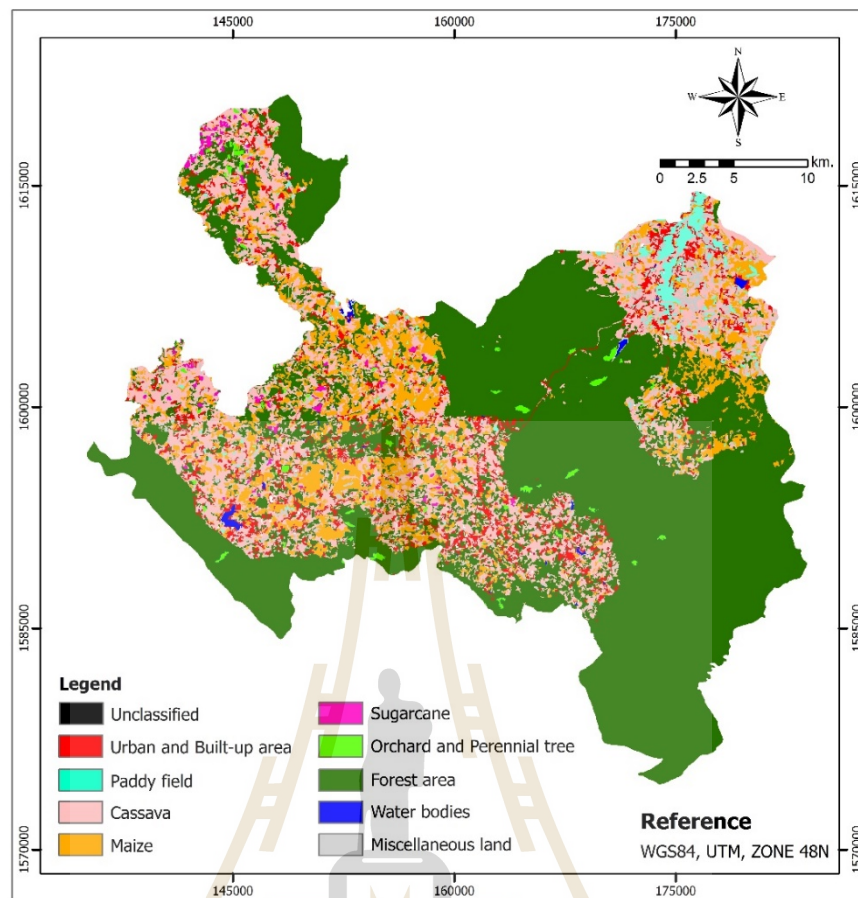


**Figure 6.4** LULC classification of 2015 of SNN with nine bands.



**Table 6.6** Error matrix and accuracy assessment of LULC classification of SNN with nine bands.

Classified LULC class	Reference data										Row Total
	UC	UB	PD	CV	MA	SU	OP	FA	WB	ML	
Unclassified (UC)	0	1								1	2
Urban and built-up area (UB)		6			1					1	8
Paddy field (PD)			4		1					5	10
Cassava (CV)				7		8	2	1			18
Maize (MA)			1		17					3	21
Sugarcane (SU)				1		5					6
Orchard and perennial trees (OP)						2	2	2			6
Forest area (FA)				3		2	4	74			83
Water bodies (WB)									9		9
Miscellaneous land (ML)		1			1					1	27
<b>Column Total</b>	<b>0</b>	<b>8</b>	<b>5</b>	<b>11</b>	<b>20</b>	<b>17</b>	<b>8</b>	<b>77</b>	<b>10</b>	<b>37</b>	<b>193</b>
<b>Producer's accuracy (%)</b>	0	75.00	80.00	63.64	85.00	29.41	25.00	96.10	90.00	72.97	
<b>User's accuracy (%)</b>	0	75.00	40.00	38.89	80.95	83.33	33.33	89.16	100	90.00	
<b>Overall accuracy (%)</b>	<b>78.24</b>										
<b>Kappa hat coefficient (%)</b>	<b>71.83</b>										

### 6.1.3 LULC classification of SNN with eleven bands

The result of LULC classification using SNN with eleven bands is summarized in Table 6.7 and distribution of LULC data is displayed in Figure 6.5.



**Table 6.7** Area and percentage of final LULC classification of SNN with eleven bands.

No.	LULC class	Area in sq.km	Percent
0	Unclassified	1.29	0.12
1	Urban and built-up area	95.84	9.09
2	Paddy field	21.74	2.06
3	Cassava	59.17	5.61
4	Maize	153.50	14.56
5	Sugarcane	4.74	0.45
6	Orchard and perennial trees	8.76	0.83
7	Forest area	673.70	63.90
8	Water bodies	4.72	0.45
9	Miscellaneous land	30.85	2.93
<b>Total</b>		<b>1,054.30</b>	<b>100.00</b>

As results, top three dominant LULC classes in the study area are forest area, maize, and urban and built-up area and cover area of 673.70 km<sup>2</sup>, 153.50 km<sup>2</sup> and 95.84 km<sup>2</sup> or 63.90%, 14.56% and 9.09% of the total study area, respectively.

In addition, the classified LULC map was further performed accuracy assessment with 193 sample points by field survey in 2017 (See Figure 5.3). Error matrix form for LULC accuracy assessment is displayed in Table 6.8. It reveals that overall accuracy is 81.35% and Kappa hat coefficient is 75.68%. Meanwhile producer's accuracy of LULC classes varies between 35.29% for sugarcane and 100% for paddy field and forest area while user's accuracy of LULC classes varies between 41.67% for cassava and 100.00% for water bodies. Based on Fitzpatrick-Lins (1981), Kappa hat coefficient between 40-80% represents moderate agreement or accuracy between the predicted map and the reference map.

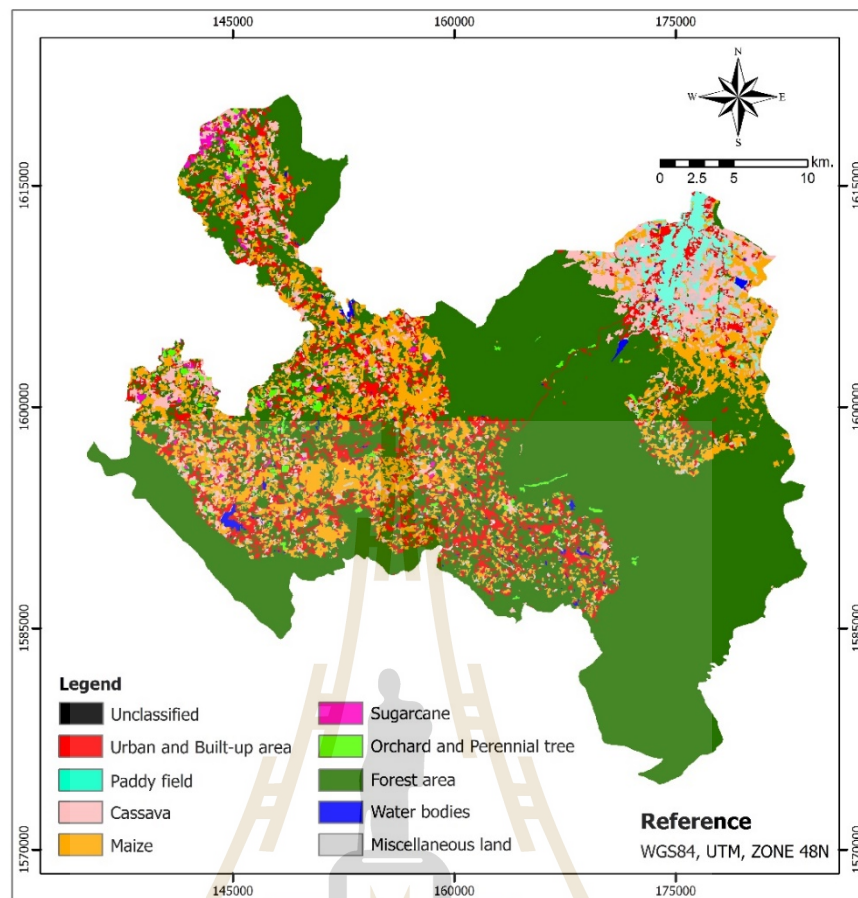


**Figure 6.5** LULC classification of 2015 of SNN with eleven bands.

**Table 6.8** Error matrix and accuracy assessment of LULC classification of SNN with eleven bands.

Classified LULC class	Reference data										Row Total
	UC	UB	PD	CV	MA	SU	OP	FA	WB	ML	
Unclassified (UC)	0	1									1
Urban and built-up area (UB)		6		1	1					3	11
Paddy field (PD)		1	5							2	8
Cassava (CV)				5		6				1	12
Maize (MA)				1	18					4	23
Sugarcane (SU)				1		6					7
Orchard and perennial trees (OP)						3	4				7
Forest area (FA)				3		2	4	77			86
Water bodies (WB)									9		9
Miscellaneous land (ML)					1					1	27
<b>Column Total</b>	<b>0</b>	<b>8</b>	<b>5</b>	<b>11</b>	<b>20</b>	<b>17</b>	<b>8</b>	<b>77</b>	<b>10</b>	<b>37</b>	<b>193</b>
<b>Producer's accuracy (%)</b>	0	75.00	100	45.45	90.00	35.29	50.00	100	90.00	72.97	
<b>User's accuracy (%)</b>	0	54.55	62.50	41.67	78.26	85.71	57.14	89.53	100	93.10	
<b>Overall accuracy (%)</b>	<b>81.35</b>										
<b>Kappa hat coefficient (%)</b>	<b>75.68</b>										

## Discussion

As results of LULC classification of SNN with three different datasets, it can be observed that area of LULC classes are rather different except sugarcane, orchards and perennial trees, and water bodies as shown in Figure 6.6.

According accuracy assessment, it reveals that LULC map of SNN that was classified with eleven bands (six multispectral bands, three spectral index bands and two physical data) provides the highest overall accuracy of 81.35% and Kappa hat coefficient of 75.68% (Figure 6.7). Likewise, producer's accuracy and user's accuracy of LULC classes of SNN with eleven bands are higher than LULC classes of SNN with six and nine bands as shown in Figure 6.8. Thus, it can be here concluded that SNN

with eleven bands is the most suitable for LULC classification using SNN method under OBIA.

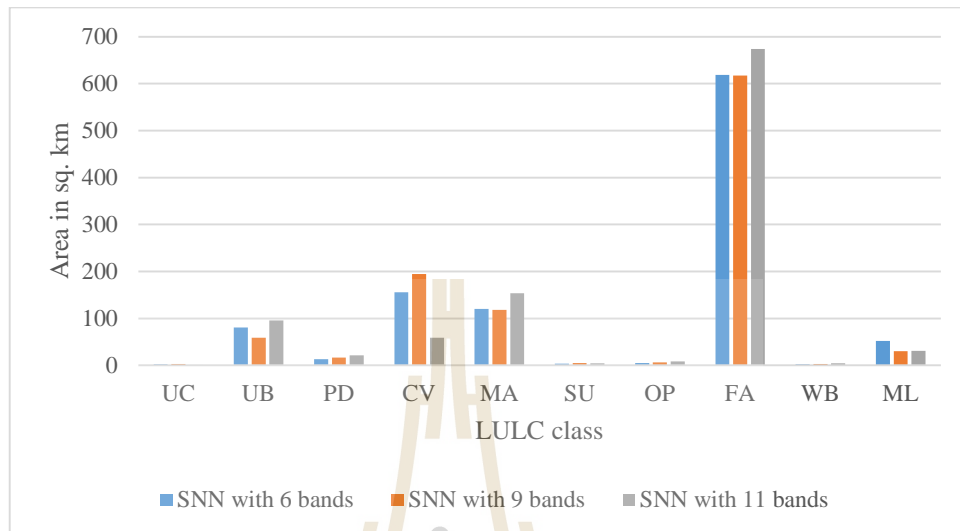


**Figure 6.6** Comparison area of LULC classification of SNN with three different dataset.

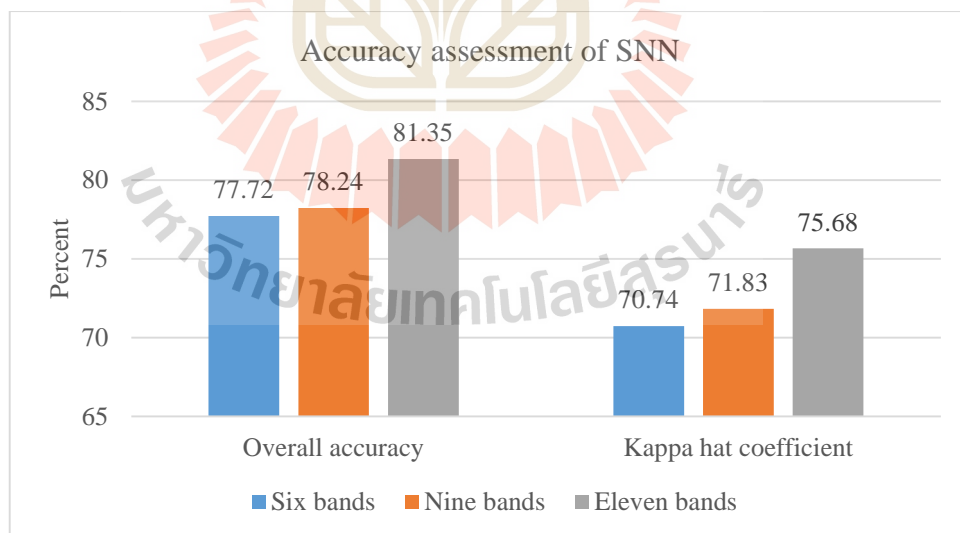


**Figure 6.7** Accuracy assessment of SNN with three different datasets.

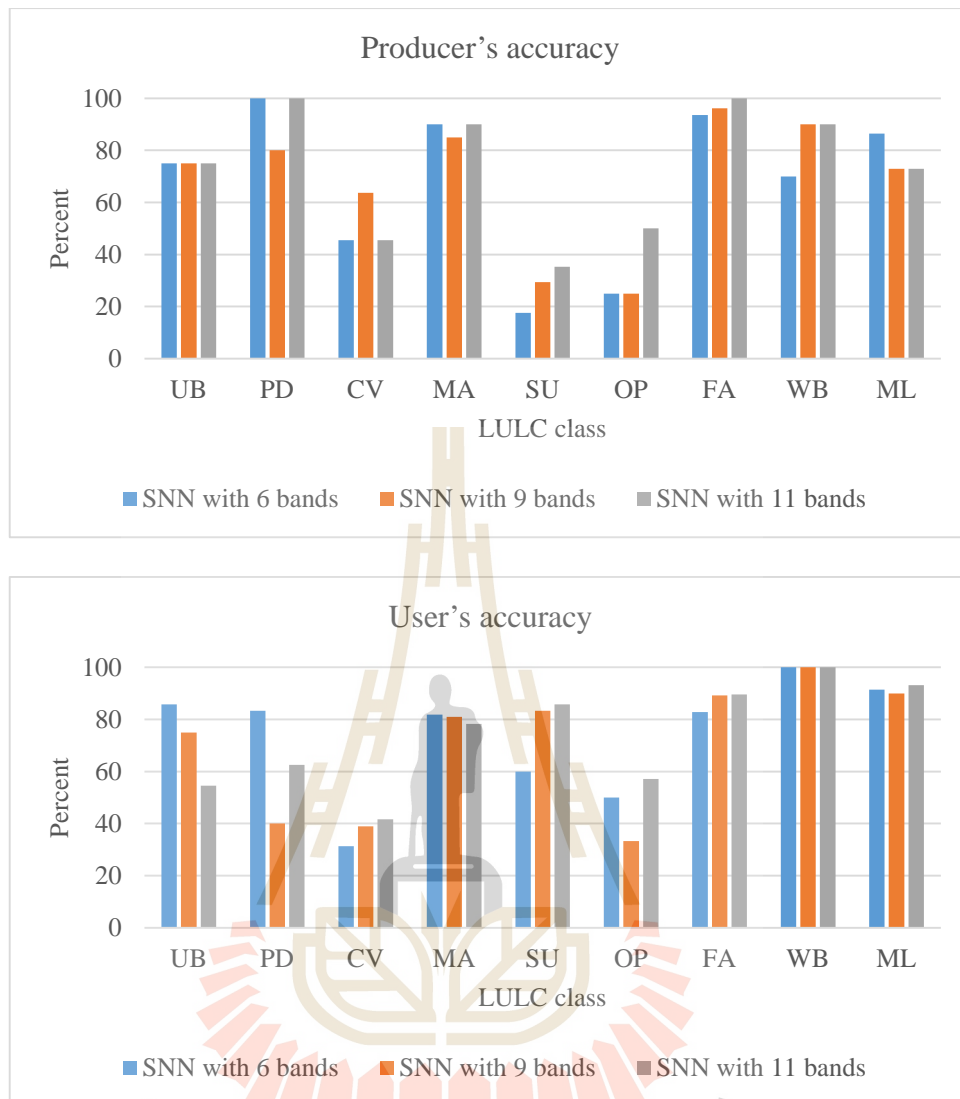


**Figure 6.8** Comparison producer's and user's accuracy of LULC classification of SNN.

However, the pairwise Z test of SNN with three different datasets based on Kappa hat analysis shows that the accuracy of LULC classification are not significantly different at the 80% confidence level since the Z-value is less than Chi square values at various confidence levels as shown in Table 6.9. This finding suggests that it should apply six bands dataset for reducing operation time for LULC classification with SNN.

**Table 6.9** Pairwise Z test of Kappa hat coefficient value for LULC extraction in SNN.

Pairwise Z test	Kappa hat	Variance	Z-Statistic	Confidential level of critical value			
				80%	90%	95%	100%
SNN with six bands	0.70801	0.00140	<b>0.20503</b>	<b>1.28</b>	<b>1.65</b>	<b>1.96</b>	<b>2.58</b>
SNN with nine bands	0.71868	0.00131					
SNN with six bands	0.70801	0.00140	<b>0.95886</b>	<b>1.28</b>	<b>1.65</b>	<b>1.96</b>	<b>2.58</b>
SNN with eleven bands	0.75689	0.00120					
SNN with nine bands	0.71868	0.00131	<b>0.76273</b>	<b>1.28</b>	<b>1.65</b>	<b>1.96</b>	<b>2.58</b>
SNN with eleven bands	0.75689	0.00120					

## 6.2 LULC classification of FSO

Five combinations of features of pan-sharpened Landsat-8 data and their properties were here applied to classify LULC with FSO including:

- (1) Brightness, Mean layer 1 to 6 (Band 2, 3, 4, 5, 6 and 7) and Max. diff.;
- (2) Brightness, Mean layer 1 to 6 (Band 2, 3, 4, 5, 6 and 7), Max. diff. and Standard deviation of layer 1 to 6 (Band 2, 3, 4, 5, 6 and 7);
- (3) Brightness, Mean layer 1 to 6 (Band 2, 3, 4, 5, 6 and 7), Max. diff., Standard deviation of layer 1 to 6 (Band 2, 3, 4, 5, 6 and 7) and ratio of layer 1 to 6 (Band 2, 3, 4, 5, 6 and 7);
- (4) Brightness, Mean layer 1 to 6 (Band 2, 3, 4, 5, 6 and 7), Max. diff., Standard deviation of layer 1 to 6 (Band 2, 3, 4, 5, 6 and 7), Ratio of layer 1 to 6 (Band 2, 3, 4, 5, 6 and 7) and three spectral indices (NDVI, MNDWI and NDBI); and
- (5) Brightness, Mean layer 1 to 6 (Band 2, 3, 4, 5, 6 and 7), Max. diff., Standard deviation of layer 1 to 6 (Band 2, 3, 4, 5, 6 and 7), Ratio of layer 1 to 6 (Band 2, 3, 4, 5, 6 and 7), three spectral indices (NDVI, MNDWI and NDBI) and six GLCM texture (homogeneity, contrast, entropy, Ang. 2<sup>nd</sup> moment and correlation).

In practice, image objects of six bands of pan-sharpened Landsat-8 data and training areas of SNN method as initial input data are firstly applied to extract optimize

features from each feature combination which provides the best separability among features. Then, the optimized features are applied to classify LULC using nearest neighbor classifier.

Results of LULC classification of FSO with different feature combinations is separately reported and discussed in the following sections.

### 6.2.1 LULC classification of FSO with feature combination # 1

Under the first combination of features of pan-sharpened Landsat-8 data and their properties including brightness, mean layer 1 to 6 (Band 2, 3, 4, 5, 6 and 7) and Max. diff., the optimized features that provide the best separability distance of 0.375 for LULC classification are Mean Layer 2, 3 and 4 and Max. diff.

The result of LULC classification using FSO with the first feature combination is summarized in Table 6.10 and distribution of LULC data is displayed in Figure 6.9.

**Table 6.10** Area and percentage of final LULC classification of FSO with feature combination # 1.

No.	LULC class	Area in sq.km	Percent
0	Unclassified	0.19	0.02
1	Urban and built-up area	116.13	11.01
2	Paddy field	67.48	6.40
3	Cassava	137.91	13.08
4	Maize	89.65	8.50
5	Sugarcane	0.47	0.04
6	Orchard and perennial trees	8.72	0.83
7	Forest area	612.28	58.07
8	Water bodies	3.65	0.35
9	Miscellaneous land	17.82	1.69
<b>Total</b>		<b>1,054.30</b>	<b>100.00</b>

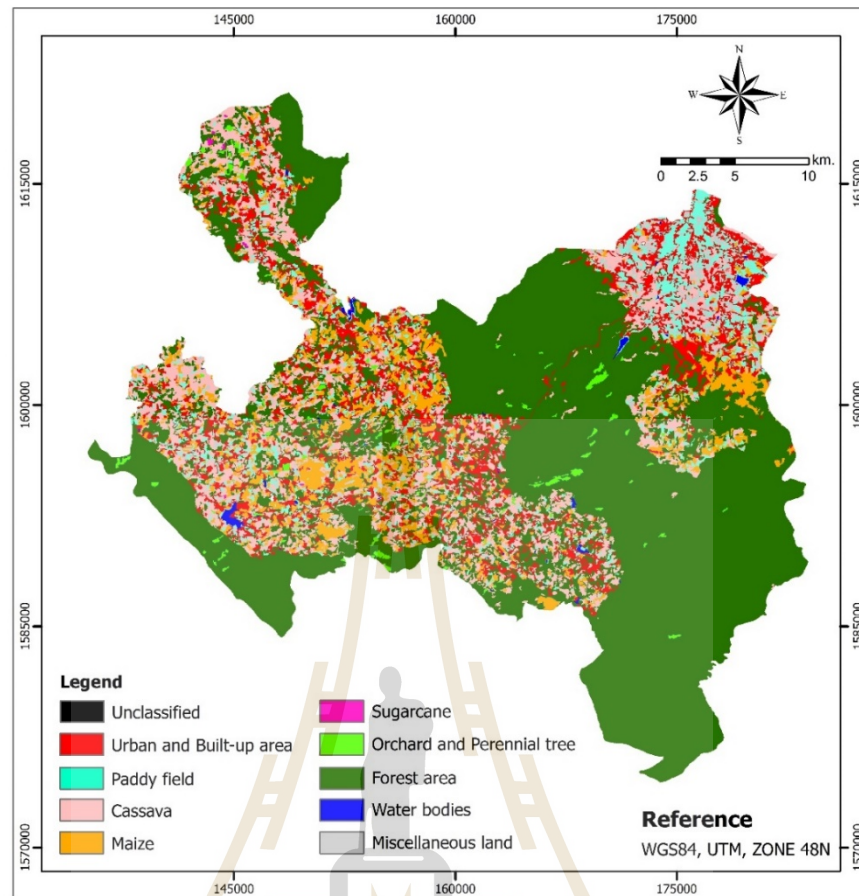


**Figure 6.9** LULC classification of 2015 of FSO with feature combination # 1.

As results, top three dominant LULC classes in the study area are forest area, cassava, and urban and built-up area and cover area of 612.28 km<sup>2</sup>, 137.91 km<sup>2</sup> and 116.13 km<sup>2</sup> or 58.07%, 13.08% and 11.01% of the total study area, respectively.

In addition, the classified LULC map was further performed accuracy assessment using 193 sample points by field survey in 2017 (See Figure 5.3). Error matrix form for LULC accuracy assessment is displayed in Table 6.11. It reveals that overall accuracy is 72.02% and Kappa hat coefficient is 63.63%. Meanwhile producer's accuracy of LULC classes varies between 0.00% for sugarcane and 94.81% for forest area while user's accuracy of LULC classes varies between 0.00% for sugarcane and





### 6.2.2 LULC classification of FSO with feature combination # 2

Under the second combination of features of pan-sharpened Landsat-8 data and their properties including brightness, mean layer 1 to 6 (Band 2, 3, 4, 5, 6 and 7), Max. diff. and standard deviation of layer 1 to 6 (Band 2, 3, 4, 5, 6 and 7), the optimize features that provide the best separability distance of 0.579 for LULC classification are Mean Layer 4 and 5, Standard deviation Layer 4, and Max. diff.

The result of LULC classification using FSO with the second feature combination is summarized in Table 6.12 and distribution of LULC data is displayed in Figure 6.10.

**Table 6.12** Area and percentage of final LULC classification of FSO with feature combination # 2.

No.	LULC class	Area in sq.km	Percent
0	Unclassified	4.51	0.43
1	Urban and built-up area	116.57	11.06
2	Paddy field	24.79	2.35
3	Cassava	136.04	12.90
4	Maize	86.06	8.16
5	Sugarcane	1.83	0.17
6	Orchard and perennial trees	10.78	1.02
7	Forest area	610.32	57.89
8	Water bodies	2.42	0.23
9	Miscellaneous land	60.97	5.78
<b>Total</b>		<b>1,054.30</b>	<b>100.00</b>

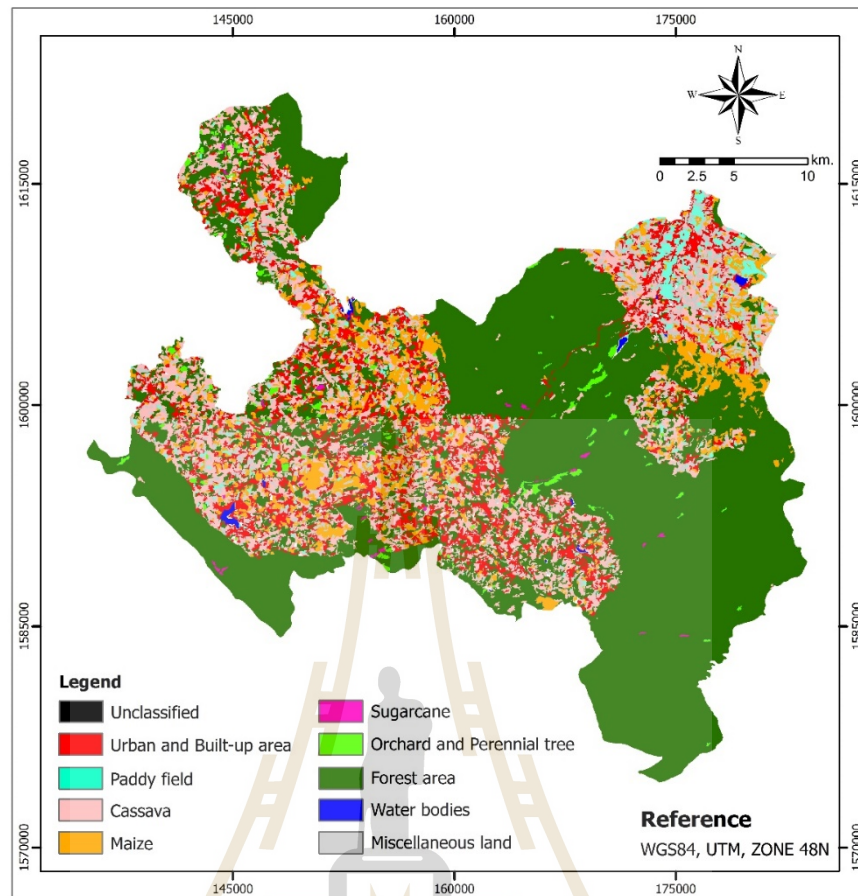


**Figure 6.10** LULC classification of 2015 of FSO with feature combination # 2.

As results, top three dominant LULC classes in the study area are forest area, cassava and urban and built-up area and cover area of 610.32 km<sup>2</sup>, 136.04 km<sup>2</sup> and 116.57 km<sup>2</sup> or 57.89%, 12.90% and 11.06% of the total study area, respectively.

In addition, the classified LULC map was further performed accuracy assessment using 193 sample points by field survey in 2017 (See Figure 5.3). Error matrix form for LULC accuracy assessment is displayed in Table 6.13. It reveals that overall accuracy is 74.61% and Kappa hat coefficient is 66.49%. Meanwhile producer's accuracy of LULC classes varies between 5.88% for sugarcane and 93.51% for forest area while user's accuracy of LULC classes varies between 40.00% for orchard and



### 6.2.3 LULC classification of FSO with feature combination # 3

Under the third combination of features of pan-sharpened Landsat-8 data and their properties including brightness, mean layer 1 to 6 (Band 2, 3, 4, 5, 6 and 7), Max. diff., standard deviation of layer 1 to 6 (Band 2, 3, 4, 5, 6 and 7) and ratio of layer 1 to 6 (Band 2, 3, 4, 5, 6 and 7), the optimize features that provide the best separability distance of 1.423 for LULC classification are Mean Layer 4 and 5, Standard deviation Layer 4, Ratio Layer 2 and 5.

The result of LULC classification using FSO with the third feature combination is summarized in Table 6.14 and distribution of LULC data is displayed in Figure 6.11.

**Table 6.14** Area and percentage of final LULC classification of FSO with feature combination # 3.

No.	LULC class	Area in sq.km	Percent
0	Unclassified	4.41	0.42
1	Urban and built-up area	132.31	12.55
2	Paddy field	29.68	2.82
3	Cassava	110.44	10.48
4	Maize	96.35	9.14
5	Sugarcane	2.96	0.28
6	Orchard and perennial trees	15.47	1.47
7	Forest area	615.09	58.34
8	Water bodies	2.28	0.22
9	Miscellaneous land	45.29	4.30
<b>Total</b>		<b>1,054.30</b>	<b>100.00</b>

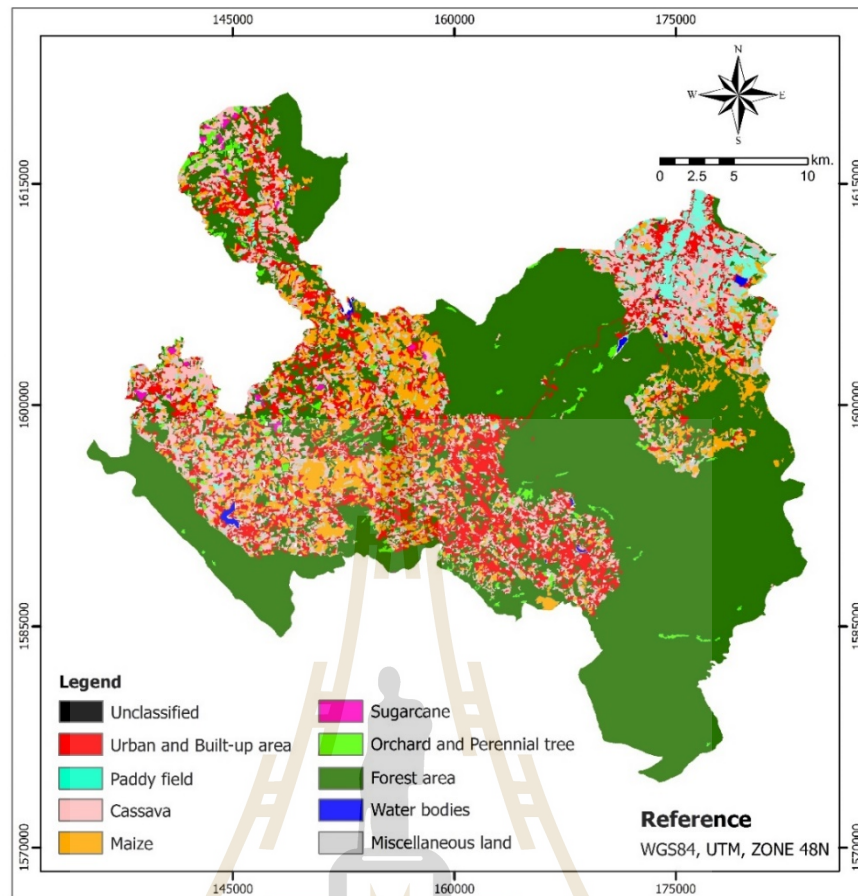


**Figure 6.11** LULC classification of 2015 of FSO with feature combination # 3.

As results, top three dominant LULC classes in the study area are forest area, urban and built-up area and cassava and cover area of 615.09 km<sup>2</sup>, 132.31 km<sup>2</sup> and 110.44 km<sup>2</sup> or 58.34%, 12.55% and 10.48% of the total study area, respectively.

In addition, the classified LULC map was further performed accuracy assessment using 193 sample points by field survey in 2017 (See Figure 5.3). Error matrix form for LULC accuracy assessment is displayed in Table 6.15. It reveals that overall accuracy is 76.17% and Kappa hat coefficient is 68.92%. Meanwhile producer's accuracy of LULC classes varies between 11.76% for sugarcane and 100% for paddy field while user's accuracy of LULC classes varies between 33.33% for orchard and

perennial trees and 100.00% for water bodies. Based on Fitzpatrick-Lins (1981), Kappa hat coefficient between 40-80% represents moderate agreement or accuracy between the predicted map and the reference map.

**Table 6.15** Error matrix and accuracy assessment of LULC classification of FSO with feature combination # 3.

Classified LULC class	Reference data										Row Total
	UC	UB	PD	CV	MA	SU	OP	FA	WB	ML	
Unclassified (UC)	0	1							2		3
Urban and built-up area (UB)		5		1	1		1	1			9
Paddy field (PD)			5							3	8
Cassava (CV)		1		8		5				7	21
Maize (MA)					18			1		1	20
Sugarcane (SU)						2	1				3
Orchard and perennial trees (OP)				1		2	2	1			6
Forest area (FA)				1		8	4	74			87
Water bodies (WB)									7		7
Miscellaneous land (ML)		1			1					1	26
<b>Column Total</b>	<b>0</b>	<b>8</b>	<b>5</b>	<b>11</b>	<b>20</b>	<b>17</b>	<b>8</b>	<b>77</b>	<b>10</b>	<b>37</b>	<b>193</b>
<b>Producer's accuracy (%)</b>	0	62.50	100	72.73	90.00	11.76	25.00	96.10	70.00	70.27	
<b>User's accuracy (%)</b>	0	55.56	62.50	38.10	90.00	66.67	33.33	85.06	100	89.66	
<b>Overall accuracy (%)</b>	<b>76.17</b>										
<b>Kappa hat coefficient (%)</b>	<b>68.92</b>										

#### 6.2.4 LULC classification of FSO with feature combination # 4

Under the fourth combination of features of pan-sharpened Landsat-8 data and their properties including brightness, mean layer 1 to 6 (Band 2, 3, 4, 5, 6 and 7), Max. diff., standard deviation of layer 1 to 6 (Band 2, 3, 4, 5, 6 and 7), ratio of layer 1 to 6 (Band 2, 3, 4, 5, 6 and 7) and three spectral indices (NDVI, MNDWI and NDBI), the optimize features that provide the best separability distance of 1.434 for LULC classification are Mean Layer 4 and 5, Standard deviation Layer 4, MNDWI, and Ratio Layer 5.

The result of LULC classification using FSO with the fourth feature combination is summarized in Table 6.16 and distribution of LULC data is displayed in Figure 6.12.

**Table 6.16** Area and percentage of final LULC classification of FSO with feature combination # 4.

No.	LULC class	Area in sq.km	Percent
0	Unclassified	4.66	0.44
1	Urban and built-up area	124.35	11.79
2	Paddy field	34.65	3.29
3	Cassava	110.16	10.45
4	Maize	92.47	8.77
5	Sugarcane	3.01	0.29
6	Orchard and perennial trees	16.24	1.54
7	Forest area	617.66	58.58
8	Water bodies	2.28	0.22
9	Miscellaneous land	48.82	4.63
<b>Total</b>		<b>1,054.30</b>	<b>100.00</b>



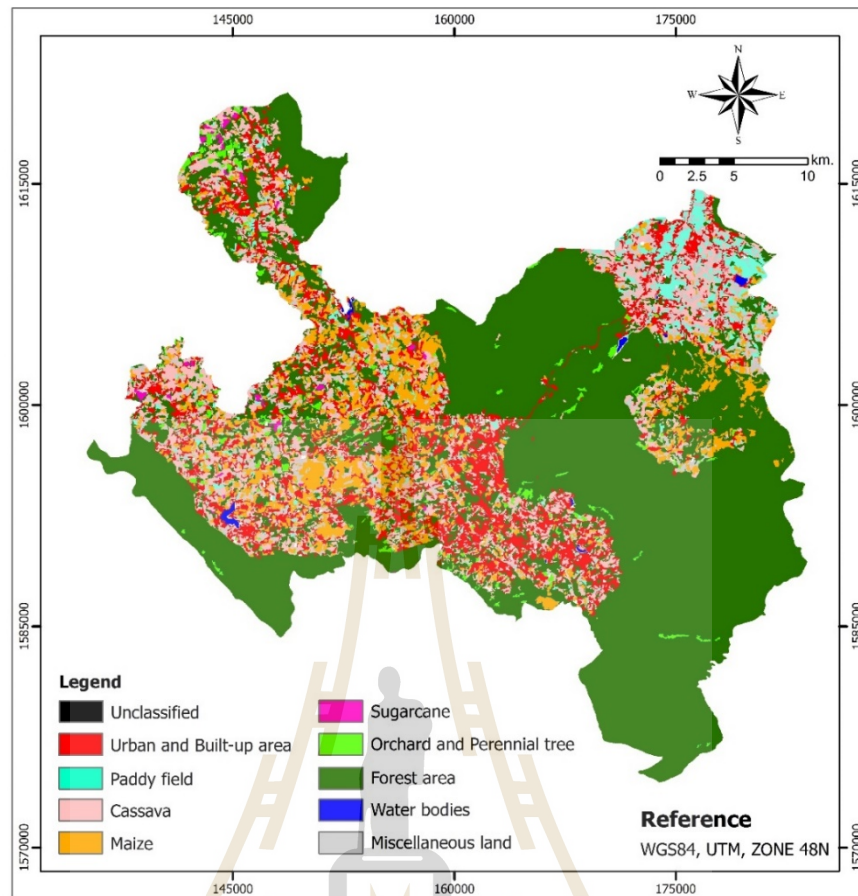


**Figure 6.12** LULC classification of 2015 of FSO with feature combination # 4.

As results, top three dominant LULC classes in the study area are forest area, urban and built-up area and cassava, and cover area of 617.66 km<sup>2</sup>, 124.35 km<sup>2</sup> and 110.16 km<sup>2</sup> or 58.58%, 11.79% and 10.45% of the total study area, respectively.

In addition, the classified LULC map was further performed accuracy assessment using 193 sample points by field survey in 2017 (See Figure 5.3). Error matrix form for LULC accuracy assessment is displayed in Table 6.17. It reveals that overall accuracy is 75.13% and Kappa hat coefficient is 67.50%. Meanwhile producer's accuracy of LULC classes varies between 11.76% for sugarcane and 100% for paddy field while user's accuracy of LULC classes varies between 31.58% for cassava and

100% for water bodies. Based on Fitzpatrick-Lins (1981), Kappa hat coefficient between 40-80% represents moderate agreement or accuracy between the predicted map and the reference map.

**Table 6.17** Error matrix and accuracy assessment of LULC classification of FSO with feature combination # 4.

Classified LULC class	Reference data										Row Total
	UC	UB	PD	CV	MA	SU	OP	FA	WB	ML	
Unclassified (UC)	0	1							2		3
Urban and built-up area (UB)		4		1	1		1	1			8
Paddy field (PD)			5							3	8
Cassava (CV)		1		6		6				6	19
Maize (MA)				1	18			1		1	21
Sugarcane (SU)						2	1				3
Orchard and perennial trees (OP)				1		2	2	1			6
Forest area (FA)				2		7	4	74			87
Water bodies (WB)									7		7
Miscellaneous land (ML)		2			1					1	27
<b>Column Total</b>	<b>0</b>	<b>8</b>	<b>5</b>	<b>11</b>	<b>20</b>	<b>17</b>	<b>8</b>	<b>77</b>	<b>10</b>	<b>37</b>	<b>193</b>
<b>Producer's accuracy (%)</b>	0	50.00	100	54.55	90.00	11.76	25.00	96.10	70.00	72.97	
<b>User's accuracy (%)</b>	0	50.00	62.50	31.58	85.71	66.67	33.33	85.06	100	87.10	
<b>Overall accuracy (%)</b>	<b>75.13</b>										
<b>Kappa hat coefficient (%)</b>	<b>67.50</b>										

### 6.2.5 LULC classification of FSO with feature combination # 5

Under the fifth combination of features of pan-sharpened Landsat-8 data and their properties including brightness, mean layer 1 to 6 (Band 2, 3, 4, 5, 6 and 7), Max. diff., standard deviation of layer 1 to 6 (Band 2, 3, 4, 5, 6 and 7), ratio of layer 1 to 6 (Band 2, 3, 4, 5, 6 and 7), three spectral indices (NDVI, MNDWI and NDBI) and six GLCM texture (homogeneity, contrast, entropy, Ang. 2<sup>nd</sup> moment and correlation), the optimize features that provide the best separability distance of 1.557 for LULC classification are GLCM Entropy (all dir.), Mean Layer 4, GLCM Homogeneity (all dir.), MNDWI, and Ratio Layer 5.

The result of LULC classification using FSO with the fifth feature combination is summarized in Table 6.18 and distribution of LULC data is displayed in Figure 6.13.

**Table 6.18** Area and percentage of final LULC classification of FSO with feature combination # 5.

No.	LULC class	Area in sq.km	Percent
0	Unclassified	2.12	0.20
1	Urban and built-up area	44.15	4.19
2	Paddy field	103.85	9.85
3	Cassava	54.39	5.16
4	Maize	42.40	4.02
5	Sugarcane	1.50	0.14
6	Orchard and perennial trees	3.69	0.35
7	Forest area	594.53	56.39
8	Water bodies	1.92	0.18
9	Miscellaneous land	205.77	19.52
<b>Total</b>		<b>1,054.30</b>	<b>100.00</b>

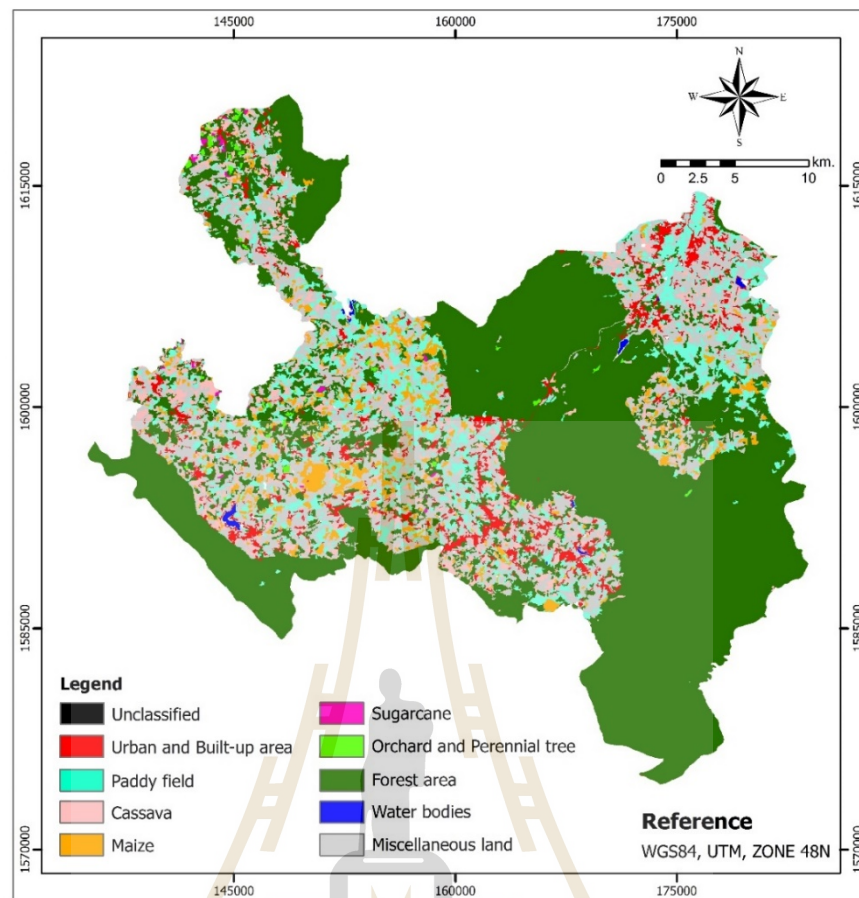


**Figure 6.13** LULC classification of 2015 of FSO with feature combination # 5.

As results, top three dominant LULC classes in the study area are forest area, miscellaneous land, and paddy field and cover area of 594.53 km<sup>2</sup>, 205.77 km<sup>2</sup> and 103.85 km<sup>2</sup> or 56.39%, 19.52% and 9.85% of the total study area, respectively.

In addition, the classified LULC map was further performed accuracy assessment using 193 sample points by field survey in 2017 (See Figure 5.3). Error matrix form for LULC accuracy assessment is displayed in Table 6.19. It reveals that overall accuracy is 73.06% and Kappa hat coefficient is 64.53%. Meanwhile producer's accuracy of LULC classes varies between 11.76% for sugarcane and 94.81% for forest area while user's accuracy of LULC classes varies between 21.43% for paddy field and

100.00% for water bodies. Based on Fitzpatrick-Lins (1981), Kappa hat coefficient between 40-80% represents moderate agreement or accuracy between the predicted map and the reference map.

**Table 6.19** Error matrix and accuracy assessment of LULC classification of FSO with feature combination # 5.

Classified LULC class	Reference data										Row Total
	UC	UB	PD	CV	MA	SU	OP	FA	WB	ML	
Unclassified (UC)	0								1		1
Urban and built-up area (UB)		7							1	1	9
Paddy field (PD)			3	1	5			2		3	14
Cassava (CV)				4		3		1			8
Maize (MA)					11		1	1		1	14
Sugarcane (SU)				1		2	1				4
Orchard and perennial trees (OP)						5	2				7
Forest area (FA)				3		7	4	73			87
Water bodies (WB)									7		7
Miscellaneous land (ML)		1	2	2	4				1	32	42
<b>Column Total</b>	<b>0</b>	<b>8</b>	<b>5</b>	<b>11</b>	<b>20</b>	<b>17</b>	<b>8</b>	<b>77</b>	<b>10</b>	<b>37</b>	<b>193</b>
<b>Producer's accuracy (%)</b>	0	87.50	60.00	36.36	55.00	11.76	25.00	94.81	70.00	86.49	
<b>User's accuracy (%)</b>	0	77.78	21.43	50.00	78.57	50.00	28.57	83.91	100	76.19	
<b>Overall accuracy (%)</b>	<b>73.06</b>										
<b>Kappa hat coefficient (%)</b>	<b>64.53</b>										

## Discussion

As results of LULC classification of FSO with five features combinations, it can be observed that area of LULC classes are rather different except water bodies as shown in Figure 6.14.

According to accuracy assessment, it reveals that FSO with feature combination # 3 that was applied features: Mean Layer 4 (Band 5) and Mean Layer 5 (Band 6), Standard deviation of Layer 4 (Band 5), Ratio Layer 2 (Band 3) and Ratio Layer 5

(Band 6) to classify LULC provides the highest overall accuracy of 76.17% and Kappa hat coefficient of 68.92% (Figure 6.15). Likewise, most of producer’s accuracy and user’s accuracy of LULC classes of FSO with feature combination # 3 are higher than others as shown in Figure 6.16. Thus, it can be here concluded that FSO with feature combination # 3 is the most suitable for LULC classification using FSO method under OBIA.

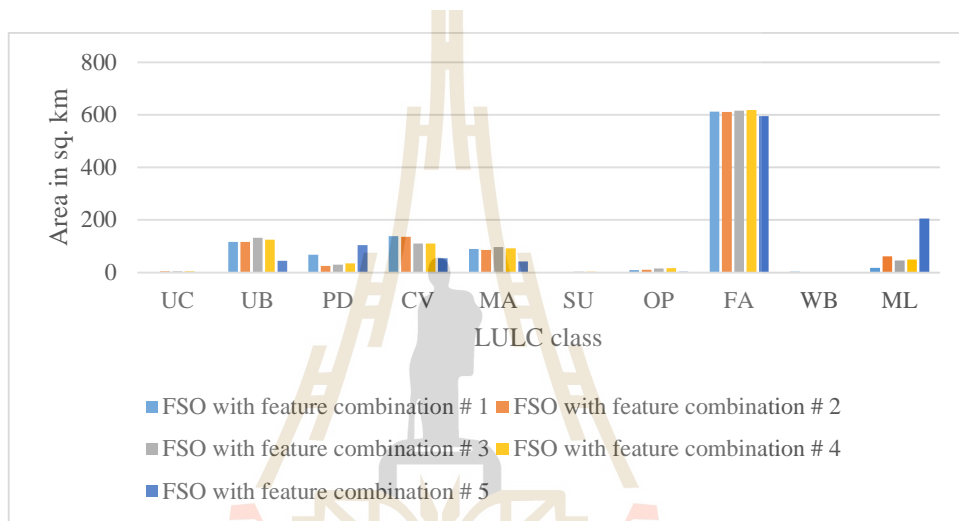


**Figure 6.14** Comparison area of LULC classification of FSO with five features combinations.

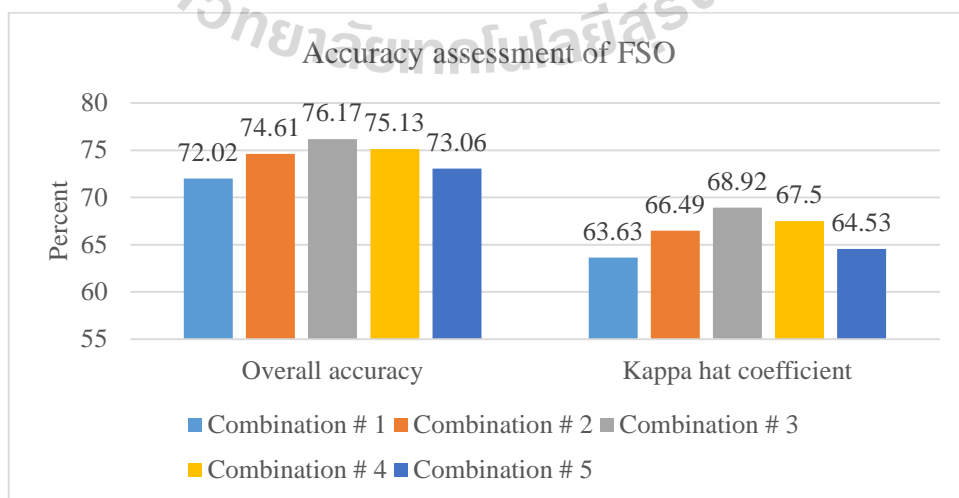


**Figure 6.15** Accuracy assessment of FSO with five different features combination.

However, the pairwise Z test of FSO with five different features combinations based on Kappa hat analysis shows that the accuracy of five LULC classifications of FSO are not significantly different at the 80% confidence level since the Z-value is less than Chi square values at various confidence levels as shown in Table 6.20.

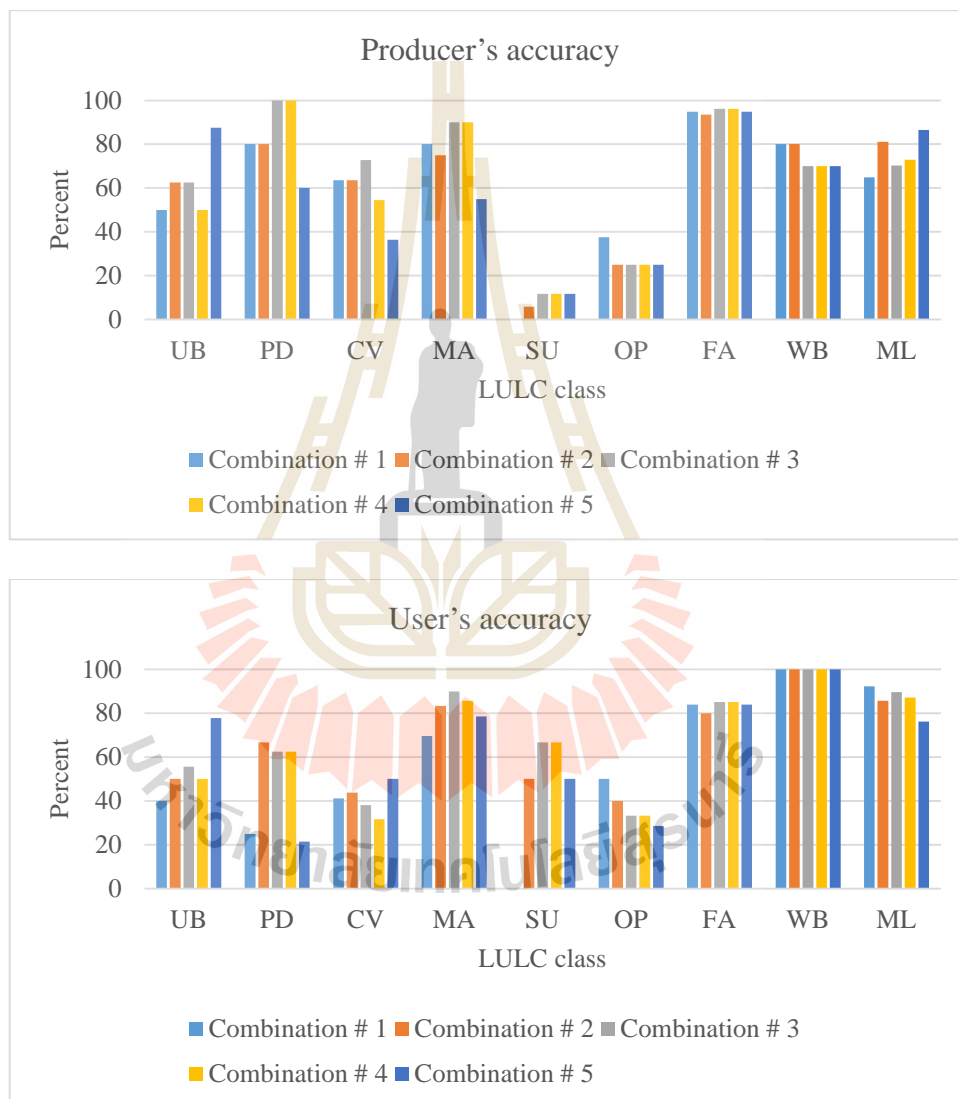


**Figure 6.16** Comparison producer's and user's accuracy of LULC classification of FSO with five different features combination.

**Table 6.20** Pairwise Z test of Kappa hat coefficient value for LULC classification with FSO.

Pairwise Z test	Kappa hat	Variance	Z-Statistic	Confidential level of critical value			
				80%	90%	95%	100%
FSO with features combination #1	0.63627	0.00150	<b>0.53349</b>	<b>1.28</b>	<b>1.65</b>	<b>1.96</b>	<b>2.58</b>
FSO with features combination #2	0.66556	0.00152					
FSO with features combination #1	0.63627	0.00150	<b>0.98745</b>	<b>1.28</b>	<b>1.65</b>	<b>1.96</b>	<b>2.58</b>
FSO with features combination #3	0.68945	0.00140					
FSO with features combination #1	0.63627	0.00150	<b>0.71959</b>	<b>1.28</b>	<b>1.65</b>	<b>1.96</b>	<b>2.58</b>
FSO with features combination #4	0.67521	0.00143					
FSO with features combination #1	0.63627	0.00150	<b>0.16597</b>	<b>1.28</b>	<b>1.65</b>	<b>1.96</b>	<b>2.58</b>
FSO with features combination #5	0.64536	0.00150					
FSO with features combination #2	0.66556	0.00152	<b>0.44194</b>	<b>1.28</b>	<b>1.65</b>	<b>1.96</b>	<b>2.58</b>
FSO with features combination #3	0.68945	0.00140					
FSO with features combination #2	0.66556	0.00152	<b>0.17768</b>	<b>1.28</b>	<b>1.65</b>	<b>1.96</b>	<b>2.58</b>
FSO with features combination #4	0.67521	0.00143					
FSO with features combination #2	0.66556	0.00152	<b>0.36749</b>	<b>1.28</b>	<b>1.65</b>	<b>1.96</b>	<b>2.58</b>
FSO with features combination #5	0.64536	0.00150					
FSO with features combination #3	0.68945	0.00140	<b>0.26738</b>	<b>1.28</b>	<b>1.65</b>	<b>1.96</b>	<b>2.58</b>
FSO with features combination #4	0.67521	0.00143					
FSO with features combination #3	0.68945	0.00140	<b>0.81767</b>	<b>1.28</b>	<b>1.65</b>	<b>1.96</b>	<b>2.58</b>
FSO with features combination #5	0.64536	0.00150					
FSO with features combination #4	0.67521	0.00143	<b>0.55094</b>	<b>1.28</b>	<b>1.65</b>	<b>1.96</b>	<b>2.58</b>
FSO with features combination #5	0.64536	0.00150					



## CHAPTER VII

### OPTIMUM METHOD FOR LULC CLASSIFICATION

Under this chapter an optimum method of PBIA or OBIA for LULC classification based on overall accuracy and Kappa hat coefficient is firstly separately reported with discussion. Then, an optimum method between PBIA and OBIA for LULC classification are then reported and discussed.

#### 7.1 Optimum method of PBIA for LULC classification

The best performance of three representative methods of PBIA according to accuracy assessment (overall accuracy and Kappa hat coefficient) include (1) MLC with nine bands, (2) ANN at learning rate of 0.1 with six bands and (3) DT without splitting samples with six bands were here compared to identify an optimum method of PBIA for LULC classification. Accuracy assessment of the best three representative methods of PBIA is presented in Table 7.1 and it is comparatively displayed in Figure 7.1. Meanwhile, producer's accuracy and user's accuracy of the best three representative methods of PBIA is presented in Figure 7.2.

**Table 7.1** Accuracy assessment of the best three representative methods of PBIA.

Method	Overall accuracy (%)	Kappa hat coefficient (%)
MLC with nine bands	86.01	81.93
ANN at learning rate of 0.1 with six bands	80.83	75.48
DT without splitting samples with six bands	82.38	77.02

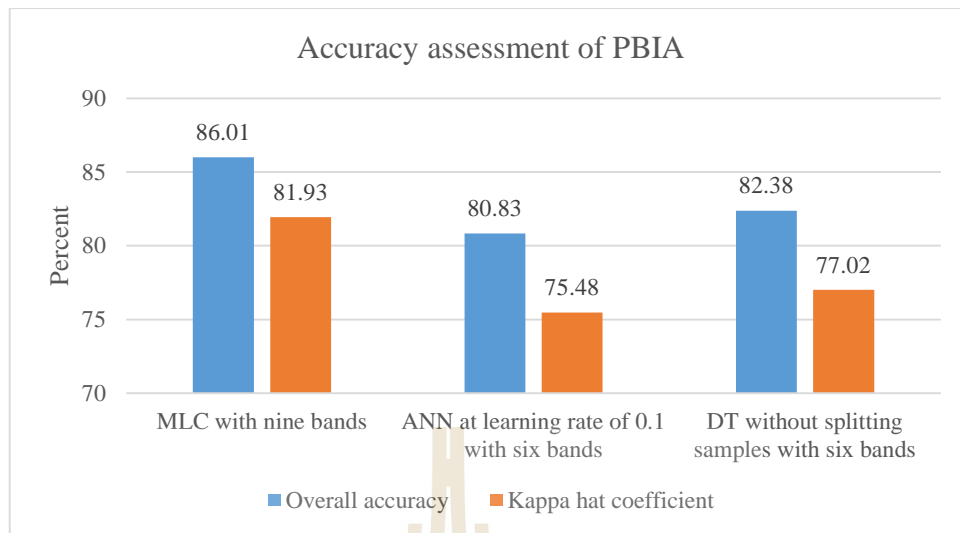


**Figure 7.1** Accuracy assessment of the best three representative methods of PBIA.

As results, it was found that the optimum method of PBIA for LULC classification in this study from pan-sharpened image of Landsat-8 data is maximum likelihood classifier (MLC) with nine bands (Band 2, 3, 4, 5, 6, and 7, NDVI, MNDWI, and NDBI). It can provide overall accuracy of 86.01% and Kappa hat coefficient of 81.93% and it represents strong agreement or accuracy between the predicted map and the reference map (Fitzpatrick-Lins, 1981). The producer's accuracy of LULC classes varies between 37.50% for orchard and perennial trees and 100.00% for paddy field and maize while user's accuracy of LULC classes varies between 27.27% for orchard and perennial trees and 100.00% for urban and built-up area and water bodies. In addition, the producer's accuracy that measures omission error and reflects efficiency of classifier shows that MLC can accurately extract most of LULC classes except orchard and perennial trees. Meanwhile, the user's accuracy that measures commission error and reflects reliability of thematic map reveals that most thematic LULC classes are reliable except orchard and perennial trees. The possible reason could be here

mentioned that because orchard and perennial trees is mixed class in this study by combining perennial trees (A4) and orchard (A5) of LDD's land use classification system. So, it consists of varieties sizes and species of perennial trees and orchard.

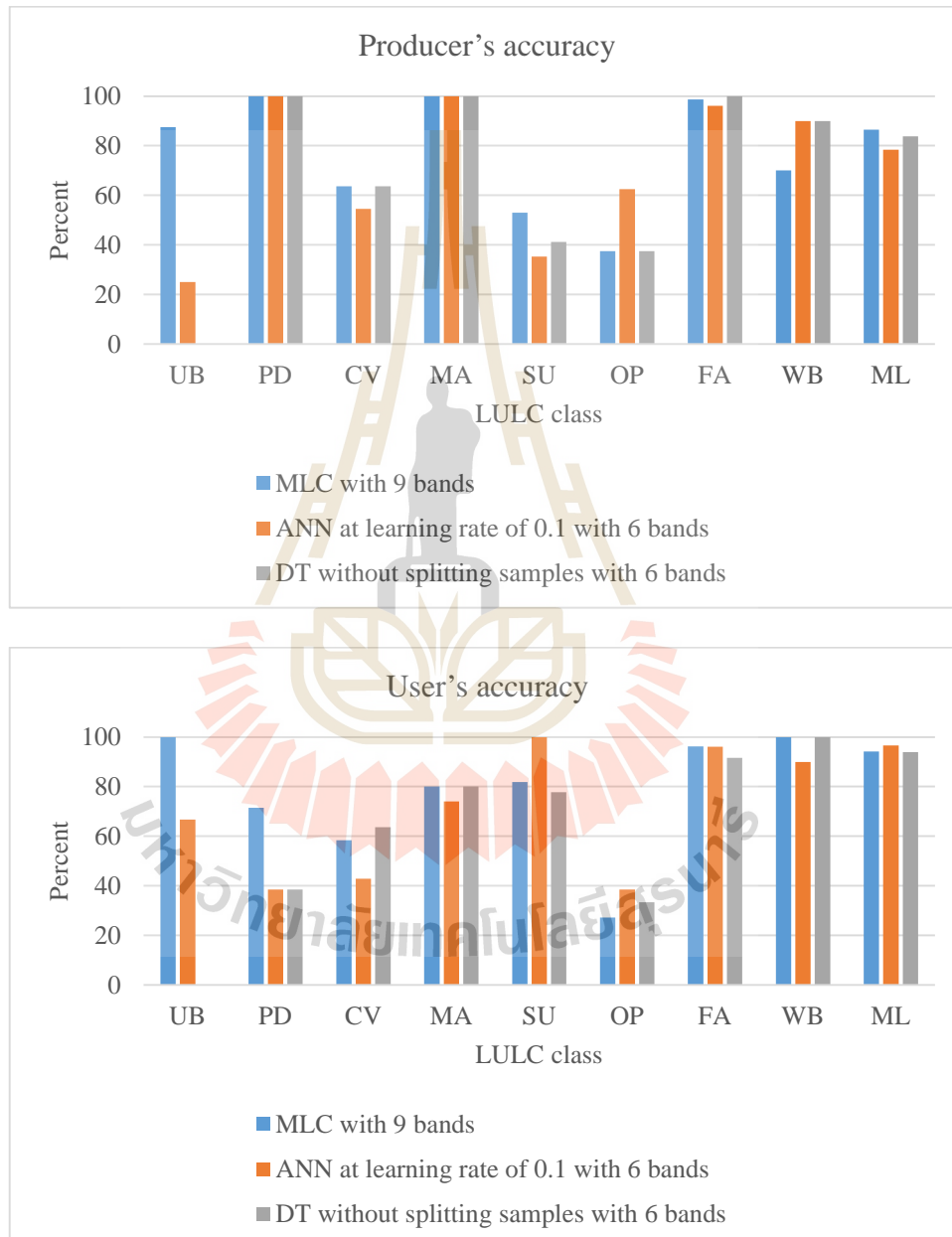


**Figure 7.2** Producer's accuracy and user's accuracy of the best three representative methods of PBIA.

The pairwise Z test among the best performance of three representative methods of PBIA is reported in Table 7.2. It was found that accuracy of MLC with nine bands for LULC classification is significantly different at the 80% confidence level from ANN at learning rate of 0.1 with six bands since the Z-value is more than Chi square values. Meanwhile, accuracy of MLC with nine bands and DT without splitting samples with six bands for LULC classification are not significantly different at the 80% confidence level. However, implementation of MLC is easier than DT. In the meantime, accuracy of DT without splitting samples with six bands and ANN at learning rate of 0.1 with six bands for LULC classification are also not significantly different at the 80% confidence level.

**Table 7.2** Pairwise Z test of among the best performance of three representative methods of PBIA.

Pairwise Z test	Kappa hat	Variance	Z-Statistic	Confidential level of critical value			
				80%	90%	95%	100%
MLC with nine bands	0.81931	0.00096	<b>1.39420</b>	<b>1.28</b>	<b>1.65</b>	<b>1.96</b>	<b>2.58</b>
ANN at learning rate of 0.1 with six bands	0.75478	0.00119					
MLC with nine bands	0.81931	0.00096	<b>1.06757</b>	<b>1.28</b>	<b>1.65</b>	<b>1.96</b>	<b>2.58</b>
DT without splitting samples with six bands	0.77023	0.00116					
ANN at learning rate of 0.1 with six bands	0.75478	0.00119	<b>0.32103</b>	<b>1.28</b>	<b>1.65</b>	<b>1.96</b>	<b>2.58</b>
DT without splitting samples with six bands	0.77023	0.00116					

## 7.2 Optimum method of OBIA for LULC classification

The best performance of two standard methods of OBIA under eCognition software according to overall accuracy and Kappa hat coefficient include (1) SNN with eleven bands: six multispectral bands and three spectral indices of pan-sharpened image of Landsat-8 and two physical data and (2) FSO with feature combination # 3: Mean Layer 4 (Band 5) and 5 (Band 6), Standard deviation Layer 4 (Band 5), Ratio Layer 2 (Band 3) and 5 (Band 6) is here compared to identify an optimum method of OBIA for LULC classification. Accuracy assessment of the best two methods of OBIA is presented in Table 7.3 and Figure 7.3. Meanwhile, producer's accuracy and user's accuracy of the best two methods of OBIA is presented in Figure 7.4.

**Table 7.3** Accuracy assessment of the best two methods of OBIA.

Method	Overall accuracy (%)	Kappa hat coefficient (%)
SNN with eleven bands	81.35	75.68
FSO with feature combination # 3	76.17	68.92

As results, it was found that the optimum method of OBIA for LULC classification in this study is standard nearest neighbor classifier (SNN) with eleven bands (Band 2, 3, 4, 5, 6, and 7, NDVI, MNDWI, NDBI, Elevation and SLOPE). It can provide overall accuracy of 81.35% and Kappa hat coefficient of 75.68% and it represents moderate agreement or accuracy between the predicted map and the reference map (Fitzpatrick-Lins, 1981). The producer's accuracy of LULC classes varies between 35.29% for sugarcane and 100% for paddy field and forest area while user's accuracy of LULC classes varies between 41.67% for cassava and 100.00% for water bodies.

The pairwise Z test among the best two methods of OBIA is reported in Table 7.4. It was found that accuracy of SNN with eleven bands for LULC classification is significantly different at the 80% confidence level from FSO with features combination #3 since the Z-value is more than Chi square values.

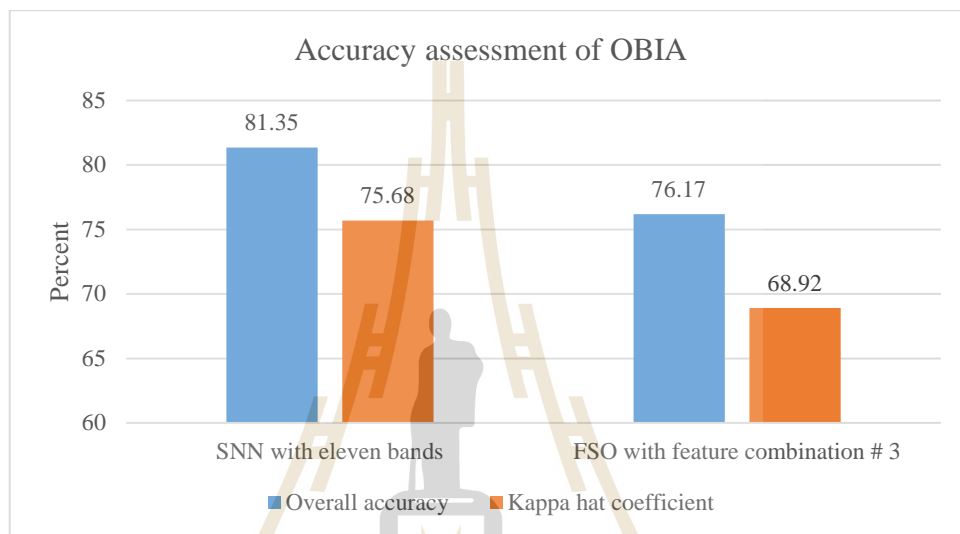


**Figure 7.3** Accuracy assessment of the best two methods of OBIA.

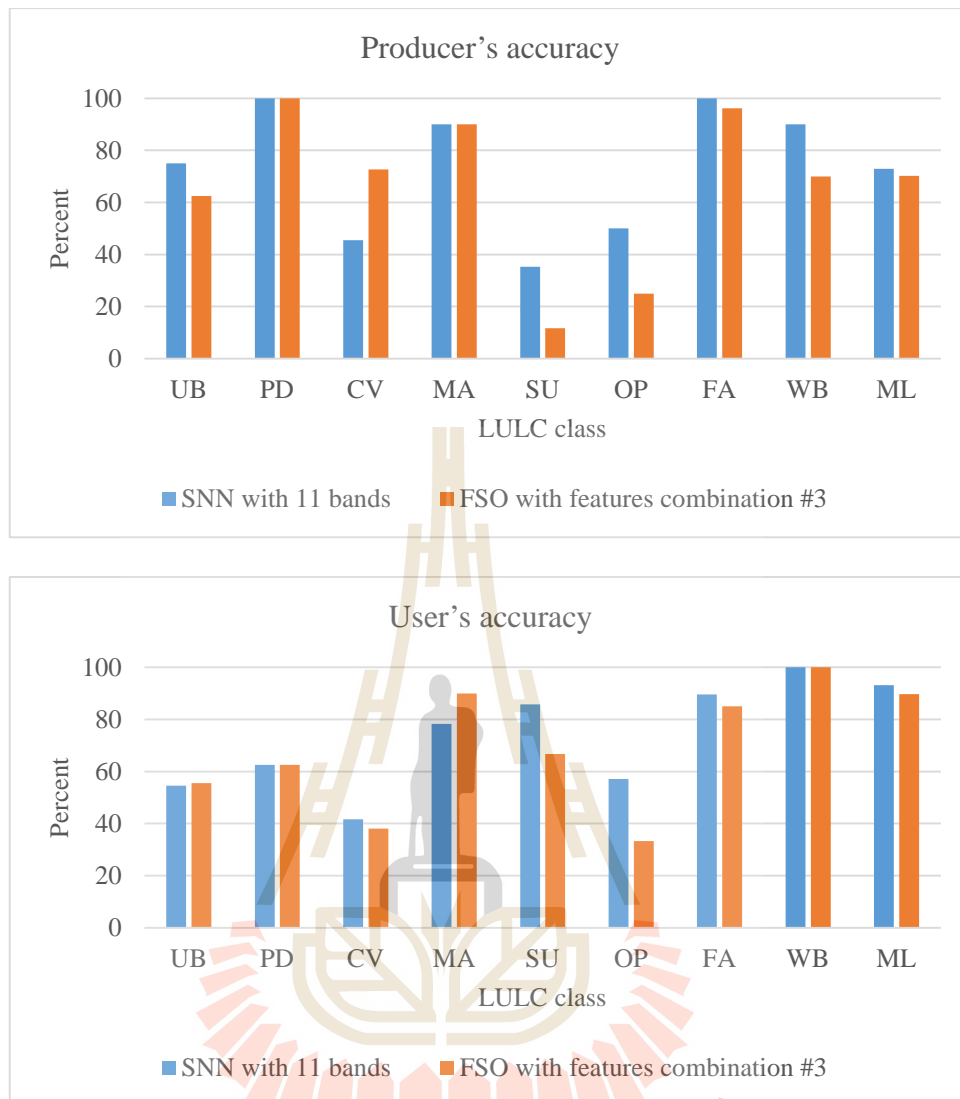


**Figure 7.4** Producer's accuracy and user's accuracy of the best two methods of OBIA.

**Table 7.4** Pairwise Z test of among the best two methods of OBIA.

Pairwise Z test	Kappa hat	Variance	Z-Statistic	Confidential level of critical value			
				80%	90%	95%	100%
SNN with eleven bands	0.75689	0.00120	1.32144	1.28	1.65	1.96	2.58
FSO with features combination #3	0.68945	0.00140					

### 7.3 Optimum method for LULC classification

The optimum method of PBIA, MLC with nine bands and OBIA, SNN with eleven bands as reported in early two sections were here compared to identify an optimum method for LULC classification. Accuracy assessment of both methods is presented in Table 7.5 and Figure 7.5. Meanwhile, producer's accuracy and user's accuracy of both methods is presented in Figure 7.6.

**Table 7.5** Accuracy assessment of the optimum method of PBIA and OBIA.

Approach	Method	Overall accuracy (%)	Kappa hat coefficient (%)
PBIA	MLC with nine bands	86.01	81.93
OBIA	SNN with eleven bands	81.35	75.68

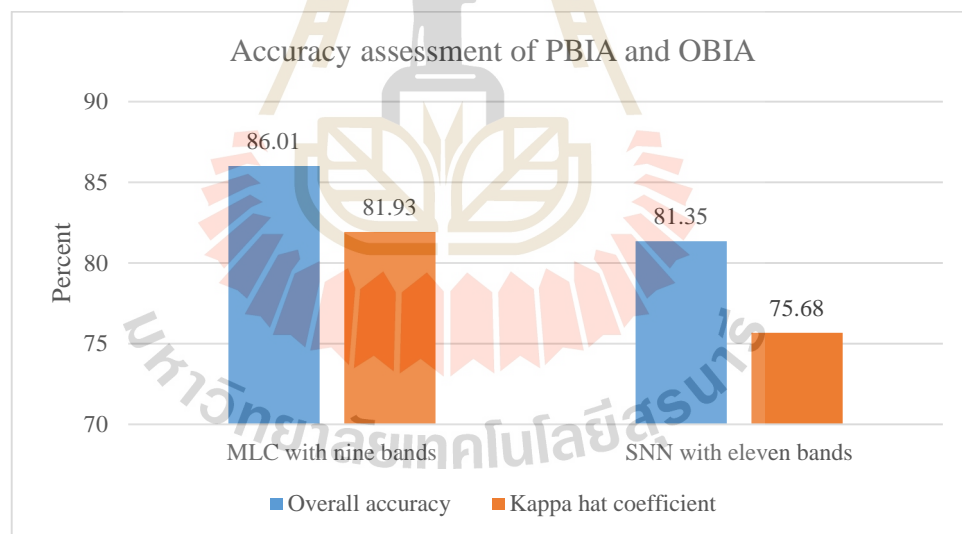


**Figure 7.5** Accuracy assessment of optimum method of PBIA and OBIA.



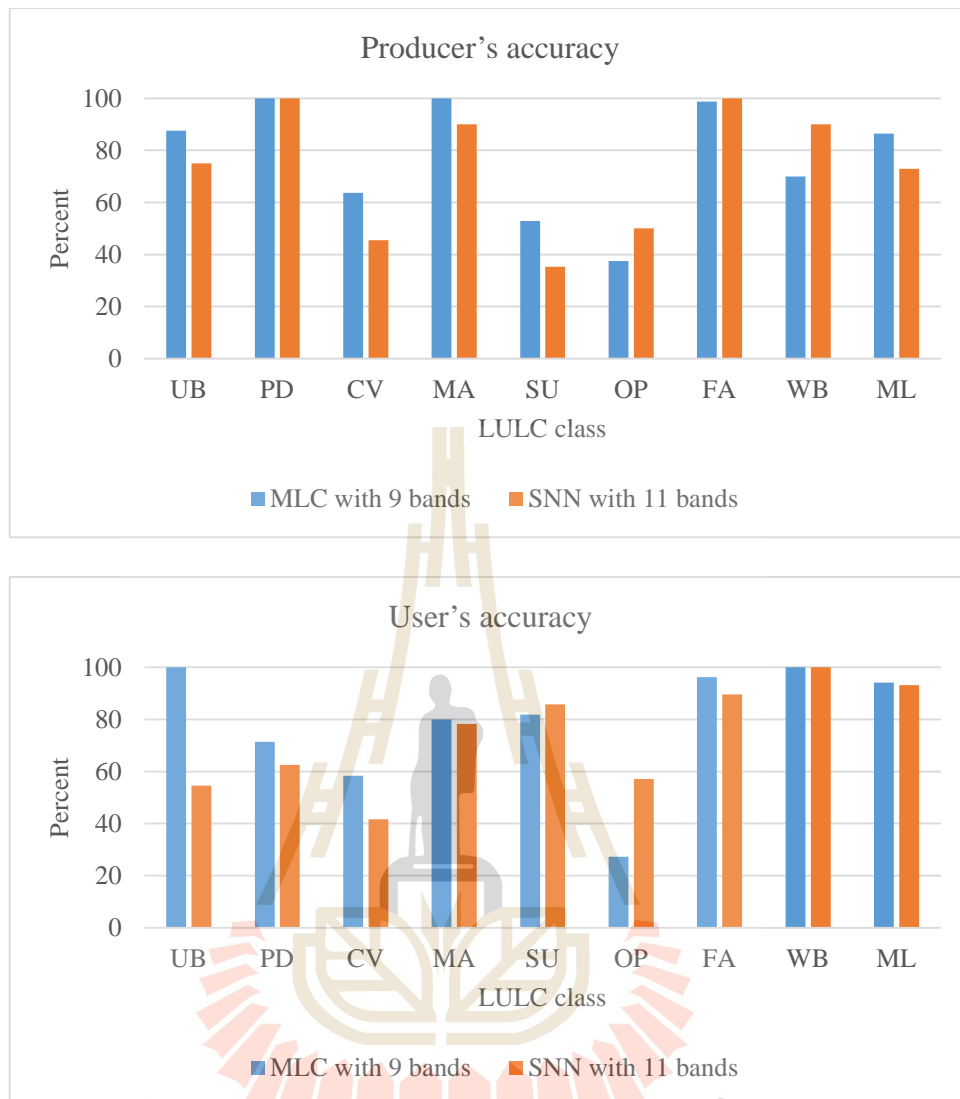


**Figure 7.6** Producer's accuracy and user's accuracy of optimum method of PBIA and OBIA.

As results, it was found that the optimum method for LULC classification in this study is maximum likelihood classifier (MLC) with nine bands (Band 2, 3, 4, 5, 6, and 7, NDVI, MNDWI, and NDBI) under ERDAS Imagine software. It can provide overall accuracy of 86.01% and Kappa hat coefficient of 81.93% and it represents strong agreement or accuracy between the predicted map and the reference map (Fitzpatrick-Lins, 1981). Most of producer's accuracy of LULC classes using MLC

with nine bands are higher than SNN with eleven bands except orchards and perennial trees, forest area and water bodies. Likewise, most of user's accuracy of LULC classes using MLC with nine bands are higher than SNN with eleven bands except sugarcane and orchards and perennial trees. The producer's accuracy of LULC classes of MLC with nine bands varies between 37.50% for orchard and perennial trees and 100.00% for paddy field and maize while user's accuracy of LULC classes varies between 27.27% for orchard and perennial trees and 100.00% for urban and built-up area and water bodies.

In addition, the pairwise Z test between the optimum method of PBIA and OBIA was calculated as result in Table 7.6. It was found that accuracy of MLC with nine bands under PBIA for LULC classification is significantly different at the 80% confidence level from SNN with eleven bands under OBIA since the Z-value, is more than Chi square values. This finding confirms that result of LULC classification with MLC with nine bands under PBIA is better than SNN with eleven bands under OBIA.

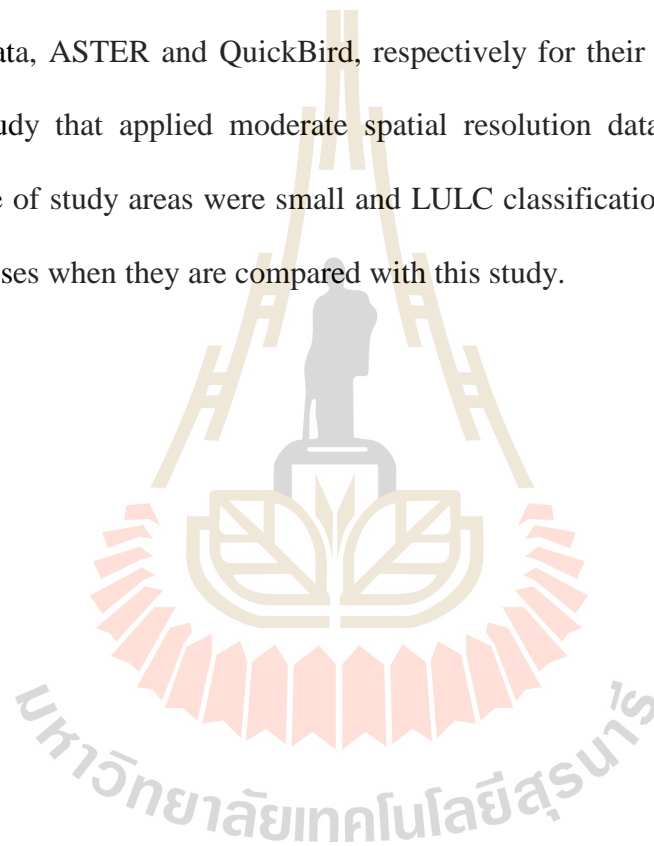
**Table 7.6** Pairwise Z test of between optimum method of PBIA and OBIA.

Pairwise Z test	Kappa hat	Variance	Z-Statistic	Confidential level of critical value			
				80%	90%	95%	100%
MLC with nine bands	0.81931	0.00096	<b>1.34428</b>	<b>1.28</b>	<b>1.65</b>	<b>1.96</b>	<b>2.58</b>
SNN with eleven bands	0.75689	0.00120					

In conclusion, it can be here concluded that MLC with nine bands of six multispectral bands and three spectral index bands (NDVI, MNDWI, and NDBI) under PBIA is the optimum method for LULC classification in this study. In practice, downloaded Landsat image is firstly preprocessed pan-sharpening and then creates

spectral indices (NDVI, MNDWI, and NDBI). After that training areas of LULC classes are selected to classify LULC map under ERDAS imagine software.

This finding is totally contrast from the previous research works of Dehvari and Heck (2009), Myint et al. (2011), Whiteside et al. (2011), and Castillejo-González et al. (2014) as mentioned in literature reviews in Chapter II. Because they applied very high spatial resolution remotely sensed data included airborne infrared image, QuickBird data, ASTER and QuickBird, respectively for their studies. It is different from this study that applied moderate spatial resolution data from Landsat 8. In addition, size of study areas were small and LULC classification system were simple with few classes when they are compared with this study.



## **CHAPTER VIII**

### **CONCLUSION AND RECOMMENDATION**

Under this chapter, major results according to objectives of the study, which were reported in Chapters V to VII, are here separately concluded and recommendations for future research and development are suggested.

#### **8.1 Conclusion**

##### **8.1.1 Optimum method of PBIA for LULC classification**

Three representative classification methods included maximum likelihood classifier (MLC), artificial neural network (ANN), and decision tree classification (DT) under pixel-based image analysis (PBIA) were firstly applied to classify LULC and then assessed accuracy with 193 sample points by field survey in 2017.

As results of LULC classification using MLC with two different datasets, it was found that MLC with nine bands of six pan-sharpened Landsat-8 and three spectral index bands (NDVI, MNDWI, and NDBI) provided better result than six bands with overall accuracy of 86.01% and Kappa hat coefficient of 81.93%. However, the pairwise Z test of MLC of two datasets based on Kappa hat analysis showed that the accuracy of both LULC classification of MLC with six and nine bands were not significantly different at the 80% confidence level.

In the meantime, results of LULC classification using ANN with learning rate of 0.1 and 0.2 and two different datasets (six and nine bands), it was found that ANN with learning rate of 0.1 and six bands of pan-sharpened Landsat-8 provided the best result with overall accuracy of 80.83% and Kappa hat coefficient of 75.48%. The pairwise Z test of LULC classification using ANN with learning rate of 0.1 and 0.2 and two different datasets (six and nine bands) based on Kappa hat analysis showed that accuracy of LULC classification maps of ANN were not significantly different at the 80% confidence level.

Meanwhile, result of DT with two methods for construction decision and three different datasets (six, nine and eleven bands) showed that DT without splitting samples and six bands of pan-sharpened Landsat-8 provided the best result with overall accuracy of 82.38% and Kappa hat coefficient of 77.02%. The pairwise Z test of LULC classification using DT with and without splitting samples and three different datasets based on Kappa hat analysis showed that accuracy of LULC classification maps of DT were not significantly different at the 80% confidence level.

According to the best performance of three representative methods of PBIA including (1) MLC with nine bands, (2) ANN at learning rate of 0.1 with six bands and (3) DT without splitting samples with six bands, it can concluded that the optimum method of PBIA for LULC classification in this study from pan-sharpened image of Landsat-8 data and its derivative spectral indices was MLC with nine bands (Band 2, 3, 4, 5, 6, and 7, NDVI, MNDWI, and NDBI). In addition, the pairwise Z test among the best performance of three representative methods of PBIA showed that accuracy of MLC with nine bands for LULC classification is significantly different at the 80% confidence level from ANN at learning rate of 0.1 with six bands.

### 8.1.2 Optimum method of OBIA for LULC classification

Two representative classification methods included standard nearest neighbor classifier (SNN) and nearest neighbor classifier with feature space optimization (FSO) under object-based image analysis (OBIA) were firstly applied to classify LULC and then assessed accuracy with 193 sample points by field survey in 2017.

As results of LULC classification of SNN with three different datasets, it was found that SNN with eleven bands of six pan-sharpened Landsat-8, three spectral index bands (NDVI, MNDWI, and NDBI) and two physical data (elevation and slope) provided better result than six and nine bands with overall accuracy of 81.35% and Kappa hat coefficient of 75.68%. However, the pairwise Z test of SNN among three datasets based on Kappa hat analysis showed that the accuracy of LULC classification of SNN within three datasets were not significantly different at the 80% confidence level.

Meanwhile, results of FSO with five features combinations, it was found that FSO with feature combination # 3 which applied features: Mean layer 4 (Band 5) and Layer 5 (Band 6), Standard deviation layer 4 (Band 5), Ratio layer 2 (Band 3) and Layer 5 (Band 6) provided the best result with overall accuracy of 76.17% and Kappa hat coefficient of 68.92%. The pairwise Z test of LULC classification using FSO among five different feature combinations based on Kappa hat analysis showed that accuracy of LULC classification maps of FSO were not significantly different at the 80% confidence level.

According to the best performance of two representative methods of OBIA including (1) SNN with eleven bands and (2) FSO with feature combination #

3, it can be concluded that the optimum method of OBIA for LULC classification in this study is SNN with eleven bands (Band 2, 3, 4, 5, 6, and 7, NDVI, MNDWI, NDBI, elevation and slope). In addition, the pairwise Z test between the best performances of two representative methods of OBIA showed that accuracy of SNN with eleven bands for LULC classification is significantly different at the 80% confidence level from FSO with feature combination # 3.

### **8.1.3 Optimum method for LULC classification**

By comparison between the best performance of two methods including (1) MLC with nine bands under PBIA and (2) SNN with eleven bands under OBIA, it can be concluded that the optimum method for LULC classification in this study was MLC with nine bands (Band 2, 3, 4, 5, 6, and 7, NDVI, MNDWI and NDBI). In addition, the pairwise Z test between the best performances of two mentioned methods showed that accuracy of MLC with nine bands for LULC classification is significantly different at the 80% confidence level from SNN with eleven bands.

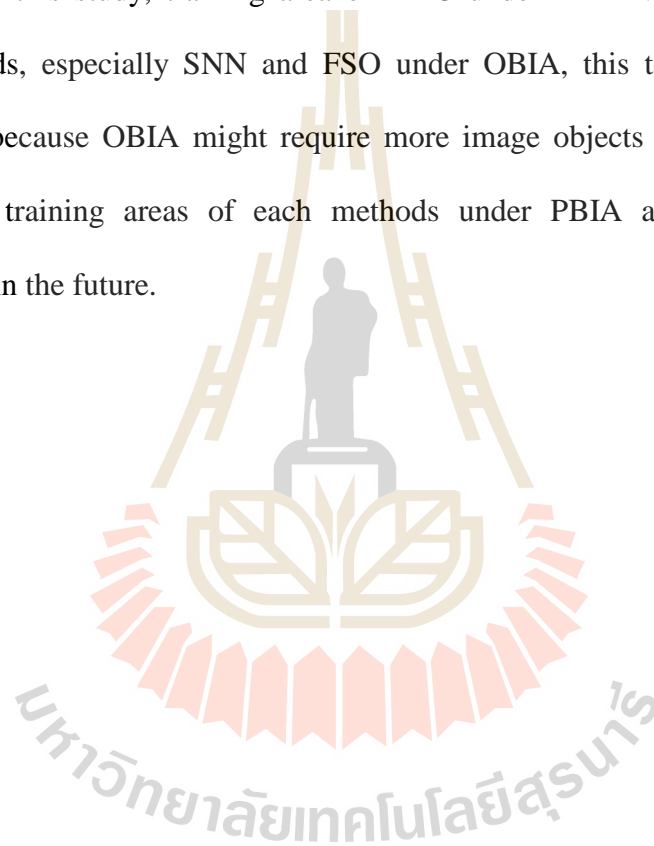
In conclusion, it can be concluded that MLC is the most appropriate method for LULC classification from moderate spatial resolution data of Landsat 8 with variety of LULC classes.

## 8.2 Recommendation

Three main objectives were here examined and implemented, the possibly expected recommendations could be made for further studies as following.

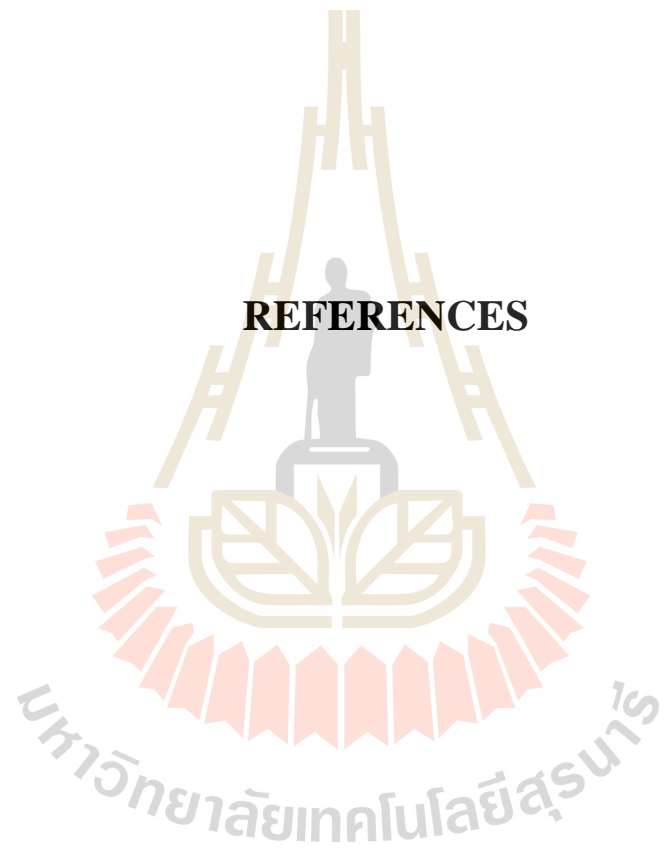
(1) PBIA and OBIA for LULC classification should be examined in different areas to verify the results in this study.

(2) In this study, training area of MLC under PBIA was here applied with other methods, especially SNN and FSO under OBIA, this technique may not be appropriate because OBIA might require more image objects as training areas. So, independent training areas of each methods under PBIA and OBIA should be investigated in the future.





## REFERENCES



## REFERENCES

- Albertz, J. (2001). **Einfuehrung in die Fernerkundung. Grundlagen der Interpretation von Luft- und Satellitenbildern.** Darmstalt: Wissenschaftliche Buchgesellschaft. Quoted by Nussbaum, S. and Menz, G. (2008) **Object-Based Image Analysis and Treaty Verification.** Berlin: Springer.
- Benz, U., Hofmann, P., Willhauck, G., Lingenfelder, I. and Heynen, M. (2004). Multi-resolution, object-oriented fuzzy analysis of remote sensing data for GIS-ready information. **ISPRS Journal of Photogrammetry & Remote Sensing.** 2004 (58): 239–258. Quoted by Nussbaum, S. and Menz, G. (2008). **Object-Based Image Analysis and Treaty Verification.** Berlin: Springer.
- Bitelli, G., Camassi, R., Gusella, R. and Mongol, A. (2004). Image change detection on urban area: The earthquake case. In **Proceedings of the ISRPS 2004 Annual Conference.** Turkey: Istanbul. Quoted by Nussbaum, S. and Menz, G. (2008). **Object-Based Image Analysis and Treaty Verification.** Berlin: Springer.
- Blaschke, T. (2004). **Towards a framework for change detection based on image objects.** Gottingen.
- Blaschke, T. (2005). A framework for change detection based on image objects. In **Gottinger Geographische Abhandlungen.** Goettingen: Goltze. Quoted by Nussbaum, S. and Menz, G. (2008). **Object-Based Image Analysis and Treaty Verification.** Berlin: Springer.

- Blaschke, T. and Strobl, J. (2001). What's wrong with pixels? Some recent developments interfacing remote sensing and GIS. **GIS - Zeitschrift für Geoinformationssysteme**. 6: 12-17. Quoted by Blaschke, T., Lang, S. and Hay, G. J. (2008). **Object-Based Image Analysis Spatial Concepts for Knowledge-Driven Remote Sensing Applications**. Berlin: Springer-Verlag.
- Blaschke, T., Lang, S. and Hay, G. J. (2008). **Object-Based Image Analysis Spatial Concepts for Knowledge-Driven Remote Sensing Applications**. Berlin: Springer-Verlag.
- Cabral, P., Gilg, J. and Painho, M. (2005). Monitoring urban growth using remote sensing, GIS and spatial metrics, remote sensing and modeling of ecosystems for sustainability. In **Proceedings of SPIE – Optics & Photonics**. USA: San Diego. Quoted by Nussbaum, S. and Menz, G. (2008). **Object-Based Image Analysis and Treaty Verification**. Berlin: Springer.
- Canty, M. J. (1999). **Fernerkundung mit Neuronalen Netzen**. Germany: Expert-Verlag. Quoted by Nussbaum, S. and Menz, G. (2008). **Object-Based Image Analysis and Treaty Verification**. Berlin: Springer.
- Castillejo-González, I. L., Pena-Barragán, J. M., Jurado-Expósito, M., Mesas-Carrascosa, F. J. and López-Granados, F. (2014). Evaluation of pixel- and object-based approaches for mapping wild oat (*Avena sterilis*) weed patches in wheat fields using QuickBird imagery for site-specific management. **European Journal of Agronomy**. (59): 57-66.

- Chandra, M., Moreira, A. and Keydel, W. (2005). Amper: Network on applied multiparameter environmental remote sensing. An EU sponsored research and training network. In **Proceedings of the IGARSS 2005 Symposium**. Korea: Seoul. Quoted by Nussbaum, S. and Menz, G. (2008). **Object-Based Image Analysis and Treaty Verification**. Berlin: Springer.
- Chunyang, H., Li, J., Zhang, J., Pan, Y. and Chen, Y. H. (2005). Dynamic monitor on urban expansion based on an object-oriented approach. In **Proceedings of the IGARSS 2005 Symposium**. Korea: Seoul. Quoted by Nussbaum, S. and Menz, G. (2008). **Object-Based Image Analysis and Treaty Verification**. Berlin: Springer.
- Cleve, C., Kelly, M., Kearns, F. R. and Moritz, M. (2008). Classification of the wildland–urban interface: A comparison of pixel- and object-based classifications using high-resolution aerial photography. **Computers, Environment and Urban Systems**. 2008(32): 317-326.
- Congalton, R. G. and Green, K. (1999). **Assessing the Accuracy of Remotely Sensed Data: Principles and Practices**. Boca Raton: Lewis Publishers.
- Congalton, R. G. and Green, K. (2009). **Assessing the Accuracy of Remotely Sensed Data: Principles and Practices**. The 2<sup>nd</sup> Edition. CRC Press.
- Cruse, B. and Hempel, C. (2005). Object based land cover mapping for Groote Eylandt: a tool for reconnaissance and land based surveys. In **Proceedings of NARGIS 2005 – APPLICATIONS IN TROPICAL SPATIAL SCIENCE. 4<sup>th</sup>–7<sup>th</sup> July Charles Darwin University**. Australia: Darwin. Quoted by Nussbaum, S. and Menz, G. (2008). **Object-Based Image Analysis and Treaty Verification**. Berlin: Springer.

- Definiens AG. (2007). **Definiens Developer 7 - User Guide**. Germany.
- Dehvari and Heck. (2009). Comparison of object-based and pixel based infrared airborne image classification methods using DEM thematic layer. **Journal of Geography and Regional Planning**. 2(4): 086-096.
- Duda, R. O., Hart, P. E. and Stork, D. G. (2001). **Pattern Classification**. USA: John Wiley & Sons. Quoted by Ongsomwang, S. (2007). **Fundamental of Remote Sensing and Digital Image Processing**. Institute of Science. Suranaree University of Technology.
- Duro, D. C., Franklin, S. E. and Dubé, M. G. (2012). A comparison of pixel-based and object-based image analysis with selected machine learning algorithms for the classification of agricultural landscapes using SPOT-5 HRG imagery. **Remote Sensing of Environment**. (118): 259-272.
- ERDAS. (2002). **ERDAS Field Guide**. Georgia: Atlanta. Quoted by Ongsomwang, S. (2007). **Fundamental of Remote Sensing and Digital Image Processing**. Institute of Science. Suranaree University of Technology.
- Fitzpatrick-Lins, K. (1981). Comparison of Sampling Procedures and Data Analysis for a Land-use and Land-cover Map. **Photogrammetric Engineering & Remote Sensing**. 55(4): 475-478.
- Gao, J. (2009). **Digital Analysis of Remotely Sensed Imagery**. New Zealand: Auckland.

- Grenzdorfer, G. (2005). Land use change in Rostock, Germany since the reunification – a combined approach with satellite data and high resolution aerial images. In **Proceedings of the ISPRS WG VII/1 Human Settlements and Impact Analysis, 3<sup>rd</sup> International Symposium Remote Sensing and Data Fusion Over Urban Areas (URBAN 2005) and 5<sup>th</sup> International Symposium Remote Sensing of Urban Areas (URS 2005)**. USA: Tempe. Quoted by Nussbaum, S. and Menz, G. (2008). **Object-Based Image Analysis and Treaty Verification**. Berlin: Springer.
- Heremans, R., Willekens, A., Borghys, D., Verbeeck, B., Valckenborgh, J. and Perneel, C. (2005). Automatic detection of flooded areas on Envisat/Asar images using an object-oriented classification technique and an active contour algorithm. In **Proceedings of the 31<sup>th</sup> International Symposium on Remote Sensing of the Environment**. Russian Federation: Petersburg. Quoted by Nussbaum, S. and Menz, G. (2008). **Object-Based Image Analysis and Treaty Verification**. Berlin: Springer.
- Jensen, J. R. (2005). **Introductory Digital Image Processing: A Remote Sensing Perspective**. Practice Hall. Quoted by Ongsomwang, S. (2007). **Fundamental of Remote Sensing and Digital Image Processing**. Institute of Science. Suranaree University of Technology.
- Keiner, L. E. (1999). Neural Network as Non-linear Function Approximators for Remote Sensing Applications. In **Information Processing for Remote Sensing**. Singapore: World Scientific.

- Kosugi, Y. and Kosaka, N. (2005). Development of agricultural GIS on Shonai area in northeast Japan using satellite data. In **Proceedings of the 26<sup>th</sup> Asian Conference on Remote Sensing**. Vietnam: Hanoi. Quoted by Nussbaum, S. and Menz, G. (2008). **Object-Based Image Analysis and Treaty Verification**. Berlin: Springer.
- Kouchi, K. and Yamazaki, F. (2005). Damage detection based on object-based segmentation and classification from high-resolution satellite images for the 2003 Boumerdes, Algeria earthquake. In **Proceedings of the 26<sup>th</sup> Asian Conference on Remote Sensing**. Vietnam: Hanoi. Quoted by Nussbaum, S. and Menz, G. (2008). **Object-Based Image Analysis and Treaty Verification**. Berlin: Springer.
- Laliberte, A., Rango, A. and Fredrickson, E. (2005). Classification of arid rangelands using an object-oriented and multi-scale approach with quick bird imagery. In **Proceedings of the ASRPS 2005**. USA: Baltimore. Quoted by Nussbaum, S. and Menz, G. (2008). **Object-Based Image Analysis and Treaty Verification**. Berlin: Springer.
- Langanke, T., Blaschke, T. and Lang, S. (2004). An object-based GIS / remote sensing approach supporting monitoring tasks in European-wide nature conservation. In **Proceedings of the Mediterranean conference on Earth Observation. First Mediterranean Conference on Earth Observation (Remote Sensing)**. 245-252. Quoted by Nussbaum, S. and Menz, G. (2008). **Object-Based Image Analysis and Treaty Verification**. Berlin: Springer.

Lillesand, T. M., Kiefer, R. W. and Chipman, J. W. (2004). **Remote Sensing and Image Interpretation**. Hoboken: John Wiley & Sons. Quoted by Nussbaum, S. and Menz, G. (2008). **Object-Based Image Analysis and Treaty Verification**. Berlin: Springer.

Matinfar, H. R., Sarmadian, F., Panah, S. K. A. and Heck, R. J. (2007). **Comparisons of object-oriented and pixel-based classification of land use/land cover types based on Landsat7, ETM+ spectral bands (case study: Arid region of Iran)**. Iran: University of Tehran.

Meinel, G. and Neubert, M. (2004). A comparison of segmentation programs for high resolution remote sensing data. In **International Archives of Photogrammetry and Remote Sensing**. Istanbul. Quoted by Blaschke, T., Lang, S. and Hay, G. J. (2008). **Object-Based Image Analysis Spatial Concepts for Knowledge-Driven Remote Sensing Applications**. Berlin: Springer-Verlag.

Moeller, M. (2005). Remote sensing for the monitoring of urban growth patterns. In **Proceedings of the ISPRS WG VII/1 Human Settlements and Impact Analysis 3<sup>rd</sup> International Symposium Remote Sensing and Data Fusion Over Urban Areas (URBAN 2005) and 5<sup>th</sup> International Symposium Remote Sensing of Urban Areas (URS 2005)**. USA: Tempe. Quoted by Nussbaum, S. and Menz, G. (2008). **Object-Based Image Analysis and Treaty Verification**. Berlin: Springer.



- Myint, S. W., Gober, P., Brazel, A., Grossman-Clarke, S. and Weng, Q. (2011). Per-pixel vs. object-based classification of urban land cover extraction using high spatial resolution imagery. **Journal of Remote Sensing of Environment.** (115): 1145-1161.
- Nussbaum, S. and Menz, G. (2008). **Object-Based Image Analysis and Treaty Verification.** Berlin: Springer.
- Office of Agricultural Economics. (2016). **Office of Agricultural Economics.** [Online]. Available: <http://www.oae.go.th/oaenew/OAE/>.
- Ongsomwang, S. (2007). **Fundamental of Remote Sensing and Digital Image Processing.** Institute of Science. Suranaree University of Technology.
- Ongsomwang, S. (2011). **Principles of Remote Sensing and Digital Image Processing.** Institute of Science. Suranaree University of Technology.
- Powers, R. P., Hermosilla, T. Coops, N. C. and Chen, G. (2015). Remote sensing and object-based techniques for mapping fine-scale industrial disturbances. **International Journal of Applied Earth Observation and Geoinformation.** (34): 51-57.
- Qiu, F. and Jensen, J. R. (2004). Opening the black box of neural networks for remote sensing image classification. **International Journal of Remote Sensing.** 25(9): 1749-1768. Quoted by Schowengerdt, R. A. (2007). **Remote Sensing: Models and Methods for Image Processing.** New York.
- Richards, J. A. and Jia, X. (1999). **Remote Sensing Digital Image Analysis.** New York: Springer Verlag. Quoted by Nussbaum, S. and Menz, G. (2008). **Object-Based Image Analysis and Treaty Verification.** Berlin: Springer.

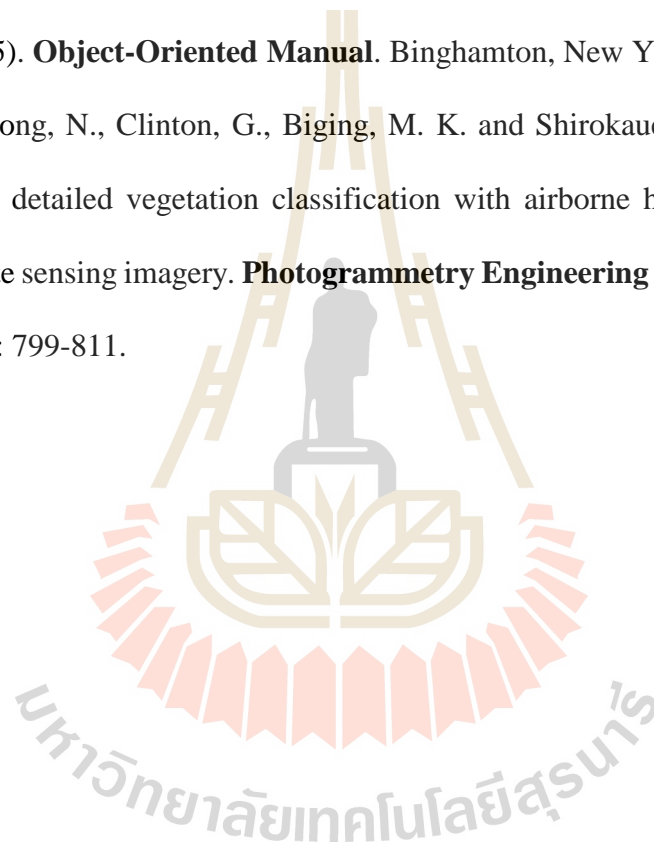
- Schowengerdt, R. A. (1997). **Remote Sensing: Models and Methods for Image Processing**. New York. Quoted by Ongsomwang, S. (2007). **Fundamental of Remote Sensing and Digital Image Processing**. Institute of Science. Suranaree University of Technology.
- Schowengerdt, R. A. (2007). **Remote Sensing: Models and Methods for Image Processing**. New York.
- Sim, S. (2005). A proposed method for disaggregating census data using object-oriented image classification and GIS. In **Proceedings of the ISPRS WG VII/1 Human Settlements and Impact Analysis 3<sup>rd</sup> International Symposium Remote Sensing and Data Fusion Over Urban Areas (URBAN 2005) and 5<sup>th</sup> International Symposium Remote Sensing of Urban Areas (URS 2005)**. USA: Tempe. Quoted by Nussbaum, S. and Menz, G. (2008). **Object-Based Image Analysis and Treaty Verification**. Berlin: Springer.
- Skidmore, A., Turner, B., Brinkhof, W. and Knowles, E. (1997). Performance of a neural network: Mapping forests using GIS and remotely sensed data. **Photogrammetric Engineering and Remote Sensing**. 63: 501-514. Quoted by Gao, J. (2009). **Digital Analysis of Remotely Sensed Imagery**. New Zealand: Auckland.
- Stehman, S. V. (2000). Practical implications of design-based sampling inference for thematic map accuracy assessment. **Journal of Remote Sensing of Environment**. 72: 34-45.
- Stehman, S. V. (2001). Statistical rigor and practical utility in thematic map accuracy assessment. **Photogrammetric Engineering & Remote Sensing**. 67: 727-734.

- Stow, D., Coulter, L., Kaiser, J., Hope, A., Service, D., Schutte, K. and Walters, A. (2003). Irrigated Vegetating Assessments for Urban Environments. **Photogrammetric Engineering & Remote Sensing**. 69(4): 381-390. Quoted by Gao, J. (2009). **Digital Analysis of Remotely Sensed Imagery**. New Zealand: Auckland.
- Tessawat, W. (2011). **A comparative accuracy assessment of expert systems and artificial neural network classification methods for identification of cassava and sugarcane areas using THEOS data**. School of Remote sensing. Institute of Science. Suranaree University of Technology.
- U.S. Geological Service. (2015). **Landsat 8**. [On-line]. Available: <http://landsat.usgs.gov/landsat8.php>.
- Wang, Z. and Bovik, A. C. (2002). A Universal Image Quality Index. **IEEE Signal Processing Letters**. 9(3): 81-84.
- Weih, R. C., Jr. and Riggan, N. D., Jr. (2010). Object-based classification vs. Pixel-based classification: Comparative importance of multi-resolution imagery. In **International Archives of the Photogrammetry, Remote Sensing and Spatial Information Sciences**. Belgium: Ghent.
- Whiteside, T. G., Boggs, G. S. and Maier, S. W. (2011). Comparing object-based and pixel-based classifications for mapping Savannas. **International Journal of Applied Earth Observation and Geoinformation**. 13: 884-893.

Witheside, T. (2005). A multi-scale object-oriented approach to the classification of multi-sensor imagery for mapping land cover in the top end. In **Proceedings of NARGIS 2005 – APPLICATIONS IN TROPICAL SPATIAL SCIENCE. 4<sup>th</sup>–7<sup>th</sup> July 2005 Charles Darwin University**. Australia: Darwin. Quoted by Nussbaum, S. and Menz, G. (2008). **Object-Based Image Analysis and Treaty Verification**. Berlin: Springer.

Wu, Q. (2015). **Object-Oriented Manual**. Binghamton, New York.

Yu, Q. P., Gong, N., Clinton, G., Biging, M. K. and Shirokauer, D. (2006). Object-based detailed vegetation classification with airborne high spatial resolution remote sensing imagery. **Photogrammetry Engineering and Remote Sensing**. 72(7): 799-811.



## CURRICULUM VITAE

**Name** Miss Salisa Saraisamrong

**Date of Birth** June 06, 1991

**Place of Birth** Nakhon Sawan, Thailand.

### **Education**

2009 - 2013 Bachelor of Science (Computer Science), Faculty of Science and Liberal Arts, Rajamangala University of Technology Isan, Nakhon Ratchasima, Thailand.

### **Grant and Fellowships**

Teaching assistants and research assistant scholarship, Suranaree University of Technology.

มหาวิทยาลัยเทคโนโลยีสุรนารี